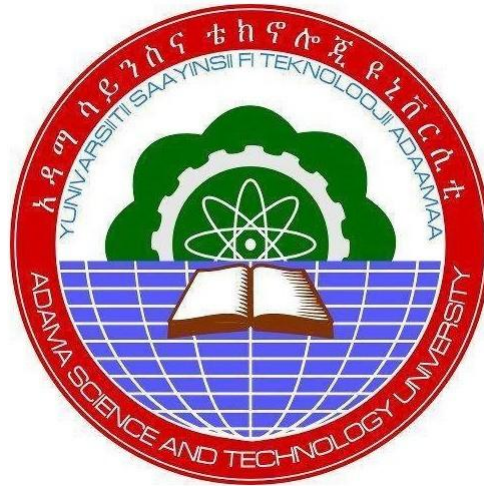


Phytochemical Investigation and In-Vitro Biological Activities evaluation of Selected Ethiopian Medicinal Plants and their Endophytes in Eastern Ethiopia



By

Prof. Aman Dekebo

Dr. Seid Mohammed

A Final Research Report Submitted to Adama Science and Technology
University

Adama, Ethiopia
March, 2025

ACKNOWLEDGEMENT

I am indebted to my PhD students Tsigu Kiros, Teshome Degifie, Hadush G/Hiwot and Dinku Senbeta for taking part in the research project. I am grateful to MSc students Terfo Yilma and Betelhem Behailu who were also involved in the project. I also thank my colleagues Prof. Yadessa Melaku and Prof. Milkyas Endale for their unreserved, invaluable support to the research project by co-advising the students who took part in the research project.

I am grateful to Adama Science and Technology University for awarding the research project. I acknowledge the World Academy of Sciences (TWAS) and the United Nations Educational, Scientific and Cultural Organization (UNESCO) under the TWAS Research Grant (RGA No. 20-274RG/CHE/AF/AC_G_FR3240314163) for the donation of instruments to our natural products research laboratory.

I would also like to thank Andong National University, South Korea, for generating MS and GC-MS data of some samples.

It is also my pleasure to thank Mr. Tariku Nefo and Taiwan Science and Technology University, Taiwan; and Dr. Mesfin Getachew and Addis Ababa University for analyzing the NMR data of some of our samples.

I am also thankful to Dr. Anteneh Belayneh, Haramaya University, for the identification of the scientific names of the studied plants.

My acknowledgement also goes to Mr. Abebe Olani, National Animal Health Diagnostic and Investigation Center (NAHDIC), Ethiopia, for conducting the MALDI-TOF MS analysis of isolated endophytic bacteria.

Professor Rajalakshmanan Eswaramoorthy, Saveetha Institute of Medical and Technical Sciences (SIMATS), Chennai, India; and Mr. Muhdin Aliye, Ph.D. student of Adama Science and Technology University, are also acknowledged for conducting the *in silico* molecular modeling of isolated compounds.

ACRONYMS

ADME	Absorption Distribution Metabolism and Excretion
ATCC	American Type Culture Collection
CFU	Colony Forming Unit
DMSO	Dimethyl Sulphoxide
DPPH	1,1-Diphenyl-2-pic-ryl-hydrazyl
FRAP	Ferric Reduction Antioxidant Power
IC ₅₀	Half Maximal Inhibitory Concentration
LBA	Luria Bertani Agar
MALDI-TOF MS	Matrix Assisted Laser Desorption Ionization- Time of Flight- Mass Spectrometry
MHA	Mueller-Hinton Agar
PDB	Protein Data Bank
TSA	Tryptic Soy Agar
TSB	Tryptic Soya Broth
¹ H-NMR	Proton Nuclear Magnetic Resonance
¹³ C-NMR	Carbon Nuclear Magnetic Resonance
DEPT-135	Distortionless Enhancement by Polarization Transfer
HRMS	High-Resolution Mass Spectrometry
CC	Column Chromatography
PTLC	Preparative Thin-Layer Chromatography
NAHDIC	National Animal Health Diagnostic and Investigation Center

TABLE OF CONTENTS

PAGES

ACKNOWLEDGEMENT.....	ii
ACRONYMS	iii
List of Tables	vii
List of Figures.....	ix
List of Appendices.....	xiii
List of Tables Appendices	xiii
List of Figure Appendices	xv
List of publication from the research project	xvi
1 Introduction.....	1
1.1 Background.....	1
1.2 Statement of the problem.....	2
1.3 Justification of the study	3
1.4 Objectives	5
1.4.1 General objective	5
1.4.2 Specific objectives	5
1.5 Significance of the study	6
2 Literature Review	6
2.1 Traditional medicinal plants and the modern medicine	6
2.2 Antimicrobial potency of medicinal plants.....	8
2.3 Endophytes and their method of isolation	9
2.4 Botanical, ethnobotanical, biological and phytochemical aspects of studied plants.....	12
2.4.1 Botanical description	12
2.4.2 Ethnobotanical uses	13
2.4.3 Biological activity.....	17
2.4.4 Chemical constituents	21
3 Materials and Methods.....	28

3.1 Description of the study area	28
3.2 Collection and authentication of the plant materials.....	29
3.3 Test microbial cultures	29
3.4 Chemicals, apparatuses and instruments	30
3.5 Extraction and isolation of compounds from plants parts	30
3.5.1 <i>Cadia purpurea</i> leaves and roots	31
3.5.2 <i>Caralluma speciosa</i> stems	39
3.5.3 <i>Gloriosa superba</i> tubers.....	43
3.5.4 <i>Gomphocarpus purpurascens</i> leaves	45
3.6 Isolation and identification of endophytic bacteria and associated compounds from <i>Gloriosa superba</i>	47
3.6.1 Isolation of endophytic bacteria.....	47
3.6.2 Morphological and microscopic characterization.....	48
3.6.3 Biochemical tests	49
3.6.4. MALDI-TOF MS Bacterial Identification.....	53
3.6.5 Culture cultivation and ethyl acetate extraction.....	53
3.6.6 Fractionation of GST5 (<i>Escherichia coli</i>) ethyl acetate extract.....	54
3.7 Instrumentation	56
3.8 <i>In vitro</i> antimicrobial activity evaluation of crude extracts of medicinal plants, and endophytes and compounds	56
3.8.1 Antibacterial activity assay	56
3.8.2 Antifungal activity assay	58
3.9 <i>In vitro</i> antioxidant activity examination evaluation of crude extracts of the medicinal plants and isolated compounds	58
3.9.1 DPPH free radical scavenging assay.....	58
3.9.2 Ferric reducing antioxidant power (FRAP) assay.....	59
3.10 <i>In silico</i> molecular modeling study.....	60
4 Results and Discussion.....	61
4.1 Structural elucidation of the isolated compounds.....	61
4.1.1 Compounds isolated from the roots and leaves of <i>Cadia purpurea</i>	61
4.1.2 Compounds isolated from <i>Caralluma speciosa</i> stems.....	68
4.1.3 Compounds isolated from <i>Gloriosa superba</i> tubers	77

4.1.4 Compound isolated from <i>Gomphocarpus purpurascens</i> leaves	79
4.1.5 Compound isolated from ethyl acetate extract of <i>Escherichia coli</i> (GST5) isolate.....	80
4.2 Morphological and biochemical characterization of isolated endophytic bacteria.....	82
4.3 Identification of isolated bacterial endophytes based on protein profile using MALDI-TOF MS analysis	84
4.4 <i>In vitro</i> antimicrobial activity evaluation.....	87
4.4.1 Antibacterial activity assay	87
4.4.2 Antifungal activity assay	103
4.5. <i>In vitro</i> antioxidant potential examination.....	104
4.5.1 DPPH free radical scavenging assay.....	104
4.5.2 Ferric reducing antioxidant power (FRAP) assay.....	113
4.6 <i>In silico</i> molecular modeling study.....	118
5 Conclusion and Recommendation.....	146
6 References.....	150
7 Appendices.....	163

List of Tables

Table 1. Ethnobotanical uses of studied plant species	16
Table 2. Biological activities of studied ethnomedicinal plant species	20
Table 3. Collected fractions of chloroform leaves extract of <i>C. purpurea</i>	33
Table 4. Fractions collected from methanol leaves extract of <i>C. purpurea</i>	34
Table 5. Collected fractions of ethyl acetate phase extract of defatted methanol extract of <i>C. purpurea</i> leaves	36
Table 6. Sub-fractions collected from Fr.6-16 of chloroform: methanol (1:1) roots extract of <i>C. purpurea</i>	38
Table 7. Collected fractions from chloroform extract of <i>C. speciosa</i> stem	41
Table 8. Fractions collected from methanol extract of <i>C. speciosa</i> stem	43
Table 9. Fractions eluted from chloroform: methanol (1:1) tuber extract of <i>G. superba</i>	44
Table 10. Collected fractions from chloroform: methanol (1:1) leaves extract of <i>G. purpurascens</i>	46
Table 11. Colony morphology and microscopic Gram-staining test	49
Table 12. Collected fractions of ethyl acetate extract of GST5 (<i>Escherichia coli</i>) endophytic bacterium culture filtrate	55
Table 13. Biochemical test results for Gram-positive endophytic bacterial isolates	83
Table 14. Biochemical test results for Gram-negative endophytic bacterial isolates	84
Table 15. MALDI-TOF MS analysis result for isolated endophytic bacteria	85
Table 16. Antibacterial activity of five leaves extracts of <i>C. purpurea</i> against <i>E. coli</i> , <i>P. aeruginosa</i> and <i>S. aureus</i> standard human pathogens	89
Table 17. Antibacterial inhibitory activity of isolated compounds 65-67 against <i>E. coli</i> , <i>P. aeruginosa</i> and <i>S. aureus</i> bacterial strains	90
Table 18. Antibacterial inhibitory action (mean \pm sd, mm) against <i>E. coli</i> , <i>P. aeruginosa</i> and <i>S. aureus</i> of five roots extracts of <i>C. purpurea</i>	92
Table 19. Antibacterial activity inhibition zone (mean \pm sd, mm) of compounds 67-70 against <i>E. coli</i> , <i>P. aeruginosa</i> and <i>S. aureus</i> bacterial strains	94
Table 20. Antibacterial activity inhibition zone (mean \pm sd, mm) on <i>E. coli</i> , <i>P. aeruginosa</i> , and <i>S. aureus</i> of <i>C. speciosa</i> stem extracts	96

Table 21. Antibacterial inhibitory values (mean \pm sd, mm) against <i>E. coli</i> , <i>P. aeruginosa</i> and <i>S. aureus</i> of compounds 71-75.....	97
Table 22. Antibacterial activity inhibitory values (mean \pm sd) of tuber extracts of <i>G. superba</i> against <i>E. coli</i> , <i>P. aeruginosa</i> and <i>S. aureus</i>	99
Table 23. Antibacterial inhibition zone diameter (mean \pm sd) of leaves extracts of <i>G. purpurascens</i> against <i>E. coli</i> , <i>P. aeruginosa</i> and <i>S. aureus</i> standard bacterial strains	101
Table 24. Antibacterial activity of isolated compounds 76, 78, 79 and 80 against <i>E. coli</i> , <i>S. aureus</i> and <i>P. aeruginosa</i> bacterial strains	102
Table 25. Antibacterial activity of ethyl acetate extracts of isolated endophytic bacteria.....	103
Table 26. Antifungal activity inhibition zone diameters (mean \pm sd, mm) against <i>Candida albicans</i> of chloroform: methanol (1:1) extracts of four plants	104
Table 27. DPPH scavenging percentage (mean \pm sd) of <i>C. purpurea</i> leaves extracts.....	105
Table 28. DPPH radical scavenging percentage (mean \pm sd) of <i>C. purpurea</i> roots extracts.	106
Table 29. DPPH radical scavenging activity percentage (mean \pm sd) of compounds 65-70 isolated from leaves and roots of <i>C. purpurea</i>	107
Table 30. Percent scavenging activity (mean \pm sd) against DPPH of <i>C. speciosa</i> stem extracts	109
Table 31. Scavenging activity percentage (mean \pm sd) against DPPH of compounds 71-75 isolated from <i>C. speciosa</i> stem extracts	110
Table 32.: Percentage inhibitory activity (mean \pm sd) of <i>G. superba</i> tubers extracts and isolated compounds 76 and 78 against DPPH free radical.....	111
Table 33. DPPH scavenging activity percentage of <i>G. purpurascens</i> leaves extracts and isolated calotropin (79).....	113
Table 34.: FRAP (mean \pm sd) of <i>C. purpurea</i> leaves extracts	114
Table 35. FRAP (mean \pm sd) of <i>C. purpurea</i> roots extracts	115
Table 36. FRAP (mean \pm sd) of compounds 65-70 isolated from <i>C. purpurea</i> leaves and roots extracts	116
Table 37. FRAP (mean \pm sd) of <i>C. speciosa</i> extracts	117
Table 38. FRAP (mean \pm sd) of isolated compounds 71-75 of <i>C. speciosa</i> stems extracts...	118
Table 39. FRAP of isolated compounds 76, 78 and 79.....	118

List of Figures

Figure 1. Structures of some compounds 1-5 reported in the early 20 th century	8
Figure 2. Structures of some antimicrobial and anticancer compounds 6-14 originated from fungal endophytes of medicinal plants.....	11
Figure 3. Structures of compounds 15-38 reported from <i>G. superba</i>	23
Figure 4. Structures of compounds 39-49 reported from <i>C. purpurea</i>	24
Figure 5. Structures of compounds 50-64 reported from different species of the genus <i>caralluma</i>	27
Figure 6. Map of the study area ¹⁷	28
Figure 7. Photo of four studied plant species. (a) <i>Cadia purpurea</i> and its root (left) part, (b) <i>Caralluma speciosa</i> , (c) <i>Gomphocarpus purpurascens</i> and (d) <i>Gloriosa superba</i> and its tuber (left) part (photo by Tsegu K., 2021)	29
Figure 8: General procedure for preparation of crude plant extracts with increasing polarity	31
Figure 9. TLC profiles of <i>n</i> -hexane (a), chloroform (b), chloroform: methanol (1:1;.....	32
Figure 10. TLC profiles of combined fractions of chloroform leaves extract of <i>C. purpurea</i>	33
Figure 11. TLC profiles of combined fractions of methanol leaves extract of <i>C. purpurea</i> ...	34
Figure 12: Acid-base extraction procedure used to isolate alkaloidal compounds from leaves of <i>C. purpurea</i>	35
Figure 13. TLC profiles of combined fractions of ethyl acetate extract of defatted methanol extract of <i>C. purpurea</i> leaves	36
Figure 14. TLC analysis of combined sub-fractions from Fr.41-52 of ethyl acetate extract of defatted methanol leaves extract of <i>C. purpurea</i>	37
Figure 15. TLC profiles of combined fractions of chloroform: methanol (1:1) roots extract of <i>C. purpurea</i>	37
Figure 16. TLC profiles of combined sub-fractions of Fr.6-16 of chloroform: methanol (1:1) roots extract of <i>C. purpurea</i>	38
Figure 17. TLC profiles of combined fractions of methanol roots extract of <i>C. purpurea</i>	39
Figure 18. TLC profiles of <i>n</i> -hexane, chloroform, chloroform: methanol (1:1), methanol and ethanol extracts of <i>C. speciosa</i> stem	40
Figure 19. TLC profiles of combined fractions of chloroform stem extract of <i>C. speciosa</i>	41

Figure 20. TLC profiles of combined sub-fractions of Fr.119-203 of chloroform <i>C. speciosa</i> stem extract	42
Figure 21. TLC profiles of combined fractions of methanol stem extract of <i>C. speciosa</i>	43
Figure 22. TLC profile of crude tuber extracts of <i>G. superba</i>	44
Figure 23. TLC profiles of combined fractions of chloroform:methanol (1:1) <i>G. superba</i> tuber extract	45
Figure 24. TLC profiles of <i>n</i> -hexane, chloroform, chloroform: methanol (1:1), methanol and ethanol extracts of <i>G. purpurascens</i> leaves.....	45
Figure 25. TLC results of combined fractions of chloroform: methanol (1:1) leaves extract of <i>G. purpurascens</i>	46
Figure 26. TLC analysis of combined sub-fractions of Fr.85-92 of chloroform: methanol (1:1) leaves extract of <i>G. purpurascens</i>	47
Figure 27. TLC profile of scraped bands on PTLC fractionated sub-fr11-25 of Fr.85-92 of chloroform: methanol (1:1) leaves extract of <i>G. purpurascens</i>	47
Figure 28. TLC profiles of ethyl acetate extracts of fermented endophytic bacterial culture filtrates.....	54
Figure 29. TLC profiles of combined sub-fractions of Fr.1-113 of GST5 (<i>Escherichia coli</i>) ethyl acetate extract.....	55
Figure 30. Structures of compounds 65-70 isolated from leaves and roots of <i>C. purpurea</i>	65
Figure 31. Structures of compounds 71-75 isolated from <i>C. speciosa</i> stem.....	74
Figure 32. Structures of compounds 76-78 isolated from <i>G. superba</i> tubers	79
Figure 33. Structure of calotropin (79) isolated from <i>G. purpurascens</i> leaves.....	80
Figure 34. Structure of 1-undecene (80) isolated from ethyl acetate extract of GST5 (<i>Escherichia coli</i>) endophytic bacterial culture	81
Figure 35. Pure colonies for certain endophytic bacterial isolates obtained from <i>G. superba</i> . (a) indicates pure colony for <i>Bacillus subtilis</i> (GSL1). (b) indicates pure colony for <i>Bacillus megaterium</i> (GSL3) with gel colony.....	86
Figure 36. Gram-staining for certain endophytic bacteria isolated from <i>G. superba</i> . (a) <i>Bacillus subtilis</i> (GSL1), (b) <i>Bacillus megaterium</i> (GSL3), (c) <i>Escherichia coli</i> (GST5) and (d) <i>Providencia rettgeri</i> (GSS1)	86

Figure 37. Endospore test for Gram-positive isolates these obtained from <i>G. superba</i> . (a) indicates endospore test for <i>Bacillus subtilis</i> (GSL1). (b) indicates endospore test for <i>Bacillus megaterium</i> (GSL3) with long rod-shaped	87
Figure 38. Percentage scavenging activity (means of duplicates) versus different concentrations of <i>Cadia purpurea</i> leaves extracts against DPPH radical. CLE, CMLE, MLE and ELE are chloroform, chloroform: methanol (1:1), methanol and ethanol leaves extract, respectively, and AA is ascorbic acid	105
Figure 39. Percentage scavenging activity against DPPH of <i>C. purpurea</i> roots extracts at different concentrations. CRE, CMRE, MRE and ERE are chloroform, chloroform: methanol (1:1), methanol and ethanol roots extracts, and AA is ascorbic acid standard	107
Figure 40. DPPH radical scavenging activity percentage (mean of duplicates) against various concentrations of compounds 65-70 isolated from leaves and roots of <i>C. purpurea</i>	108
Figure 41. DPPH radical scavenging percentage (%) versus different concentrations of <i>C. speciosa</i> crude extracts and ascorbic acid (HE-hexane extract, CE-chloroform extract, CME-chloroform: methanol extract, ME-methanol extract, EE-ethanol extract, AA-ascorbic acid)	109
Figure 42. DPPH radical scavenging percentage (%) versus different concentrations ($\mu\text{g/mL}$) of compounds 71-75 isolated from <i>C. speciosa</i> stems and standard ascorbic acid (AA)	110
Figure 43. Percentage scavenging activity against DPPH radical versus concentration ($\mu\text{g/mL}$) of <i>G. superba</i> tuber extracts and isolated compounds 76 and 78. CTE, CMTE and MTE are chloroform, chloroform: methanol (1:1) and methanol tubers extract, respectively.	112
Figure 44. DPPH radical scavenging activity percentage versus concentration ($\mu\text{g/mL}$) of <i>purpurascens</i> leaves extracts and isolated calotropin (79)	113
Figure 45. Ligand-protein interaction (a) and 3D representation (b) between compound 65 and <i>E. coli</i> gyraseB enzyme (6F86).....	121
Figure 46. Ligand-protein interaction (a) and 3D representation (b) of compound 65 against <i>S. aureus</i> pyruvate kinase (3T07).....	122
Figure 47. Ligand-protein interaction (a) and 3D representation (b) of compound 65 against human peroxiredoxin (1HD2)	123
Figure 48. Ligand-protein interaction (a) and 3D representation (b) between apigenin-7- <i>O</i> -neohesperidoside (66) and <i>E. coli</i> gyraseB enzyme (6F86).....	124

Figure 49. Ligand-protein interaction (a) and 3D representation (b) between apigenin-7- <i>O</i> -neohesperidoside (66) and <i>S. aureus</i> pyruvate kinase (3T07)	125
Figure 50. Ligand-protein interaction (a) and 3D representation (b) between apigenin-7- <i>O</i> -neohesperidoside (66) and human peroxiredoxin 5 (1HD2).....	126
Figure 51. Ligand-protein interaction (a) and 3D representation (b) between calpurnine (67) and <i>E. coli</i> gyraseB enzyme (6F86)	127
Figure 52. Ligand-protein interaction (a) and 3D representation (b) between calpurnine (67) and <i>S. aureus</i> pyruvate kinase enzyme (3T07)	128
Figure 53. Ligand-protein interaction (a) and 3D representation (b) between calpurnine (67) and human peroxiredoxin 5 (1HD2)	129
Figure 54. Ligand-protein interaction (a) and 3D representation (b) between compound 68 and <i>E. coli</i> gyraseB protein (6F86).....	130
Figure 55. Ligand-protein interaction (a) and 3D representation (b) between compound 68 and <i>S. aureus</i> pyruvate kinase (3T07).....	131
Figure 56. Ligand-protein interaction (a) and 3D representation (b) between compound 68 and human peroxiredoxin 5 (1HD2).....	132
Figure 57. Ligand-protein interaction (a) and 3D representation (b) between bis-(2-hydroxybutyl) phthalate (69) and <i>E. coli</i> gyraseB protein (6F86).....	133
Figure 58. Ligand-protein interaction (a) and 3D representation (b) between bis-(2-hydroxybutyl) phthalate (69) and <i>S. aureus</i> pyruvate kinase (3T07).....	134
Figure 59. Ligand-protein interaction (a) and 3D representation (b) between bis-(2-hydroxybutyl)phthalate (69) and human peroxiredoxin 5 (1HD2).....	135
Figure 60. Ligand-protein interaction (a) and 3D representation (b) between compound 65 and <i>P. aeruginosa</i> PqsA (5OE3).....	136
Figure 61. Ligand-protein interaction (a) and 3D representation (b) between apigenin-7- <i>O</i> -neohesperidoside (66) and <i>P. aeruginosa</i> PqsA (5OE3)	137
Figure 62. Ligand-protein interaction (a) and 3D representation (b) between calpurnine (67) and <i>P. aeruginosa</i> PqsA (5OE3).....	138
Figure 63. Ligand-protein interaction (a) and 3D representation (b) between compound 68 and <i>P. aeruginosa</i> PqsA (5OE3).....	139

Figure 64. Ligand-protein interaction (a) and 3D representation (b) between bis-(2-methylheptyl) phthalate (70) and <i>P. aeruginosa</i> PqsA (5OE3).....	140
Figure 65. Ligand-protein interaction (a) and 3D representation (b) between calotropin (79) and <i>P. aeruginosa</i> PqsA (5OE3).....	141
Figure 66. Ligand-protein interaction (a) and 3D representation (b) between chloramphenicol and <i>E. coli</i> gyraseB enzyme (6F86).....	142
Figure 67. Ligand-protein interaction (a) and 3D representation (b) between chloramphenicol and <i>S. aureus</i> pyruvate kinase (3T07).....	143
Figure 68. Ligand-protein interaction (a) and 3D representation (b) between chloramphenicol and <i>P. aeruginosa</i> PqsA (5OE3).....	144
Figure 69. Binding interaction (a) and 3D structure (b) between ascorbic acid and human peroxiredoxin 5 (1HD2).....	145

List of Appendices

List of Tables Appendices

Appendix Table 1. ^1H , ^{13}C and DEPT-135 NMR (CDCl_3) spectroscopic data of compound 65.....	163
Appendix Table 2. ^1H , ^{13}C and DEPT-135 NMR (CD_3OD) spectral data of apigenin-7- <i>O</i> -neohesperidoside (66).....	164
Appendix Table 3. ^1H , ^{13}C and DEPT-135 NMR (CDCl_3) data of 13- <i>O</i> -pyrrolecarboxyl lupanine (67) and literature data.....	164
Appendix Table 4. ^1H , ^{13}C and DEPT-135 NMR (CDCl_3) spectral data of compound 68...	166
Appendix Table 5. ^1H , ^{13}C and DEPT-135 NMR (CDCl_3) spectral data for bis-(2-hydroxybutyl) phthalate (69).....	166
Appendix Table 6. ^1H , ^{13}C and DEPT-135 NMR (CD_3OD) data of compound 70 and di-(2-methylheptyl)phthalate.....	167
Appendix Table 7.: ^1H , ^{13}C and DEPT-135 NMR (CDCl_3) spectral data of heptacos-1-ene (71).....	167
Appendix Table 8. ^1H , ^{13}C and DEPT-135 NMR (CDCl_3) spectral data of di-(2-ethylhexyl)phthalate (72).....	169

Appendix Table 9. ^1H , ^{13}C and DEPT-135 NMR (CDCl_3) spectroscopic data of the aglycone moiety of compound 73	170
Appendix Table 10. ^1H , ^{13}C and DEPT-135 NMR (CDCl_3) spectral data for the sugar moieties of compound 73	172
Appendix Table 11. ^1H , ^{13}C and DEPT-135 NMR (CDCl_3) spectral data of compound 74	173
Appendix Table 12. ^1H , ^{13}C and DEPT-135 NMR (CDCl_3) spectral data for the aglycone moiety of compound 75	174
Appendix Table 13. ^1H , ^{13}C and DEPT-135 NMR (CDCl_3) spectroscopic data for the sugar moieties of compound 75	175
Appendix Table 14. ^1H , ^{13}C and DEPT-135 NMR (CDCl_3) spectral data of β -sitosterol (76) and β -sitosterol oleate (77).....	176
Appendix Table 15. ^1H , ^{13}C and DEPT-135 NMR (CDCl_3) spectral data of 1,2-dipropyl phthalate (78)	178
Appendix Table 16. ^1H , ^{13}C and DEPT-135 NMR (CD_3OD) data of calotropin (79).....	178
Appendix Table 17. ^1H , ^{13}C and DEPT-135 NMR (CDCl_3) data of 1-undecene (80).....	179
Appendix Table 18. Molecular binding capacity of isolated compounds 65-69 and chloramphenicol against <i>E. coli DNA gyraseB</i> (PDB ID: 6F86) for antibacterial activity....	180
Appendix Table 19. Molecular binding capacity of isolated compounds 65-69 and chloramphenicol against <i>S. aureus pyruvate kinase</i> (PDB ID: 3T07) for antibacterial activity	180
Appendix Table 20. Molecular binding capacity of isolated compounds 65-69 and ascorbic acid against <i>human peroxiredoxin 5</i> (PDB ID: 1HD2) for antioxidant activity	181
Appendix Table 21. Molecular binding capacity of isolated compounds 65-68, 70 and 79, and chloramphenicol against <i>P. aeruginosa PqsA</i> (PDB ID: 5OE3) for antibacterial activity	182
Appendix Table 22. Drug-likeness property prediction of isolated compounds 65-69, 70 and 79.....	183
Appendix Table 23. ADME property prediction of isolated compounds 65-69, 70 and 79.	184
Appendix Table 24. Predication of toxicity property of isolated compounds 65-69, 70 and 79	184

List of Figure Appendices

Appendix Figure 1. Representatives of emerging endophytic bacteria of plant segments on TSA medium containing Petri plate. (a) <i>B. subtilis</i> (GSL2), (b) <i>B. megaterium</i> (GSL3), (c) <i>E. coli</i> (GSS11), (d) <i>E. coli</i> (GST5), (e) <i>B. amyloliquefaciens</i> (GSS7) and (f) <i>Providencia rettgeri</i> (GSS1).....	185
Appendix Figure 2. Representatives of sub-cultured (pure) endophytic bacterial isolates. (a) indicates for <i>Bacillus subtilis</i> (GSL1), (b) indicates <i>Bacillus megaterium</i> (GSL3) with gel colony, (c) indicates for <i>Bacillus subtilis</i> (GSL2) and (d) indicates <i>B. amyloliquefaciens</i> (GSS7)	186
Appendix Figure 3. Representatives of Gram-positive (purple color) and Gram-negative (red color) endophytic bacterial isolates. (a) <i>Bacillus subtilis</i> (GSL1), (b) <i>Bacillus megaterium</i> (GSL3), (c) <i>Escherichia coli</i> (GST5) and (d) <i>Providencia rettgeri</i> (GSS1).....	187
Appendix Figure 4. Representatives of spore forming endophytic bacteria against Gram-staining (a-d) and spore-staining (e & f) tests. (a) <i>B. subtilis</i> (GSL2), (b) <i>B. subtilis</i> (GSS2), c) <i>B. amyloliquefaciens</i> (GSS7), (d) <i>B. subtilis</i> (GSS8), (e) <i>B. subtilis</i> (GST8) and (f) <i>B. subtilis</i> (GST1)	188
Appendix Figure 5. MALDI-TOF MS analysis data of endophytic bacteria isolated from leaves, stems and tubers of <i>Gloriosa superba</i>	189
Appendix Figure 6. Representatives of antimicrobial inhibition zones of extracts, isolated compounds and ethyl acetate extracts of endophytic bacterial cultures	191

List of publication from the research project

1. Degfie, T., Endale, M., Begna, T., Jung, C. and Dekebo, A., 2025. GC-MS profiling and in silico pharmacokinetic properties of essential oils hydrodistilled from leaves of *Capparis tomentosa* and *Cadaba rotundifolia*. *Bull. Chem. Soc. Ethiop.*, 39(2), 351-366.
2. Kiros, T., Melaku, Y., Jung, C., Hu, X. and Dekebo, A., 2024. Endophytes as Potential Contenders of Their Host Plants for Bioactive Drug Discovery: A Review. *Traditional Resources and Tools for Modern Drug Discovery: Ethnomedicine and Pharmacology*, pp.499-525
3. Degfie, T., Endale, M., Aliye, M., Eswaramoorthy, R., Nefo Duke, T. and Dekebo, A., 2024. In Vitro Antibacterial, Antioxidant, Cytotoxicity Activity, and In Silico Molecular Modelling of Compounds Isolated from Roots of *Hydnora johannis*. *Biochem. Res. Int.*, 2024(1), p.3713620.
4. Gebrehiwot, H., Ensermu, U., Dekebo, A., Endale, M. and Hunsen, M., 2024. Exploring the medicinal potential of *Senna siamea* roots: an integrated study of antibacterial and antioxidant activities, phytochemical analysis, ADMET profiling, and molecular docking insights. *Appl. Biol. Chem.*, 67(1), 1-22.
5. Gebrehiwot, H., Dekebo, A., Shenkute, K., Ensermu, U. and Endale, M., 2024. Chemical composition, antibacterial and antioxidant activities of essential oils from *Cyphostemma adenocaula* and *Ziziphus spinachristi*. *Bull. Chem. Soc. Ethiop.*, 38(1),167-186.
6. Kiros, T., Eswaramoorthy, R., Mohammed, S., Dekebo, A. and Melaku, Y., 2023. Compounds with antibacterial and antioxidant activities from *Cadia purpurea*. *Nat. Prod. Res.*, 37(16), pp.2672-2680.
7. Kiros, T., Mohammed, S., Dekebo, A. and Melaku, Y., 2023. In silico pharmacokinetics properties and *in vitro* bioactivities of pregnane derivatives and other compounds from stems of *Caralluma speciosa*. *Nat. Prod. Commun.*, 18(12), p.1934578X231220110.

8. Kiros, T., Mohammed, S., Melaku, Y., Tesfa, T., Dekebo, A., 2023. Isolation and identification of endophytic bacteria and associated compound from *Gloriosa superba* and their antibacterial activities. <https://doi.org/10.1016/j.heliyon.2023.e22104>.
9. Ebu SM, Adem MA, **Dekebo A.** Olani A, Isolation and identification of endophytic bacterial isolates from the leaves, roots, and stems parts of *Artemisia annua*, *Moringa oleifera*, and *Ocimum lamiifolium* Plants, 2023. *Curr. Microbiol.* 80, 405.
10. Kiros, T., Eswaramoorthy, R., Mohammed, S., **Dekebo, A.** and Melaku, Y., 2023. Non-Alkaloidal compounds from tubers of *Gloriosa superba* and their *in vitro* and *in silico* Antibacterial and Antioxidant Activities. *Curr. Bioact. Compd.*, 19(8), 2-15.
11. Degfie, T., Endale, M., Tafese, T., **Dekebo, A.** and Shenkute, K., 2022. *In vitro* antibacterial, antioxidant activities, molecular docking, and ADMET analysis of phytochemicals from roots of *Hydnora johannis*. *Appl. Biol. Chem.*, 65(1), 1-13.
12. Degfie, T., Ombito, J.O., Demissie, T.B., Eswaramoorthy, R., **Dekebo, A.** and Endale, M., 2022. Antibacterial and Antioxidant Activities, *in silico* Molecular Docking, ADMET and DFT Analysis of Compounds from Roots of *Cyphostemma cyphopetalum*. *Adv. App. l Bioinforma. Chem.*, 15, pp.79-97. DOI: [10.2147/AABC.S377336](https://doi.org/10.2147/AABC.S377336).
13. Kiros, T., Eswaramoorthy, R., Seid Mohammed, **Dekebo, A.** and Melaku, Y. 2022. Compounds with antibacterial and antioxidant activities from *Cadia purpurea*. *Nat. Prod Res.*, 2022. <https://doi.org/10.1080/14786419.2022.2130302>.
14. Kiros, T., Eswaramoorthy, R., Melaku, Y. and **Dekebo, A.**, 2022. *In Vitro* Antibacterial and Antioxidant Activities and Molecular Docking Analysis of Phytochemicals from *Cadia purpurea* Roots. *J. Trop. Med.*, 2022. <https://doi.org/10.1155/2022/4190166>.
15. Dinku, W., Park, S.B., Jeong, J.B., Jung, C., **Dekebo, A.**, 2022. Chemical composition and anti-inflammatory activity of essential oils from resin of *Commiphora* species. *Bull. Chem. Soc. Ethiop.*, 36(2), 399-415.

ABSTRACT

The development of chemo-resistance by microbes, severe adverse effects associated with synthetic old antibiotics, unavailability of newer drugs, genetic variability of microbial strains and the re-emergence/emergence of opportunistic pathogens are among the challenges attributed to the crises of the current world medicine. This has led to the resurrection of the world research on natural sources, mainly medicinal plants and associated microbes (endophytes) to get possible non-toxic, affordable and effective novel natural drugs. This research project work intended to investigate phytochemical constituents, evaluate *in vitro* antibacterial (against *Staphylococcus aureus* ATCC 25923, *Pseudomonas aeruginosa* ATCC 27853 and *Escherichia coli* ATCC 25922), antifungal (against *Candida albicans* ATCC 10231) and antioxidant (via DPPH free radical and FRAP assays) activities of *Gomphocarpus purpurascens* (leaves), *Gloriosa superba* (tubers), *Cordia purpurea* (roots and leaves) and *Caralluma speciosa* (stems). These plants are among the top cited and ethnomedicinally valued plants found in the prehistoric Harla town and its surroundings, Dire Dawa, Ethiopia. We also proposed to conduct similar investigation on *Portulaca oleracea*, *Rhynchosia erlangeri* and *Leucas stachydiformis*. However, it was difficult to collect samples sufficient for the proposed study after even though repeatedly visited their proposed habitat. Thus, investigation of these plants were excluded and replaced by some other medicinal plants. The results of those replaced plants which were published and shown in the list of publications of this research project. In this study, we also isolated possible endophytic bacteria and associated secondary metabolite from *Gloriosa superba* (stems, leaves and tubers). The molecular binding capacity of the isolated compounds **65-69** was assessed against *E. coli* DNA gyraseB (PDB ID: 6F86), *S. aureus* pyruvate kinase (PDB ID: 3T07) and human peroxiredoxin 5 (PDB ID: 1HD2) enzymes using AutoDock vina version 4.2 software. The compounds **65-68**, **70** and **79** were also docked against *P. aeruginosa* PqsA (5OE3) enzyme. The phytochemical investigation resulted in isolation of 17 compounds; six (**65-70**) from *C. purpurea* (**65** and **66** from leaves, **68-70** from roots and **67** from both), five (**71-75**) from *C. speciosa* (stems), three (**76-78**) from *G. superba* (tubers), one (**79**) from *G. purpurascens* (leaves) and another one (**80**) from ethyl acetate extract of *Escherichia coli* (GST5) endophytic bacterium. The structures of these isolated compounds were established based on FT-IR, GC-MS and NMR analysis and comparison with reported data. Compound **65**, the epoxy-lignan (**68**) and bis-(2-hydroxybutyl) phthalate (**69**) were found as new compounds. Based on the biochemical and MALDI-TOF MS analyses, thirty endophytic bacteria were isolated from leaves, stems and tubers of *G. superba* and classified into *Bacillus* spp. (66.7%), *Escherichia* spp. (26.7%), *Providencia* spp. (3.3%) and *Corynebacterium* spp. (3.3%). Calpurnine (**67**) and apigenin-7-O-neohesperidoside (**66**) displayed a better antibacterial activity against *E. coli* (18.5 ± 0.02 mm and 12.1 ± 0.1 mm, respectively) and *P. aeruginosa* (10.6 ± 0.01 mm and 14.5 ± 0.01 mm, respectively) at a maximum concentration (1000 $\mu\text{g/mL}$). All extracts and isolated compounds of *G. superba*, *C. purpurea* and *G. purpurascens* displayed better antibacterial activity against *P.*

aeruginosa than chloramphenicol (7.2 ± 0.6 to 8.2 ± 0.6 mm) almost at all concentrations. The chloroform: methanol (1:1) stems extract of *C. speciosa* was found to give a promising antifungal activity against *C. albicans* with higher diameter of inhibition zone (17.17 ± 1.04 mm) recorded at the higher concentration (100, 000 $\mu\text{g/mL}$), compared to Ketoconazole (17.67 ± 2.52 at 10 $\mu\text{g/disc}$). The antioxidant activity data indicated that apigenin-7-O-neohesperidoside (**66**) and calpurnine (**67**) provided a good DPPH radical scavenging potential with IC_{50} values of 6.21 and 8.67 $\mu\text{g/mL}$, respectively, comparable to ascorbic acid (4.82 $\mu\text{g/mL}$) at similar concentrations. All the extracts of *G. superba* tubers and *G. purpurascens* leaves also exhibited a strong DPPH scavenging activity with IC_{50} values of 1.1-3.2 $\mu\text{g/mL}$ equivalent to ascorbic acid (1.0-1.3 $\mu\text{g/mL}$). The molecular docking study revealed that compound **65**, calpurnine (**67**) and compound **68** showed stronger binding affinity (-6.5, -7.4 and -7.3 kcal/mol, respectively) to 6F86 enzyme than chloramphenicol (-6.4 kcal/mol). Whereas all the compounds **65-69** showed a better binding energy to 3T07 and 1HD2 than chloramphenicol (-4.6 kcal/mol) and ascorbic acid (-4.5 kcal/mol), respectively. The compounds **65**, **66**, **67**, **68** and **79** also recorded higher docking scores (-7.9, -10.9, -8.1, -7.8 and -10.3 kcal/mol, respectively) against 5OE3 than chloramphenicol (-7.0 kcal/mol). Apigenin-7-O-neohesperidoside (**66**) was found violated three rules of the Lipinski's rule of five (with molecular weight > 500 g/mol, hydrogen-acceptor > 10 and hydrogen-donor > 5). Compound **68**, bis-(2-methylheptyl)phthalate (**70**) and calotropin (**79**) were also found violated, each, one rule of the Lipinski's rule of five (with hydrogen-donor > 5, LogP > 4.15 and molecular weight > 500 g/mol), respectively. Apigenin-7-O-neohesperidoside (**66**) and calotropin (**79**) were found as immunotoxic and mutagenic; and immunotoxic and cytotoxic isolates, respectively. Compounds **65** and **68** were also found as immunotoxic and mutagenic isolates, respectively. This finding provided an assertion to the possibility of exploration of endophytic bacteria and associated chemical constituents from their host plants in the context of Ethiopia as it was reported herein for the first time; and this would be a basis for similar works to be done in the future. Finally, it is recommended to do further instrumental analysis including the 2D-NMR and HRMS to fully confirm the structures of the newly isolated compounds **65**, **68** and **69**. The present study also recommends further molecular characterization of the isolated endophytic bacteria using 16S rRNA gene sequencing to identify them in strain level. Further extensive biochemical investigations would also be needed on the aforementioned plant species, by giving a special emphasis to the *G. superba* and *G. purpurascens* plants, to explore additional bioactive phytochemicals and endophytic microbes.

Keywords: *Cadia purpurea*, *Caralluma speciosa*, *Gloriosa superba*, *Gomphocarpus purpurascens*, phytochemicals, antimicrobial activity, antioxidant activity, endophytic bacteria, In silico molecular modeling

1 Introduction

1.1 Background

The world's most effective medicines have been derived from natural sources. Medicinal plants and microbes are the most well-known and paramount sources of natural products which are being studied for their potential bioactive compounds. Among the plant species found on our planet, nearly 20,000 are used for medicinal purposes¹. In Africa, including Ethiopia, people often chooses traditional healing systems as a primary health care to treat various infectious and non-infectious ailments. The economical unaffordability and limited access to Western medicine, antibiotic-resistance developed by microbes, side effects associated with synthetic drugs and trust in herbal medicines are some of the reasons attributed to the importance of using medicinal plants². Due to these factors, researchers are increasingly turning their attention once again to medicinal plant-based natural products looking for new bioactive chemotherapeutic agents. The need for new medicinal plant-based drugs, mainly antimicrobial agents, is even more urgent in the context of developing countries where bacterial and fungal causing infectious diseases are so rampant³.

Medicinal plants have also been known as reservoirs of untold numbers of internal microbes, the so called endophytes. Endophytes are the plant-associated microbes (mostly filamentous fungi and bacteria) living within the living tissues of their hosts without any visible hurt. Endophytic fungi and bacteria have shown symbiotic interaction with their host plant in which both sides are mutually benefited^{4,5}. The improved resistance of some plant species to biotic and abiotic stresses is believed due the correlation with the endophytic natural products^{4,6}. The strong endophyte-host plant association enables endophytes to take advantage of producing a diversified number of secondary metabolites as compared to epiphytes. This has been ascertained by several bioactive secondary metabolites which have been discovered and reported from various endophytic microbes^{4,6,7}. In the world modern medicine, drugs have a latent toxicity effect to animal and human tissues, which is currently the major concern. It is therefore expected that endophyte-originated bioactive compounds may have less toxicity effect on the normal cell, as they do not harm the eukaryotic host system (hence symbiotic interaction). This is a great advantage to search potential alternative chemotherapeutic agents that are highly effective, having minor environmental impact and less toxicity effect on human and animal cells^{6,8}. The previously reported

effective drugs originated from endophytes have inspired the world research to look further at endophytes ones again as sources of alternative drug. As a result, endophytes have currently been gained a significant interest in the world for searching diverse and novel bioactive drugs⁶.

Medicinal plants play a continuous role in basic healthcare system, especially in many developing countries. In developing countries, including Ethiopia, about 80% of the world's population is dependent on medicinal plant-based traditional medicines for primary health care⁹. More than 95% of the traditional remedy preparations in Ethiopia are also of plant origin^{10,11}. The cultural diversity and acceptability of healers, psychological comfort, lack of adequate healthcare services, economic unaffordability and perceived efficacy against certain type of diseases as compared to modern medicines^{10,11} are some of the reasons people from developing countries to rely on traditional medicine. The traditional medicines and their traditional preparations have paramount importance in treating of various infectious diseases in Ethiopia¹². Besides to their direct antimicrobial potency, medicinal plants have also been a continual sources of new precursors and/or "lead compounds" used to synthesize modern antibiotic drugs¹³. However, the efforts made on the chemico-biology research of traditional medicinal plants in Ethiopia are limited regardless of the rich biodiversity of the country. Regarding the endophytes, also only a few of them have been investigated though thousands of millions of different endophytic species do exist on our planet. Moreover, the study on endophytic microbes as potential sources of bioactive compounds is relatively less explored area of study.

Continuous and extensive research works on the chemical constituents and biological activity of potentially valuable Ethiopian plant species and associated endophytic microbes is therefore important to increase the chance of finding novel bioactive compounds and advance modern medicine.

1.2 Statement of the problem

In recent years, the development of chemo-resistance, due to continuous use of antibiotics, by human pathogenic microbial has been commonly reported from all over the world. In addition, antibiotics are sometimes associated with adverse effects on immunocompromised host body which include hypersensitivity, headache, vomiting and allergic reactions. The ability of microbial strains to undergo genetic variability and the re-emergence/emergence

of opportunistic pathogens (due to weakened immune system) are other challenges to the current world medicine. This has created immense clinical problem in the treatment of infectious diseases. These highlight a great need for the discovery and development of non-toxic, affordable and effective novel natural drugs. One approach is conducting a continuous chemical and biological research on local medicinal plants and their endophytes to look for possible new bioactive drugs². This is because, drugs originated from medicinal plants and their associated microbes, have incomparable structural diversity, relatively small molecular weight (< 2000 Dalton), less toxicity nature and greater bioavailability¹⁴.

1.3 Justification of the study

In Ethiopia, it is reckoned that about 6500-7000 higher plant species are found as reported in the flora of the country¹⁰. Of these, 800-1000 plant species are being used in the traditional health care system making the country one of the most diverse floristic regions in the world^{10,15}. However, the research works done hitherto on these medicinal plants have been mostly of producing inventories and checklists, which remained more of a survey nature and their outputs, were merely listing of plants. Among the reckoned number of plant species mentioned above, only a handful of them have been scientifically researched for their bioactive compounds. Moreover, as to our knowledge, no research works were reported thus far on the chemical constituents and biological activities of endophytes and associated secondary metabolites in Ethiopia. It is therefore greatly needed to conduct a comprehensive scientific investigation on the chemical constituents and biological activities of most selected medicinal plants found in Dire Dawa and its surrounding areas, Eastern Ethiopia and their endophytes (based on their ethnobotanical knowledge).

In the Eastern Ethiopia, including the Eastern Hararge zone and Dire Dawa administrative city, indigenous people of the area use several medicinal plants for various traditional medicinal purposes. For instance, like many other rural communities in Ethiopia, the use of traditional medicinal plants play a vital role in human and livestock healthcare systems in the pastoral and agro-pastoral communities of Hararge zone. According to the ethnobotanical studies reported by Belayneh *et al.*¹⁶, a total of 51 plant species were reported and documented as traditional medicinal plants against human ailments in the Erer valley of Babile wereda, Eastern Hararge zone. Also, 83 traditional medicinal plant species were documented from Harla town and its surrounding area, Dire Dawa. Harla and the entire

catchment areas are the prehistoric places where the Oromo people currently inhabit. It is believed that these people were the descendants of the former Harla people of the Harla kingdom who had been ruled between 13th to 16th centuries. The Harla kingdom are expected to be the guardians of valuable indigenous knowledge on the use of traditional medicinal plants. According to Belayneh and Bussa report¹⁷, there is even an endemic plant species named after this prehistoric place called *Aloe harlana* Reynolds due to its availability only in Harla place. In addition, the share of medicinal plants and the value of the associated indigenous knowledge of the current Oromo communities of the area and in Dengego mountains and valley complex are expected to be high¹⁷. In Harla and Dengego Mountains and Valleys complex harbour about 83 traditional medicinal plant species against 81 human ailments which are distributed across 70 genera and 40 Families.¹⁷ About 57.8% of these traditional medicinal plant species belong to ten Families. Asteraceae had the largest number of plant species (10, 12%), followed by Fabaceae (8, 9.6%), Euphorbiaceae (6, 7.2%) and Cucurbitaceae (5, 6%). Aloaceae and Lamiaceae had each 4 plant species, Asclepiadaceae, Boraginaceae and Capparidaceae each has 3 species, and Apocynaceae has 2 species. About 71% of these medicinal plant species were reported by different authors in twenty three articles who conducted researches on traditional medicinal plants in the different parts of Ethiopia wherein about 44% of them were reported for similar ailments.¹⁷

Based on the ethnomedicinal study reported by Belayneh and Bussa¹⁷ *Gloriosa superba*, *Cadia purpurea*, *Caralluma speciosa* and *Gomphocarpus purpurascens* (endemic to Ethiopia) are among the preferred and most frequently cited ethnomedicinal plants found in the prehistoric Harla town and its surroundings. To the best of our knowledge, The phytochemical and biological studies conducted on the above plant species were few in number. According to Belayneh and Bussa¹⁷ the leaves, fruits, seeds, branches, pods and nectars are the most applied parts of the surveyed plant species, including the above plant species, which account for 60% of the total traditional preparations. The large biodiversity and long history of traditional medicinal practices of the study area justified the importance of the present work which aimed to investigate secondary metabolites, and evaluate their *in silico* and *in vitro* biological activities from leaves of *G. purpurascens*, tubers of *G. superba*, roots and leaves of *C. purpurea* and stems of *C. speciosa*. According to the phytochemical literature reviews of the aforementioned plant species (section 2.4.4), the stems, leaves,

tubers and seeds of *G. superba* were claimed as reservoirs of various endophytes. Accordingly, a preliminary work was made in this study to isolate possible endophytic bacteria and associated secondary metabolite from *G. superba* (stems, leaves and tubers) to shed light on the study of endophytes in the context of Ethiopia.

1.4 Objectives

1.4.1 General objective

The general objective of this work was to investigate, and study *in silico* and *in vitro* biological activities of secondary metabolites, and isolate endophytic bacteria from selected medicinal plants of surrounding Dire Dawa, Ethiopia.

1.4.2 Specific objectives

The specific objectives were to:

- Extract *Gomphocarpus purpurascens* (leaves), *Gloriosa superba* (tubers), *Cadia purpurea* (roots and leaves) and *Caralluma speciosa* (stems) using *n*-hexane, chloroform, chloroform: methanol (1:1), ethanol and methanol solvents through successive extraction technique; and *Cadia purpurea* leaves via acid-base extraction method;
- Isolate potential endophytic bacteria and associated compounds from stems, leaves and tubers of *Gloriosa superba*, and identify them using MALDI-TOF MS technique;
- Isolate secondary metabolites from crude plant extracts and ethyl acetate extracts of endophytic bacteria using chromatographic techniques (CC, PTLC); and elucidate their structures by the means of spectroscopic techniques (FT-IR and NMR);
- Evaluate *in vitro* antibacterial potency of plant extracts, ethyl acetate extracts of certain endophytic bacteria and isolated compounds against *Staphylococcus aureus* ATCC 25923, *Pseudomonas aeruginosa* ATCC 27853 and *Escherichia coli* ATCC 25922;
- Assess *in vitro* antifungal activity of chloroform: methanol (1:1) extracts of all studied plant species against *Candida albicans* ATCC 10231 using agar-disc diffusion method;
- Evaluate the antioxidant activity of plant extracts and isolated compounds via DPPH free radical and FRAP assays;
- Study the molecular binding capacity of some of the isolated compounds through docking against *E. coli* DNA gyraseB (6F86), *S. aureus* pyruvate kinase (3T07), *P.*

aeruginosa PqsA (5OE3) and human peroxiredoxin 5 (1HD2) protein models using AutoDock vina version 4.2 docking program;

- Predict the drug-likeness, ADME and toxicity characteristics of some of the isolated compounds by SwissADME, PreADMET and OSIRIS property explorer software.

1.5 Significance of the study

- The ethnobotanical uses of Ethiopian medicinal plants need a scientific evaluation to provide basic understanding of the plants' efficacy and lend further support to the widespread use of the traditional medicine in health care systems. Hence the importance of the present study may lay in providing a scientific rationale to support the purported folkloric usages of the selected plants of the Harla town and its surroundings, Dire Dawa, Ethiopia and their endophytic bacteria by investigating their chemical constituents and evaluating their *in vitro* antimicrobial and antioxidant activity. This dissertation study in general may have the following significances: Evaluating the *in vitro* antimicrobial and antioxidant effect of selected medical plant species used by the local community;
- Providing bioactive compounds which may be used for designing of new analogues having either better therapeutic potency or reduced cytotoxicity effect;
- Obtaining potential endophytic bacterial isolates which may have bio-nano-technological applications;
- Providing a scientific evidence to support the claimed ethnomedicinal uses of the selected plant species;
- Laying a scientific base for both the modern and traditional medicines by providing a bridge between the modern and traditional claims of about the medicinal uses of the selected plant species.

2 Literature Review

2.1 Traditional medicinal plants and the modern medicine

Medicinal plant, also called botanical medicine or phytomedicine, refers to the use of different parts (seeds, berries, roots, leaves, bark, flowers, etc.) of a plant for curative purposes. The use of medicinal plants as traditional therapeutic agents may be traced back to at least 60,000 years, according to fossil records¹⁸. Since then, people all over the world have traditionally been utilizing medicinal plants for the treatment, control and management of various diseases. It has also been recorded that Hippocrates, who was a Greek philosopher,

used approximately 400 different plant species for medicinal purposes. These plant species were later used as a standard medical reference in the ancient Western medicine¹⁹. The traditional Chinese medicine (TCM), traditional Japanese medicine (TJM), traditional Korean medicine (TKM), Russian herbal medicine, Ayurvedic of India and traditional medicine in Africa are also some of the recorded traditional medicines¹⁸. Currently, the above mentioned types of traditional medicines are incorporated into the modern pharmacopeia of corresponding country. The traditional Chinese medicine (TCM), for instance, is practiced side by side with the modern medicine. In India also, medicinal plants are still widely practiced via the Ayurvedic medicine²⁰.

Earlier to the 19th century, medicinal plants were administered mostly in the form of crude drugs such as herbal teas, tinctures, decoctions, syrups, poultices and herbal formulations²¹. However, during the late 19th and early 20th century, scientists began extracting, purifying, isolating and identifying active ingredients from various parts of medicinal plants¹⁹. These efforts led and paved a way to the beginning of the era of modern medicine²². For example morphine (**1**), the first pharmacologically-active commercial natural product, was isolated from *Papaver somniferum* (Opium poppy) as a powerful pain reliever and narcotic²²(Figure 1). Quinine (**2**), isolated from *Cinchona* plant species, is another effective anti-malarial drug²² reported in this era. Taxol (**3**) and vincristine (**4**) isolated from *Taxus brevifolius* and *Catharanthus roseus*, respectively, are other known anti-cancer drugs. Serpentine (**5**), known as anti-hypertension drug, was also reported in this era from the root of the Indian plant, *Rauwolfia serpentina*^{19,22}. Traditional medicinal plants have also been known as origins of “building block” chemicals used in the research and development of synthetic drugs²². Aspirin is a good example, developed in 1953 from salicylic acid (identified as the active ingredient in *Salix* spp. and *Populus* spp.) via structural modification²³. Unfortunately, the interest on medicinal plants and their products as sources of drugs had shown a decline for several years. This was because of the discovery of already known natural drugs (due to lack of advanced techniques for de-replication purpose), and scarcity of the medicinal plant sources and genetic intellectual property issues. However, the emergence and re-emergence of pathogens with multi-drug resistance have forced researchers and other stakeholders to renew their interest on biological sources, predominantly, medicinal plants¹⁹. Nowadays, the direct use of medicinal plants for traditional medicine still continuous in many countries,

especially, in the developing world. For instance, 60% of the world's population depends on traditional medicine and 80% of the population in developing countries depends almost entirely on traditional medical practices to fulfill their primary health care needs²⁴. Also, medicinal plants continue to contribute significantly to modern prescription drugs by providing “lead compounds” and scaffolds²². Consequently, there is a continuous need for searching and discovering of diversified bioactive agents from the botanical sources and their associated microbes²⁴

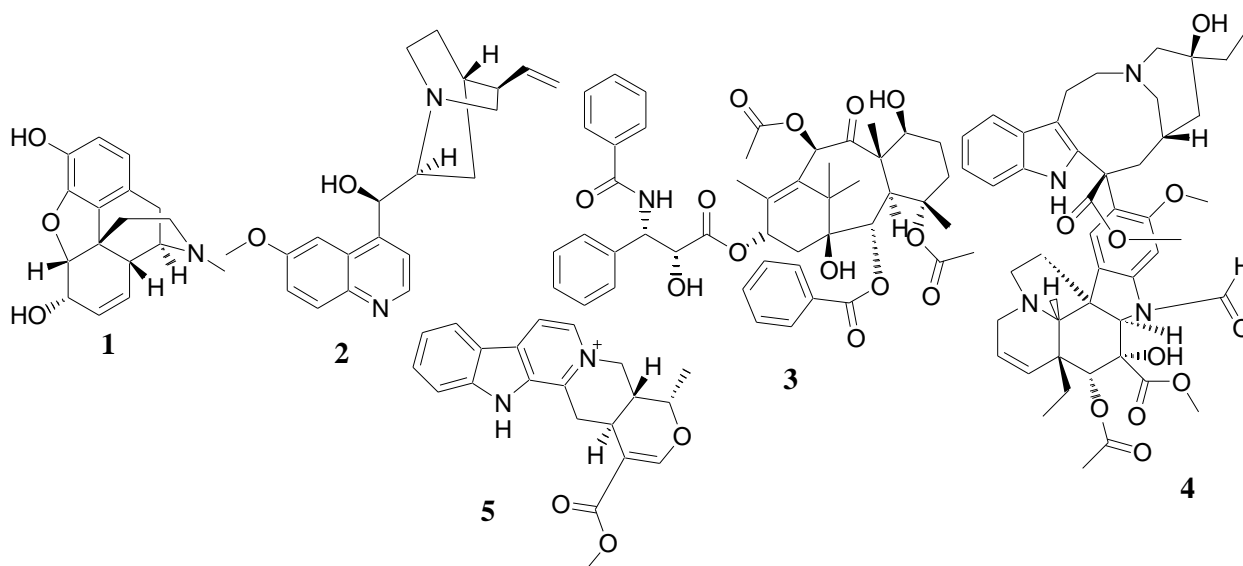


Figure 1. Structures of some compounds 1-5 reported in the early 20th century

2.2 Antimicrobial potency of medicinal plants

Research works supporting the beneficial roles of the chemical constituents of medicinal plants and their endophytic microbes against various diseases are based on the chemical's mechanism of action using the *in vitro*, *ex vivo* and *in vivo* bioassaying techniques. In other words, the antimicrobial activity of medicinal plants and endophytes is attributed to their chemical constituents. Infectious diseases caused by microbial are the world's leading cause of premature deaths, killing large number of people every day²⁵. Morbidity and mortality due to diarrhea continue to be a major problem in many developing countries^{25,26}, for example. In recent years, human pathogenic microbial resistance to antibiotic drugs has been commonly reported from all over the world. With the continuous use and misuse of antibiotics, microbes have become resistant. In addition to this problem, antibiotics are sometimes associated with adverse effects on host body including hypersensitivity,

vomiting, headache and allergic reactions. This has created immense clinical problem in the treatment of infectious diseases. There is thus a great need for alternative drugs effective against current antibiotic resisting pathogens and opportunistic pathogens. One approach is to screen local medicinal plants for possible pharmacological properties and isolation of bioactive agents having a high biological potential²⁵.

Medicinal plants are rich sources of potential and powerful drugs which are used as antimicrobial agents. The different parts of medicinal plants are the one responsible for the origin of such active chemical constituents²⁷. The use of plant extracts and phytochemicals, both with known antimicrobial properties, can be of great significance in therapeutic treatments, which still practiced all over the globe. In the last few years, a number of scientific studies have been conducted in different countries to prove such efficiency²⁸. These studies have revealed that medicinal plants have a powerful antimicrobial potency and exhibit synergistic activity against antibiotic resistant microbes, in which people all over the world uses them as an alternative and complementary therapy. This is because, medicinal plants contain mixture of compounds which have an advantage such as fewer side effects, better patient tolerance, less expensive, acceptance due to long history of use and being renewable in nature, over other synthesized antibiotic drugs²⁹.

2.3 Endophytes and their method of isolation

Medicinal plants produce unique and divergent secondary metabolites and harbor many of the hitherto unknown microbial species. Currently, endophytes have been confirmed for their ability to mimic the biosynthesis chemistry of their host plant to produce same or alternative bioactive compounds. Searching and producing natural products from endophytic microbes via fermentation is a cost-effective, continuous, less toxic, very effective and environmental friendly. This may help to reduce the need to harvest slow-growing and rare plant species, and conserve the world's ever diminishing biodiversity. Because of these rationales, scientists and researchers have turned their attention back to the microbial world. Besides to their pharmaceutical application, endophytes have also played a great role in biotechnology (such as in agriculture, biotransformation, biodegradation/bioremediation process), in nanotechnology and as a source of biofuels and extracellular enzymes. It is, therefore, noteworthy to explore endophytes from their host medicinal plants claimed as a source of bioactive compounds³⁰. Among the nearly 300,000

plant species that exist on the earth, each individual plant is expected to host one or more endophytes⁶. Unfortunately, only a few of these plants (mainly grasses) have been studied in detail relative to their endophytic biodiversity. Accordingly, the opportunity to find new and beneficial endophytic microbes among the diversity of plants in different ecosystems is considerable⁶. Many researchers have attempted to isolate and document endophytic microbes, especially filamentous fungi and examine their antimicrobial activities from various medicinally important plants. Intern, numerous bioactive natural products have been investigated and reported from those endophytic isolates. For instance, the antibacterial compounds, benzomalvin A (**6**) and penitrems A (**7**) were reported from the *Taxus brevifolia* originated *Penicillium spp.* endophytic fungus³¹. Besides, 5 α ,9 α -epidioxy-sterol (**8**) and compound **9** were isolated from *Aspergillus niger*, a fungal endophyte isolated from *Avicennia marina* plant species³². The antibacterial and antifungal compound, asperpyrone A (**10**), was also obtained from *Aspergillus spp.* endophytic fungus, isolated from the *Melia azedarach* plant³³. Moreover, some anticancer compounds such as dothiorelone F (**11**)³⁴, sclerotiorin (**12**)³⁵, secoemestrin D (**13**)³⁶ and daldinone C (**14**)³⁷ were reported from *Dothiorella spp.*, *Cephalotheca faveolata*, *Emericella spp.* and *Hypoxyton truncatum*, respectively, fungal endophytes of the plant species, *Aegiceras corniculatum*, *Eugenia jambolana*, *Astragalus lentiginosus* and *Artemisia annua*, respectively. The structures of compounds **6-14** are presented in Figure 2. However, the endophytes which have been studied in detail are still few in number with respect to their huge biodiversity. Thus, conducting an intensive research on the chemistry of the endophytes may lead to discovery of novel bioactive compounds.

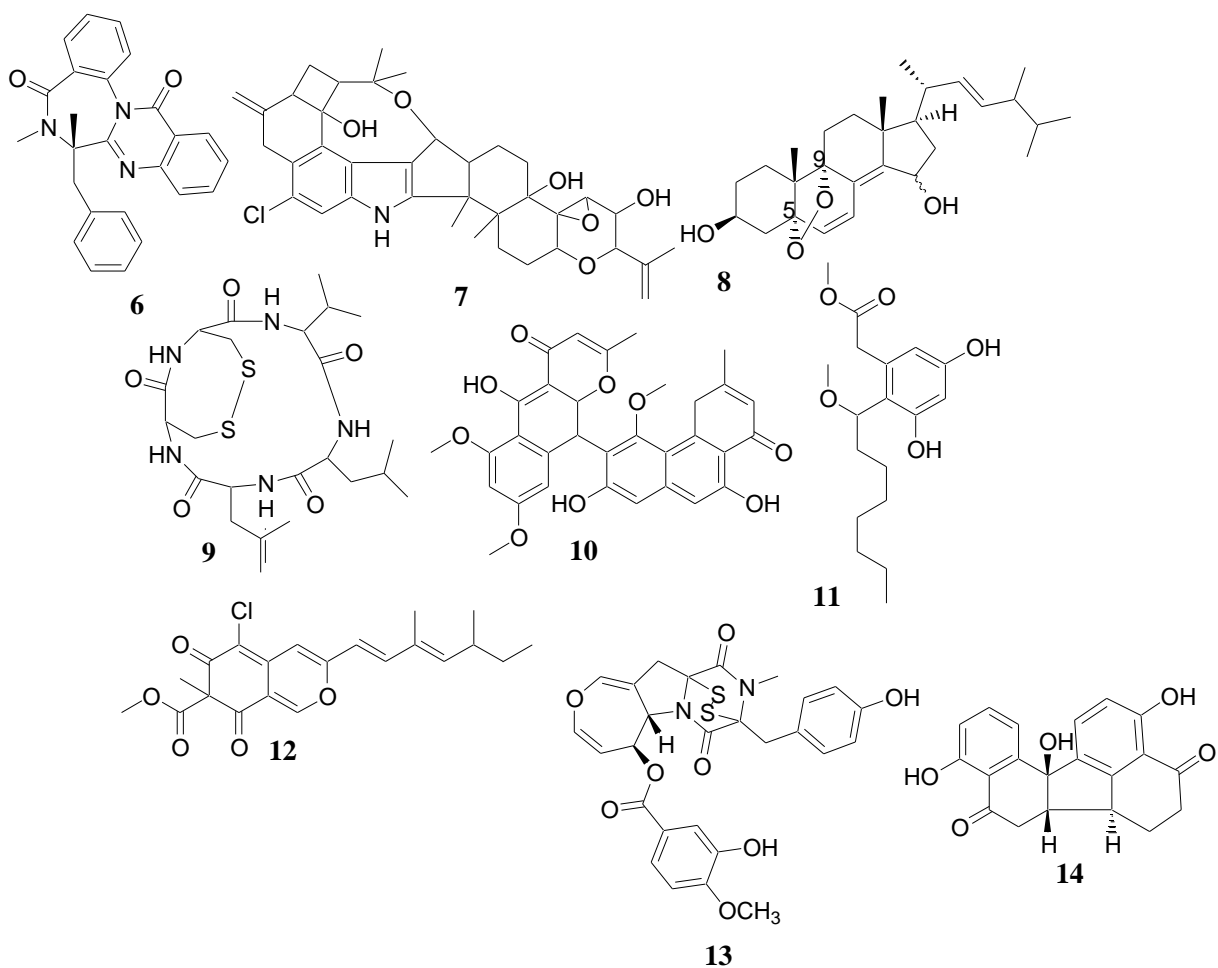


Figure 2. Structures of some antimicrobial and anticancer compounds **6-14** originated from fungal endophytes of medicinal plants

In the study of endophytes, identifying a plant material suspected as reservoir of potential endophytes and selecting the appropriate isolation method are the two critical steps. In other words, focusing on the methods and rationale used to provide the opportunities for endophyte exploitation with the probability of producing novel active metabolites is very vital. According to several reviewed articles, plant species: 1) growing in areas of great biodiversity (like tropical rainforest and mangrove forests) and under the influence of biotic/abiotic stress; 2) showing no symptoms of disease while surrounded by plants infected by phyto-pathogens; 3) occupying unique environmental settings like ancient land masses; and 4) having ethno-botanical uses, extreme age or interesting endemism nature are

expected as reservoirs of many potential endophytes thereby helpful to the discovery of bioactive drugs^{38,39}. It is therefore our hope that the medicinal plant species selected for the present study may fulfill some of the above plant selection criteria.

In exploration of endophytes, the isolation procedure is another important step. The procedure is expected to be sensitive enough to target the endophytic microbes by eliminating the epiphytes from the plant surface. That is, the isolation procedure must be adapted to the respective tissues and microbes, since some isolation procedures are suitable only for certain plant tissues, whereas others favor local or systemic colonizers. The isolation procedures of endophytes generally involve washing and surface sterilization of the plant parts using different protocols. The surface sterilized plant parts are then either powdered or cut into small segment followed by placing directly onto appropriate culture plate agar aseptically. Finally, the plate is incubated at 37 °C for 48 hr to observe the emergence of possible endophytic microbial colonies^{40,7}.

2.4 Botanical, ethnobotanical, biological and phytochemical aspects of studied plants

Cadia purpurea, *Caralluma speciosa*, *Gloriosa superba* and *Gomphocarpus purpurascens* are among the most cited plant species in Harla town and its surrounding areas as per the ethnomedicinal document reported by Belayneh and Bussa¹⁷. Regarding the ethnobotanical and phyto-biological features of these plant species, some research articles and reviews have been reported so far (see sub sections 2.4.1 to 2.4.4). Reviewed in the present research study is those of the above plant species with special emphases on their botanical, ethnobotanical, biological and phytochemical aspects based on the available scientific literature.

2.4.1 Botanical description

G. superba L. (synonymically known as *G. simplex*, *G. abyssinica* and *G. speciosa*) belongs to the genus *Gloriosa* and family Colchicaceae. It is an erect or climbing annual herb and tuberous poisoning tropical medicinal plant growing up to 3 m height^{41,42}. It is commonly known as glory lily in English. It exhibits a hollow stem about 6 m, emerging from its tuberous underground stem every year in rainy season. Leaves are etiolated, alternate, sessile, lanceolate and spear shaped with curved end, which helps them to climb and creep. The flowers of *G. superba* have characteristics of brilliant wavy edged yellow and red colors that have been observed every year from November to March⁴³. Fruits of this poisoning plant are oblong, ellipsoid capsule and its seeds are numerous and rounded⁴¹. *G. superba*

grows widespread in *Acacia-Commiphora*, *Combretum-Termianlia* woodland, in open places in forest edges on well-drained soils, in thickets on roadsides and along ditches, about 400-2500 m altitudes⁴². In Africa, it is widely distributed in Senegal, Ethiopia, Somalia and South Africa. *G. simplex*, *G. grandiflora*, *G. lutea*, *G. planti*, *G. longifolia*, *G. rotheschildiana* and *G. sudanica* are also some of the species categorized under the genus, *Gloriosa*. *G. superba* is much known as an industrial medicinal crop for its high content of colchicine, especially in South India, which is widely collected from the wild habitat and marketed⁴¹.

C. purpurea (Fabaceae) is unarmed shrub with 0.8-5 m height and its leaves up to 17 cm long. Flowers are on axillary short shoots, hanging and its petals about 30 mm long, which are cream, turning wine-red and falling quickly. *C. purpurea* inhabits rift valley escarpment, bush land, commonly in altitudes about 1300-2700 m. In Ethiopia, it is found in Tigray, Welo, Shewa, Hararge and Bale regions. *C. purpurea* is also found in Eritrea, Yemen, Oman, North Somalia and North Kenya⁴⁴.

C. speciosa (Asclepiadaceae) is a succulent perennial herb, exhibiting a stem procumbent up to 30 cm long. Its flowers have a particular strong smelling and imitating mature carrion in a very close situation. *C. speciosa* grows in *Acacia* woodland and bush land, and is found in most Ethiopian regions, Sudan, Somalia, Uganda, Kenya and Tanzania⁴⁵.

G. purpurascens A.Richs. (synonyms: *Asclepias purpurascens* and *Gomphocarpus fruticosus*) belongs to the family, Apocynaceae, sub-family, Asclepiadaceae. It has a stem with 2 cm height and grows in open rocky ground and disturbed areas. *G. purpurascens* occurs in most Ethiopian regions and is endemic to highland regions of Ethiopia and Eritrea⁴⁶.

2.4.2 Ethnobotanical uses

G. superba has been known for its wide ethnomedicinal application in which all of its parts have been used for various therapeutic purposes (Table 1). Various parts of the plant are used to treat spleen complaints, sores, tumors, syphilis, CNS depressant and sexual dysfunction^{41,47}. *G. superba* is also used as an embolic in labor, purgative, anthelmintic and cure against leprosy, colic, chronic ulcers, hemorrhoids, skin parasites and head lice^{48,49}. For instance, the tuberous root of the plant is used to reduce a joint pain affected with arthritis⁵⁰. The sap from the leaves tip is used as smoothening agent for pimples and skin

eruptions; and leaves are used to treat ulcers, piles and expel placenta. The seed of *G. superba* is used to cure cancer, for relieving rheumatic pain and as a muscle relaxant⁴¹. The different parts of *G. superba* have a wide variety of uses in the traditional medicine of different countries in tropical Africa. In Congo, for example, crushed leaves are applied to the chest to treat asthma. In Tanzania also, there is an experience of using the plant to heal a wound by burning and applying its ash. The plant juice is also drunk in the same country for antimalarial activity purpose. Zambian people uses the tuber as part of a preparation for impotence and as abortifacient⁵¹. Because of the presence of colchicine, powdered tuber is commonly used as a suicidal agent and to commit homicide in Kenya and Tanzania⁵¹. More surprisingly, in India, a small amount of the tuber paste of the plant is applied externally on head to accelerate childbirth and the rhizome paste is also applied to the lower part of stomach for easing childbirth⁴¹. Moreover, the rhizome and its starch has been reported as abortifacient⁵² in early stage of pregnancy and useful in gonorrhoea in India. *G. superba* extracts are also found to contain monoethyl ester of 2, 6-dihydroxybenzoic acids having neutralizing potential against snake venom and are used as remedy for snakebite in India⁵³. In Dire Dawa and its surrounding areas of Eastern of Ethiopia, the leaves of *G. superba* are used for the treatment of toothache, epilepsy, skin cyst, tumor or “*Keledo*”, gallstone and gangrene¹⁷.

In Ethiopia, the root of *C. purpurea* is widely used for the treatment of severe wounds⁵⁴ and the leaves are applied to heal fire burn by mixing the powder with coffee⁵⁵ (Table 1). The nectar of *C. purpurea* is also applied for reducing gastritis, heart burn and pyrosis¹⁷. The leaves are also used for the treatment of wound infection and nail inflammation in Eritrea⁵⁶. The genus *Caralluma* is composed of about 260 species used as food in many parts of the world. In India, for example, fruits and young shoots of *C. edulis* are used as a vegetable⁵⁷. The plant species under this genus are mainly consumed for the treatment of obesity (Table 1). For instance, *C. adscendens fimbriata* is used as an appetite suppressant by ethnic populations of middle India⁵⁸. The appetite suppressant and weight loss properties of *Caralluma* species, as claimed in Indian traditional records, are believed due to the presence of pregnane glycosides (C₂₁ steroidal compounds), which are the major bioactive constituents of *Caralluma* species. This is because pregnane glycosides isolated and reported from an African plant, *Hoodia* species, are confirmed for their appetite suppressant

and antiobesity property⁵⁹. Moreover, *Caralluma* species is used for the treatment of human ailments like malaria, inflammation, hyperglycemia, ulcers and cancer. The species *C. attenuate*, for example, is used for curing diabetes and its juice together with black pepper is recommended for the treatment of migraine⁶⁰. The juice of *C. stalagmifera* mixed with black pepper is also recommended for treating migraine, and a decoction of its fresh stems for treating diabetes. *C. tuberculata* and *C. fimbriata* are also applied for treating rheumatism, diabetes, leprosy, paralysis, joint pains, fever, inflammation and pyretic⁵⁷. In Dire Dawa and its surroundings of Eastern Ethiopia, the stem and sap of *C. spiciosa* are used for treatment of skin cyst and tumor or “*Keledo*”, gangrene, poison, swollen body part or “*Gofla*”, wound and itching skin¹⁷. The leaves of *G. purpurascens* are used for treatment of itching skin and evil eye in the same place¹⁷.

G. purpurascens is an annually grown endemic plant to Ethiopia and it is a shrubby perennial herb. This plant has many reported uses in traditional medicine; the dried leaf part is applied topically for the treatment of eczema, evil eye, and itching skin; fresh leaf or stem latex is applied topically for warts and used as part of a formula for Rhesus Factor problems in pregnancy (shotelay); a pound of fresh or dry root bark is used for febrile illness, abdominal pain, hemorrhoids, and wounds (livestock).¹⁷ The ethnobotanical uses of the selected plant species discussed above are summarized below (Table 1).

Table 1. Ethnobotanical uses of studied plant species

Scientific name	Family	Vernacular name (Oromifa)	Habit	Traditional medicinal uses (treatments)	PU	Reference
<i>C. purpurea</i>	Fabaceae	Cheeka	Sh	For severe wounds	R	17, 54-56
				For gastritis, heart burn and pyrosis	N	
				For wound infection and nail inflammation	L	
<i>C. speciosa</i>	Asclepiadaceae	Yaa'ii Beeraa	HP	For skin cyst, tumor or “ <i>Keledo</i> ”, gangrene and swollen body or “ <i>Gofla</i> ”	St	17
				For poison, wound and itching skin	Sa	
<i>G. superba</i>	Colchicaceae	Harmel Kubra	Sh	For toothache, epilepsy, skin cyst, tumor or “ <i>Keledo</i> ”, gallstone, gangrene, ulcers, piles and expel placenta	L	17,41, 47-51
				For intestinal worms, bruises, infertility, inflammation, ulcers, bleeding piles, skin diseases, leprosy, snakebites and impotence	R	
				For cancer, rheumatic and pain	S	
<i>G. purpurascens</i>	Asclepiadaceae	Ari-Yuyo	HA	For itching skin and evil eye	L	17

Notes: PU-part used, Sh-shrub, HA-herb annual, HP-herb perennial, Sa-sap, R-roots, L- leaves, S-Seeds, St-stems, N-nectar

2.4.3 Biological activity

The well-known alkaloids of *G. superba*, colchicine (**15**) and gloriosine (**29**), are used in treatment of gout and rheumatism⁴¹. According to Hemaiswarya *et al.*⁶¹, the petroleum, methanolic and aqueous tuber extracts of *G. superba* showed a promising activity against the Gram-negative bacteria, *Escherichia coli* (8 ± 1 to 66.7 ± 1.5 mm), *Proteus vulgaris* (15 ± 2 to 30.0 ± 2.0 mm) and *Salmonella typhi* (7.0 ± 1.0 to 10.0 ± 1.0 mm) at the MIC values of 50-100 $\mu\text{g/mL}$; whereas they did not show any activity against the Gram-positive, *Bacillus subtilis* and *Staphylococcus aureus* bacteria, compared to chloramphenicol (15-27 mm at 30 $\mu\text{g/disc}$). The mentioned extracts also exhibited a strong inhibitory activity (50%-100% inhibition) against the growth of *Aspergillus niger* and *Mucor*, in comparison to the nystatin drug (with 100% inhibition) at 1000 $\mu\text{g/mL}$ ⁶¹. The *n*-butanol fraction of methanol extract of *G. superba* rhizomes also showed remarkable antifungal activity against *Candida albicans* and *Candida glaberata* (90% inhibition) and *Trichophyton longifusus* (78% inhibition), followed by the chloroform fraction against *Microsporium canis* (80% inhibition), in reference to miconazole and amphotericin (up to 97% inhibition) at 400 $\mu\text{g/mL}$. The *n*-butanol fraction also showed highest antibacterial activity (23 mm, 88% inhibition) against the *S. aureus* followed by the methanol extract (16 mm, 59% inhibition) with respect to imipinem standard (27 mm) at 100 $\mu\text{g/mL}$ ^{41,62}.

Moreover, methanol extracts of different parts (peel, rhizomes, leaves, flowers and seeds) of *G. superba* were also evaluated for their *in vitro* antifungal activities. Of these, the seed (82.45%) and rhizome (82.06%) extracts were found as strong inhibitors of the fungus, *Fusarium oxysporum*⁶³ at 100% concentration. Besides, the chloroform, methanol and petroleum ether tuber extracts of *G. superba* also showed very low ED₅₀ value (0.02, 0.49 and 2.07 $\mu\text{g/mL}$, respectively) against p388 cell line, compared to 5-fluoro-uracil(5-FU) standard drug (0.0189 $\mu\text{g/mL}$)⁶⁴. The rhizomes alcoholic extract and its subsequent fractions of chloroform, ethyl acetate, *n*-butanol and aqueous extracts of *G. superba* also presented promising enzyme inhibitory activity against lipoxygenase (66.7% to 90.10% inhibition) at 240 $\mu\text{g}/200 \mu\text{L}$ ⁶⁵. The ethanolic, benzene and aqueous tuber extracts of *G. superba* displayed a good antioxidant activity against DPPH radical (IC₅₀ values of 42.16, 59.71 and 149.84 $\mu\text{g/mL}$, respectively)^{66,67}. The aqueous, chloroform and alcoholic extracts of *G. superba* tubers, stems and leaves showed a pronounced aphrodisiac activity in male albino rats at

dose of 500 mg/kg body weight, compared with the standard Sildenafil citrate (5 mg/kg body weight)⁶⁸. The alcoholic hot continuous tuber extract of *G. superba* also displayed good antibacterial antifungal activities against *E. coli* (13.1 mm), *P. aeruginosa* (21.33 mm) and *Klebsiella oxytoca* (11.5 mm), and *C. albicans* (13 mm) at 20% concentration, compared to tetracycline (30 µg/disc, 11.97-13 mm) and amphoterecin-B (10 µg/disc, 11.6 mm). This extract was also found with effective anthelmintic activity on earthworms up to 100 mg/mL dose, compared to the standard piperazine citrate (10 mg/mL)⁶⁹.

All parts of *G. superba* are extremely poisonous, especially the tuber part, having an inhibitory action on cellular division resulting in diarrhea, depressant action on bone marrow, alopecia, vomiting, purging, stomachache and burning sensation. The rhizome and seed parts of the plant are also very toxic⁴¹. According to Wink and Wyk report⁷⁰, even more than 40 mg of the principal phyto-constituent of *G. superba*, colchicine, causes death within 3 days.

Caralluma species have been extensively used for the treatment of various ailments, according to several reported biological studies. The medicinal properties of *Caralluma* species have been attributed to their pregnane glycoside constituents. For instance, pregnane glycosides isolated from *C. penicillata*, *C. tuberculata* and *C. russelliana* showed antitrypanosomal and antiplasmodial potency^{71,72}. The ethanolic extract of *C. tuberculata* was also found as gastric mucosa protective. In addition, *C. arabica* was reported for its antiinflammatory, antihyperglycemic, antinociceptive, gastric mucosa protective and antiulcer properties⁷³. *C. umbellata* was also evaluated for antiinflammatory and antinociceptive activity. *C. fimbriata* was another species studied for its antifungal and anthelmintic activities^{57,74}. According to the biological study reported by Jitwasinkul and Charoensuksai⁷⁵, the hydroethanolic extract of fresh *C. spiciosa* showed cytotoxic, antiproliferative and proapoptotic activities against two cancer cell lines, namely, HN22 (Head-and-neck cancer) and HT29 (colon cancer). Therefore, *C. spiciosa* can be considered as a promising candidate for further studies which may lead to the discovery of a new “lead” for anticancer agents.

To the best of our knowledge, no research works were reported so far on the biological uses of *C. purpurea* and *G. purpurascens* plant species except one study⁷⁶ which reported the antimicrobial activity of leaves of *G. purpurascens*. According to this study, three

concentrations (150, 300 and 600 mg/mL) of the ethanol and methanol leaves extracts of *G. purpurascens* were tested against some bacterial pathogens and *C. albicans* fungal strain. These extracts scored respective inhibition zone values of 6.09 ± 0.18 to 6.90 ± 0.40 mm and 9.19 ± 0.07 to 13.20 ± 0.1 mm against *E. coli*; 9.51 ± 0.1 to 12.7 ± 0.15 mm and 7.1 ± 0.01 to 8.2 ± 0.01 mm against *S. aureus*; 9.01 ± 0.01 to 9.77 ± 0.15 mm and 9.8 ± 0.01 to 13.8 ± 0.10 mm against *P. aeruginosa*; and 6.34 ± 0.04 to 6.64 ± 0.04 mm and 8.01 ± 0.01 to 13.79 ± 0.01 mm against *C. albicans*. The reported result was compared with the tetracycline (13.09 - 25.65 mm at 0.025 mg/mL) and ketoconazole (7.87 ± 2.18 mm at 25 mg/mL) standard drugs. The biological activity reviewed above of the studied ethnomedicinal plants is summarized in the following table (Table 2).

Table 2. Biological activities of studied ethnomedicinal plant species

Name of plant species	Biological activity	Plant part/extract	Reference
<i>G. superba</i>	Antibacterial against both Gram-positive and Gram-negative	Aqueous, methanol and petroleum root tuber extracts	41, 61-67
	Antifungal against <i>Fusarium oxysporum</i>	Methanol extracts of rhizomes, leaves, flower and seeds	63
	Antiinflammatory and analgesic effect	Hydro-alcoholic extract of aerial part	41
	Cytotoxic against p388 cell line	Chloroform, methanol and petroleum ether tuber extracts	41
	Anticoagulant	Methanol and aqueous leaves extracts	41
	Antioxidant	Ethanol tuber extract	66
	Antiarthritic	Chloroform tuber extract	67
<i>C. speciosa</i>	Cytotoxic, antiproliferative and proapoptotic activities against Head-and-neck (HN22) and colon (HT29) cancer cell lines, appetite suppressant	Hydro-ethanolic fresh stem extract	75
<i>C. purpurea</i>	*	*	*
<i>G. purpurascens</i>	Antibacterial activity	Ethanol and methanol leaves extracts	76

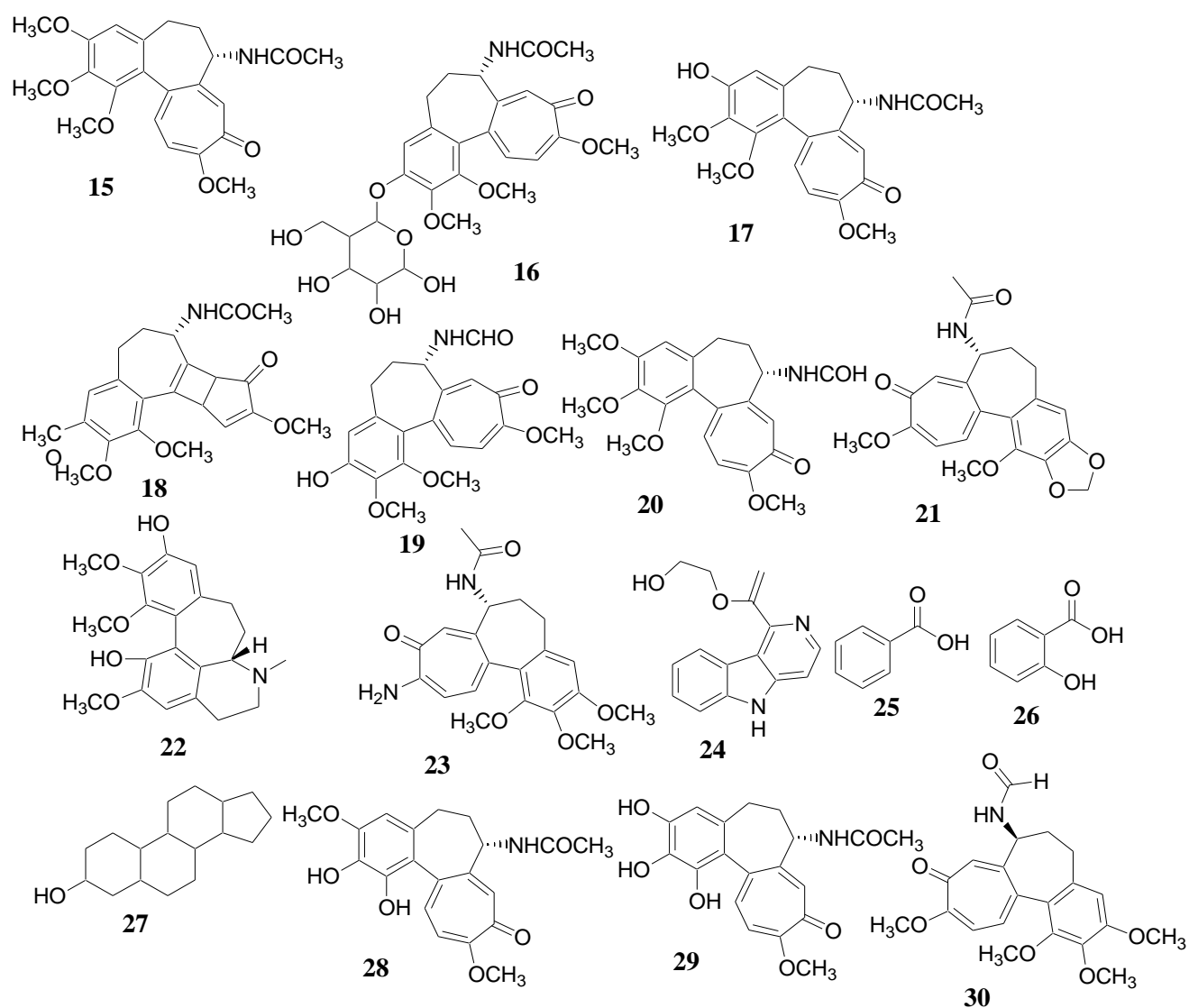
Note: * indicates no research works reported so far till the preparation of this final report as to our knowledge

2.4.4 Chemical constituents

The ethnomedicinal importance of the poisoning plant, *G. superba*, is due to the presence of various phyto-constituents, especially alkaloids in almost all parts of the plant, including colchicine (**15**), colchicoside (**16**) and 3-demethyl colchicine (**17**). It is highly believed that the medicinal importance of *G. superba* is mainly attributed to the principal bioactive compounds, colchicine (**15**) and colchicoside (**16**), which are greatly demanded in the global market. Other tropolone alkaloids such as lumicolchicine (**18**), 3-demethyl-N-formyl-N-deacetylcolchicine (**19**), 3-demethylcolchicine (**17**) and N-formyl-N-deacetylcolchicine (**20**) were reported from the whole plant, mainly from the roots and rhizomes parts^{41,49}. Besides, nineteen tropolane and three non-tropolone alkaloids were isolated from the corms and seeds of Indian *G. superba*. Of these, cornigerine (**21**), (S)-(+)-floramultine (**22**), colchicamide (**23**) and isoperlolryrine (**24**) were identified⁷⁷. The tubers were also reported for their phyto-constituents such colchicine (**15**), benzoic acid (**25**), salicylic acid (**26**), sterols (**27**), 1, 2-didemethyl colchicines (**28**), 2, 3-didemethylcolchicine (**29**), colchicoside (**16**) and gloriosine (**30**)⁴¹. Colchicine (**15**), colchicoside (**16**), 2-demethylcolchicine (**31**), 3-O-demethylcolchicine (**17**) and N-formyl-N-deacetylcolchicine (**20**) were also isolated from the ethanol seed extract of *G. superba* as active alkaloids⁷⁸. Moreover, non-alkaloidal compounds such as β -sitosterol-D-glucoside (**32**), luteolin (**33**), orcinol (**34**) and 2-hydroxy-6-methoxybenzoic acid (**35**) were reported from the seeds and rhizomes of *G. superba*⁷⁹. The flower of *G. superba* was also confirmed for its chemical constituents such as luteolin (**33**), 3-demethylcolchicine (**17**), 2-demethylcolchicine (**31**) and 3-demethylcolchicine-glucosides (**36**)⁸⁰. Colchicine (**15**), gloriosine (**30**), 2-hydroxy 6-methoxy benzoic acid (**35**) and β -sistosterol-D-glucoside (**32**) were reported as active principles of the leaves part⁴¹.

In addition to the phytochemicals isolated directly from *G. superba*, some endophytic fungi were also isolated and identified from various part of the plant. For instance, a total of 233 fungal endophyte isolates were identified and reported from a total of 450 segments of roots, stems and leaves parts. Of these, a large and diversified number of endophytic fungi were recovered from the root part than the other parts of the plant. *Bipolaris cynodontis*, *B. specifera*, *Fusarium oxysporum* and *F. solani* were found as dominant colonizers of the root part together with *Talaromyces pinophilus*, *Oidiodendron spp.* and *Colletotrichum gleosporioides*. These isolated endophytic fungi were categorized under seven morphotypes,

namely, *Hyphomycetes* (65.21%), *Dothideomycetes* (13.04%), *Coelomycetes* (8.69%), *Sordariomycetes* (4.34%), *Eurotiomycetes* (4.34%), *Leotiomycetes* (4.34%) and *Zygomycetes* (4.34%)⁸¹. *Phomopsis* species was another endophytic fungus reported from the tuber part of *G. superba* and used to produce the known anticancer agent, colchicine⁸². Two endophytic fungi, namely, *Alternaria solani* and *Penicillium funiculosum* were also identified from *G. superba* and used in the biosynthesis of antimicrobial Silver nanoparticles⁸³. Some compounds such as compound (37) and compound (38) were also isolated from the endophytic fungus, *Aspergillus* species, isolated from the seed part of *G. superba*⁸⁴. The chemical structures of the compounds 15-38 are presented in Figure 3.



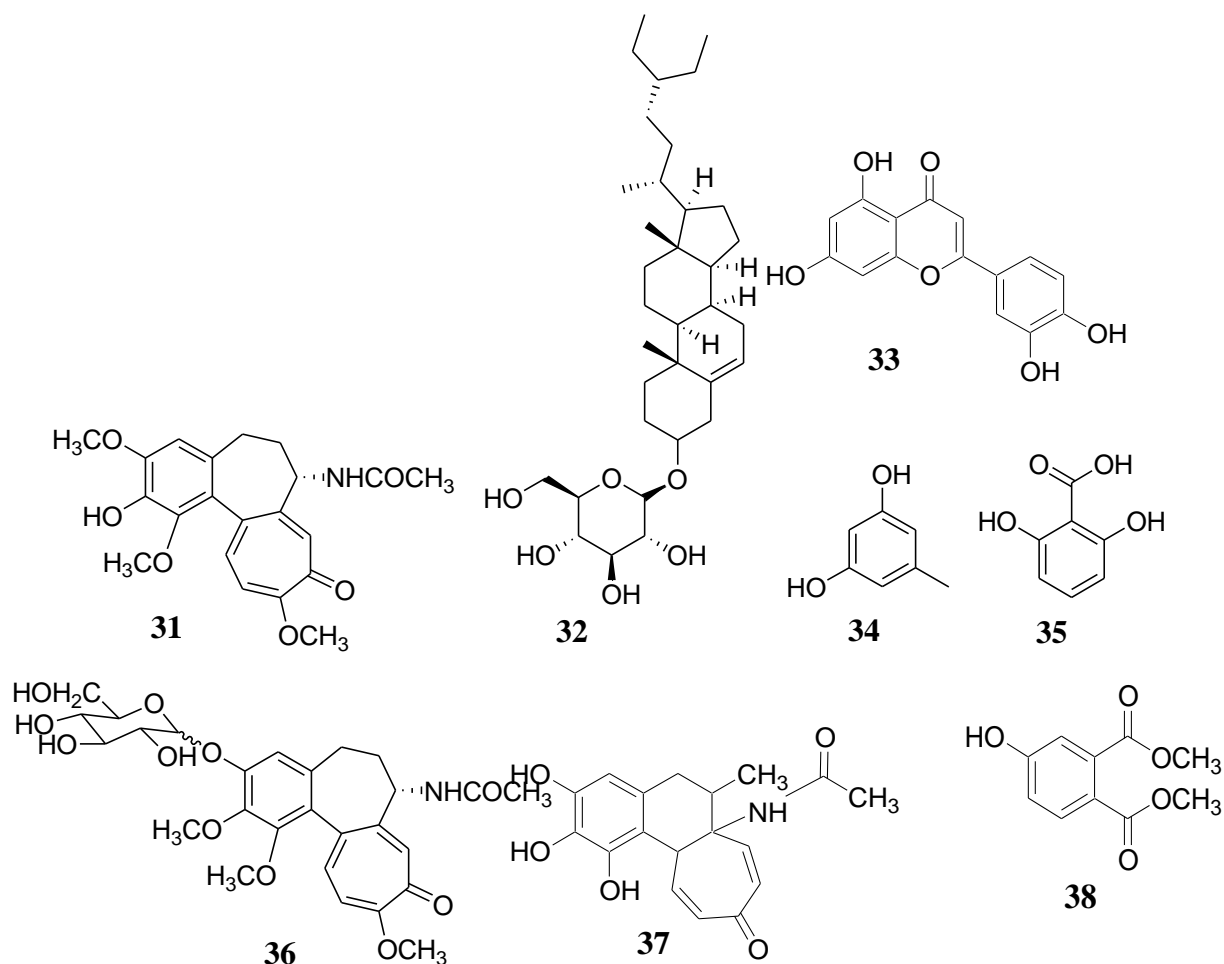


Figure 3. Structures of compounds **15-38** reported from *G. superba*

Previously, some phytochemical constituents, mainly flavonoids and alkaloids, were isolated and reported from different parts of *C. purpurea*. For example, the flavonoids apigenin (**39**), apigenin 7-*O*-glucoside (**40**) and chrysoeriol (**41**) were isolated from ethanol leaves extract by concentrating, diluting with 1N acetic acid, extracting with diethyl ether followed by chromatographic fractionation of the diethyl ether extract⁸⁵. Three quinolizidine alkaloids (**42-44**) were also detected from *C. purpurea* through spectroscopic analysis⁸⁶. According to Van Rijk and Radema⁸⁷, 1-sparteine (**45**), lupanine (**46**), α -amyrin (**47**) and cadiamine (**48**) were isolated from the leaves and twigs of *C. purpurea*. 13-ethoxylupanine (**49**), a novel, naturally occurring, derivative of lupanine (**46**) was isolated from the ethanol and chloroform extracts of *C. purpurea* by column chromatography on alumina eluted with diethyl ether: chloroform (95:5) and identified by thin-layer chromatography and mass

spectroscopy⁸⁸. The leaves of *C. purpurea* were also studied for their luteolin (**33**) content⁸⁹. The chemical structures of the compounds **39-49** reported from *C. purpurea* are shown in Figure 4.

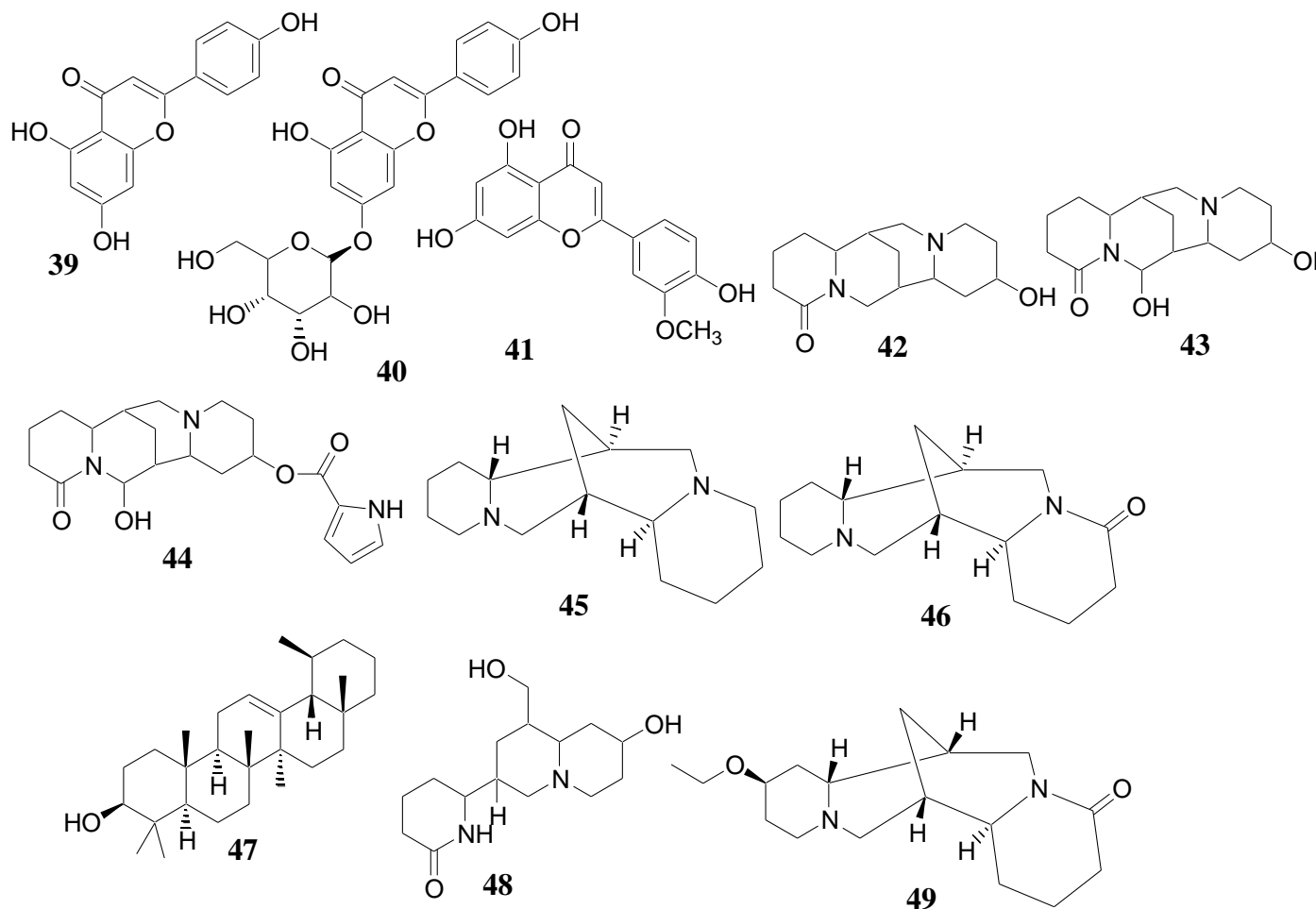
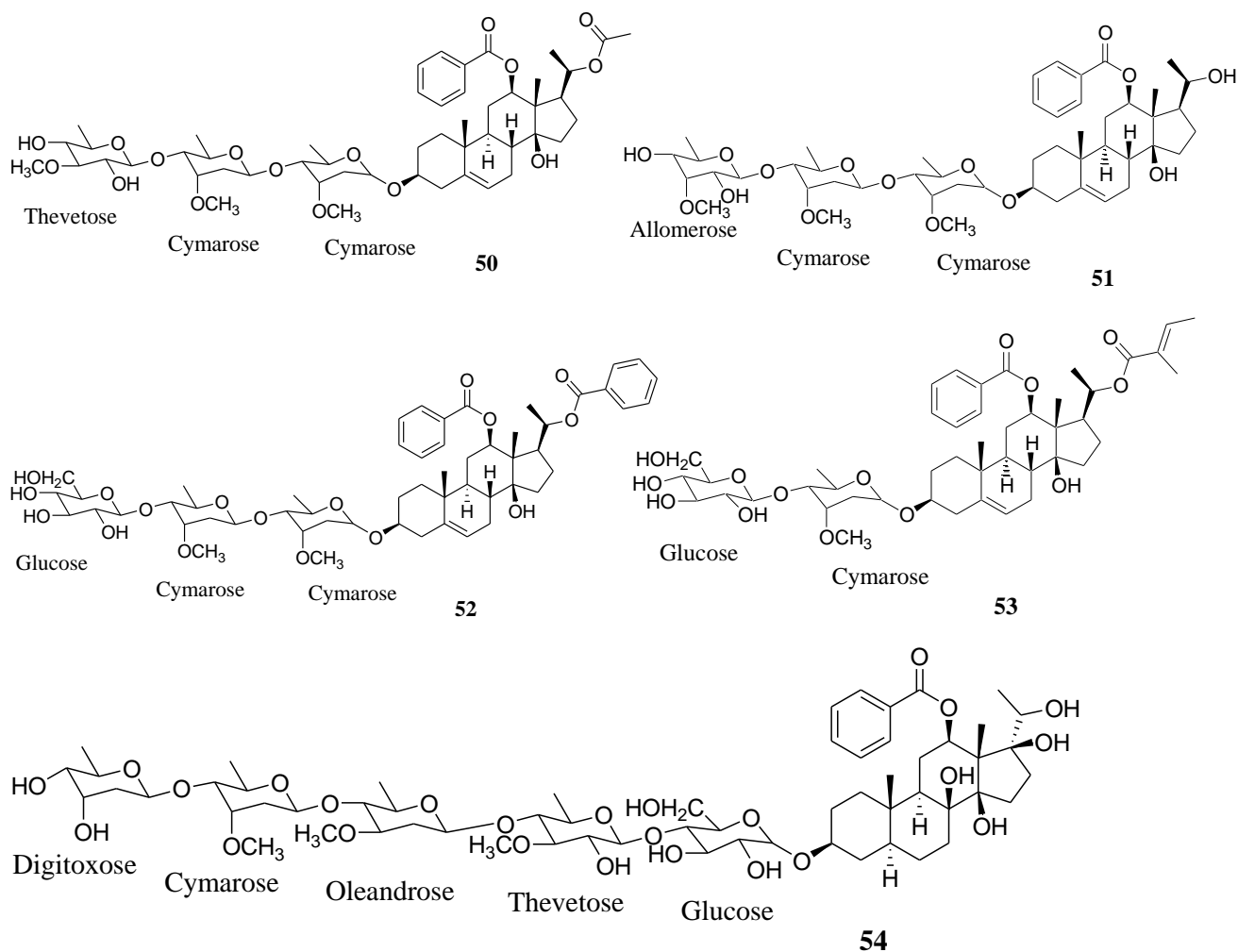
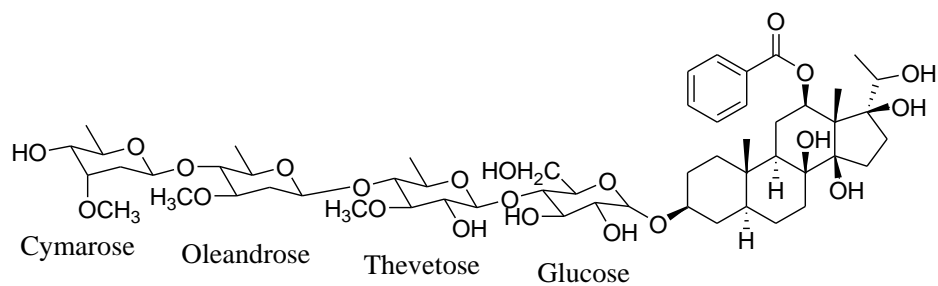


Figure 4. Structures of compounds **39-49** reported from *C. purpurea*

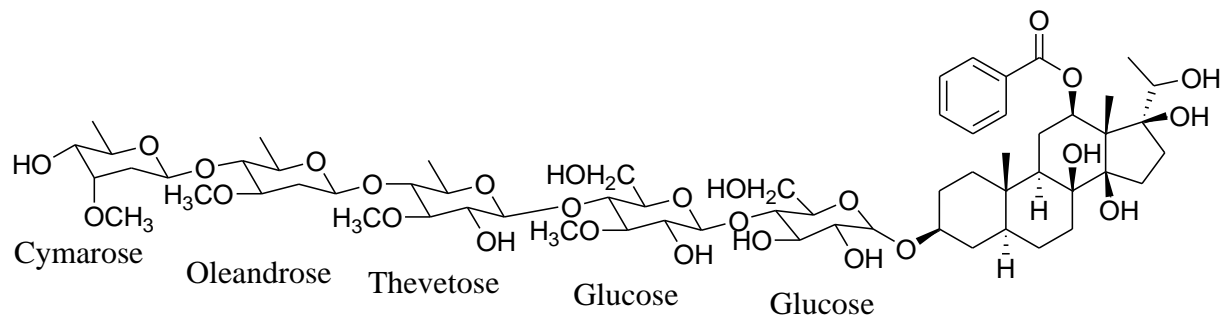
Many phytochemical constituents have been isolated and identified from the genus *Caralluma* as reported in various phytochemical studies. The chemical constituents reported from the genus *Caralluma* are mainly pregnane glycosides, types of steroidal glycosides. Besides, megastigmane glycosides and few flavones have also been isolated from some species of the genus⁹⁰. For instance, four clyated pregnane glycosides **50-53** were identified from the chloroform and *n*-butanol fractions of ethanol extract of the aerial parts of *Caralluma sinaica*⁹¹. Five pregnane glycosides **54-58** were also reported from stems

*Marsdenia tenacissima*⁹². In addition, three pregnane oligoglycosides **50-61** and other pregnane glycosides **62-64** were reported from the stems of *Hemidesmus indicus*⁹³ and whole part of *C. dalzielii*⁹⁴, respectively. Moreover, eighteen fatty acids, four hydrocarbons and β -sitosterol were isolated from the ethyl acetate fraction of vegetative part of *C. edulis*⁹⁵. Seventy four volatile compounds and several fatty acids were also identified from stem and fruit parts of *C. europaea*⁹⁶. But, to the best of our knowledge, no phytochemical constituents were reported from *C. speciosa*. The structures of compounds **50-64** are depicted in Figure 5.

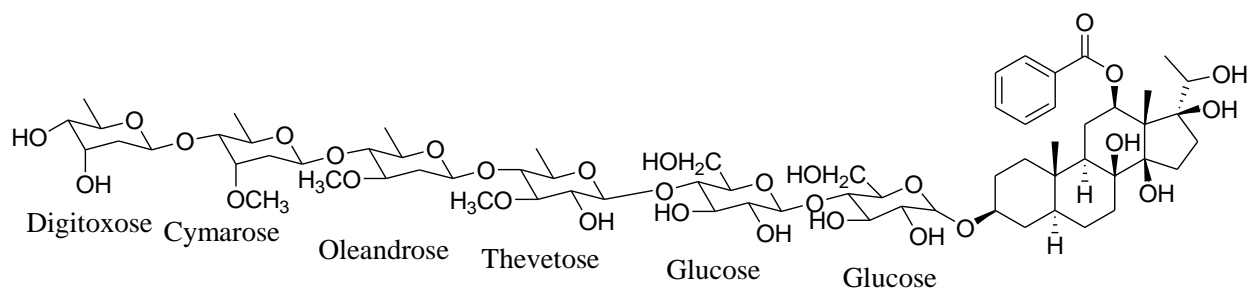




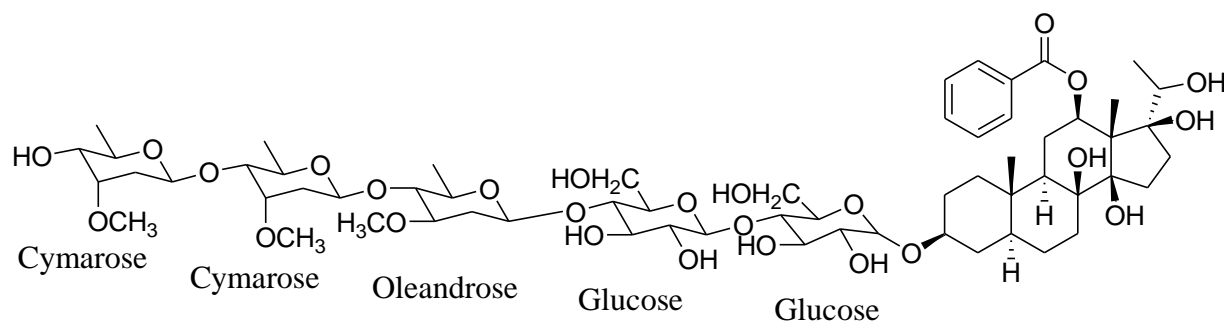
55



56



57



58

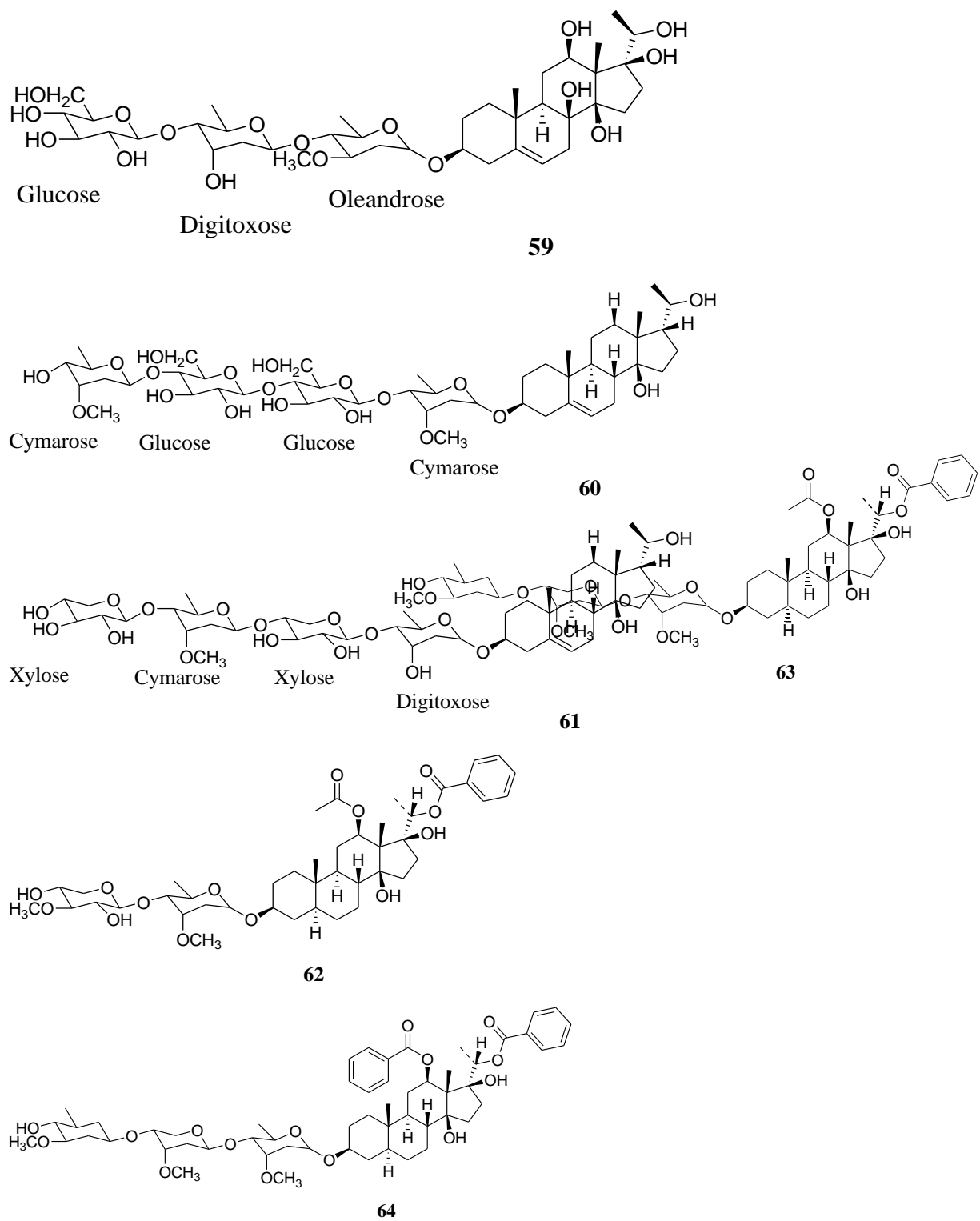


Figure 5. Structures of compounds 50-64 reported from different species of the genus *caralluma*

Generally, previously reported research works on the chemical constituents and biological activity of various parts of the selected plant species mentioned above and their endophytes found in Harla town and its surrounding places were very limited. That is why we are highly interested in these plant species and their associated bacterial endophytes to investigate their chemical constituents, and evaluate *in vitro* antimicrobial and antioxidant activities. The leaves of *G. purpurascens*, stems, leaves and tubers of *G. superba*, roots and leaves of *C. purpurea* and stems of *C. speciosa* were considered in the present dissertation work.

3 Materials and Methods

3.1 Description of the study area

The present study covered the areas ranging from Harla town up to its surrounding villages which are found under Dire Dawa administrative city, Eastern Ethiopia, located at 515 km East of Addis Ababa. These areas are delimited with coordinates of 9°27' and 9°39'N latitude and 41°38' and 42°20'E longitude with elevation ranges between 950-2260 m above sea level. The mean annual temperature is about 22.8 °C, ranging from a mean minimum of 16.2 °C to mean maximum of 30.4 °C. The mean annual rainfall in the surrounding areas ranges from about 1,000-600 mm¹⁷ (Figure 6).

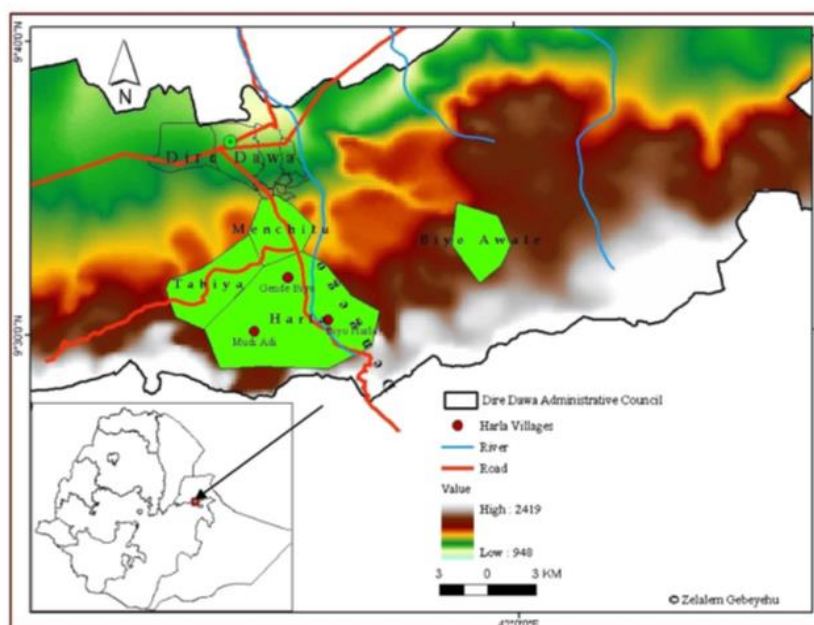


Figure 6. Map of the study area¹⁷

3.2 Collection and authentication of the plant materials

Roots and leaves of *C. purpurea* (Figure 7a), stems of *C. speciosa* (Figure 7b), leaves of *G. purpurascens* (Figure 7c) and tubers of *G. superba* (Figure 7d) were collected from the aforementioned study areas during June to October 2019/20/21. A voucher specimen of each plant was collected and pressed on newspaper, separately for taxonomic identification. The taxonomic identification process was conducted at the herbarium of Haramaya University by Dr Anteneh Belayneh for the confirmation of the botanical name of the plant species reported elsewhere. Voucher specimens of *C. purpurea* (voucher number, AHU178), *C. speciosa* (voucher number, AHU111), *G. superba* (voucher number, AHU110) and *G. purpurascens* (voucher number, AHU126) were deposited at the herbarium of Haramaya University. Collected plant parts were washed with tap water and dried in shade at room temperature. The dried plant samples were ground into powder with electrical blender. Powdered samples were stored in an airtight container and kept at 4 °C refrigerator until extraction process was commenced.

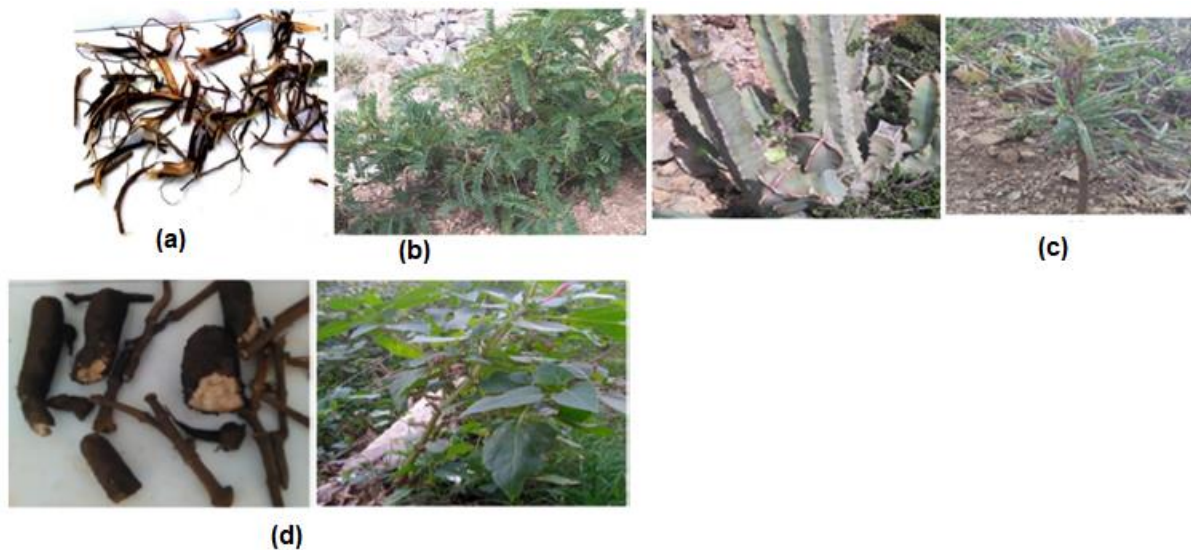


Figure 7. Photo of four studied plant species. (a) *Cadia purpurea* and its root (left) part, (b) *Caralluma speciosa*, (c) *Gomphocarpus purpurascens* and (d) *Gloriosa superba* and its tuber (left) part (photo by Tsegu K., 2021)

3.3 Test microbial cultures

Three human standard bacterial pathogens, viz., *Staphylococcus aureus* (*S. aureus*, ATCC 25923), *Escherichia coli* (*E. coli*, ATCC 25922) and *Pseudomonas aeruginosa* (*P.*

aeruginosa, ATCC 27853), and *Candida albicans* ATCC 10231 fungal strain were obtained from Ethiopian Public Health Institute (EPHI).

3.4 Chemicals, apparatuses and instruments

Chemicals: TLC visualizing reagents (iodine vapor, Wagner's reagent, vanillin/MeOH/H₂SO₄), analytical grade organic solvents (methanol, ethanol, *n*-hexane, ethyl acetate, chloroform, dichloromethane, acetone), inorganic reagents (NaOH, 5% sodium hypochlorite, anhydrous Na₂SO₄, 10% Na₂CO₃, ferric chloride, potassium ferricyanide, 0.2 M potassium phosphate buffer, BaCl₂, BaCl₂.H₂O), culture media (MHA, TSA, TSB, PDA etc) and others (trichloroacetic acid, DMSO, chloramphenicol standard, ketoconazole standard, carbendazim standard, 0.1 N tartaric acid, 230-400 mesh size silica gel, ascorbic acid, acetic acid, DPPH free radical) were used.

Apparatuses and instruments: Pre-coated aluminum TLC sheet silica gel 60 F₂₅₄ (Merck), TLC chamber, capillary tube, PTLC, glass column, waring commercial laboratory blender (Torrington, CT., USA), suction filtration and Petri plates, digital melting point (SMP10, Bibby Scientific, UK), orbital shaker (Hy-5A, Movel Scientific Instrument CO. Ltd., China), rotary evaporator (Rotary vacuum, Jainsons, India), incubator (Binder B28, Germany), autoclave (tuttnauer 3150EL, Israel), UV- lamp cabinet (UVP Chromato-Vue C-70G, Analytik Jena, USA), UV-Vis spectrophotometer (Cecil CE4001 UV/VIS, Cambridge, England), Spectrum 65 FT-IR (PerkinElmer, 4000-400 cm⁻¹), EI GC-MS spectrometry (7890B and 5977A, Agilent Technologies, USA), MALDI-TOF MS (Biotype, Bruker), ¹H (400 MHz) and ¹³C (100 MHz) NMR spectroscopy (BRUKER ACQ 400 AVANCE) were employed.

3.5 Extraction and isolation of compounds from plants parts

Total extraction of each plant material was conducted by mixing with organic solvents in the ratio of 1:10 (plant material/solvent, g/mL). Briefly, dried and ground plant material was defatted with *n*-hexane (3x), filtered using suction filtration followed by solvent evaporation using rotary evaporator. The remaining marcs, after *n*-hexane extractions, were successively extracted with chloroform, chloroform: methanol (1:1), ethanol and methanol solvents followed by filtration and concentration. The general procedure applied for the preparation of these crude extracts used to isolate phytochemical constituents, is shown below (Figure

8). Obtained crude extracts were subjected to *in vitro* antibacterial, antifungal and antioxidant activities assay, and chromatographic fractionations.

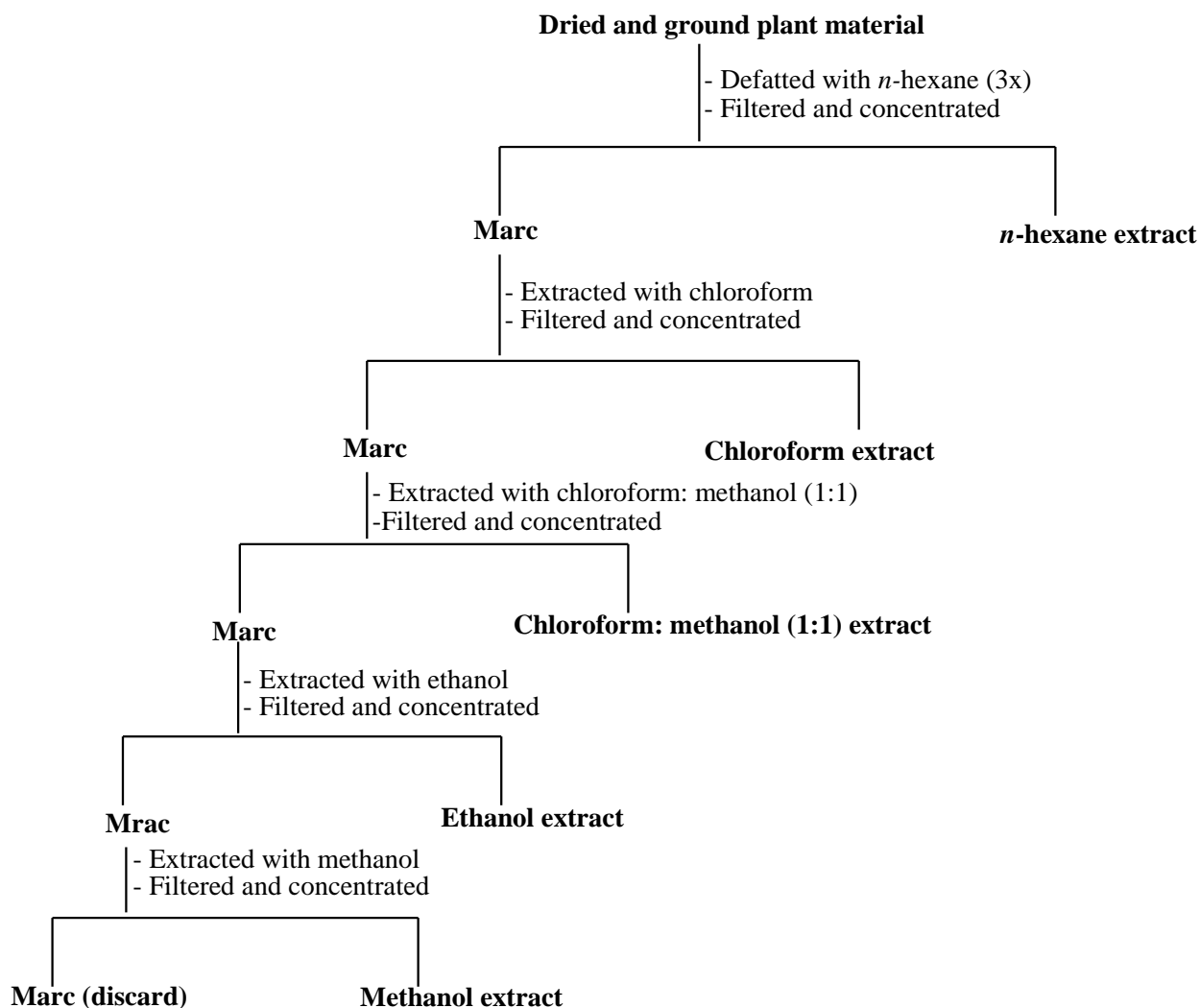


Figure 8: General procedure for preparation of crude plant extracts with increasing polarity

3.5.1 *Cadia purpurea* leaves and roots

Shed dried powder (100 g) of each part was defatted with *n*-hexane (3x) for 24 hr, filtered by suction filtration, concentrated by rotary evaporator at reduced pressure and weighed the crude extract of the roots (0.60 g) and the leaves (2.50 g). The marc after *n*-hexane extracts of roots (99.00 g) and leaves (97.00 g) extracts were then extracted with chloroform, filtered and concentrated affording 0.57 and 1.82 g, respectively. The remaining marc after chloroform extracts of the roots (98.00 g) and leaves (94.00 g) were further extracted with chloroform: methanol (1:1), filtered and concentrated to obtain 4.67 and 7.87 g of the roots

and leaves extracts, respectively. The remaining roots (93.00 g) and leaves (85.00 g) marc of the chloroform: methanol (1:1) extracts were extracted with ethanol, filtered and concentrated obtaining 0.20 and 0.28 g, respectively. Finally, marc of the ethanol roots (92.00 g) and leaves (84.00 g) extracts were subjected to methanol extraction overnight, filtered and concentrated resulting in 4.78 and 8.04 g, respectively. Obtained crude extracts of each plant parts were subjected to *in vitro* antibacterial and antioxidant activity assay and TLC guided fractionation.

The *n*-hexane, chloroform, chloroform: methanol (1:1), methanol and ethanol crude extracts of the roots and leaves parts were first subjected to TLC analysis using *n*-hexane/EtOAc (3:1), CHCl₃/acetone (3:1), CHCl₃/MeOH (1:1), EtOAc/MeOH/AcOH (3:1:0.1) and 100% EtOH, respectively, as developing solvents and UV-lamp (254 and 365 nm) followed by vanillin/H₂SO₄ as visualization methods. Then, to target compounds with medium and high polarity, those crude extracts expected to have such compounds and taking their TLC profiles (Figure 9) into consideration, were fractionated over silica gel column chromatography.

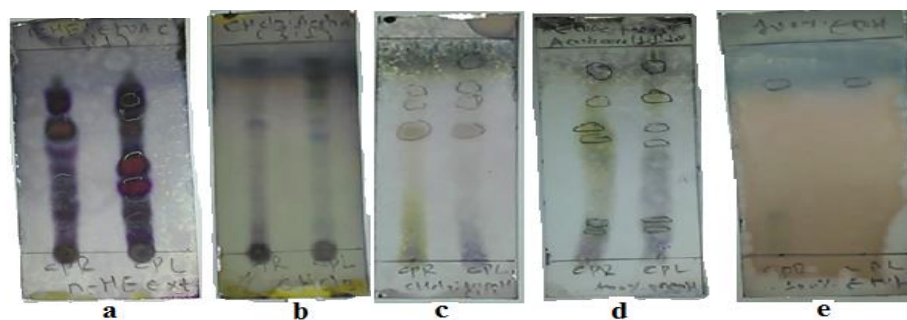


Figure 9. TLC profiles of *n*-hexane (a), chloroform (b), chloroform: methanol (1:1; c), methanol (d) and ethanol (e) crude extracts of the roots (left) and leaves (right) of *C. purpurea*

Fractionation of chloroform leaves extract

The chloroform crude leaves extract (1 g) was dissolved in MeOH (20 mL) and adsorbed on 10 g silica gel. The adsorbed sample was chromatographed over column chromatography packed with silica gel (150 g). Elution was accompanied with CHCl₃/acetone with increasing polarity and one hundred ten fractions were collected (Table 3). Collected fractions were subjected to TLC analysis with different ratio of CHCl₃/acetone as

developing solvent and UV-lamp (254 and 365 nm) and iodine vapor as visualization methods. And fractions with similar spot (s) were combined and their TLC analysis was performed (Figure 10).

Table 3. Collected fractions of chloroform leaves extract of *C. purpurea*

Fraction no.	Solvent system	Volume (mL)
1-4	100% Chloroform	15-25
5-19	100% Chloroform	10-40
20-25	100% Chloroform	25-40
26-38	CHCl ₃ /acetone (3:1)	15-25
39-42	CHCl ₃ /acetone (3:1)	10
43-51	CHCl ₃ /acetone (3:1)	10
52-78	CHCl ₃ /acetone (3:1)	10-25
79-94	100% acetone	10-30
95-110	100% Aacetone	10-25

Fr.90-94

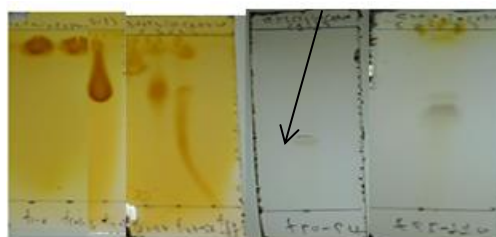


Figure 10. TLC profiles of combined fractions of chloroform leaves extract of *C. purpurea*

The TLC profile of Fr.90-94 appeared as single spot on TLC with R_f value of 0.4 (CHCl₃/acetone; 1:1) using acetone as eluent and afforded compound **65** (26 mg).

Fractionation of methanol leaves extract

The methanol leaves extract (5 g) was dissolved in MeOH (50 mL), adsorbed on 50 g silica gel and fractionated over CC packed with silica gel (250 g). Eighty one fractions were collected with EtOAc/MeOH with increasing polarity (Table 4). Collected fractions were

applied on TLC developed with EtOAc/MeOH/AcOH (3:1:0.1) and visualized UV-lamp and iodine vapor. Fractions exhibiting better and similar spot(s) were combined and subjected to TLC analysis (Figure 11) using the same mobile phase with same ratio and visualization method mentioned above.

Table 4. Fractions collected from methanol leaves extract of *C. purpurea*

Fraction no.	Solvent system	Volume (mL)
1-23	100% EtOAc	10
24-31	100% EtOAc	10-25
32-36	100% EtOAc	25
37-52	EtOAc/MeOH (3:1)	10
53-57	EtOAc/MeOH (1:1)	10
58-72	EtOAc/MeOH (1:1)	10
73-81	100% MeOH	20

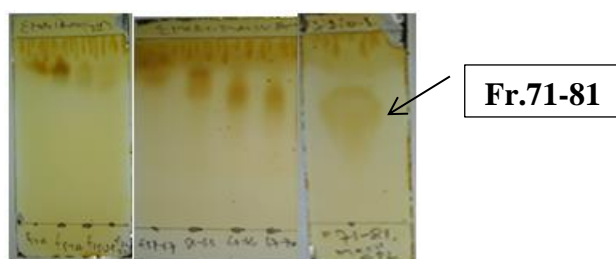


Figure 11. TLC profiles of combined fractions of methanol leaves extract of *C. purpurea*

The TLC profile of Fr.71-81 was observed as better spot, concentrated and subjected to characterization resulted in compound **66** (25 mg).

Acid-base extraction for isolation of alkaloidal constituent

Leaves powder (100 g) of *C. purpurea* was subjected to “acid-base shake-out” extraction technique to isolate possible alkaloidal constituent, following the general procedure described by Satyajit *et al.*¹⁴ and depicted in Figure 12. Briefly, the mentioned amount was defatted with *n*-hexane (3x 1L) and the last defatted marc (89 g) was extracted with methanol by placing on orbital shaker overnight. Methanol extract was filtered using suction filtration

and filtrate was concentrated by rotary evaporator at reducing pressure affording 12 g. This crude yield (12 g) was suspended in 0.1N tartaric acid and titrated to pH 5 with 10% Na₂CO₃. It was then partitioned in ethyl acetate by prior saturation with water. The ethyl acetate phase was separated and dried over Na₂SO₄ anhydrous. The remaining aqueous-acidic phase was basified with 10% Na₂CO₃, to pH 11, followed by partitioning with ethyl acetate for five rounds. All ethyl acetate phases were then combined; dried over Na₂SO₄, filtered and concentrated affording 0.8 g.

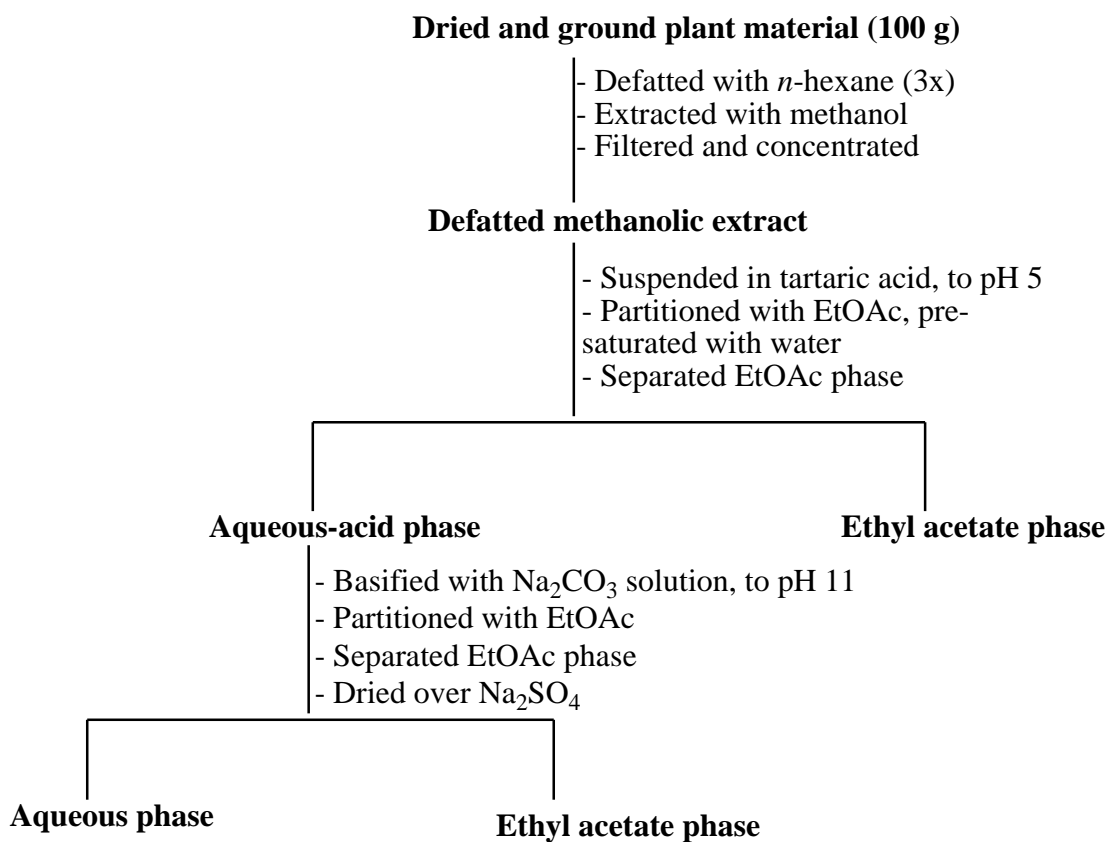


Figure 12: Acid-base extraction procedure used to isolate alkaloidal compounds from leaves of *C. purpurea*

The TLC profile of ethyl acetate portion together with the remaining basified aqueous layer were analyzed using EtOAc/MeOH/AcOH (1:1:0.1) as mobile phase; and UV-lamp followed by iodine vapor and Wagner's reagent as visualization methods. Based on the obtained TLC result, the ethyl acetate phase, which showed a positive response to Wagner's reagent, was subjected to silica gel CC fractionation to target possible alkaloidal constituent(s).

The ethyl acetate extract (0.8 g) was adsorbed on silica gel (5 g) and subjected to prepacked column with silica gel slurry (150 g). Elution was started with 100% EtOAc followed by EtOAc/MeOH with different ratio in polarity wise. A total of sixty fractions were collected (Table 5). The TLC profile of collected fractions was observed with the developing solvents, *n*-hexane/EtOAc/AcOH (3:1:0.1), DCM/EtOAc/ACO_H (3:1:0.1), EtOAc/MeOH/AcOH (9:1:0.1) and EtOAc/MeOH/AcOH (3:1:0.1) under the visualization methods UV-lamp followed by iodine vapor and Wagner's reagent. Fractions showing similar spot(s) were combined and re-subjected to TLC analysis using the same mobile phases and visualization techniques stated above (Figure 13).

Table 5. Collected fractions of ethyl acetate phase extract of defatted methanol extract of *C. purpurea* leaves

Fraction No.	Solvent system	Volume (mL)
1-8	100% EtOAc	20 each
9-12	“	20 each
13-20	EtOAc/MeOH (9:1)	25 each
21-28	EtOAc/MeOH (3:1)	20 each
29-40	“	10 each
41-52	“	10 each
53-56	“	20 each
57-60	EtOAc/MeOH (1:1)	20 each

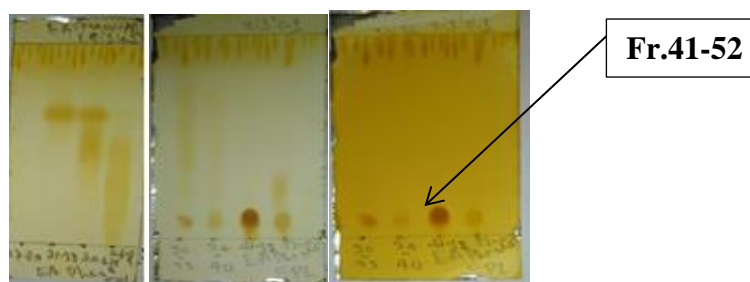


Figure 13. TLC profiles of combined fractions of ethyl acetate extract of defatted methanol extract of *C. purpurea* leaves

From the obtained TLC results of the combined fractions (Figure 13), Fr.41-52 (500 mg) was found to be reactive against Wagner's reagent with minor purity and was further purified over silica gel CC as follows.

Fr.41-52 (300 mg) was dissolved in methanol (2 mL), adsorbed on silica gel (2 g), concentrated and fractionated over silica gel CC (50 g). Elution was begun with 100% DCM and continued with gradients of DCM/EtOAc (90/10, 70/30 and 50/50), 100% EtOAc and EtOAc/MeOH (90/10 and 75/25) which resulted in collection of seventy sub-fractions (5 mL, each). Sub-fractions with similar TLC composition, under the solvent systems of 100% DCM, DCM/EtOAc/AcOH (3:1:0.1) and EtOAc/MeOH/AcOH (3:1:0.1), and visualizing agents of iodine and Wagner's reagent, were combined. Of the combined sub-fractions (Figure 14), sub-fr61-70 showed a positive response against Wagner's reagent, concentrated (67 mg) and characterized resulting in compound **67**.

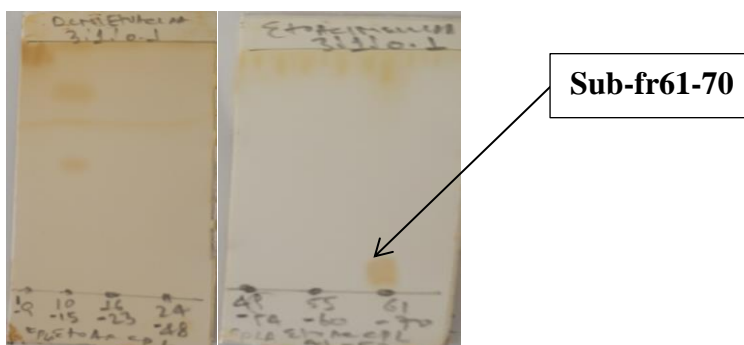


Figure 14. TLC analysis of combined sub-fractions from Fr.41-52 of ethyl acetate extract of defatted methanol leaves extract of *C. purpurea*

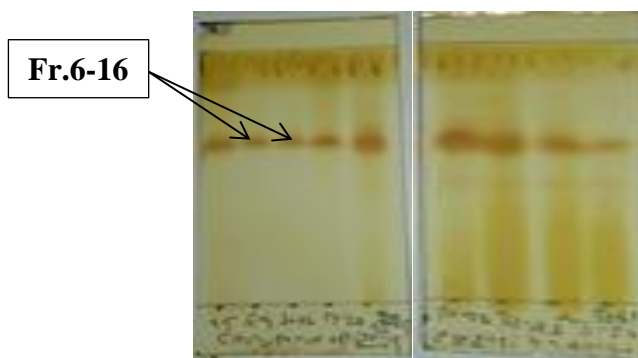


Figure 15. TLC profiles of combined fractions of chloroform: methanol (1:1) roots extract of *C. purpurea*

The TLC profile (Figure 15) displayed a major spot with R_f value 0.6 shown in all fractions. Fr.6-16 was further fractionated over silica gel CC as follows.

300 mg of Fr.6-16 was dissolved in methanol, adsorbed on silica gel (2 g), concentrated and refractionated over silica gel CC (50 g). eighty eight sub-fractions (Table 6) were eluted with DCM/EtOAc/MeOH solvent systems of varied polarity. The TLC profile of collected sub-fractions was examined with the solvent systems, DCM/*n*-hexane (3:1), DCM, DCM/EtOAc/AcOH (9:1:0.1 and 1:1:0.1), EtOAc/DCM/AcOH (3:1:0.1) and EtOAc/MeOH/AcOH (3:1:0.1) and visualizing methods of UV-lamp (254 and 365 nm) and vanillin (Figure 16). Among them, sub-fractions 17-19 and 42-48 were found to be good in purity and afforded compounds **68** and **69**, respectively.

Table 6. Sub-fractions collected from Fr.6-16 of chloroform: methanol (1:1) roots extract of *C. purpurea*

Sub-fraction no.	Solvent system	Volume (mL)
1-20	100% DCM	5
21-31	DCM/EtOAc (90:10)	5
32-46	DCM/EtOAc (70:30)	5
47-56	DCM/EtOAc (50:50)	5
57-64	EtOAc/DCM (70:30)	5
65-74	100% EtOAc	5
75-88	EtOAc/MeOH (90:10)	10

The figure shows four TLC plates. The first three plates correspond to sub-fractions 17-19, and the fourth plate corresponds to sub-fractions 42-48. Arrows from the table point to the spots on the plates. The spots are located at approximately the same R_f value (around 0.6) in all plates, indicating a major component in each fraction.

Figure 16. TLC profiles of combined sub-fractions of Fr.6-16 of chloroform: methanol (1:1) roots extract of *C. purpurea*

Fractionation of methanol roots extract

The methanol roots extract (3 g) was dissolved in MeOH (30 mL) and adsorbed on 10 g silica gel. The adsorbed sample was chromatographed over silica gel column chromatography (200 g) and eighty fractions were collected using EtOAc/MeOH. That is, fractions 1-30 (15 mL) were collected with increasing gradient of MeOH in EtOAc, while fractions 31-88 (10-20 mL) were collected with isocratic mode using EtOAc: MeOH (1:1). Collected fractions were subjected to TLC analysis using EtOAc/MeOH/AcOH (3:1:0.1) and EtOAc/MeOH/AcOH (1:1:0.1) as developing solvents visualized under UV-lamp and iodine vapor. Fractions showing similar spot (s) were combined, subjected to TLC analysis (Figure 17), concentrated and their amount was determined.

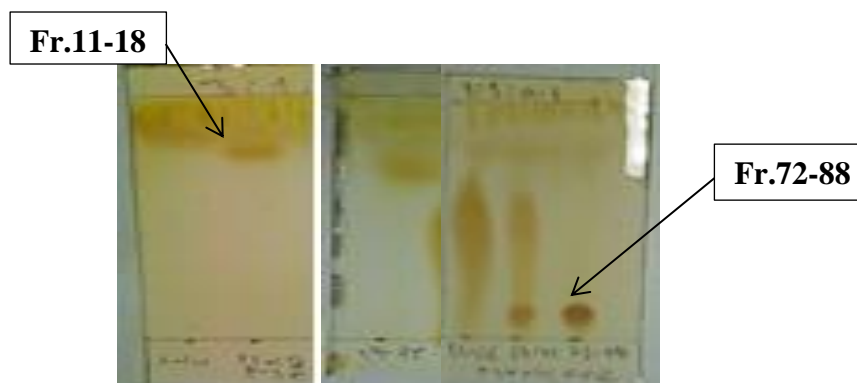


Figure 17. TLC profiles of combined fractions of methanol roots extract of *C. purpurea*

As shown from Figure 17, Fr.11-18 and Fr.72-88 were seen as better spots, concentrated and resulted in compounds **70** (45 mg) and **67** (300 mg).

3.5.2 *Caralluma speciosa* stems

Finely ground *C. speciosa* stem (0.5 kg) was defatted with *n*-hexane (3x) via shaking on orbital shaker for 24 hr followed by filtration with suction filtration and solvent evaporation by rotary evaporator leading to yellow *n*-hexane extract residue (6 g). Then, the remaining last marc, after defatting with *n*-hexane, was successively extracted with chloroform, chloroform: methanol (1:1), ethanol and methanol which afforded the corresponding crude extracts of 19, 18.9, 8 and 10 g. Prior to fractionation, the TLC profiles of the five different *C. speciosa* stem extracts, *n*-hexane, chloroform, chloroform: methanol (1:1), methanol and ethanol, were observed using solvent systems: *n*-hexane/DCM/AcOH (1:1:0.1), DCM/EtOAc/AcOH (1:1:0.1) and EtOAc/MeOH/AcOH (3:1:0.1). UV-lamp (254 and 365

nm) followed by iodine vapor was applied to visualize the developed TLC chromatograms (Figure 18).

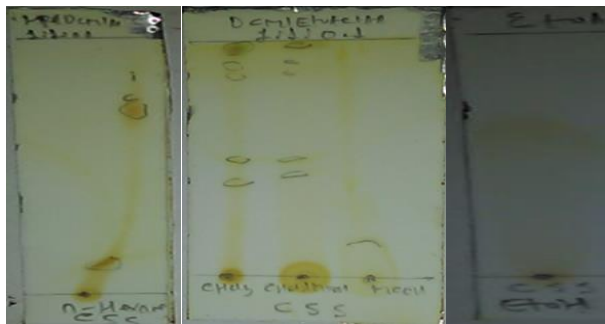


Figure 18. TLC profiles of *n*-hexane, chloroform, chloroform: methanol (1:1), methanol and ethanol extracts of *C. speciosa* stem

Based on the TLC analysis (Figure 18), the chloroform and methanol extracts were selected for silica gel column chromatographic separation as follows.

Fractionation of chloroform extract

Dark brown chloroform extract (15 g) of *C. speciosa* stem was solubilized in chloroform (100 mL), adsorbed on silica gel (20 g) and dried using rotary evaporator. Adsorbed and concentrated sample was then applied onto column CC packed with silica gel slurry (200 g). Three hundred twenty five fractions were collected using the eluents *n*-hexane/DCM/EtOAc/acetone with different ratio (Table 7). And their TLC profile was analysed using *n*-hexane/DCM/AcOH (3:1:0.1 and 1:1:0.1), DCM/EtOAc/AcOH (9:1:0.1, 4:1:0.1, 3:1:0.1 and 1:1:0.1) and EtOAc/acetone/AcOH (9:1:0.1, 3:1:0.1 and 1:1:0.1); and visualized under UV-lamp assisted iodine vapor. Similar fractions were merged and re-analyzed their TLC analysis (Figure 19).

Table 7. Collected fractions from chloroform extract of *C. speciosa* stem

Fraction No.	Eluents	Volume (mL)
1-26	100% <i>n</i> -hexane	50 each
27-46	<i>n</i> -Hexane/DCM (3:1)	50 each
47-68	<i>n</i> -Hexane/DCM (1:1)	50 each
69-81	<i>n</i> -Hexane/DCM (1:3)	50 each
82-130	100% DCM	25-50 each
131-159	DCM/EtOAc (9:1)	25 each
160-177	DCM/EtOAc (4:1)	50 each
178-200	DCM/EtOAc (3:2)	25 each
201-220	DCM/EtOAc (1:1)	25 each
221-236	DCM/EtOAc (1:4)	25 each
237-252	DCM/EtOAc (1:9)	25 each
253-268	100% EtOAc	25 each
269-280	EtOAc/acetone (9:1)	25 each
281-290	EtOAc/acetone (3:2)	25 each
291-300	EtOAc/acetone (1:1)	25 each
301-307	EtOAc/acetone (2:3)	25 each
308-315	EtOAc/acetone (1:9)	25 each
316-325	100% acetone	50 each

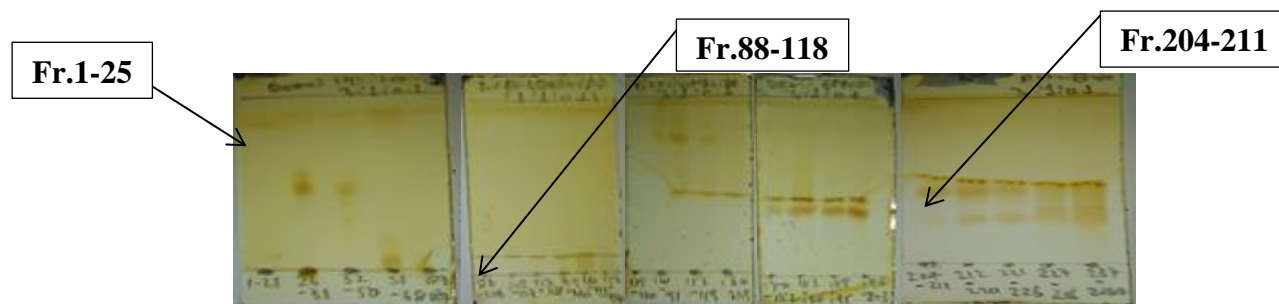


Figure 19. TLC profiles of combined fractions of chloroform stem extract of *C. speciosa*

Among the combined fractions (Figure 19), Fr.1-25 (eluted with *n*-hexane), Fr.88-118 (eluted with DCM) and Fr.204-211 (eluted with DCM/EtOAc, 1:1) were observed as promising fractions which yielded compounds **71** (104 mg), **72** (186 mg) and **73** (104 mg), respectively.

Fr.119-203 (yellowish gel, 600 mg) was further re-fractionated to give one hundred thirty five sub-fractions using DCM (fractions 1-27, 10 mL), 9:1 of DCM/EtOAc (fractions 28-52, 10 mL), 3:1 of DCM/EtOAc (fractions 53-63, 10 mL), 4:1 of CHCl₃/EtOAc (fractions 64-85, 10 mL), 3:2 of CHCl₃/EtOAc (fractions 86-120, 10 mL), 1:1 of CHCl₃/EtOAc (fractions 121-125, 20 mL) and EtOAc (fractions 126-135, 20 mL). The TLC analysis of collected sub-fractions was conducted using *n*-hexane/DCM/AcOH (1:1:0.1), DCM/EtOAc/AcOH (9:1:0.1) and *n*-hexane/EtOAc/AcOH (1:1:0.1) under the visualization agents UV-lamp and iodine vapor. Similar sub-fractions were combined and subjected to TLC evaluation (Figure 20). Among them, sub-fr70-120 (eluted with CHCl₃/EtOAc, 3:2) showed a comparatively better purity on TLC which yielded compound **74** (127 mg).

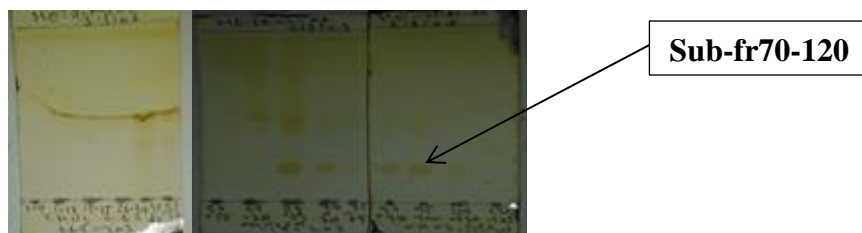


Figure 20. TLC profiles of combined sub-fractions of Fr.119-203 of chloroform *C. speciosa* stem extract

Fractionation of methanol extract

Methanol extract (9 g) of *C. speciosa* stem was dissolved in MeOH (25 mL), adsorbed on silica gel (10 g) and applied on CC packed with silica gel (150 g). Using DCM/EtOAc/MeOH as eluents in increasing ratio of polarity, one hundred sixty seven fractions were collected (Table 8) and subjected to TLC profiling using different developing solvents with varied ratio of polarity (*n*-Hexane/DCM/AcOH, 1:1:0.1; DCM/EtOAc/AcOH, 9:1:0.1; EtOAc/MeOH/AcOH, 9:1:0.1; EtOAc/MeOH/AcOH, 4:1:0.1 and EtOAc/MeOH/AcOH, 1:1:0.1) under UV-lamp and iodine vapor detection techniques. Fractions with similar R_f on TLC were combined and their TLC identity was again determined using same technique (Figure 21).

Table 8. Fractions collected from methanol extract of *C. speciosa* stem

Fraction No.	Solvent system	Volume (mL)
1-29	100% DCM	50
30-42	DCM/EtOAc (9:1)	25
43-60	DCM/EtOAc (4:1)	20
61-71	DCM/EtOAc (3:2)	20
72-83	DCM/EtOAc (1:4)	20
84-105	100% EtOAc	20
106-121	EtOAc/MeOH (9:1)	25
122-150	EtOAc/MeOH (3:1)	25
151-167	EtOAc/MeOH (1:1)	20

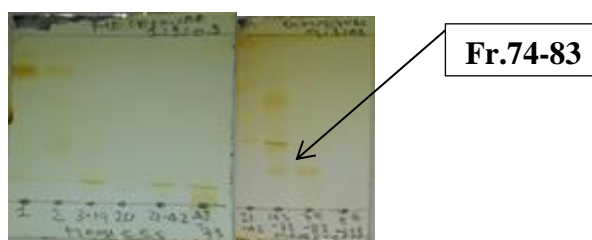


Figure 21. TLC profiles of combined fractions of methanol stem extract of *C. speciosa*

As per the TLC profile (Figure 21), Fr.74-83 (eluted with DCM/EtOAc, 1:4) provided compound **75** (157 mg).

3.5.3 *Gloriosa superba* tubers

Shed dried tuber powder (400 g) of *G. superba* was extracted successively with *n*-hexane (3x), chloroform, chloroform:methanol (1:1) and methanol via shaking, to afford dry residue of 2, 1.3, 11 and 17 g, respectively. The TLC profile of the extracts was analysed using DCM/EtOAc/AcOH (3:1:0.1) and visualized with UV-lamp and vanillin/MeOH/H₂SO₄ (3:95:5) (Figure 22). Then, the chloroform: methanol (1:1) residue (8 g) was dissolved in methanol, adsorbed on silica gel and chromatographed over silica gel CC (150 g). Three hundred sixteen fractions were collected (Table 9) using *n*-hexane, *n*-hexane/DCM (90/10 to 20/80), DCM, DCM/EtOAc (90/10 to 10/90), EtOAc and EtOAc/MeOH (95/5 to 50/50). The TLC analysis of collected fractions was performed using different solvent systems (*n*-hexane/DCM, 1:1 up to EtOAc/MeOH/AcOH, 1:1:0.1) under the detection methods of UV-

lamp (254 nm) and vanillin reagent. Fractions with similar TLC profile were combined and again subjected to TLC examination (Figure 23). Among them, Fr.1-45 (23 mg), Fr.46&47 (4 mg), Fr.48&49 (6 mg), Fr5.0 (3 mg), Fr.51-53 (12 mg), Fr.54-72 (15 mg), Fr.110-115 (12 mg), Fr.116-129 (21 mg), Fr.195-211 (46 mg) and Fr.257-273 (50 mg) were found with comparatively better purity regardless of their amounts. Fr.110-115, Fr.116-129 and Fr.257-273 furnished compounds **76** (21 mg), **77** (6 mg) and **78** (50 mg), respectively.

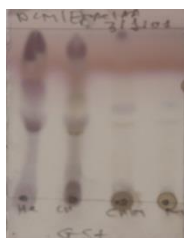


Figure 22. TLC profile of crude tuber extracts of *G. superba*

Table 9, Fractions eluted from chloroform: methanol (1:1) tuber extract of *G. superba*

Fraction No.	Solvent system	Volume (mL)
1-12	100% <i>n</i> -hexane	25
13-24	Hexane/DCM (90/10)	“
25-34	Hexane/DCM (80/20)	“
35-44	Hexane/DCM (70/30)	“
45-55	Hexane/DCM (60/40)	“
56-65	Hexane/DCM (40/60)	“
66-75	Hexane/DCM (20/80)	“
76-115	100% DCM	“
116-150	DCM/EtOAc (90/10)	20
151-160	DCM/EtOAc (80/20)	“
161-171	DCM/EtOAc (70/30)	“
172-181	DCM/EtOAc (60/40)	“
182-194	DCM/EtOAc (50/50)	“
195-204	DCM/EtOAc (50/60)	“
205-216	DCM/EtOAc (30/70)	“
217-230	DCM/EtOAc (20/80)	“
231-240	DCM/EtOAc (10/90)	“
241-270	100% EtOAc	10
271-275	EtOAc/MeOH (95/5)	10
276-292	EtOAc/MeOH (90/10)	20
293-300	EtOAc/MeOH (80/20)	20
301-316	EtOAc/MeOH (50/50)	20

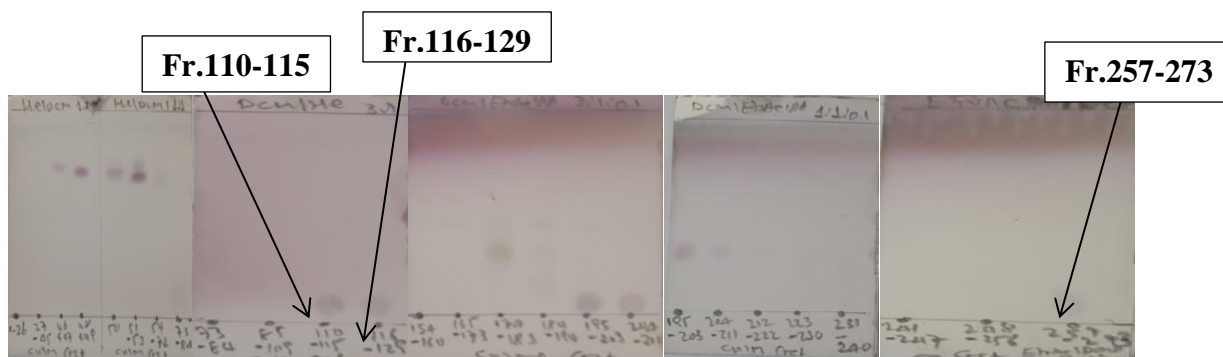


Figure 23. TLC profiles of combined fractions of chloroform:methanol (1:1) *G. superba* tuber extract

3.5.4 *Gomphocarpus purpurascens* leaves

Powdered leaves (500 g) of *G. purpurascens* was successively extracted with *n*-hexane, chloroform, chloroform: methanol (1:1), ethanol and methanol following the procedure stated in Figure 8. It was then resulted in a dark yellow *n*-hexane extract (18 g), a dark gel chloroform extract (6 g), a green gel chloroform: methanol extract (53 g), a green yellowish ethanol extract (27 g) and a light brown gel methanol extract (43 g). The TLC analysis of each extract was performed using *n*-hexane/ CHCl_3 /AcOH (1:1:0.1) for *n*-hexane, *n*-hexane/EtOAc/AcOH (1:1:0.1) for chloroform and chloroform: methanol (1:1) and EtOAc/MeOH/AcOH (9:1:0.1) for ethanol and methanol extracts. UV-lamp and iodine vapor were used as visualization techniques (Figure 24).



Figure 24. TLC profiles of *n*-hexane, chloroform, chloroform: methanol (1:1), methanol and ethanol extracts of *G. purpurascens* leaves

Then, the chloroform: methanol (1:1) extract was subjected to further fractionation process over silica gel CC. That is, green gel (30 g) was dissolved in chloroform: methanol (1:1, 150 mL), adsorbed on silica gel (40 g) and concentrated. Adsorbed powder was then applied over silica gel CC (200 g) and eluted with *n*-hexane/ CHCl_3 /EtOAc/MeOH of different

polarity ratio. Three hundred seventy six fractions were collected (Table 10). After observing on their TLC profiles using *n*-hexane/EtOAc/AcOH (3:1:0.1&1:1:0.1) and EtOAc/MeOH/AcOH (9:1:0.1), fractions with similar R_f value were merged and subjected for further TLC analysis (Figure 25).

Table 10. Collected fractions from chloroform: methanol (1:1) leaves extract of *G. purpurascens*

Fraction No.	Eluents	Volume (mL)
1-18	<i>n</i> -Hexane/CHCl ₃ (9:1)	50 each
19-26	<i>n</i> -Hexane/CHCl ₃ (1:1)	
27-40	<i>n</i> -Hexane/CHCl ₃ (1:4)	
41-60	“	25 each
61-64	100% CHCl ₃	50 each
65-115	100% CHCl ₃	25 each
116-136	CHCl ₃ /EtOAc (9:1)	25 each
137-150	CHCl ₃ /EtOAc (3:1)	
151-161	CHCl ₃ /EtOAc (3:2)	
162-204	CHCl ₃ /EtOAc (1:1)	25 each
205-219	CHCl ₃ /EtOAc (2:3)	
220-230	CHCl ₃ /EtOAc (1:3)	
231-240	CHCl ₃ /EtOAc (1:9)	25 each
241-271	100% EtOAc	25 each
272-280	EtOAc/MeOH (95:5)	
281-288	EtOAc/MeOH (90:10)	
289-333	EtOAc/MeOH (90:10)	20 each
334-376	EtOAc/MeOH (85:15)	25 each

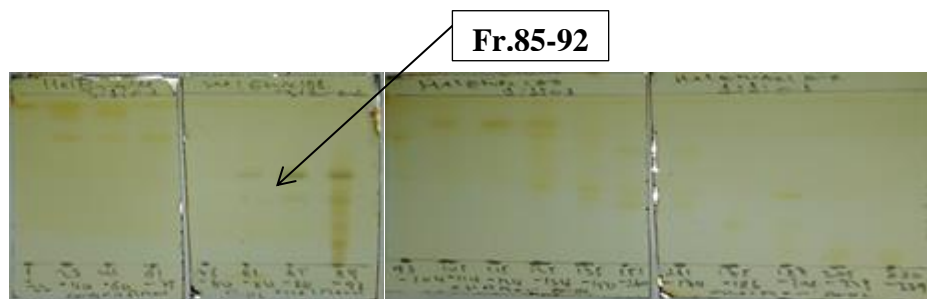


Figure 25. TLC results of combined fractions of chloroform: methanol (1:1) leaves extract of *G. purpurascens*

Dark gel (100 mg) of Fr.85-92 was re-fractionated using silica gel CC (30 g) to give sixty sub-fractions after being eluted with CHCl₃/EtOAc in different polarity ratio. According to

the TLC result, sub-fractions exhibiting similar spot (s) were combined and their TLC profile was again analyzed by UV-lamp followed by iodine vapor (Figure 26).

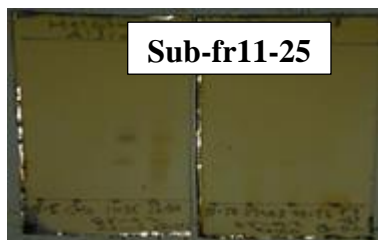


Figure 26. TLC analysis of combined sub-fractions of Fr.85-92 of chloroform: methanol (1:1) leaves extract of *G. purpurascens*

The sub-fraction 11-25 (Figure 26) exhibited two spots with close R_f values. This sub-fraction was then concentrated (30 mg), and further purified on PTLC using *n*-hexane/EtOAc/AcOH (3:1:0.1) which resulted in compound **79** (12 mg) after TLC analysis (Figure 27).

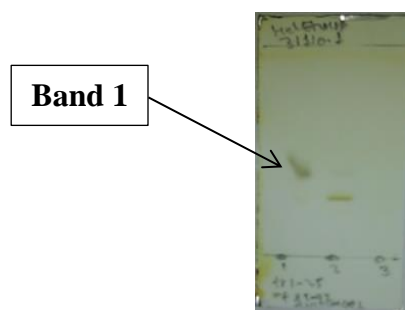


Figure 27. TLC profile of scraped bands on PTLC fractionated sub-fr11-25 of Fr.85-92 of chloroform: methanol (1:1) leaves extract of *G. purpurascens*

3.6 Isolation and identification of endophytic bacteria and associated compounds from *Gloriosa superba*

3.6.1 Isolation of endophytic bacteria

Collected leaves, stems and tubers of *G. superba* were thoroughly washed with tap water to remove attached debris and excess epiphytes. Subsequently, plant tissues were surface sterilized by sequential immersion in 95% (v/v) ethanol (10 s), 5% (v/v) aqueous solution of sodium hypochlorite (2-5 min) and 70% (v/v) ethanol (2 min). Finally, the surface sterilization process was ended by rinsing the plant tissues three times with autoclaved distilled water (to remove excess sterilants) and dried on aluminium foil. All steps in the sterilization procedure were conducted under aseptic condition. Surface sterilized explants

were cut into small segments (2 cm) using sterilized knife and 15 segments of each part were seeded on Petri dishes containing tryptic soy agar (TSA) (g/L) (pancreatic digest of casein, 15.0; peptic digest of soybean meal, 5.0; sodium chloride, 5.0; agar, 15.0; pH 7.3±0.2 at 25 °C) medium augmented with antifungal drug (carbendazim). At the same time, aliquot of last tissue washing was inoculated on TSA for sterility checking. All plates were incubated at 37 °C for 48 hr in duplicates. After incubation, emergence of endophytic bacteria was observed and number of segments colonized by bacterial endophytes was counted. No colony growth was observed in the last washing of the plant tissues, indicative of safe surface sterilization. Out of the emerged bacterial colonies, 30 of colonies with distinct feature (10 from leaves, 12 from stems and 8 from tubers) were sub-cultured several times in fresh TSA until getting pure colonies. Finally, single colony isolates were kept at 4 °C for biochemical and MALDI-TOF MS characterizations. Other duplicates of these pure colonies were preserved at -20 °C using 50% (v/v) glycerol for further sub-culture.

3.6.2 Morphological and microscopic characterization

The colony morphological features (color, form, elevation and margin), on the Petri dish, of all the 30 endophytic bacterial isolates were noted and presented in Table 11. Besides, each isolates were subjected to Gram-staining analyses using standard staining procedure; and their response toward Gram-staining reagent and shape were identified using Olympus microscope. Those spore forming isolates were further subjected to spore staining test using Malachite green reagent to confirm their spore forming ability.

Table 11. Colony morphology and microscopic Gram-staining test

Isolates	Colony morphology				Gram-staining	Shape	Spore forming
	Form	Color	Elevation	Margin			
GSL1	Rhizoid	White grey	Umbonate	Lobate	+	Bacilli	+
GSL2	Rhizoid	White grey	Umbonate	Lobate	+	Bacilli	+
GSL3	Rhizoid	White grey	Umbonate	Lobate	+	Bacilli	+
GSL4	Rhizoid	White grey	Umbonate	Lobate	+	Bacilli	+
GSL5	Irregular	White purple	Umbonate	Undulate	+	Bacilli	+
GSL6	Irregular	White purple	Umbonate	Undulate	-	Rod	-
GSL7	Irregular	White green	Umbonate	Undulate	+	Cocci	-
GSL8	Irregular	Orange	Flat	Undulate	-	Rod	-
GSL9	Irregular	White brown	Flat	Undulate	-	Rod	-
GSL10	Irregular	Light orange	Flat	Undulate	-	Rod	-
GSS1	Rhizoid	White grey	Umbonate	Lobate	-	Rod	-
GSS2	Rhizoid	White grey	Umbonate	Lobate	+	Bacilli	+
GSS3	Rhizoid	White grey	Umbonate	Lobate	+	Bacilli	+
GSS4	Rhizoid	White grey	Umbonate	Lobate	+	Bacilli	+
GSS5	Rhizoid	White grey	Umbonate	Lobate	+	Bacilli	+
GSS6	Rhizoid	White grey	Umbonate	Lobate	+	Bacilli	+
GSS7	Rhizoid	White grey	Umbonate	Lobate	+	Bacilli	+
GSS8	Rhizoid	White grey	Umbonate	Lobate	+	Bacilli	+
GSS9	Rhizoid	White grey	Umbonate	Lobate	+	Bacilli	+
GSS10	Irregular	Brown	Crateriform	Undulate	+	Bacilli	-
GSS11	Irregular	White	Crateriform	Undulate	-	Rod	-
GSS12	Irregular	Brown	Crateriform	Undulate	+	Rod	+
GST1	Rhizoid	White grey	Umbonate	Lobate	+	Bacilli	+
GST2	Circular	Light orange	Raised	Entire	-	Rod	-
GST3	Rhizoid	White grey	Umbonate	Lobate	+	Bacilli	+
GST4	Circular	Light brown	Raised	Entire	-	Rod	-
GST5	Circular	Light brown	Raised	Entire	-	Rod	-
GST6	Rhizoid	Light brown	Umbonate	Undulate	+	Bacilli	+
GST7	Rhizoid	Light brown	Umbonate	Undulate	+	Bacilli	+
GST8	Circular	Brown	Raised	Entire	+	Bacilli	+

3.6.3 Biochemical tests

Both the Gram-positive and Gram-negative endophytic bacterial isolates were subjected to various biochemical tests based on the flow-chart of Bergey's manual of determinative bacteriology¹⁰⁰ to systematically identify them.

Catalase test: All the Gram-positive isolates were subjected to catalase test using a hydrogen peroxide reagent. Briefly, bacterial isolates were inoculated into LB agar (g/L) (tryptone, 10.0; yeast extract powder, 5.0; sodium chloride, 10.0; pH 7.2 ± 0.2). It was incubated at 37 °C for 24 hr. From 24 hr old culture, colonies were taken and placed on

cover slide. A 1 to 2 drops of hydrogen peroxide reagent were added to these endophytic bacterial isolates. Bubble gas formation was checked for these isolates. According to Bergey's manual¹⁰⁰ those isolates forming a spore were further subjected to biochemical tests to tentatively identify in species level as follows.

Starch hydrolysis (amylase test): among the Gram-positive isolates, those spore formers were subjected to starch hydrolysis test to check the presence of amylase enzyme using iodine solution. Few colonies of each isolates were streaked onto a starch agar (g/L) plate (peptone, 5.0; beef extract, 3.0; soluble starch, 2.0; agar, 15.0; pH 7.0) and incubated at 37 °C for 24 hr. After 24 hr incubation, 2-3 drops of iodine solution (10%) were added directly onto the plates. Then, after 10-15 min the absence of a blue black color was monitored.

Voges-Proskauer (VP) test: Isolates showing a positive response toward starch hydrolysis were tested against VP reagents. 48 hr old pure cultures of endophytic bacterial isolates were grown on MR-VP broth medium (glucose phosphate broth) (g/L) (pancreatic digest of casein, 3.5; peptic digest of animal tissue, 3.5; dextrose, 5.0; mono-potassium phosphate, 5.0 at 25 °C and 7±0.2 pH). The broth was gently heated to completely dissolve the ingredients and 1 mL aliquots were pipetted into culture tubes. The culture tubes were sterilized at 121 °C for 15 min and incubated at 35-37 °C for a minimum of 48 hr. A 18 drops (0.5 mL) of Barritt's reagent A (α -naphthol, 5% v/v) and 4 drops (0.2 mL) of Barritt's reagent B (KOH) were added into the culture tube with 1 mL. Then, the tubes were vigorously shaken for 1 min to achieve complete aeration. These tubes were then allowed to stand for 30 min and examined for the formation of pinkish red color. The cell diameter of isolates found as VP positive was measured to check whether their width was $\geq 1\mu\text{m}$ or not while those VP negative isolates were checked for the presence of swollen cell.

Motility test: The motility test was performed for the recent endophytic bacterial isolates. Briefly, sulfide indole motility (SIM) agar medium (g/L) (peptone, 30.0; beef extract, 3.0; peptonized iron, 0.2; agar, 3.0 and $\text{Na}_2\text{S}_2\text{O}_3 \cdot 5\text{H}_2\text{O}$, 0.025 at pH 7.3 \pm 0.2 and 25 °C) was prepared in 1000 mL distilled water. Pure isolates of these endophytes were inoculated into labeled test tubes containing SIM agar medium by means of stab inoculation. The cultures were then incubated at 37 °C for 24 hr. Finally, the motility was observed whether the diffuse zone of growth is restricted or not to the line of inoculation.

Citrate test: Citrate tests were carried out for those endophytic bacteria isolates, which exhibited a diameter of $\leq 1\mu\text{m}$ and non-swollen cell, using Simmon's citrate agar (SCA) (g/L) (ammonium dihydrogen phosphate, 1.0; MgSO_4 , 0.2; K_2HPO_4 , 1.0; $\text{Na}_3\text{C}_6\text{H}_5\text{O}_7$, 2.0; , NaCl, 5.0; bromothymol blue, 0.08 and bacteriological agar, 15.0 at 37 °C and 6.8 ± 0.2 pH). Briefly, a 24.28 g of SCA medium was added in 1000 mL of pure distilled water. The solution is then heated 100 °C. The dissolved medium is then dispensed into tubes and sterilized in an autoclave at 121 °C for 15 min. Once the autoclaving process was completed, the tubes were taken out and cooled at a slanted position at 40-45 °C. Pure colonies were taken from an 18 hr old culture with a sterile inoculating loop and inoculated onto slanted tubes with SCA medium and aerobically incubated at 37 °C for up to 4 days. Finally, the color change from green to blue was observed.

Effect of salt concentration: The endophytic isolates were also checked for their growth tolerance to salt concentration by inoculating few colonies of each isolate onto Tryptic soy agar (g/L) (pancreatic digest of casein, 15.0; peptic digest of soybean meal, 5.0; sodium chloride, 5.0; agar, 15.0; pH 7.3 ± 0.2 at 25 °C) medium supplemented with 6.5% NaCl concentration. After 24 hr incubation, growth of each isolate was checked.

Oxidase reaction test: The reaction towards oxidase reagent of all Gram-negative isolates was analyzed by ripping few colony of new culture of each isolates onto oxidase reagent containing filter paper and the immediate formation of intense purple color was monitored.

Lactose and glucose fermentation test: The formation of yellow color and gas bubble after 24 hr incubation of active cultures on purple broth base indicates that the isolate(s) are lactose and glucose fermenter(s) and gas producer(s), which is indicative of positive reaction toward carbohydrates.

Methyl red (MR) test: MR-VP broth medium (glucose phosphate broth) (g/L) (pancreatic digest of casein, 3.5; peptic digest of animal tissue, 3.5; dextrose, 5.0; mono-potassium phosphate, 5.0 at 25 °C and 7 ± 0.2 pH) was prepared and gently heated to completely dissolve the ingredients and 5 mL aliquots were transferred into culture tubes. These tubes with endophytic bacterial culture were autoclaved at 121 °C for 15 min. The cultures were then incubated at 37 °C for a minimum of 48 hr in ambient air. After incubation, 5 drops of methyl red reagent was added to MR-VP broth and the color change (from yellow to red) in the broth medium was observed.

Indole test: Fresh culture of each isolates was inoculated into a Hi media tryptophan broth (g/L) (Casein enzymatic hydrolysate, 10.0; sodium chloride, 5.0; final pH 7.5 ± 0.2), incubated for 18-24 hr followed by addition of Kovacs indole reagent (0.5 mL) to the broth culture. Then, an observation was made in the formation of a pinkish red color ring on the top of the broth with in few seconds which is an indication of the production of indole from the amino acid tryptophan via deamination and hydrolysis reaction by the enzyme tryptophanase.

Ornithine test: This test is used to check the ability of bacterial isolates to produce decarboxylase enzyme. Actively grown colony of each isolate was inoculated into a test tube which contained a motility-indole-ornithine (MIO) medium (g/L) (Casein enzymatic hydrolysate, 10.0; peptic digest of animal tissue, 10.0; yeast extract, 3.0; L-ornithine hydrochloride, 5.0; dextrose, 1.0; bromocresol purple, 0.02; agar, 2.0; final pH 6.5 ± 0.2 at 25 °C). The test tubes were then incubated for 24 hr at 37 °C and observed for color change from yellow to turbid purple.

Lysine decarboxylase (LDC) test: The lysine iron agar (LIA) medium (g/L) (peptone, 5.0; yeast extract, 3.0; glucose, 1.0; L-lysine, 10.0; ferric ammonium citrate, 0.5; sodium thiosulphate, 0.04; bromocresol purple, 0.02; agar, 15.0; final pH at 25 °C 6.7 ± 0.2) was prepared as per the manufacturer's procedure and dispensed in test tubes. Culture of each isolates was inoculated into the test tubes and incubated at 37 °C for about 24 hr. The change in color from yellow to purple was then monitored.

Phenylalanine test: A slant of phenylalanine agar medium (g/L) (yeast extract, 3.0; sodium chloride, 5.0; DL-phenylalanine, 2.0; disodium hydrogen phosphate, 1.0; agar, 15.0; final pH 7.3 ± 0.2 at 25 °C) was prepared in test tubes and freshly grown culture of each isolate was streaked onto the slant surface. After incubation for 18-24 hr at 37 °C, 4-5 drops of ferric chloride solution (10%, w/v) was added directly to the slant followed by shaking the tube and observing for the development of a dark green color within 1-5 min.

Urease test: Actively grown colony of each isolates was inoculated onto urea agar slant (g/L) (urea, 20; sodium chloride, 5.0; mono potassium phosphate, 2.0; peptone, 1.0; dextrose, 1.0; phenol red, 0.012; agar, 15.0; final pH 6.7 ± 0.2 at 25 °C) in test tube and incubated for 24 hr at 37 °C. The development of a pink color was then examined indicative of the production of urease enzyme.

3.6.4. MALDI-TOF MS Bacterial Identification

The Matrix-Assisted Laser Desorption/Ionization Time-of-Flight Mass Spectrometry (MALDI-TOF MS) analysis was carried out to confirm the identity of endophytic bacterial isolated. Briefly, all isolates were initially purified and representative single colonies of each isolate were smeared as a thin film directly into a spot on MALDI target plate using a tooth applicator. The MALDI-TOF MS target plate was overlaid with 1 μ L of 70% (v/v) formic acid and allowed to dry at room temperature. Immediately the spot was overlaid with 1 μ L of matrix solution (10 mg/mL α -cyano-4-hydroxy cinnamic acid, 50% acetonitrile and 2.5% trifluoroacetic acid) and allowed to dry at room temperature. The resulting spectra of protein part of each isolate were compared with reference spectra by using the Biotyper 3.1 software (Bruker MALDI Biotyper, UK). The identification score cutoff values were applied to each measurement according to the manufacturer's instructions. Isolates with a score of ≥ 2.0 for a given species were considered high confidence identification to the species level; 1.70-1.99 were considered low confidence identification; and 0.00-1.69 were characterized as no organism identification possible. *E. coli* ATCC 25922 was used as a standard for calibration and quality control.

3.6.5 Culture cultivation and ethyl acetate extraction

Six isolates of endophytic bacteria, namely, GST8 (*B. subtilis*), GST2 (*E. coli*), GST5 (*E. coli*), GST4 (*E. coli*), GSL5 (*B. subtilis*) and GSS7 (*B. amyloliquefaciens*), were selected as representatives and subjected to fermentation process to cultivate and scale up of the respective cultures for extraction of secondary metabolites. A single colony of each isolate was picked up and inoculated in separate Erlenmeyer flask (500 mL) containing tryptone soya broth (TSB, 250 mL) aseptically and placed on orbital shaking incubator (121 rpm at 28 °C) for 8 days avoiding of any antibiotics. Fermented cultures were filtered using muslin cloth and cell free culture filtrates were liquid-liquid partitioned with equal amounts of ethyl acetate. The ethyl acetate phases were separated; dried over Na₂SO₄ anhydrous and concentrated using rotavapor leading to 0.2, 2.6, 3.5, 0.044, 0.064 and 0.16 g crude yields for GST8 (*B. subtilis*), GST2 (*E. coli*), GST5 (*E. coli*), GST4 (*E. coli*), GSL5 (*B. subtilis*) and GSS7 (*B. amyloliquefaciens*) isolates, respectively. The chemical profile of all these ethyl acetate extracts was monitored with TLC analysis using DCM/EtOAc/Acetic acid

(3:1:0.1) solvent system and UV-lamp followed by vanillin/MeOH/H₂SO₄ (0.3:95:5) visualizing techniques (Figure 28).



Figure 28. TLC profiles of ethyl acetate extracts of fermented endophytic bacterial culture filtrates

Finally, the ethyl acetate extract of GST5 (*E. coli*) isolate (3.5 g) was fractionated over silica gel column chromatography as follows.

3.6.6 Fractionation of GST5 (*Escherichia coli*) ethyl acetate extract

A yellowish powder (3.0 g) of ethyl acetate extract was reconstituted in EtOAc (30 mL), adsorbed on 10 g of silica gel and applied over CC packed with DCM saturated silica gel (150 g). Elution was started with 100% DCM, followed by gradient of DCM/EtOAc and ended with EtOAc/MeOH (95/5) to collect one hundred thirteen fractions (Table 12). Collected fractions were analyzed for their TLC profiles using DCM/EtOAc/AcOH (9:1:0.1 and 3:1:0.1) under the visualizing techniques, UV-lamp (254 and 365 nm) and iodine vapor. Fractions with similar chemical profile were combined and their TLC analysis was conducted.

Table 12. Collected fractions of ethyl acetate extract of GST5 (*Escherichia coli*) endophytic bacterium culture filtrate

Fraction No.	Solvent system	Volume (mL)
1-12	DCM/EtOAc (90/10)	50
13-18	DCM/EtOAc (80/20)	50
19-25	DCM/EtOAc (60/40)	50
26-32	DCM/EtOAc (40/60)	50
33-40	DCM/EtOAc (20/80)	50
41-100	100% EtOAc	20
101-113	EtOAc/MeOH (95/50)	20

Unfortunately, the combined fractions exhibited similar TLC profile both under iodine and vanillin visualizing reagents with DCM/EtOAc/AcOH (3:1:0.1) as a solvent system. Hence, all the fractions (1-113) were recombined, concentrated (200 mg) and subjected to silica gel CC separation as follows. Fr1-113 (200 mg), after dissolved in ethyl acetate and adsorbed on silica gel, was sub-fractionated on CC packed with 30 mg of silica gel solvated with 100% DCM. Fifty sub-fractions were eluted using 100% DCM, DCM/EtOAc (80/20 and 60/40) and 100% EtOAc solvent systems. After TLC examination under the solvent systems of 100% DCM and DCM/EtOAc/AcOH (9:1:0.1) and detection methods of UV-lamp and vanillin, sub-fraction 1-5, sub-fraction 9-12, sub-fraction 13-16, sub-fraction 17-19 and sub-fraction 21-50 were combined and subjected to TLC analysis (Figure 29).

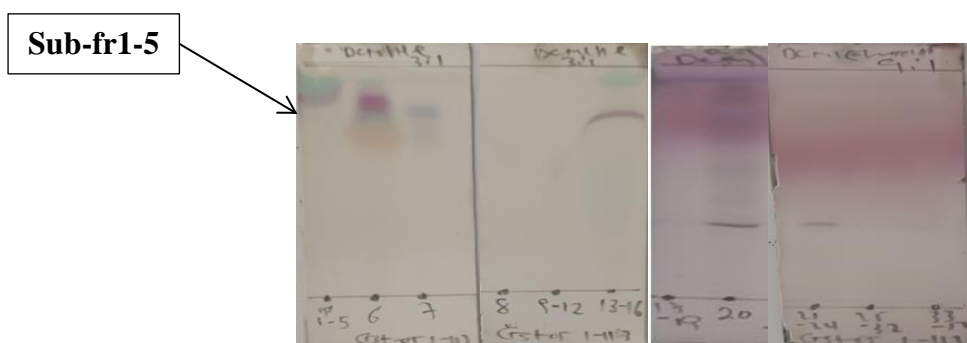


Figure 29. TLC profiles of combined sub-fractions of Fr.1-113 of GST5 (*Escherichia coli*) ethyl acetate extract

Among the combined sub-fractions (Figure 29), sub-fr1-5 indicated a better purity on TLC and afforded compound **80** (20 mg).

3.7 Instrumentation

All the NMR (^1H , ^{13}C and DEPT-135) experiments were performed on a BRUKER ACQ 400 AVANCE spectrometer operating at 400 MHz (for ^1H) and 100 MHz (for ^{13}C and DEPT-135) equipped with a 5 mm proton probe under a temperature of 298 K with topspin software (version 2.1). All chemical shifts (δ_{ppm}) of the spectra were recorded relative to an internal TMS reference. Spectral data were processed using MestReNova software (Mestrelab Research S.L., version 12). The FT-IR experimental process was run on Spectrum 65 FT-IR (PerkinElmer) in the wavenumbers range of 4000-400 cm^{-1} with 4 cm^{-1} resolution and 4 number of scans using the KBr pellets. The measured ASCII data were then converted and processed via OriginPro2019b.Win software into FT-IR spectral graphs (% transmittance versus wavenumbers in cm^{-1}). The GC-MS instrumentation were done on 7890B (Agilent Technologies, USA) equipped with an HP 5MS non-polar column (internal diameter of 30 m \times 250 μm and 0.25 μm of film thickness). Helium was used as carrier gas with a flow rate of 1 mL/min. The injector temperature was set at 230 $^{\circ}\text{C}$ and the injection mode was a split mode with 10:1 of split ratio. The oven temperature was initially set at 40 $^{\circ}\text{C}$ for 5 min and was elevated to 250 $^{\circ}\text{C}$ with a rate of 6 $^{\circ}\text{C}/\text{min}$ held for 20 min. The total run-time was 60 min. The MS part was run on 5977A Network (Agilent Technologies) and operated in the EI mode at 70 eV. All spectra were scanned from 50-650 m/z range and compounds were identified by comparing their mass spectra with those possible compounds searched from the database of NIST11 (National Institute of Standards and Technology, Gaithersburg, USA). Relative amounts of identified compounds were calculated based on the peak areas of the total ion chromatograms (TIC). The MALDI-TOF MS analysis was carried out at NAHDIC, Ethiopia using the direct smear method (MALDI Biotyper 3.1. User Manual, Bruker Daltonics Inc.).

3.8 *In vitro* antimicrobial activity evaluation of crude extracts of medicinal plants, and endophytes and compounds

3.8.1 Antibacterial activity assay

The antibacterial activity for both crude extracts of medicinal plants and endophytes and isolated compounds of each studied plants was evaluated against three standard human pathogens, namely, *Staphylococcus aureus* (*S. aureus*, ATCC 25923), *Escherichia coli* (*E. coli*, ATCC 25922) and *Pseudomonas aeruginosa* (*P. aeruginosa*, ATCC 27853) bacterial

strains. Experimental activity was conducted at microbiology laboratory of medical laboratory department, Haramaya University. Agar medium disc-diffusion technique was followed to evaluate the antibacterial effectiveness of each extracts and compound isolates using the standard protocols of Clinical and Laboratory Standards Institute (CLSI).

In this study, pure MHA media (Hi media) was prepared according to the manufacturer's general instruction. 0.5 McFarland standard solution was also prepared by adding 0.5 mL of 0.048 M BaCl₂ (1.175% W/V, BaCl₂.H₂O) to 99.5 mL of 0.18 M H₂SO₄ (1% V/V) with constant stirring to bring to 10⁸ CFU/mL solution^{50,101}.

Freshly grown colonies (3-5) of similar morphology of the respective bacterial species were transferred with a sterile inoculating loop aseptically into a liquid medium (saline solution). And the turbidity was adjusted to be equal with 0.5 McFarland standard solution (10⁸ CFU/mL). Then, each bacterial suspension was inoculated onto Petri plates containing the MHA by swapping with cotton swap. A sterilized Whatman No. 1 filter paper discs (6 mm in diameter) were prepared using a puncher for loading tested solution.

A stock solution of each extracts (200 mg in 2 mL) and isolated compounds (5 mg in 5 mL) of each studied plant was prepared in 4% DMSO. Three concentrations of 50,000, 25,000 and 12,500 µg/mL were prepared from stock solutions of each extracts using the two fold serial dilution method¹⁰². Four various solutions , 500, 300, 100 and 50 µg/mL of each compounds were also prepared from their corresponding stock solutions. Whereas each ethyl acetate extract of each culture filtrate of GST8 (*B. subtilis*), GST2 (*E. coli*), GST5 (*E. coli*), GST4 (*E. coli*), GSL5 (*B. subtilis*) and GSS7 (*B. amyloliquefaciens*) endophytic bacteria was tested against individual bacterium at concentration of 1000 µg/mL. Chloramphenicol impregnated standard disc (30 µg) and DMSO solvent were served as positive and negative control, respectively. Thereafter, each concentration (100 µL) was loaded onto separate paper discs (as thick as the chloramphenicol disc) followed by putting the discs onto the Petri plates containing the bacterial culture inoculated MHA and incubated them at 37 °C for 18-24 hr. Inhibition zones were indicated by clear area around the paper disc which were measured by caliper (in mm) to evaluate the degree of susceptibility of the bacterial strains to the tested analytes. Each experiment was done in duplicate aseptically and result was presented as mean ± standard deviation after statistical analysis with SPSS software (version 20).

3.8.2 Antifungal activity assay

The chloroform: methanol (1:1) extracts of *C. purpurea* (leaves and roots), *C. speciosa* (stems), *G. superba* (tubers) and *G. purpurascens* (leaves) were assessed for their antifungal activity against *Candida albicans* ATCC 10231 using the disc diffusion method. A PDA medium was prepared as per the instruction of the manufacturer. The chloroform: methanol (1:1) extracts of the plants were selected among other extracts because of their relatively highest yields and compounds were better separated during TLC. Analysis. The PDA containing plate was then inoculated with *Candida albicans* suspension by streaking with a sterilized swab very well. Similar to the antibacterial activity experiment, four concentrations (12,500, 25,000, 50,000 and 100,000 $\mu\text{g/mL}$) of the chloroform:methanol extracts of the plants were prepared in DMSO and 100 μL amount of each concentration was loaded onto sterile Whatman filter paper disc (6 mm) and impregnated discs were placed onto the surface of the inoculated agar plates using sterile forceps. Commercial Ketoconazole/Tilt disc (10 $\mu\text{g/disc}$) was used as a positive control. Then, the PDA plates were sealed with Para film and incubated at 27 °C for 3-5 days for fungal growth. After incubation, the diameters of the zone of inhibition around each disc were measured using caliper (in mm). Experiments were conducted in duplicate and results were expressed in mean and standard deviation.

3.9 *In vitro* antioxidant activity examination evaluation of crude extracts of the medicinal plants and isolated compounds

The *in vitro* antioxidative effect of crude extracts and isolated compounds of investigated plant species was evaluated via two assays, DPPH free radical and ferric reducing antioxidant power (FRAP).

3.9.1 DPPH free radical scavenging assay

DPPH free radical trapping power of crude extracts and isolated compounds, including a standard antioxidant ascorbic acid, was evaluated by adopting the procedure of Khorasani Esmaeili *et al.*¹⁰³ with some modification. Six different concentrations, 500, 250, 150, 100, 50 and 25 $\mu\text{g/mL}$ of crude extracts, isolated compounds and ascorbic acid (AA) were prepared from corresponding stock solutions (1 mg/mL in MeOH). To each of the above

concentrations, freshly prepared DPPH solution (2 mL, 0.004% w/v in MeOH) was added followed by incubating for 30 min at room temperature. After incubation, each concentration was subjected to UV-Vis spectrophotometer read at 517 nm to measure their absorbance. The analyte free DPPH solution and Ascorbic acid (AA) in methanol were used as negative and positive controls, respectively. The antioxidant potential of each tested analyte was evaluated in terms of percentage scavenging activity using the following formula (1):

$$\text{DPPH scavenging activity (\%)} = \left(1 - \frac{A}{A_0}\right) \times 100\% \quad (1)$$

Where, A and A₀ are absorbance of DPPH containing tested samples including AA and negative control (DPPH solution, 0.004% w/v in MeOH), respectively.

DPPH free radical trapping power of extracts and compounds was compared with that of ascorbic acid (AA), also expressed in terms of IC₅₀ (the concentration needed to scavenge the total DPPH radicals by 50%). This IC₅₀ value was obtained from the regression equation derived from percentage scavenging activity versus concentration graph of each tested samples. The experimental activity was repeated twice and were subjected to statistical analysis and described as mean ± standard deviation.

3.9.2 Ferric reducing antioxidant power (FRAP) assay

The working principle of ferric reducing antioxidant power assay is expressed in terms of the ferric ion (Fe³⁺)-ligand complex reduction by antioxidants to the ferrous ion (Fe²⁺) complex under acidic condition which can be monitored via the formation of intense blue color. In the present study, ferric reducing power of crude plant extracts and isolated compounds was studied by employing the experimental procedure stated by Do *et al.*¹⁰⁴ with little change. In brief, the assay involved the following experimental steps. Similar to DPPH assay mentioned above, six different concentrations (500, 250, 150, 100, 50 and 25 µg/mL in H₂O) of each sample was prepared in test tubes from stock solution (1 mg/mL in H₂O, each). Then, each concentration was mixed with 0.2 M potassium phosphate buffer (2 mL, pH 6.6) and potassium ferricyanide (2.5 mL, 10% w/v) solutions followed by incubation at 40 °C for 30 min. Trichloroacetic acid (2.5 mL, 10% w/v) was then added to the incubated solutions; centrifuged for 10 min at 3000 rpm and a supernatant (5 mL) of each solution was mixed with distilled water (2 mL) and ferric chloride (0.5 mL, 0.1% w/v). Same preparation was also followed for the positive control, ascorbic acid. Lastly, absorbance of each reacted

mixtures was read at 700 nm UV-Visible spectrophotometer. The ferric ion reducing power of each tested extracts and compounds was determined by the increase in absorbance recorded in duplicate and compared with ascorbic acid. Recorded individual absorbance was subjected to SPSS (version 20) of statistical software to express as mean \pm standard deviation.

3.10 *In silico* molecular modeling study

The molecular binding capacity of the isolated compounds **65-69** was studied by docking against *E. coli* gyraseB (PDB ID: 6F86), *S. aureus* pyruvate kinase (PDB ID: 3T07) and human peroxiredoxin 5 (PDB ID: 1HD2) protein models. The compounds **65-68, 70** and **79** were also docked against the *P. aeruginosa* PqsA (5OE3) enzyme. The molecular docking analysis was performed using the AutoDock vina tools (version 4.2) to predict the potential binding mode of isolated compounds into the selected protein models. Polar hydrogen atoms and Gasteiger partial atomic charges were added. All rotatable bonds of the compounds, defined by default of the program, were allowed to rotate during the automated docking process. Then prepared protein and compound structures were saved in the PDBQT format suitable for calculating energy grid maps and analysed using Autodock vina. The maintaining space of the grid box was considered at 0.375 Å with the grid box size of 46×46×46 Å points. The Lamarckian genetic algorithm (LGA) program with an adaptive whole method search in the AutoDock vina was chosen to calculate the different conformers of compounds. After 200 independent docking runs for each compound, a cluster analysis was done. In accordance to the root mean squared deviation (RMSD), tolerance of 2.0 Å conformations was clustered and ranked by energy. The conformation with the best scored pose between the protein models and isolated compounds with the lowest binding energy was considered for the compounds. The molecular docking results were analysed based on the binding energy (kcal/mol) and number of binding interactions between catalytic amino residues and isolated compounds. The drug-likeness, ADME and toxicity property predictions of the isolated compounds were also computed by SwissADME, PreADMET and OSIRIS property explorer software.

4 Results and Discussion

In this study, four plant species, namely, *C. purpurea* (leaves and roots), *C. speciosa* (stems), *G. superba* (tubers) and *G. purpurascens* (leaves) were extracted through successive solvent extraction technique and investigated for their phytochemical constituents, *in vitro* antimicrobial and antioxidant activities. Besides, the leaves of *C. purpurea* were studied for isolation of possible alkaloidal constituent by applying the “acid-base shake-out” extraction method. During the course of this study, an attempt for the first time was also made to explore endophytic bacteria from the leaves, stems and tubers of *G. superba*. The overall results of the present finding are discussed below.

4.1 Structural elucidation of the isolated compounds

4.1.1 Compounds isolated from the roots and leaves of *Cadia purpurea*

The phytochemical investigation of different extracts of *C. purpurea* leaves and roots led to the isolation and identification of six compounds (Figure 30), two from the leaves (**65** and **66**), three from the roots (**68**, **69** and **70**) and one from both (**67**).

Compound 65: It was found as dark brown amorphous (26 mg); R_f 0.4 ($\text{CHCl}_3/\text{acetone}$; 1:1).

In the ^1H (400 MHz), ^{13}C and DEPT-135 (100 MHz) NMR spectra, an olefinic methine carbon signal at δ_C 122.6 (C-6) together with its multiplet proton signal at δ_H 5.27 (H-6) and a quaternary carbon signal at δ_C 138.9 (C-5) were observed. Besides, olefinic terminal methylene and methine carbon signals were existed at δ_C 113.9 (C-24) and 139.3 (C-23), respectively, in the ^{13}C spectrum, along with methylene proton signals (δ_H 4.85, *cis* H-24, br d, $J = 10.55$ Hz; δ_H 4.92, *trans* H-24, br d, $J = 17.02$ Hz) and multiplet methine proton signal at δ_H 5.73 (H-23, m) in the ^1H spectrum. The ^{13}C and DEPT-135 spectra showed 22 identifiable signals attributed to 24 carbon atoms and belonged to 11 methylene (δ_C 29.3, 39.7, 29.1, 22.6, 33.8, 27.1, 66.7, 31.9 and 113.9; C-1/2, C-4, C-7, C-11, C-12, C-15/16, C-21, C-22 and C-24) of which the latter is terminal sp^2 methylene; 8 methine (δ_C 73.9, 122.6, 38.6, 49.9, 56.6, 55.9, 45.8 and 139.4; C-3, C-6, C-8, C-9, C-14, C-17, C-20 and C-23); 2 methyl (δ_C 13.9 and 14.0; C-18 and C-19); and 3 quaternary carbons (δ_C 138.9, 42.1 and 48.8; C-5, C-10 and C-13) of which the former is sp^2 quaternary carbon. Moreover, the ^1H spectrum supported the presence of two methyl groups which were identified by observing

two singlet proton signals at δ_{H} 0.80 (18-CH₃) and 0.94 (19-CH₃) integrated to three proton numbers each. Furthermore, the two carbon signals at δ_{C} 73.9 and 66.7 along with multiplet and doublet of doublet proton signals at δ_{H} 3.63 (H-3, m) and 3.91 (H-21, dd, $J = 1.79$ and 1.79 Hz), were due to the presence of hydroxylated methine (C-3) and methylene (C-21) carbon atoms, respectively, implied that compound **65** exhibited a secondary and primary alcohol groups. The compiled NMR data is presented in Table 13 (¹H, ¹³C and DEPT-135 NMR spectral data: See Appendix Table 1). The IR spectrum also provided additional information regarding the presence of hydroxyl groups which showed an absorption band at 3426 cm^{-1} . In addition, the IR spectrum showed three peaks at 2918-2848, 1622 and 1462 cm^{-1} which corresponded to the -CH, exocyclic C=C and C-O stretchings, respectively. In the EI GC/MS spectrum, a [M-3]⁻ peak was observed at m/z 354.9 (C₂₄H₃₈O₂, calculated for 358) along with a base peak at m/z 68.1 (C₅H₈, calculated for 68) and three other intense fragment peaks at 95.0 (C₇H₁₁), 82.0 (C₆H₁₀) and 123.2 (C₈H₁₁O). The general skeletal structure of compound **65** was found to be closely related to a tetracyclic sesterterpene type of steroid with the presence of two olefinic bonds, one is endocyclic double bond between C-5 and C-6) and the second double bond is exocyclic olefinic bond between C-23 and C-24). Based on the overall spectral information, the chemical structure of compound **65** was determined as 2,3,4,7,8,9,10,11,12,13,14,15,16,17-tetradecahydro-17-(1-hydroxypent-4-en-2-yl)-10,13 dimethyl-1H-cyclopenta[a]phenanthren-3-ol (Figure 30), which was found as new compound.

Compound 66: It was obtained as white yellowish powder (25 mg); mp. 250-253 °C (lit. value 251-253°C)⁹⁷; R_f 0.7 (EtOAc/MeOH/AcOH; 3:1:0.1)..

In the ¹H spectrum (Appendix Table 2), two clear doublet proton signals were occurred at δ_{H} 6.48 (H-6, d, $J = 2.02$ Hz) and 6.82 (H-8, d, $J = 2.02$ Hz) which were due to the *meta* coupling between H-6 and H-8 of A-ring of glycone flavone type of flavonoid with AB spin system and small coupling constants (⁴J). Besides, two additional doublet proton signals (integrated to two symmetric protons, each) were shown at δ_{H} 7.94 (H-2'/6', d, $J = 8.69$ Hz) and 6.98 (H-3'/5', d, $J = 8.69$ Hz) which indicated the presence of two protons with an AA'BB' spin pattern of *para* substituted aromatic B-ring (H-2'/6' and H-3'/5'). The sharp singlet proton signal at δ_{H} 6.71 was assigned to H-3 of the aglycone unit of compound **66**¹⁰⁵. From ¹³C and DEPT-135 spectra, eight quaternary carbon signals were identified, of which

one was due to the carbonyl carbon of the C-ring (δ_C 181.2, C-4), two were ascribed to the hydroxylated carbons of the A-ring (δ_C 160.1, C-5 and δ_C 163.9, C-7); and the remaining five were belong to C-2 (δ_C 161.5), C-9 (δ_C 156.1), C-10 (δ_C 105.6), C-1' (δ_C 120.2) and a hydroxyl bearing C-4' (δ_C 160.0). In the IR spectrum, absorption bands at 3426 (sharp intense), 1657, 1602 and 1170-1038 cm^{-1} were shown due to the hydroxyls (OHs), carbonyl (C=O), C=C and C-O stretching, respectively, of the dehydroflavone part. The chemical shifts and multiplicities of the aglycone flavone backbone of compound **66**, in the NMR spectra, were found in strong agreement with reported data¹⁰⁶ of same structure regardless of the peak intensity of the carbons (observed weak in compound **66**, which might be due to short scanning time).

Furthermore, two doublet proton signals were observed at δ_H 5.25 (H-1'', d, $J = 7.46$ Hz) and 5.31 (H-1''', d, $J = 1.70$ Hz) along with two oxygenated carbon signals at δ_C 99.6 (C-1'') and 101.4 (C-1''') indicative of the presence of two anomeric carbons. This ascertained that the dehydroflavone portion of compound **66** contained disaccharide moieties. One of the two sugar moieties was recognized as glucose (the inner one) known by the existence of a hydroxylated sp^3 methylene group signal at δ_H 3.93 (H-6'', m) and δ_C 59.4 (C-6'') together with the anomeric carbon signal at δ_C 99.6 (C-1'') and its corresponding doublet proton signal at δ_H 5.31 (H-1''', d, $J = 1.70$ Hz). The second sugar unit was identified as a rhaminose (the terminal one) due to the presence of characteristic doublet proton signal at δ_H 1.36 (H-6''', d, $J = 6.17$ Hz) and a carbon signal at δ_C 15.5 (C-6''') of the methyl group of the saccharide. The remaining proton signals of the two sugar units were appeared as multiplets at the proton chemical shift range of 3.57-3.98, except for the methine protons attached to C-4'' and C-4''', respectively, of the glucose and rhaminose sugars which were observed as triplet signals at δ_H 3.40-3.45 (H-4''/4''', t, $J = 18.32$ Hz). The IR spectrum also showed a peak at 2918 cm^{-1} which represents -CH stretching of the aliphatic groups of the sugar moieties. The doublet signal of H-8 at δ_H 6.82 ($J = 2.02$ Hz) and carbon signal of C-7 at δ_C 163.9 of the A-ring were found in the downfield shift with respect to H-6, suggesting that the disaccharide chain was affixed to C-7. The obtained spectral data was compiled as shown in Table 14. Based on the spectral information and reported data¹⁰⁶ for same compound, the structure of compound **66** was identified as apigenin-7-*O*-rhaminoglucoside, also known as apigenin-7-*O*-neohesperidoside (Figure 30). To our

information, compound **66** was reported herein for the first time from the leaves of *C. purpurea*.

Compound 67: It was obtained both as white brown amorphous (67 mg) from alkaloidal crude leaves extract and yellow powder (300 mg); m.p. 151-154 °C (lit. value, 153-154 °C)⁹⁸ from methanol roots extract; R_f 0.2 (EtOAc/MeOH/AcOH; 1:1:0.1).

The ¹H spectrum (Appendix Table 3) displayed a total of twenty seven integrated proton signals attributed to a methine –CH-N- (δ_{H} 4.36, H-6, m), a methylene –CH₂-N- (δ_{H} 4.57, H-10, d, $J = 4.54$ Hz) and other aliphatic groups. The proton spectrum also showed two deshielded broad singlet signals at δ_{H} 6.97 (1H, H-4', br s) and 6.95 (1H, H-6', br s), and an olefinic methine signal at δ_{H} 6.24 (1H, H-5', dd, $J = 6.23, 6.22$ Hz). A broad singlet proton signal was also observed at δ_{H} 4.98, which might be due to the presence of a 2^o amine group. The resulted ¹³C and DEPT spectra showed twenty carbon signals attributed to a quaternary carbon of an amide group (δ_{C} 171.9, C-2), nine methylene carbons (δ_{C} 33.0, 19.4, 26.5, 33.9, 27.3, 46.9, 36.4, 28.4 and 49.9; C-3, C-4, C-5, C-7, C-8, C-10, C-12, C-14 and C-15, respectively), and five methine carbons (δ_{C} 60.7, 32.4, 57.5, 67.6 and 51.9; C-6, C-9, C-11, C-13 and C-17, respectively). The remaining five carbon signals belonged to two quaternary carbon signals appeared at δ_{C} 160.0 (ester C=O, C-1') and 122.8 (C-2'), and three olefinic methine carbon signals shown at δ_{C} 123.3, 110.3 and 116.2 (C-4', C-5' and C-6', respectively). The obtained NMR spectral information highlighted the presence of a lupanine portion of a quinolizidine type of alkaloid along with an esterified pyrrolicarboxyl substituent. In the FT-IR spectrum, absorption bands of amide carbonyl functional group and –CH stretching of *trans* quinolizidine of the lupanine structure were observed at the wavenumbers of 1616 (lactam C=O) and 2910-2841 cm⁻¹, respectively. Besides, the IR spectrum showed absorption bands at 1692 and 3238 (broad) cm⁻¹ which belonged to the ester carbonyl functional group (C=O) and –NH stretching, respectively, of the pyrrolicarboxyl substituent. A similar lupanine alkaloidal compound with esterified pyrrolicarboxyl as a substituent at C-13 was also reported in literature¹⁰⁷. The NMR spectra and FT-IR spectrum of compound **67** isolated from the roots part were also found to be the same to the one discussed above. The overall NMR spectral result (Table 15) of compound **67** was found to be closely matched with the data reported by Asres *et al.*¹⁰⁷ for calpurnine isolated from leaves of Ethiopian *Calpurnia aurea* subsp. *aurea*. Taking into account the

resulted spectral values and in comparison to reported data¹⁰⁷ of calpurnine, the structure of compound **67** was deduced as 13-*O*-pyrrolicarboxyl lupanine (Figure 30).

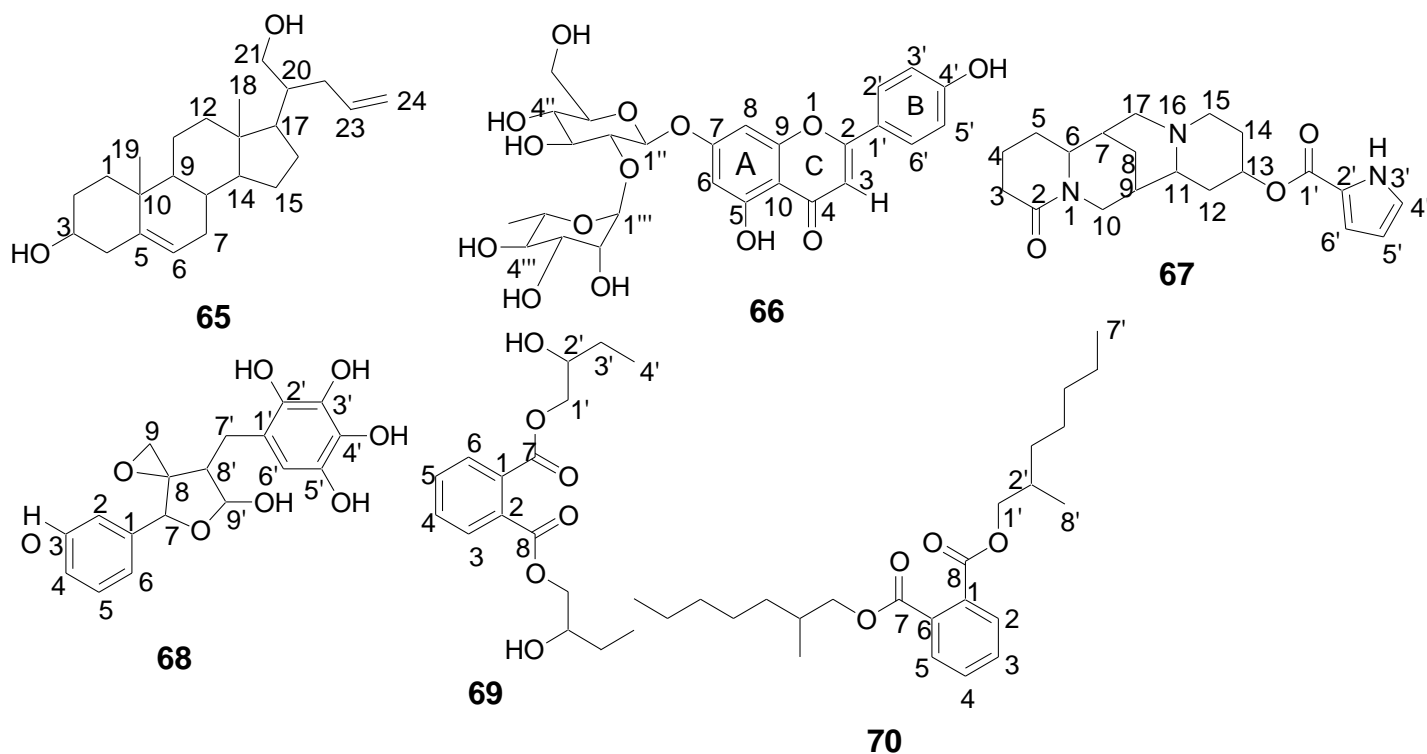


Figure 30. Structures of compounds **65-70** isolated from leaves and roots of *C. purpurea*

Compound 68: It was found as colorless amorphous (10 mg); R_f 0.2 (100% DCM).

The ^1H spectrum (Appendix Table 4) showed a proton signal at δ_{H} 7.37 (1H, H-5, br d, $J = 8.3$) and two broad singlet signals at δ_{H} 6.72 (1H, H-6) and 6.43 (1H, H-4) of the aromatic region. Additionally, the ^1H spectrum displayed two unprecedented upshifted aromatic proton signals at δ_{H} 5.92 (1H, H-2, d, $J = 1.6$) and 5.90 (1H, H-6', d, $J = 1.7$) which might be due to a long range coupling (4J) of aromatic protons resulted in small coupling constants. The proton signal at δ_{H} 5.48 (1H, H-9', d, $J = 6.7$) along with another overlapped singlet proton signal at δ_{H} 5.46 (1H, H-7) indicated the existence of hydroxylated and oxygenated protons, respectively. The additional information obtained from the ^1H spectrum was the occurrence of two multiplet signals at δ_{H} 3.67 (1H, H-8') and 2.37 (2H, H-7') which were due to a methine and methylene protons, respectively, of aliphatic group. In the aliphatic region a singlet proton signal, integrated for two protons, was also observed at δ_{H} 1.25 (2H, H-9) indicative of the presence of methylene group positioned at a quaternary carbon.

In the corresponding ^{13}C spectrum, eighteen carbon signals were appeared at δ_{C} 157.0 (C-3), 156.7 (C-5'), 154.2 (C-1), 148.1 (C-2'), 141.7 (C-3'), 132.1 (C-5), 117.9 (C-4'), 112.7 (C-1'), 109.8 (C-6), 104.7 (C-4), 103.7 (C-2), 101.3 (C-6'), 93.9 (C-9'), 78.5 (C-7), 77.2 (C-8, concealed by the solvent peak), 66.5 (C-9), 40.2 (C-8') and 29.7 (C-7'). The DEPT-135 spectrum, in its downfield region, confirmed the existence of seven quaternary signals at δ_{C} 157.0 (C-3), 156.7 (C-5'), 154.2 (C-1), 148.1 (C-2'), 141.7 (C-3'), 117.9 (C-4') and 112.7 (C-1'), and five methine signals at δ_{C} 132.1 (C-5), 109.8 (C-6), 104.7 (C-4), 103.7 (C-2) and 101.3 (C-6') suggestive of the occurrence of two unsymmetrically hydroxylated aromatic rings. The DEPT-135 spectrum also indicated the presence of unprecedented upfield quaternary signal at δ_{C} 77.2 (C-8); three methine signals at δ_{C} 93.9 (C-9'), 78.5 (C-7) and 40.2 (C-8'); and two methylene signals at δ_{C} 29.7 (C-7') and 66.5 (C-9). The overall spectral information indicated that compound **68** contained two unsymmetrical benzene rings bridged with four carbons and having different hydroxylation pattern. Of the 18 total carbons, six were appeared as a hydroxylated trihydrofuran and epoxide form which shared a quaternary carbon (δ_{C} 77.2, C-8). In summary, the combined NMR spectral data inferred that compound **68** was found to be a new epoxy lignan derivative and its proposed structure is shown in Figure 30.

Compound 69: It was isolated as yellow amorphous (10 mg); R_f 0.3 ((DCM/EtOAc/AcOH, 9:1:0.1).

The ^1H NMR spectrum (Appendix Table 5) showed two proton signals (each integrated for two protons) at δ_{H} 7.72 (2H, H-3/6, dd, $J = 3.2, 3.7$) and 7.53 (2H, H-4/5, dd, $J = 3.2, 3.7$) indicative of the presence of two protons of symmetrical *ortho* disubstituted aromatic ring with AA'BB' spin system. In addition, a quartet signal with large coupling constant was observed at δ_{H} 4.37 (4H, H-1'/1'', $J = 21.4$) which revealed the presence of two symmetric oxygenated methylene protons. Furthermore, the ^1H spectrum showed the existence of a multiplet signal at δ_{H} 3.81 (2H, H-2'/2'') which was due to the appearance of two hydroxylated symmetric methine protons. In the aliphatic region of the ^1H spectrum, a multiplet signal was also shown at δ_{H} 1.25 (4H, H-3'/3'') which belonged to two equivalent methylene groups. A triplet proton signal was also observed at δ_{H} 0.89 (6H, H-4'/4'', $J = 11.0$) implied the presence of terminal methyl group.

In the corresponding ^{13}C spectrum, eight signals were observed at δ_{C} 167.7 (C-7/8), 132.2 (C-1/2), 128.9 (C-3/6), 130.9 (C-4/5), 77.2 (C-2'/2''), 61.7 (C-1'/1''), 29.7 (C-3'/3'') and 14.1 (C-4'/4''), which attributed to sixteen carbon atoms. The DEPT-135 spectrum indicated the presence of four signals (two =CH-, one -CH- and one -CH₃) pointing upward and two signals (-CH₂-O- and -CH₂-) pointing downward. The resulted ^{13}C and DEPT-135 spectra also showed the presence of two quaternary carbons at δ_{C} 167.7 (C-7/8). Based on the the overall spectral information, the structure of compound **69** was established as bis-(2-hydroxybutyl) phthalate, a new phthalate derivative (Figure 30).

Compound 70: Compound **70** was obtained as yellow brown amorphous (45 mg); R_f 0.6 (DCM/EtOAc/AcOH (1:1:0.1)).

The ^1H NMR spectrum showed a methylene signal at δ_{H} 4.24 (H-1'/1'', dd, $J = 1.82, 2.11$ Hz), integrated for four protons. Besides, proton signals at δ_{H} 0.98 (d, $J = 7.28$ Hz) and 0.94 (t, $J = 10.98$ Hz), each integrated for six protons, implying that there were four methyl groups, in which the first two (C-8'/8''-CH₃) were attached to an sp³ methine carbons (C-2'/2'') while the latter two (C-7'/7''-CH₃) were found to be terminals affixed to the sp³ methylene carbons (C-6'/6''). The presence of two symmetric sp³ methine groups were also confirmed by the proton signal at δ_{H} 1.71 (H-2'/2'', m) in the ^1H spectrum. Another eight symmetric methylene protons were appeared at δ_{H} 1.36 as multiplet integrated for a total of sixteen protons. Furthermore, two proton signals (integrated for two protons each) at δ_{H} 7.74 (H-2/5, dd, $J = 3.68, 3.68$ Hz) and 7.64 (H-3/4, dd, $J = 3.68, 3.68$ Hz) were indicative of four symmetric aryl protons having same coupling pattern.

From the ^{13}C and DEPT-135 NMR spectra, twelve intense carbon peaks were showed which ascribed for twenty four carbon atoms. These twelve signals belonged to two ester carbonyl carbons (δ_{C} 167.9, C-7/8), two oxymethylene carbons (δ_{C} 67.7, C-1'/1''), two methine carbons (δ_{C} 38.8, C-2'/2''), six aromatic carbons (δ_{C} 132.2, C-1/6; δ_{C} 128.5, C-2/5; δ_{C} 131.0, C-3/4), two terminal methyl carbons (δ_{C} 13.1, C-7'/7''), two side chain methyl carbons (δ_{C} 10.1, C-8'/8'') and eight aliphatic methylene carbons (δ_{C} 23.6, C-3'/3''; δ_{C} 28.7, C-4'/4''; δ_{C} 30.2, C-5'/5''; δ_{C} 22.7, C-6'/6''). ^1H , ^{13}C and DEPT-135 NMR spectral values are summarized in Appendix Table 6; The IR spectrum showed three peaks at 1727, 1282 and

745 cm^{-1} , which were due to the presence of ester C=O, C-O and –CH stretches of aromatic protons, respectively. The GC-MS data indicated a peak at retention time of 37.03 min and a molecular ion peak $[\text{M}]^+$ at m/z of 390. This was found to be compatible with the molecular composition of $\text{C}_{24}\text{H}_{38}\text{O}_4$. Based on these spectral information, the structure of compound **70** was deduced as di-(2-methylheptyl) phthalate (Figure 30) which was also reported by Rameshthangam and Ramasamy¹⁰⁸.

Most of the phthalates and their derivatives are petrochemicals which have been used as plasticizers in chemical industry to improve the plasticity and flexibility of the industrial products^{109,110}. For the past several decades, phthalates have been known as totally synthetic compounds and environmental pollutants of industrial origin than biogenic source. However, this perception has been changed following the isolation of many phthalic compounds like di-(2-ethylhexyl) phthalate¹¹¹, dibutyl phthalate (DBP)¹¹⁰, from unpolluted natural sources such as algae, bacteria, fungi, higher plants, etc. Owing to this, there are controversies among researchers on the real origin of these compounds. Some argue that those phthalates isolated from living organisms are industry origins which leached to the environment and later absorbed by the organisms. Others have different point of view saying that phthalates can be biogenic or endogenous naturally originated from the bio-sources^{110,112}. The latter idea has been supported by a reported experimental evidence in which natural phthalate biosynthesis was observed in two labeled alga via the analysis of the natural abundance ^{14}C content of two isolated phthalates, dibutyl phthalate (DBP) and di-(2-ethylhexyl) phthalate (DEHP), and compared with industry originated standard plasticizers of the two. The shikimic acid pathway was the proposed and recognized biosynthetic pathway of the phthalates like DBP^{110,113}. However, researchers still believe that further experimental evidences are needed to judge phthalates can really be natural products than they are totally antropogenic origin.

4.1.2 Compounds isolated from *Caralluma speciosa* stems

Previously reported phytochemical studies on the genus *Caralluma* have revealed that members of this genus have been dominated by the C-21 steroidal like compounds, known as pregnanes. Such classes of compounds exhibit in common fused tetracyclic skeletal structure with mainly two methyl groups at C-10 and C-13 and two extended carbon-chain

at C-17 position. Pregnane compounds differ to each other by the presence or absence of different sugar units and other aglycone esterified groups (such as acetyl, benzoyl and tigloyl) at different position of the basic skeleton⁹¹. In the present investigation three pregnane derivatives (**73**, **74** and **75**) and two non-pregnane compounds (**71** and **72**) (Figure 31) were isolated from chloroform and methanol extracts. This is the first of their isolation from the stems part of *C. speciosa*. The detailed structural interpretation of the compounds is communicated as follows.

Compound 71: It was isolated as yellow powder (104 mg); R_f 0.95 (*n*-Hexane/EtOAc/AcOH; 1:1:0.1).

From the ^1H , ^{13}C and DEPT-135 NMR spectra, aliphatic proton and carbon signals (including methyl group) were observed at δ_{H} 0.88-2.04 and δ_{C} 14.6- 34.3 ppm, respectively. Briefly, in the ^1H spectrum, a multiplet methine signal at δ_{H} 5.80 (1H, H-2) and a doublet of doublet methylene signal at δ_{H} 4.96 (2H, dd, H-1, $J = 16.4, 11.1$ Hz) were appeared to indicate the presence of an olefinic bond. It also displayed three aliphatic methylene multiplet signals, integrated for two, four and forty two protons, respectively, at δ_{H} 2.06 (2H, H-3), 1.38 (4H, H-4/26) and 1.25 (42H, H-5 to H-25) and a triplet methyl signal at δ_{H} 0.88 (3H, H-27, $J = 12.87$ Hz). The existence of the olefinic bond was also evidenced by the appearance of methine (=CH-) and methylene (=CH₂) carbon signals at δ_{C} 139.8 (C-2) and 114.5 (C-1), respectively, in the ^{13}C and DEPT-135 spectra. The ^{13}C and DEPT-135 spectra also showed six aliphatic carbon signals, which attributed to twenty five carbons, at δ_{C} 34.3 (C-3), 32.4 (C-25), 29.9 (C-5 and -6), 30.2 (C-4 and C-7 to C-24), 23.2 (C-26) and 14.6 (C-27). The absence of any quaternary carbon signal in the DEPT-135 spectrum also confirmed that compound **71** was a member of a straight chain alkene. See Appendix Table 7 for detailed ^1H , ^{13}C and DEPT-135 spectral data. In the IR spectrum, an intense peak was observed at 2918-2848 cm^{-1} indicative of CH- stretching of alkyl including methyl groups. Additionally, a strong -C=C- stretching and =CH- bending bands were shown at 1462 and 717 cm^{-1} , respectively. The GC/MS spectrum shows a major chromatogram peak at the retention time of 40.73 min and a weak molecular ion peak at m/z of 380.4 in the positive ion mode which was compatible with the molecular weight of 378 $[\text{M}+2]^+$. Besides, a base peak at m/z of 57.1 was observed which represents the chemical composition of C₄H₉ (MW, 57). Moreover, three fragment ions were appeared at m/z of 71.1, 85.1 and 55.1, which

belong to the elemental compositions C₅H₁₁ (MW, 70), C₆H₁₃ (MW, 85) and C₄H₇ (MW, 55), respectively. This led to the assignment of entire molecular formula of compound **71** as C₂₇H₅₄. Based on the above spectral information, the structure of compound **71** was deduced as heptacos-1-ene (Figure 31).

Compound 72: It was found as dark semisolid (186 mg); R_f 0.3 (*n*-Hexane/EtOAc/AcOH; 1:1:0.1).

From the ¹H NMR spectrum, two doublet of doublet signals were observed at δ_H 7.53 (2H, dd, *J* = 4.45, 4.87 Hz) and 7.70 (2H, dd, *J* = 4.45, 4.87) due to the protons of symmetrical *ortho* disubstituted aromatic ester with an AA'BB' spin system. The spectrum also showed an intense multiplet proton signal at the chemical shift range of 1.25-1.36, integrated for a total of 16 protons, indicated the presence of eight methylene (-CH₂-) protons at similar chemical environment. In addition, aliphatic proton signal was observed at δ_H 4.21 (4H, br t, *J* = 12.38 Hz) for two set of oxygenated methylenes neighboring with a multiplet signal at δ_H 2.33 (2H) of methine protons. The ¹H spectrum also showed a doublet of doublet signal at δ_H 0.89 (6H, dd, *J* = 9.83, 12.04) due to two symmetric methyl protons adjacent to two non-equivalent methylene protons; and a triplet signal at δ_H 0.78 (6H, t, *J* = 8.56) for two symmetric methyl protons next to two equivalent methylene protons, each.

In the ¹³C spectrum, three aromatic carbon signals at δ_C 128.6, 130.7 and 132.2 along with an ester carbonyl carbon signal at δ_C 167.6 were observed which were due to the presence of two symmetrically esterified benzoic aromatic groups; and this was supported by the DEPT-135 spectrum in which two quaternary carbon signals (132.2 and 167.6) and a signal at δ_C 68.0 (C-1/1') of two symmetric oxygenated methylene carbons were revealed. The DEPT-135 spectrum also indicated the presence of an intense methine carbon signal at δ_C 38.5 (C-2/2') together with two consecutive methyl carbon signals at δ_C 10.8 and 13.9 ascribed to two equivalent methyl groups, each.

The IR spectrum showed an absorption peak of the ester carbonyl group (C=O) of the phthalate unit at 1734 cm⁻¹ together with the C-O and aromatic C-H stretching at wavenumbers of 1274 and 731 cm⁻¹, respectively. It also displays an intense peak at 2918-2855 cm⁻¹ which represents the -CH stretching of the long chain alkyl groups. From the GC/MS spectrum, a molecular ion peak at *m/z* 390 in the EI-MS and major peak with retention time of 37.031 min in the GC, was observed which is compatible with the

molecular formula of C₂₄H₃₈O₄ (calculated MW, 390). A base peak at *m/z* 149.0 (calcd. 149.0 for C₈H₅O₃) was also obtained, including four relatively intense product ions at *m/z* 167.0 (C₈H₇O₄, calcd. MW, 167), 57.1 (C₄H₉, calcd. MW, 57), 71.0 (C₅H₁₁, calcd. MW, 71) and 279.0 (C₁₆H₂₃O₄, calcd. MW, 279). Taking into account the spectral information discussed above and compared with reported data^{111,114}, the structure of compound **72** was elucidated as di-(2-ethylhexyl) phthalate (Figure 31). This compound **72** is reported herein for the first time from the genus, *Caralluma*.

Compound 73: It was obtained as yellow brown amorphous (104 mg); R_f 0.85 (DCM/EtOAc/AcOH; 3:1:0.1).

It is observed that the ¹H and ¹³C NMR spectra contained many complicated aliphatic proton and carbon signals at δ_H 0.88-2.02 and δ_C 10.5- 55.7 ppm, respectively. This showed that compound **73** contained a pregnane nucleus in its entire structure. The ¹H spectrum also showed three multiplet signals at δ_H 3.30-3.33 (1H, m, H-3), 4.76-4.79 (1H, br d, H-12, *J* = 9.91 Hz) and 5.32-5.39 (1H, m, H-20) due to three oxymethinic protons at C-3, C-12 and C-20, respectively, of the pregnane skeleton. An oxygenated quaternary carbon (-C-OH) signal at δ_C 86.5 was also observed in the DEPT-135 spectrum, assigned to C-14 of the pregnane skeleton⁹¹. Besides, the three neighboring singlet proton signals observed at δ_H 1.04 (3H, s, H-18), 0.88 (3H, s, H-19) and 1.24 (3H, s, H-21) assigned to three methyl groups at C-18, C-19 and C-21, respectively, of the pregnane backbone; and a multiplet signal observed at the δ_H range of 1.64-1.79 belonged to three methine protons (H-5, H-8 and H-9) at C-5, C-8 and C-9, and a methylene protons (H-11) at C-11 (Appendix Table 9). The overall spectral data of the pregnane aglycone (mostly considered as the nucleus of all pregnane compounds of the genus, *caralluma*) is in close agreement with spectral information in literature⁹¹. The ¹H spectrum also showed the presence of two consecutive doublet of doublet and broad triplet signals at δ_H 7.88-7.92 (2H, dd, H-3'/7'; *J* = 7.74, 7.74 Hz) and 8.14-8.18 (2H, br t, H-3'/7'; *J* = 18.32 Hz) integrated for two protons each; two pseudo triplet signals at δ_H 7.24-7.28 (2H, t, H-4'/6'; *J* = 12.95 Hz) and 7.30-7.34 (2H, t, H-4'/6'; *J* = 12.95 Hz) integrated for two protons each; and triplet of triplet and broad quartet signals at δ_H 7.49-7.59 (1H, tt, H-5'; *J* = 12.95, 14.10 Hz) and 7.68-7.73 (1H, br q, H-5'; *J* = 26.07 Hz) which were due to *ortho*, *meta* and *para* protons (at C-3'/7', C-4'/6' and C-5',

respectively) of two benzoyl units with AA'BB'C type of spin system. This confirmed that the pregnane core possessed two set of esterified groups positioned at C-12 and C-20 (Appendix Table 9).

From the ^{13}C spectrum, those three signals shown at δ_{C} 73.8, 86.5 and 70.4 were attributed to three oxygenated carbon signals (C-12, C-14 and C-20, respectively) of the pregnane part (Appendix Table 9). Besides, the three consecutive signals at δ_{C} 10.5, 12.5 and 19.2 were because of the presence of three methyl carbons (C-18, C-19 and C-21, respectively) of the pregnane unit. Furthermore, six carbon signals were observed at δ_{C} 129.2 (C-3'/7', *ortho* carbons of the benzoyl-12), 129.6 (C-3'/7', *ortho* carbons of benzoyl-20), 127.9 (C-4'/6', *meta* carbons of the benzoyl-12), 128.3 (C-4'/6', *meta* carbons of the benzoyl-20), 132.3 (C-5', *para* carbon of the benzoyl-12) and 132.8 (C-5', *para* carbon of the benzoyl-20). The presence of the two ester groups of the benzoyl moieties (at C-12 and C-20) was also witnessed by the presence of two ester carbonyl carbon signals at δ_{C} 165.8 (C-12) and 166.4 (C-20) in the ^{13}C spectrum. In the DEPT-135 spectrum, seven quaternary signals were confirmed; three signals at δ_{C} 35.2, 53.2 and 86.5 due to the C-10, C-13 and C-14 (oxygenated with OH) of the pregnane unit; two signals at δ_{C} 130.4 and 130.5 belong to C-2' of the two benzoyl groups; and the remaining two signals at δ_{C} 165.8 and 166.4 due to the two carbonyl carbons of the benzoyl ester groups. The overall ^{13}C and DEPT-135 data of the aglycone part of compound **73** were found to be in a good correlation with the one from literature state⁹¹. The ^1H spectrum also showed many multiplet signals of oxymethinic protons in the chemical shift range of 3.53-4.98 ppm. This indicated the presence of sugar moieties within the pregnane unit. The number of consecutively connected saccharide units can be recognized by the number of anomeric carbon signals at around δ_{C} 90-110 and anomeric proton signals at δ_{H} 4-5 ppm⁹¹. In our case, the presence of two intense carbon signals at δ_{C} 95.3 (C-1'') and 99.1 (C-1''') in the ^{13}C spectrum together with two proton signals at δ_{H} 4.96-4.98 (1H, br d, H-1'', $J = 10.52$ Hz) and 4.89-4.90 (1H, br d, H-1''', $J = 6.89$ Hz) in the ^1H spectrum inferred that there were two anomeric carbons and associated protons which belong to two interlinked sugar moieties. In addition, two proximate carbon signals at δ_{C} 57.0 (C-7'') and 57.7 (C-7''') along with two intense singlet proton signals at δ_{H} 3.53 (3H, s, H-7'') and 3.54 (3H, s, H-7''') were observed which ascribed to two methoxy (MeO-) groups. This revealed that the two sugar units were cymarose-I (C-1'') and

cymarose-II (C-1''')⁹¹. Besides, the presence of two methyl groups at δ_C 17.9 and 18.1 (C-6'' and C-6''', respectively) and at δ_H 1.32 (6H, br s, H-6'' and H-6''') in combination with the methylene carbon signal (δ_C 36.1, C-5'' and C-5''') and multiplet proton signal (δ_H 1.64-1.79, 4H, m, H-5'' and H-5''') was additional evidence to the two sugar moieties to be cymarose-I and II. In reference to reported data for similar compound⁹¹, the disaccharide units were attached to the pregnane unit at C-3 (δ_C 72.2) by taking into account the strong 3J correlation between the aglycone pregnane proton H-3 (δ_H 3.30-3.33, 1H, m) and the anomeric carbon C-1'' (δ_C 95.3) of cymarose-I in the HMBC spectrum. The interlinkage of the sugar chain was identified from HMBC spectrum showing 3J correlations between H-1''' (δ_H 4.89-4.90, 1H, br d) and C-4'' (δ_C 82.3). The IR spectrum also provided supportive information by showing major bands at 3420, 2918-2848, 1713 and 710 cm^{-1} which belong to hydroxyl, alkyl, carbonyl and aromatic groups, respectively. Based on the spectroscopic data (Appendix Tables 9 and 10) and the comparison with reported data of similar compounds^{91,92,93}, the structure of compound **73** was proposed as 12 β ,20-*O*-dibenzoyl-14 β -hydroxy-5 α ,6 dihydropregane-3-*O*- β -cymaropyranosyl-(1 4)- β -cymaropyranoside (Figure 31).

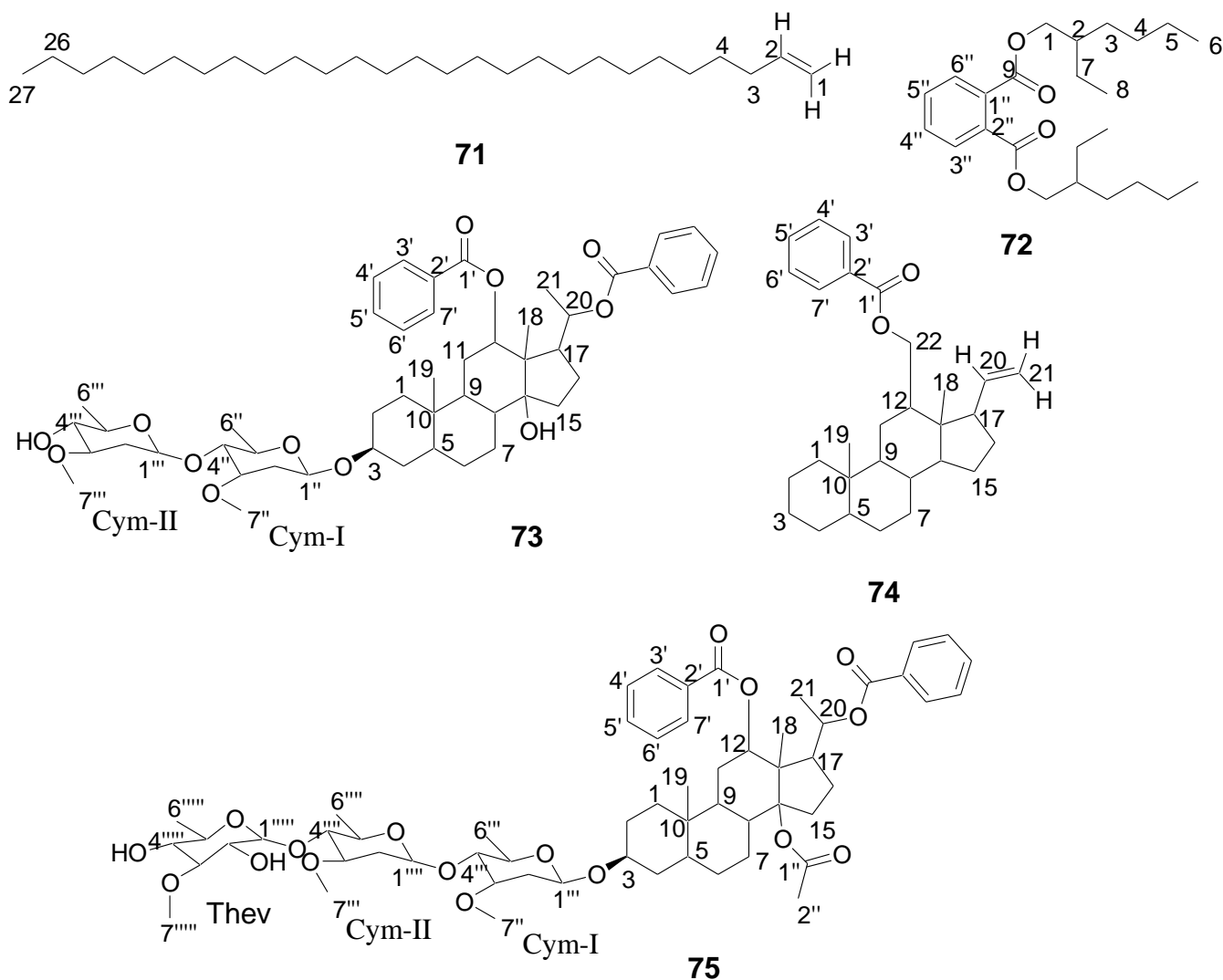


Figure 31. Structures of compounds **71-75** isolated from *C. speciosa* stem

Compound 74: It was isolated as yellowish amorphous (127 mg); R_f 0.35 (Hexane/EtOAc/AcOH; 1:1:0.1).

The acquired 1H , ^{13}C and DEPT-135 spectra confirmed the presence of a pregnane aglycone nucleus as in compound **73**. Unlike to compounds **73** and **75**, however, no glycoside units were observed and instead an olefinic bond between C-20 and C-21 was presented in the pregnane skeleton of compound **74**. This was evidenced by the appearance of a multiplet at δ_H 6.83 (1H, m, H-20), and two doublet at δ_H 5.33 (1H, d, H-21, $J = 15.20$, *cis*) and 5.78 (1H, d, H-21, $J = 17.40$, *trans*) proton signals in the 1H spectrum which belong to the olefinic protons (methine

and methylene) of the pregnene. The ^{13}C spectrum also showed two carbon signals at δ_{C} 139.3 (C-20) and 114.1 (C-21) for terminal olefinic methine (=CH-) and methylene (=CH₂) carbons, respectively, (Appendix Table 11). Furthermore, the NMR spectra showed the presence of methylenoxy-benzoyl ester moiety positioned at C-12 of the aglycone pregnane unit of compound **74**. This was confirmed by the presence of an oxygenated methylene carbon signal at δ_{C} 68.3 (C-22) in the ^{13}C and DEPT-135 spectra and methylene proton signal at δ_{H} 4.98 (2H, m) in the ^1H spectrum. Moreover, a carbon signal at δ_{C} 167.9 (C-1') from the ^{13}C spectrum, for the ester carbonyl, a broad singlet at δ_{H} 8.04 (2H, br s, H-3'/7') and two broad triplets at δ_{H} 7.57 (2H, br t, H-4'/6', $J = 17.70$ Hz) and 7.80 (1H, br t, H-5', $J = 16.82$ Hz) proton signals in the ^1H spectrum were observed to indicate the presence of an esterified benzoyl substituent. But, herein, it is very important to note that the attachment of the benzoyl ester moiety outside the pregnane aglycone nucleus (C-22) of compound **74** was unprecedented in other pregnane compounds. That is, pregnane compounds are known by containing glycoside and/or non-sugar (like benzoyl, acetoxy, tigloyl) moieties attached either within the tetracyclic rings or at C-20 of the pregnane skeleton. The phenomenon in which the benzoyl ester moiety presented at C-22 of compound **74** might be either due to the presence of additional methyl group at C-12 or a methyl ester of benzoyl substituent which latter was incorporated to the non-methylated (at C-12) of the basic pregnane structure.. The IR absorption bands at 1733, 1274 and 710 cm^{-1} were suggestive of ester carbonyl, C-O and aromatic group of the esterified phenyl moiety. The absorption peaks shown at 2918-2848 and 1462 cm^{-1} were belong to the stretching of C-H alkyl groups and C=C, respectively, of the pregnane skeleton. The GC analysis shows a major peak at retention time of 45.01 min with a corresponding weak molecular ion peak at m/z 426 $[\text{M}+6]^+$ of the ES-MS. This is matched with the proposed molecular formula ($\text{C}_{29}\text{H}_{40}\text{O}_2$, calculated MW, 420). Besides, a base peak at m/z 97.1 (C_7H_{13} , MW: 97) is observed together with three intense fragment ions at m/z of 57.1 (C_4H_9 , MW: 57), 83.1 (C_6H_{11} , calculated MW 83) and 69.1 (C_5H_9 , MW: 69). On the basis of the above information, we proposed the chemical structure of compound **74** as ((5R,8R,9S,10S,12R,13R,14R,17R)-hexadecahydro-10,13-dimethyl-17-vinyl-1H cyclopenta[a]phenanthren-12-yl)methyl benzoate (Figure 31).

Compound 75: It was obtained as brown gel (157 mg); R_f 0.23 (DCM/EtOAc/AcOH; 9:1:0.1).

The ^1H , ^{13}C and DEPT-135 spectral feature (Appendix Table 12) of compound **75** was found to be resemble to that of compound **73**. That is, in compound **75** also, two set of benzoyl ester groups attached to the pregnane skeleton at C-12 and C-20 were observed in which their spectral data were compatible with that of compound **73** with a slight change both in chemical shift and multiplicities. The only notable difference was the presence of two exclusive spectral information observed from the spectral results of compound **75**. The first one was the appearance of one additional terminal glycoside unit assigned as thevetose (they) identified by the presence of three additional major carbon signals at δ_{C} 104.7, 61.0 and 18.2 attributed to another anomeric (C-1'''''), methoxy (C-7''''') and methyl (C-6''''') carbons. The presence of this glycoside unit was further confirmed by the corresponding broad doublet (δ_{H} 4.27, 1H, br d, H-1''''', $J = 4.26$ Hz), singlet (δ_{H} 3.77, 3H, s, H-7''''') and broad singlet (δ_{H} 1.34, 3H, br s, H-6''''') signals of the anomeric, methoxy and methyl protons, respectively, in the ^1H spectrum. The second information was the incorporation of an acetyl moiety to the pregnane aglycone skeleton of compound **75** attached at C-14 (δ_{C} 87.1). This was witnessed by the presence of a deshielded signal of methyl protons at δ_{H} 2.81 (3H, s, H-2'') along with their carbon signal at δ_{C} 22.3 (C-2'') in the ^1H and ^{13}C NMR spectra (Appendix Table 12 and 13). Moreover, a downshielded carbon signal at δ_{C} 175.7 (C-1'') was recognized in the ^{13}C and DEPT-135 spectra due to the quaternary carbonyl carbon of the acetyl group⁹¹. The small increment in chemical shift (+0.6 ppm) of C-14 (δ_{C} 87.1) in this compound in comparison to C-14 (δ_{C} 86.5) of compound **73** might also be further assertion to the incorporation of acetyl moiety to the pregnane nucleus of compound **75** at C-14⁹¹. Some supportive absorption bands were also observed in the IR spectrum at wavenumbers (cm^{-1}) of 3426 (OH stretches), 2918-2848 (alkyl C-H stretching), 1713 (carbonyl groups), 1455 (C-O stretching) and 710 (aromatic groups). Based on the spectral data presented above, the structure of compound **75** was identified to be \Rightarrow 12 β ,20-*O*-dibenzoyl-(1 \rightarrow 4) β -acetyl-5 α ,6-dihydropregane-3-*O*- β -thevetopyranosyl-(1 4)- β -cymaropyranosyl-(1 4)- β -cymaropyranoside (Figure 31).

4.1.3 Compounds isolated from *Gloriosa superba* tubers

Compound 76: It was found as white powder (21 mg); R_f 0.3 (DCM/*n*-hexane, 3:1); mp. 134-135 °C (lit. value, 134-135 °C)⁹⁹.

The ¹H NMR spectrum showed a total of fifty integrated protons attributed to nine methine (CH), eleven methylene (CH₂), six methyl (CH₃) and one hydroxyl (OH) groups. The appearance of a multiplet signal at δ_H 5.36 (1H, H-6) indicated the presence of an olefinic methine proton. A multiplet signal at δ_H 3.56 (1H, H-3) was indicative of a methine proton attached to a hydroxylated carbon and the multiplet signal at δ_H 2.31 (2H, H-4) was due to the methylene (CH₂) protons attached to the hydroxylated carbon. The appearance of two singlet signals at δ_H 0.67 (3H, H-18) and 1.00 (3H, H-19) was a confirmation of the existence of two methyl groups positioned at quaternary carbons. Besides, three doublet signals, integrated for three protons each, were observed at δ_H 0.92 (3H, H-21, d, $J = 6.46$), 0.84-0.86 (3H, H-27, d, $J = 7.68$) and 0.82 (3H, H-26, d, $J = 1.92$), suggestive of the presence of three methyl groups positioned at tertiary carbons. A broad triplet signal at δ_H 0.76-0.80 (3H, H-29, br t, $J = 16.18$) was also appeared to represent a methyl group affixed at a secondary carbon. The remaining methine and methylene protons were appeared as multiplet signals at δ_H 1.25-1.86 and that of the OH proton at 1.92 as singlet. The ¹³C and DEPT-135 spectra (Appendix Table 14) displayed twenty nine clear carbon signals for three were quaternary, six methyl (CH₃), nine methine (CH) and eleven methylene (CH₂) groups appeared at δ_C 140.8 (C-5), 121.8 (C-6), 56.8 (C-14), 71.8 (C-3), 56.0 (C-17), 50.1 (C-9), 45.8 (C-24), 42.3 (C-13), 42.3 (C-4, overlapped), 39.8 (C-12), 37.1 (C-1), 36.5 (C-10), 36.2 (C-20), 33.9 (C-22), 31.9 (C-7), 31.9 (C-8, overlapped), 31.7 (C-2), 29.7 (C-23), 29.1 (C-25), 28.3 (C-16), 24.3 (C-15), 23.1 (C-28), 21.1 (C-11), 19.8 (C-26), 19.4 (C-19), 19.0 (C-27), 18.8 (C-21), 12.0 (C-29) and 11.9 (C-18). The quaternary carbon at δ_C 140.8 (C-5) along with the methine carbon signal at δ_C 121.8 (C-6) witnessed the existence of an olefinic bond between C-5 and C-6. The signal appeared at δ_C 71.8 (C-3) revealed the presence of oxygenated carbon. The overall NMR spectral data of compound **76** is in agreement with values reported in literature⁹⁹ for β -sitosterol. Hence, the structure of compound **76** was suggested as β -sitosterol (Figure 32).

Compound 77: It was obtained as colorless semisolid (6 mg); R_f 0.6 (*n*-Hexane/DCM, 1:1). The acquired ^1H , ^{13}C and DEPT-135 spectra ((Appendix Table 14)), revealed that compound **77** was also found as β -sitosterol derivative with the presence of monounsaturated fatty acid ester as substituent. In the ^1H spectrum, two multiplet proton signals were observed at δ_{H} 5.38 and 5.40 (integrated for one proton, each) which belonged to an olefinic methine protons. Besides, in the aliphatic region of the ^1H spectrum, many overlapped multiplet methylene protons and a triplet signal (δ_{H} 0.90, 3H, t, $J = 5.79$ Hz) of methyl group of fatty acid were appeared. The ^{13}C and DEPT-135 spectra also supported the presence of monounsaturated fatty acid substituent by showing a carbonyl carbon signal at δ_{C} 173.3, two olefinic carbon signals at δ_{C} 130.0 and 129.8, fourteen methylene carbon signals at δ_{C} 23.1-34.7 and a methyl carbon signal at δ_{C} 14.1. This information led to the identification of the monounsaturated fatty acid to be oleic acid ester which was incorporated to the β -sitosterol skeleton at C-3, recognized by the comparatively downfield methine proton (δ_{H} 4.65, H-3) and carbon (δ_{C} 73.7) signals. The overall spectral interpretation of the β -sitosterol part remained the same as compound **76**. Based on these spectral data ((Appendix Table 14)), the structure of compound **77** was elucidated as β -sitosterol oleate (Figure 32).

Compound 78: It was found as a yellow semisolid (50 mg), R_f 0.4 (EtOAc/DCM/AcOH, 9:1:0.1)

The ^1H NMR spectrum presented two broad triplet signals at δ_{H} 7.73 (2H, H-3/6, br t, $J = 7.98$) and 7.53 (2H, H-4/5, br t, $J = 7.98$) each integrated for two protons, which is an indicative of the existence of four aromatic methine protons. A multiplet signal resonated at δ_{H} 4.39 for four protons (4H, H-1'/1'') was also observed representing two symmetrically oxygenated methylene protons (-CH₂-O-). Besides, a triplet signal of six protons observed at δ_{H} 0.89 (6H, H-3'/3''), t, $J = 11.18$) was an indication for the existence of two equivalent terminal methyl groups. Moreover, in the aliphatic region, a multiplet proton signal was shown at δ_{H} 1.36 (4H, H-2'/2''), which attributed to four protons. The ^{13}C spectrum (Appendix Table 15) displayed seven signals appeared at δ_{C} 167.7 (C-7/8), 132.2 (C-1/2), 131.0 (C-4/5), 128.9 (C-3/6), 61.7 (C-1'/1''), 29.7 (C-2'/2'') and 14.1 (C-3'/3''). These carbon signals represented a total of fourteen carbons, and assigned to four quaternary (two C=O and two -C-), four aromatic methine (=CH-), two oxygenated methylene (-CH₂-O-), two aliphatic methylene (-CH₂-) and two methyl (-CH₃) groups as confirmed by the DEPT-

135 spectrum. The compiled spectral data (Appendix Table 15) directed to the structural elucidation of compound **78** as 1,2-dipropyl phthalate (Figure 32).

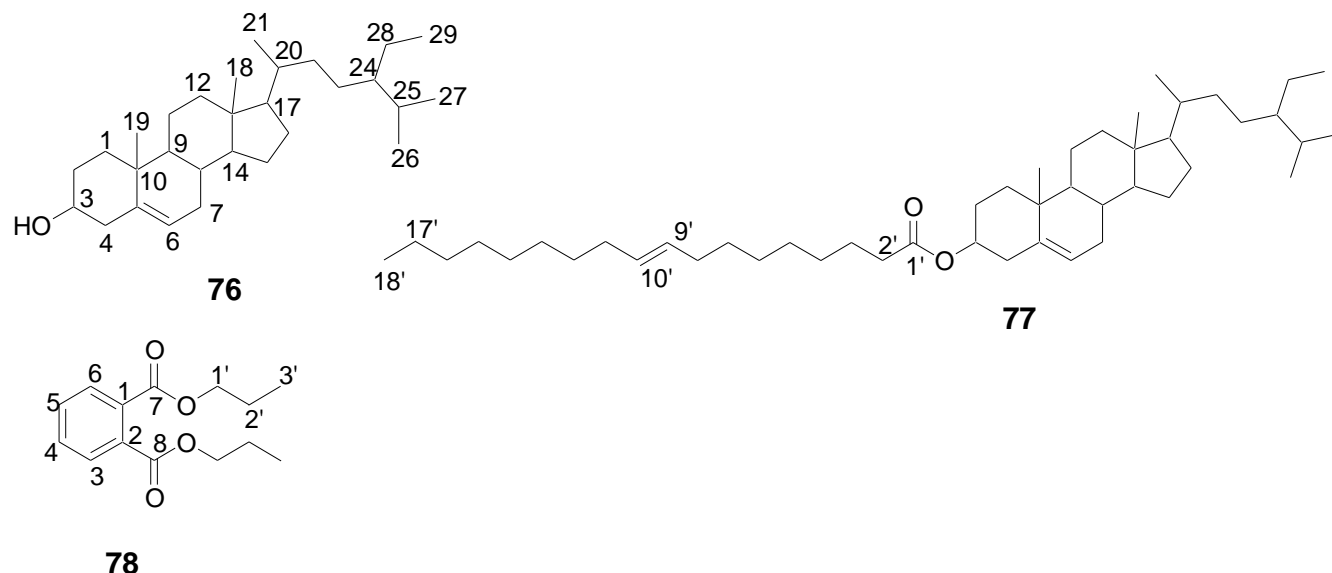


Figure 32. Structures of compounds **76-78** isolated from *G. superba* tubers

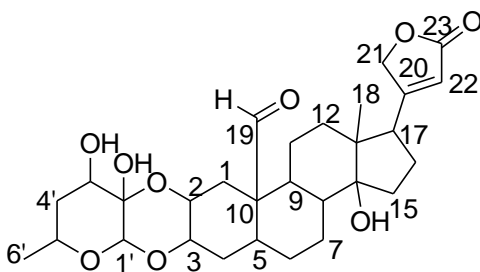
4.1.4 Compound isolated from *Gomphocarpus purpurascens* leaves

Compound 79: It was observed as black gel (12 mg); R_f 0.4 (*n*-Hexane/EtOAc/AcOH, 3:1:0.1)

In the ^1H NMR spectrum (Appendix Table 16) of compound **79**, a deshielded singlet signal at δ_{H} 10.05 (1H, H-19) is due to the aldehydic proton, while a doublet signal at δ_{H} 5.93 (1H, H-22, d, $J = 7.35$) is due to an olefinic methine proton. Moreover, a broad singlet signal was observed at δ_{H} 4.72 (1H, H-1') suggestive of oxygenated methine proton (-O-CH-O-). In addition, a broad doublet signal (integrated for two protons) was observed at δ_{H} 4.53 (2H, H-21, br d, $J = 24.52$) which underlined the occurrence of methylenoxy methylene protons (-CH₂-O-). The ^1H spectrum also confirmed the presence of three additional oxygenated methine protons which appeared as a broad doublet at δ_{H} 4.0 (1H, H-2, br d, $J = 6.06$) and multiplets at δ_{H} 3.89 (1H, H-3) and 3.45 (1H, H-5'). A hydroxylated methine proton (-CH-OH) was also found as a multiplet signal at δ_{H} 3.64 (1H, H-3'). In the aliphatic region, a doublet of doublet signal was appeared at δ_{H} 2.85 (1H, H-17, dd, $J = 10.2, 6.4$) implying the presence of a methine proton attached to a tertiary carbon adjacent to a quaternary olefinic carbon. Moreover, a doublet at δ_{H} 0.94 (3H, H-6', d, $J = 7.1$) and singlet at δ_{H} 0.83 (3H, H-18) signals were observed to confirm the presence of two methyl groups positioned at an

oxygenated tertiary and quaternary carbons, respectively. In the aliphatic region, additional twelve multiplet signals were shown at δ_{H} 2.47 which ascribed to nine different methylene (18H, H-1, H-4, H-6, H-7, H-11, H-12, H-15, H-16 and H-4') and three methine (3H, H-5, H-8 and H-9) groups.

The corresponding ^{13}C and DEPT-135 spectra presented twenty nine unsymmetrical recognizable signals which attributed to seven quaternary, one hydroxylated methine (-CH-OH), four oxygenated methine (-O-CH-O-), one oxygenated methylene (-CH₂-O-), one olefinic methine (=CH-), four aliphatic methine (-CH-), nine aliphatic methylene (-CH₂-) and two methyl (-CH₃) groups. Two of the seven quaternary signals, appeared at δ_{C} 208.0 (C-19) and 175.9 (C-23 overlapped), corresponded to the aldehyde and furan carbonyl carbons, respectively; and the remaining five were belong to two aliphatic carbons at δ_{C} 52.6 (C-10) and 49.0 (C-13), two hydroxylated carbons at δ_{C} 90.4 (C-2') and 84.4 (C-14), and one olefinic carbon at δ_{C} 175.9 (C-20 overlapped). The signal at δ_{C} 116.6 (C-22) was ascribed to the olefinic methine carbon and the one at δ_{C} 71.9 (C-3') belonging to the hydroxylated methine carbon. The signal resonated at δ_{C} 73.9 (C-21) represented the oxygenated methylene carbon. The overall spectral data (Appendix Table 16) is in agreement with the reported data in the literature for calotropin¹¹⁶ and compound **79** (Figure 33).



79

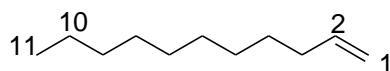
Figure 33. Structure of calotropin (**79**) isolated from *G. purpurascens* leaves

4.1.5 Compound isolated from ethyl acetate extract of *Escherichia coli* (GST5) isolate

Compound 80: It was obtained as colorless oily sample (20 mg); R_f 0.9 (DCM/*n*-hexane, 3:1).

In the ^1H NMR spectrum (Appendix Table 17), a multiplet signal was distinguished at δ_{H} 5.82 for an olefinic methine proton (=CH-). Besides, two doublet signals were observed at

δ_{H} 4.99 (1H, H-1, d, $J = 17.33$ Hz) and 4.93 (1H, H-1, d, $J = 9.76$ Hz) attributed to a *trans* and *cis* protons, respectively, of an olefinic methylene group. Furthermore, the spectrum showed three signals of aliphatic methylene protons and methyl group at the aliphatic region which appeared at the chemical shift values of δ_{H} 2.04 (2H, H-3, br q or m), 1.26 (14H, H-4, H-5, H-6, H-7, H-8, H-9 and H-10, m) and 0.88 (3H, H-11, t, $J = 13.5$ Hz). This information suggests that the isolated compound contained a terminal olefinic bond which was also supported by the presence of two carbon signals at δ_{C} 139.3 (C-2) and 114.1 (C-1) in the ^{13}C and DEPT-135 spectra, which ascribed to the methine and methylene carbons of the alkene group. Moreover, the ^{13}C spectrum demonstrated additional nine carbon signals which represented a total of nine carbon atoms belonging to eight different methylene at δ_{C} 33.8 (C-3), 31.9 (C-9), 29.6 (C-5), 29.5 (C-6), 29.4 (C-7), 29.2 (C-4), 28.9 (C-8) and 22.7 (C-10) and one methyl at δ_{C} 14.1 (C-11) groups. This overall NMR spectral information (Appendix Table 17) inferred that the structure of compound **80** was identified as 1-undecene (Figure 34). Previous research works reported that 1-undecene was produced naturally by some bacterial microbes, mainly *Pseudomonas* species, originated from different types of natural sources. For instance, Tagele *et al.*¹¹⁷ reported that 1-undecene was isolated as the dominant semi-volatile compound from the culture of *Pseudomonas chlororaphis* subsp. *Aurantiaca* strain, isolated from the rhizosphere soil of maize. Zhou *et al.*¹¹⁸ also claimed that *Pseudomonas fluorescens*, isolated as endophytic bacterium from *Atractylodes lancea* seedlings, was found producing 1-undecene. The fatty acid biosynthesis pathway is the means for the production of 1-undecene by the *Pseudomonas* species with the help of a gene *undA* originated from the bacterium^{117,119}. According to one report¹²⁰, 1-undecene, isolated from *Pseudomonas aeruginosa*, was served as olfactory signal which induced a flight and fight responses in worms like *Caenorhabditis elegans* thereby enabling them to defend from bacterial infections.



80

Figure 34. Structure of 1-undecene (80) isolated from ethyl acetate extract of GST5 (*Escherichia coli*) endophytic bacterial culture

4.2 Morphological and biochemical characterization of isolated endophytic bacteria

The leaves and stems segments supported maximum endophytic bacterial emergence (13, 86.7% each), while the minimum bacterial count was observed in the tuber segments (11, 73.3%). From the emerging endophytic bacteria (Appendix Figure 1-), 30 pure isolates (10 from leaves, 12 from stems and 8 from tubers), after several sub-culturing (Figure 35 and Appendix Figure 2), were selected as potential endophytic bacteria with distinct morphological and colony color (Table 11). Among the 30 isolated bacteria, 17 displayed a rhizoid, 9 an irregular and 4 a circular colony forms. Besides, 15 isolates exhibited a white grey color (GSL1, GSL2, GSL3, GSL4, GSS1, GSS2, GSS3, GSS4, GSS5, GSS6, GSS7, GSS8, GSS9, GST1 and GST3), 4 a white brown (GST4, GST5, GST6 and GST7), 3 a brown (GSS10, GSS12 and GST8), 2 a white purple (GSL5 and GSL6), another 2 a light orange (GSL10 and GST2) and the remaining 3 were observed as white green (GSL7), orange (GSL8) and white (GSS11).

The Gram-staining test result (Table 11, Figure 36 and Appendix Figure 3) showed that 21 of the 30 isolates were confirmed as Gram-positive while the remaining 9 were found to be Gram-negative isolates. Out of the 21 Gram-positive isolates, 19 (GSL1, GSL2, GSL3, GSL4, GSL5, GSS2, GSS3, GSS4, GSS5, GSS6, GSS7, GSS8, GSS9, GSS10, GST1, GST3, GST6, GST7 and GST8) exhibited a rod-shape while the rest two (GSL7 and GSS11) were observed as *cocci*. Besides, 19 isolates (GSL1, GSL2, GSL3, GSL4, GSL5, GSS2, GSS3, GSS4, GSS5, GSS6, GSS7, GSS8, GSS9, GSS12, GST1, GST3, GST6, GST7 and GST8) were found to be spore formers (Table 11, Figure 37 and Appendix Figure 4). According to Bergey's manual, those spore bearing isolates were recognized as *Bacillus* spp. In the present study, various biochemical reactions indicated that all the Gram-positive isolates were found to be positive for the presence of catalase and amylase enzymes with the strongest response (++++) for GSL4 and GSS6, and moderate response (++) for GSL2 isolate particularly against the catalase enzyme (Table 13). Following the Bergey's manual of method of identification, out of the 19 spore forming bacterial isolates, 17 (GSL1, GSL2, GSL4, GSS1, GSS3, GSS4, GSS5, GSS6, GSS7, GSS8, GSS9, GSS12, GST1, GST3, GST6, GST7 and GST8) were found to be positive for VP test while the remaining 2 (GSL3 and GL5) were negative. All the VP positive spore forming isolates exhibited a cell with diameter of < 1 μ m. Those VP negative spore formers were examined under microscope for

the presence of swollen cell and none of them showed any colony with exceptional size. Besides, the entire spore forming bacterial isolates showed a positive response to citrate test and grown at 6.5% NaCl concentration. Regarding the Gram-negative bacterial isolates, they provided different responses toward various biochemical tests (Table 13). All the isolates were found with a negative response toward oxidase, Vogues-Proskauer (VP), citrate, lysine decarboxylase (LDC), phenylalanine (phe) and urea biochemical tests except the GSS1 isolate (*Providencia rettgeri*), which reacted positively to citrate and phenylalanine (phe) tests. Besides, all the Gram-negative isolates were found motile and showed a positive response to methyl red (MR), indole and ornithine biochemical tests. Furthermore, all isolates, except GSS1 (*Providencia rettgeri*), were found to be as lactose and glucose fermenters, and gas/acid producers.

Table 13. Biochemical test results for Gram-positive endophytic bacterial isolates

Isolates	Cat	Starch hydrolysis (amylase)	VP	Cell diameter $\geq 1\mu\text{m}$	Mot	Swollen cell	Cit	Salt tolerance (6.5% NaCl)
GSL1	+	+	+	-	+	-	+	+
GSL2	++	+	+	-	+	-	+	+
GSL3	+	+	-	-	+	-	+	+
GSL4	+++	+	+	-	+	-	+	+
GSL5	+	+	-	-	+	-	+	+
GSS2	+	+	+	-	+	-	+	+
GSS3	+	+	+	-	+	-	+	+
GSS4	+	+	+	-	+	-	+	+
GSS5	+	+	+	-	+	-	+	+
GSS6	+++	+	+	-	+	-	+	+
GSS7	+	+++	+	-	+	-	+	+
GSS8	+	+	+	-	+	-	+	+
GSS9	+	+	+	-	+	-	+	+
GSS12	+	+	+	-	+	-	+	+
GST1	+	+	+	-	+	-	+	+
GST3	+	+	+	-	+	-	+	+
GST6	+	+	+	-	+	-	+	+
GST7	+	+	+	-	+	-	+	+
GST8	+	+	+	-	+	-	+	+

Note: **Cat**-Catalase test, **VP**-Vogues-Proskauer test, **Mot**- Motility test, **Cit**-Citrate test, + = slight response, ++ = moderate response, +++ = strong response, - = negative response

Table 14. Biochemical test results for Gram-negative endophytic bacterial isolates

Bacterial isolates	Biochemical tests											
	Ox	Lac	Glu	VP	MR	Mot	Ind	Orn	Cit	LDC	Phe	Urea
GSL6	-	+	+	-	+	+	+	+	-	-	-	-
GSL8	-	+	+	-	+	+	+	+	-	-	-	-
GSL9	-	+	+	-	+	+	+	+	-	-	-	-
GSL10	-	+	+	-	+	+	+	+	-	-	-	-
GSS1	-	-	-	-	+	+	+	+	+	-	+	-
GSS11	-	+	+	-	+	+	+	+	-	-	-	-
GST2	-	+	+	-	+	+	+	+	-	-	-	-
GST4	-	+	+	-	+	+	+	+	-	-	-	-
GST5	-	+	+	-	+	+	+	+	-	-	-	-

Key: **Ox**-Oxidase test, **Lac**-Lactose fermentation test, **Glu**-Glucose fermentation test, **VP**-Voges-Proskauer test, **MR**-Methyl Red test, **Mot**-Motility test, **Ind**-Indole test, **Orn**-Ornithine test, **Cit**-Citrate test, **LDC**-Lysine decarboxylase test, **Phe**-Phenylalanine test, **Urea**-Urease test

4.3 Identification of isolated bacterial endophytes based on protein profile using MALDI-TOF MS analysis

Based on the MALDI-TOF MS analysis (Table 15 and Appendix Figure 5), 26 out of the 30 endophytic bacterial isolates were identified in which 20 were found to be with score values of ≥ 2.0 and 6 were identified with score values of ≥ 1.7 . They were generally classified into *Bacillus* spp., *Escherichia* spp. and *Providencia* spp. Among them, 17 isolates (GSL1- *B. subtilis*, GSL2- *B. subtilis*, GSL4- *B. subtilis*, GSL5- *B. subtilis*, GSL7- *B. subtilis*, GSS2- *B. subtilis*, GSS4- *B. subtilis*, GSS5- *B. subtilis*, GSS6- *B. subtilis*, GSS7- *B. amyloliquefaciens*, GSS8- *B. subtilis*, GSS9- *B. subtilis*, GSS12- *B. atrophaeus*, GST1- *B. subtilis*, GST3- *B. amyloliquefaciens* subsp. *plantarum*, GST6- *B. subtilis* and GST7- *B. subtilis*) were from *Bacillus* spp., 8 isolates (GSL6- *E. coli*, GSL8- *E. coli*, GSL9- *E. coli*, GSL10- *E. coli*, GSS11- *E. coli*, GST2- *E. coli*, GST4- *E. coli* and GST5- *E. coli*) were identified as *Escherichia* strains and 1 (GSS1- *Providencia rettgeri*) was confirmed as *Providencia* strain. Whereas two isolates (GSL3- *B. megaterium* and GSS3- *B. subtilis*) were not totally detected (with zero score value) and two other isolates (GSS10- *Corynebacterium* spp. and GST8- *B. subtilis*) were found with no possibility of organism

identification (with score values of < 1.7). These unidentified isolates might be new endophytic bacterial isolates. Based on the biochemical and MALDI-TOF MS characterizations, majority of the 30 isolates (66.7%) were found within the *Bacillus* spp. followed by the *Escherichia* spp. (26.7%). The remaining isolates were found to be *Providencia* spp. (3.3%) and *Corynebacterium* spp. (3.3%). Bacterial isolates from stem part of the plant dominated majority of the *Bacillus* spp.

Table 15. MALDI-TOF MS analysis result for isolated endophytic bacteria

Isolates	ID No.	Organism name	Score value
GSL1	20599	<i>Bacillus subtilis</i>	2.07
GSL2	22202	<i>Bacillus subtilis</i>	2.06
GSL3	20601	No peaks found (* <i>Bacillus megaterium</i>)	0.00
GSL4	22203	<i>Bacillus subtilis</i>	1.83
GSL5	20603	<i>Bacillus subtilis</i>	2.00
GSL6	22204	<i>Escherichia coli</i>	2.01
GSL7	22205	<i>Bacillus subtilis</i>	2.03
GSL8	22206	<i>Escherichia coli</i>	2.25
GSL9	22207	<i>Escherichia coli</i>	2.29
GSL10	20608	<i>Escherichia coli</i>	2.23
GSS1	20587	<i>Providencia rettgeri</i>	2.34
GSS2	22190	<i>Bacillus subtilis</i>	1.85
GSS3	22191	No peaks found (* <i>Bacillus subtilis</i>)	0.00
GSS4	22192	<i>Bacillus subtilis</i>	1.94
GSS5	20591	<i>Bacillus subtilis</i>	2.09
GSS6	22193	<i>Bacillus subtilis</i>	2.00
GSS7	20593	<i>Bacillus amyloliquefaciens</i>	1.86
GSS8	22194	<i>Bacillus subtilis</i>	2.02
GSS9	22195	<i>Bacillus subtilis</i>	2.03
GSS10	22196	No organism identification possible (* <i>Corynebacterium</i> spp.)	1.34
GSS11	22197	<i>Escherichia coli</i>	2.25
GSS12	20598	<i>Bacillus atrophaeus</i>	1.86
GST1	22198	<i>Bacillus subtilis</i>	2.17
GST2	20580	<i>Escherichia coli</i>	2.16
GST3	20581	<i>Bacillus amyloliquefaciens</i> subsp. <i>plantarum</i>	1.93
GST4	20582	<i>Escherichia coli</i>	2.18
GST5	22199	<i>Escherichia coli</i>	2.33
GST6	22200	<i>Bacillus subtilis</i>	2.15
GST7	22201	<i>Bacillus subtilis</i>	2.26
GST8	20586	No organism identification possible (* <i>Bacillus subtilis</i>)	1.44

* Isolates were identified based on biochemical tests

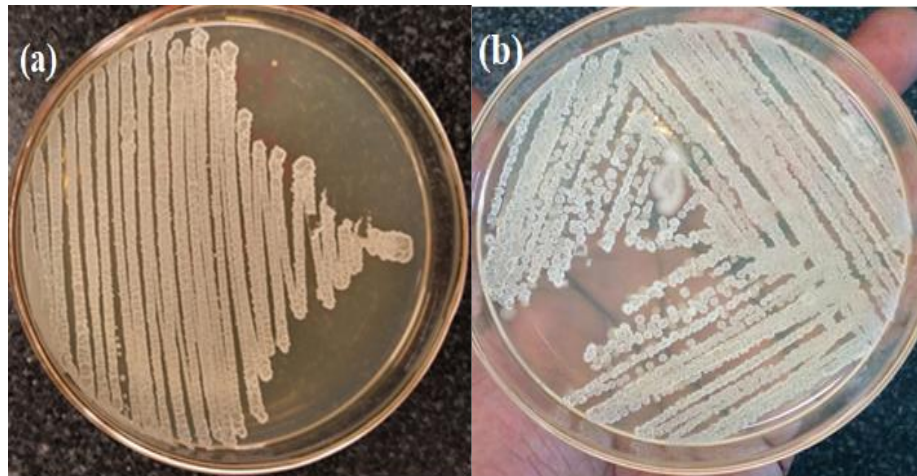


Figure 35. Pure colonies for certain endophytic bacterial isolates obtained from *G. superba*. (a) indicates pure colony for *Bacillus subtilis* (GSL1). (b) indicates pure colony for *Bacillus megaterium* (GSL3) with gel colony

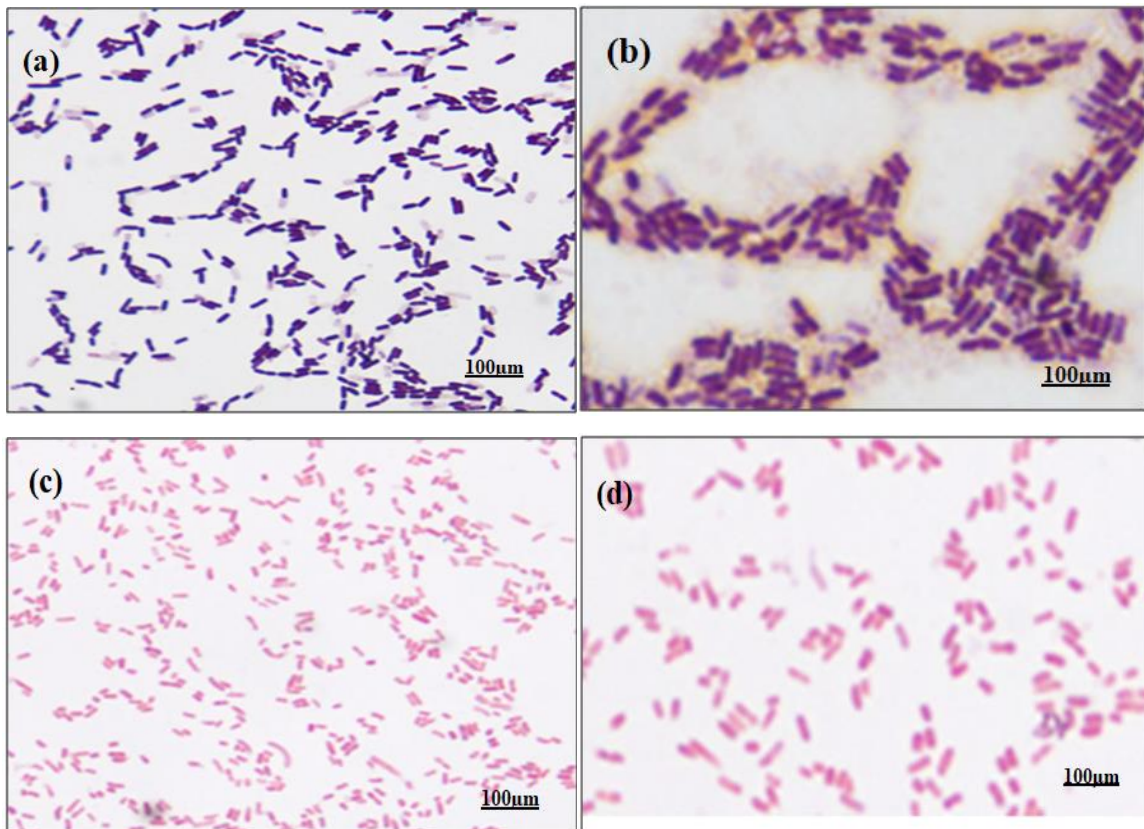


Figure 36. Gram-staining for certain endophytic bacteria isolated from *G. superba*. (a) *Bacillus subtilis* (GSL1), (b) *Bacillus megaterium* (GSL3), (c) *Escherichia coli* (GST5) and (d) *Providencia rettgeri* (GSS1)

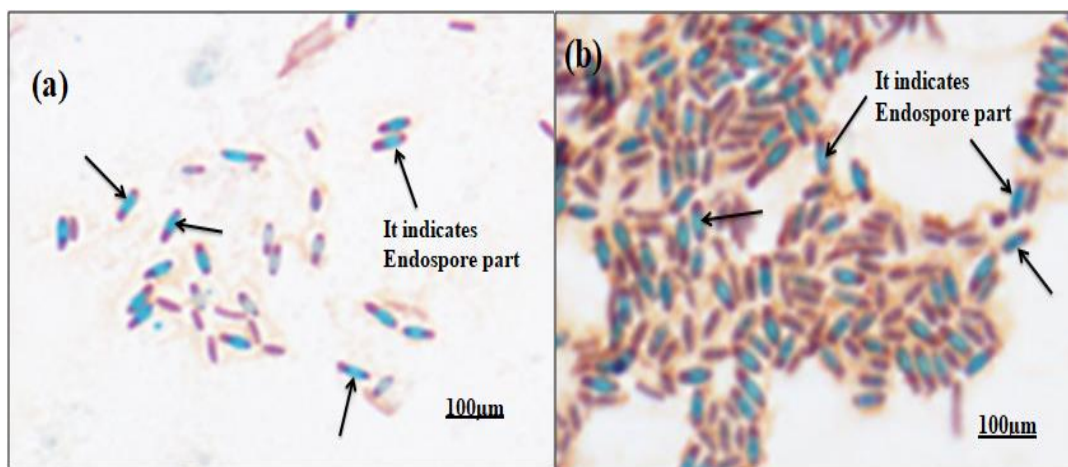


Figure 37. Endospore test for Gram-positive isolates these obtained from *G. superba*. (a) indicates endospore test for *Bacillus subtilis* (GSL1). (b) indicates endospore test for *Bacillus megaterium* (GSL3) with long rod-shaped

4.4 *In vitro* antimicrobial activity evaluation

4.4.1 Antibacterial activity assay

Cadia purpurea leaves and roots

In this investigation, four varied concentrations (100,000, 50,000, 25,000 and 12,500 µg/mL) of *n*-hexane, chloroform, chloroform: methanol (1:1), methanol and ethanol leaves and roots extracts; and five different concentrations (1000, 500, 300, 100 and 50 µg/mL) of isolated compounds **65-70** of *C. purpurea* were studied for *in vitro* antibacterial potency against *E. coli*, *S. aureus* and *P. aeruginosa* human pathogens. Resulted zone of inhibition, expressed as mean \pm standard deviation (in mm) of each tested extract and compound including the antibiotic agent (chloramphenicol, 30 µg) against each pathogen, is presented in [Tables 16 and 17](#), respectively, (for the leaves part), and in [Tables 16 and 17](#) (for the roots part). As a general rule, chemical agents showing an inhibitory zone of ≥ 7 mm are considered significantly active against tested bacterial culture²⁸. Similarly, in the present study, extracts and compounds showing a mean of inhibition zones with diameter less than 7 mm were considered as not active against the tested bacterial pathogens at the tested concentration(s). As reported in Table 16, all the tested concentrations of the chloroform, chloroform: methanol (1:1) and alcoholic leaves extracts showed an activity (inhibition zone of ≥ 7 mm) up to 12,500 µg/mL concentration against *E. coli* with the greater inhibitory value (15.7 ± 0.1 mm) recorded for ethanol extract followed by methanol (15.3 ± 0.4 mm) and chloroform (15.0 ± 0.1 mm) extracts at the maximum dose of 100,000 µg/mL. However, the *n*-hexane

leaves extract did not indicate any activity at all concentrations against *E. coli*. The inhibitory activity produced by all leaves extracts against *E. coli* at all concentrations, however, was found weak compared to chloramphenicol (23.1 ± 0.4 mm, at $30 \mu\text{g}$). On the other hand, *S. aureus* showed a total resistance against all leaves extracts at all tested concentrations, whereas it was sensitive to chloramphenicol (inhibited zone of 19.8 ± 0.3 mm). The *n*-hexane leaves extract showed a potent inhibitory activity against *P. aeruginosa* strain at all concentrations with minimum and maximum inhibition zone values of 10.2 ± 0.3 mm and 13.1 ± 0.1 mm recorded for $12,500 \mu\text{g/mL}$ and $100,000 \mu\text{g/mL}$ concentrations, respectively. The *n*-hexane and chloroform leaves extracts in general exhibited an activity against *P. aeruginosa* better than chloramphenicol (8.2 ± 0.6 mm) at all concentrations.

Table 16. Antibacterial activity of five leaves extracts of *C. purpurea* against *E. coli*, *P. aeruginosa* and *S. aureus* standard human pathogens

Bacterial strains	Concentration (µg/mL)	Inhibition zone (mean ± sd, mm) of leaves extracts					Chloramphenicol disc (30 µg/disc)
		<i>n</i> -Hexane	CHCl ₃	CHCl ₃ : MeOH (1:1)	MeOH	EtOH	
<i>E. coli</i>	12,500	0.0	12.0 ± 0.1 ^A	7.0 ± 0.0 ^B	12.3 ± 0.2 ^A	14.0 ± 0.01 ^C	23.1 ± 0.4
	25,000	0.0	13.1 ± 0.1 ^D	7.4 ± 0.1 ^E	13.1 ± 0.1 ^D	14.6 ± 0.1 ^F	
	50,000	0.0	14.0 ± 0.1 ^G	7.6 ± 0.1 ^H	14.4 ± 0.01 ^G	15.2 ± 0.01 ^I	
	100,000	0.0	15.0 ± 0.1 ^J	12.9 ± 0.5 ^K	15.3 ± 0.4 ^J	15.7 ± 0.1 ^J	
<i>P. aeruginosa</i>	12,500	10.2 ± 0.3 ^L	8.4 ± 0.01 ^M	0.0	6.5 ± 0.1 ^N	7.1 ± 0.01 ^O	8.2 ± 0.6
	25,000	10.6 ± 0.3 ^P	10.0 ± 0.1 ^P	0.0	6.8 ± 0.01 ^Q	7.3 ± 0.1 ^R	
	50,000	12.0 ± 0.3 ^S	11.6 ± 0.1 ^T	8.6 ± 0.2 ^U	8.5 ± 0.01 ^U	8.1 ± 0.1 ^U	
	100,000	13.1 ± 0.1 ^V	12.1 ± 0.3 ^W	9.0 ± 0.1 ^Y	10.4 ± 1.1 ^Z	9.4 ± 0.01 ^Y	
<i>S. aureus</i>	12,500	0.0	0.0	0.0	0.0	0.0	19.8 ± 0.3
	25,000	0.0	0.0	0.0	0.0	0.0	
	50,000	0.0	0.0	0.0	0.0	0.0	
	100,000	0.0	0.0	0.0	0.0	0.0	

Note: samples with mean diameter inhibition values of <7 mm were considered as not active

Means with different uppercase letters across rows are significantly different at (p<0.05).

Table 17 showed that, among the isolated compounds, the calpurnine (**67**) was found with an activity comparable to chloramphenicol (23.5 ± 0.3 mm at 30 μg) against *E. coli* up to 50 $\mu\text{g/mL}$ (10.6 ± 0.0 mm) with the maximum inhibitory value (17.5 ± 0.0 mm) recorded at 1000 $\mu\text{g/mL}$. Whereas this compound did not indicate any positive effect against *S. aureus* at all concentrations. On the contrary, this compound **67** exhibited an activity better than the chloramphenicol (8.2 ± 0.6 mm) against *P. aeruginosa* at concentrations of 1000 $\mu\text{g/mL}$ (10.6 ± 0.01 mm), 500 $\mu\text{g/mL}$ (9.1 ± 0.1 mm) and 300 $\mu\text{g/mL}$ (8.6 ± 0.01 mm). The apigenin-7-*O*-neohesperidoside (**66**) compound exerted a positive influence on the growth of *E. coli* at all concentrations with better inhibition zone values recorded at 1000 $\mu\text{g/mL}$ (12.1 ± 0.1 mm) and 500 $\mu\text{g/mL}$ (11.9 ± 0.02 mm). But, compared to compound **67** and chloramphenicol, the observed activity against *E. coli* of compound **66** was found weak. On the other hand, however, compound **66** possessed a better activity against *P. aeruginosa* strain at all concentrations with greater inhibition zone values (10.9 ± 0.01 to 14.5 ± 0.01 mm) than chloramphenicol (8.2 ± 0.6 mm). The *S. aureus* strain was found with a complete resistance against compound **66** at all concentration. Compound **65** only showed a better activity against *P. aeruginosa* up to 300 $\mu\text{g/mL}$ concentration (8.4 ± 0.01 to 9.0 ± 0.01 mm) than the chloramphenicol (8.2 ± 0.6 mm)

Table 17. Antibacterial inhibitory activity of isolated compounds **65-67** against *E. coli*, *P. aeruginosa* and *S. aureus* bacterial strains

Bacterial strains	Concentrations ($\mu\text{g/mL}$)	Inhibition zone diameter (mean \pm sd, mm) of compounds 65-67			
		Compound 65	Compound 66	Compound 67	Chloramphenicol disc (30 $\mu\text{g/disc}$)
<i>E. coli</i>	50	6.8 ± 0.0	7.1 ± 0.1	10.6 ± 0.02	23.5 ± 0.3
	100	7.0 ± 0.02	10.5 ± 0.1	11.0 ± 0.02	
	300	8.5 ± 0.02	10.8 ± 0.02	13.8 ± 0.02	
	500	8.5 ± 0.1	11.9 ± 0.02	15.2 ± 0.0	
	1000	8.9 ± 0.1	12.1 ± 0.1	17.5 ± 0.02	
<i>P. aeruginosa</i>	50	7.0 ± 0.01	10.9 ± 0.01	7.0 ± 0.01	8.2 ± 0.6
	100	7.6 ± 0.01	11.7 ± 0.01	7.5 ± 0.01	
	300	8.4 ± 0.01	12.4 ± 0.01	8.6 ± 0.01	
	500	8.7 ± 0.01	13.2 ± 0.01	9.1 ± 0.1	
	1000	9.0 ± 0.01	14.5 ± 0.01	10.6 ± 0.01	
<i>S. aureus</i>	50	6.3 ± 0.02	0.0	0.0	18.8 ± 0.4
	100	6.4 ± 0.02	0.0	0.0	
	300	6.5 ± 0.02	0.0	0.0	
	500	6.6 ± 0.02	6.5 ± 0.02	0.0	
	1000	8.7 ± 0.02	6.6 ± 0.02	0.0	

Note: mean inhibition values <7 mm were considered as inactive

Table 18 indicated that, *n*-hexane, chloroform and chloroform: methanol (1:1) roots extracts were found effective against *E. coli* (> 7 mm) at all tested concentrations with the maximum diameters of inhibition zone of 13.8 ± 0.0 mm, 11.1 ± 0.0 mm and 10.7 ± 0.1 mm, respectively, recorded at the maximal concentration of 100,000 $\mu\text{g/mL}$, which were slightly comparable to chloramphenicol (24.5 ± 0.3 mm at 30 μg dose). The *S. aureus* strain was found to be susceptible only to the *n*-hexane and methanol roots extracts up to the 25,000 $\mu\text{g/mL}$ dose (7.6 ± 0.0 to 10.2 ± 0.5 mm and 7.3 ± 0.0 to 8.7 ± 0.0 mm, respectively). On the other hand, the chloroform: methanol (1:1) roots extract exerted a positive action on the growth of *P. aeruginosa* at all tested dilutions (8.0 ± 0.0 to 10.0 ± 0.1 mm). However, the methanolic and ethanolic roots extracts scored a slightly lower inhibitory values (7.4 ± 0.0 to 8.7 ± 0.1 mm and 7.1 ± 0.0 to 8.3 ± 0.1 mm, respectively) against *P. aeruginosa* at the doses up to 25,000 $\mu\text{g/mL}$. Generally, a better activity against *E. coli* was noted in the non-alcoholic roots extracts though it looked like less as compared to the chloramphenicol (24.5 ± 0.3 mm at dose of 30 μg). Whereas the inhibitory action indicated by almost all roots extracts against *S. aureus* at all concentrations, was observed weak in reference to chloramphenicol (18.8 ± 0.4 mm). To the contrary, the inhibition zone values, scored by the extracts against *P. aeruginosa*, were found even better than that of chloramphenicol (7.2 ± 0.6 mm).

Table 18. Antibacterial inhibitory action (mean \pm sd, mm) against *E. coli*, *P. aeruginosa* and *S. aureus* of five roots extracts of *C. purpurea*

Bacterial culture	Concentration ($\mu\text{g/mL}$)	Diameter of inhibition area in mm (mean \pm sd) of extracts and chloramphenicol					
		<i>n</i> -Hexane	Chloroform	Chloroform: methanol (1:1)	Methanol	Ethanol	Chloramphenicol (30 $\mu\text{g/disc}$)
<i>E. coli</i>	12,500	8.3 \pm 0.0 ^A	7.2 \pm 0.0 ^B	7.0 \pm 0.0 ^B	6.5 \pm 0.0 ^C	0.0	24.5 \pm 0.3
	25,000	9.3 \pm 0.0 ^D	8.7 \pm 0.0 ^E	7.2 \pm 0.0 ^F	6.8 \pm 0.0 ^G	0.0	
	50,000	10.2 \pm 0.4 ^H	9.6 \pm 0.3 ^I	9.0 \pm 0.3 ^I	8.3 \pm 0.1 ^J	7.6 \pm 0.0 ^K	
	100,000	13.8 \pm 0.0 ^L	11.1 \pm 0.4 ^M	10.7 \pm 0.1 ^N	9.6 \pm 0.1 ^O	8.0 \pm 0.0 ^P	
<i>P. aeruginosa</i>	12,500	7.3 \pm 0.2 ^V	7.7 \pm 0.0 ^V	8.0 \pm 0.0 ^W	0.0	0.0	7.2 \pm 0.6
	25,000	7.7 \pm 0.0 ^X	8.2 \pm 0.1 ^Y	8.4 \pm 0.2 ^Y	7.4 \pm 0.0 ^X	7.1 \pm 0.0 ^X	
	50,000	8.4 \pm 0.1 ^Z	8.9 \pm 0.0 ^{AA}	9.7 \pm 0.1 ^{BB}	7.7 \pm 0.1 ^{CC}	7.4 \pm 0.0 ^{CC}	
	100,000	8.9 \pm 0.2 ^{DD}	9.8 \pm 0.1 ^{EE}	10.0 \pm 0.1 ^{FF}	8.7 \pm 0.1 ^{DD}	8.3 \pm 0.1 ^{DD}	
<i>S. aureus</i>	12,500	0.0	0.0	0.0	0.0	0.0	18.8 \pm 0.4
	25,000	7.6 \pm 0.0 ^Q	0.0	0.0	7.3 \pm 0.0 ^Q	0.0	
	50,000	8.9 \pm 0.1 ^R	0.0	0.0	7.5 \pm 0.0 ^S	0.0	
	100,000	10.2 \pm 0.5 ^T	0.0	0.0	8.7 \pm 0.0 ^U	0.0	

Note: samples with mean diameter inhibition values of <7 mm were considered as not active

Means with different uppercase letters across rows are significantly different at (p<0.05).

As it can be seen in Table 19, compound **67** presented better inhibitory activity against *E. coli* up to 50 µg/mL with greater zone of inhibition (18.5 ± 0.0 mm) recorded at the higher concentration of 1000 µg/mL, slightly comparable to chloramphenicol (21.5 ± 0.3 mm at dose of 30 µg). Whereas this compound **67** was found to be totally inactive against *S. aureus* at all concentrations. Compounds **68** and **69** possessed a mild activity against *E. coli* (8.2 ± 0.2 mm and 7.5 ± 0.2 mm, respectively) and *P. aeruginosa* (8.7 ± 0.0 mm and 9.2 ± 0.5 , respectively) only at the higher concentration (1000 µg/mL). Compound **70** displayed a moderate activity against *E. coli* at all concentrations (> 7 mm) with inhibition zones laid in the range of 7.2 ± 0.1 to 10.3 ± 0.0 mm. All compounds **67**, **68**, **69** and **70** possessed an activity stronger than the chloramphenicol (7.2 ± 0.6 mm) against *P. aeruginosa* almost at all dilutions. Table 19, in general, revealed that compound **67** provided a notable activity against *E. coli*, comparable to chloramphenicol. However, against *S. aureus* strain, all the compounds **67**, **68**, **69** and **70** exhibited a negligible activity up to 1000 µg/mL in comparison to the chloramphenicol (18.8 ± 0.4 mm). But, surprisingly, the chloramphenicol had faced a strong and unprecedented resistant from *P. aeruginosa* which led to even a smaller inhibition zone value (7.2 ± 0.6 mm) than that of the compounds. Overall, the resulted inhibitory potential of the roots extracts and isolated compounds **67**, **68**, **69** and **70** was found to be slightly comparable against *E. coli*, very weak against *S. aureus* and stronger against *P. aeruginosa* in reference to chloramphenicol.

Table 19. Antibacterial activity inhibition zone (mean \pm sd, mm) of compounds **67-70** against *E. coli*, *P. aeruginosa* and *S. aureus* bacterial strains

Bacterial pathogens	Concentration ($\mu\text{g/mL}$)	Inhibition zone (mean \pm sd, mm) of compounds 67-70				
		Compound 67	Compound 68	Compound 69	Compound 70	Chloramphenicol disc (30 $\mu\text{g/disc}$)
<i>E. coli</i>	50	9.6 \pm 0.0	6.8 \pm 0.3	6.4 \pm 0.1	7.2 \pm 0.1	21.5 \pm 0.3
	100	10.0 \pm 0.0	7.4 \pm 0.0	6.6 \pm 0.1	7.5 \pm 0.0	
	300	13.8 \pm 0.0	7.8 \pm 0.0	6.8 \pm 0.1	8.6 \pm 0.0	
	500	16.2 \pm 0.0	7.9 \pm 0.1	7.2 \pm 0.1	8.9 \pm 0.0	
	1000	18.5 \pm 0.0	8.2 \pm 0.2	7.5 \pm 0.2	10.3 \pm 0.0	
<i>P. aeruginosa</i>	50	7.2 \pm 0.0	7.0 \pm 0.3	6.9 \pm 0.5	7.1 \pm 0.0	7.2 \pm 0.6
	100	7.5 \pm 0.0	7.9 \pm 1.0	7.9 \pm 0.4	7.3 \pm 0.0	
	300	8.6 \pm 0.0	8.0 \pm 0.3	8.0 \pm 0.3	7.6 \pm 0.0	
	500	9.1 \pm 0.1	8.3 \pm 0.3	8.9 \pm 0.2	7.7 \pm 0.0	
	1000	10.6 \pm 0.0	8.7 \pm 0.0	9.2 \pm 0.5	9.0 \pm 0.1	
<i>S. aureus</i>	50	0.0	0.0	6.2 \pm 0.1	0.0	18.8 \pm 0.4
	100	0.0	6.4 \pm 0.0	6.8 \pm 0.2	0.0	
	300	0.0	6.7 \pm 0.0	7.3 \pm 0.1	0.0	
	500	0.0	7.9 \pm 0.1	7.5 \pm 0.1	8.4 \pm 0.0	
	1000	0.0	8.1 \pm 0.1	7.7 \pm 0.1	9.1 \pm 0.1	

Caralluma speciosa stems

The obtained *in vitro* antibacterial effectiveness results of five extracts (*n*-hexane, chloroform, 1:1 of chloroform: methanol, methanol and ethanol) and five isolated compounds **71-75** of *C. speciosa* stems were compiled in Tables 20 and 21, respectively.

As Table 20 indicated the maximum inhibitory zone (8.65 ± 1.63 mm) against *E.coli* at the maximum concentration (100,000 $\mu\text{g/mL}$) was recorded by chloroform followed by methanol (7.09 ± 0.88 mm) extracts. The chloroform extract also exhibited the next higher inhibition area (7.13 ± 0.71 mm) against the same bacterial pathogen at 50,000 $\mu\text{g/mL}$. Whereas *n*-hexane, chloroform: methanol (1:1) and ethanol did not show any activity against *E. coli* at all tested concentration. Besides, all the extracts, except ethanol, were found with a totally zero inhibition value against the methicillin-resistant *S. aureus* bacterium at all concentrations. Ethanol extract was the only which showed some degree of inhibitory effect (7.55 ± 0.25 mm) at the higher concentration (100,000 $\mu\text{g/mL}$) on this *S. aureus* strain. All the extracts were also observed with no activity against *P. aeruginosa* bacterium at all tested dilutions (Table 20).

Table 20. Antibacterial activity inhibition zone (mean \pm sd, mm) on *E. coli* *P. aeruginosa*, and *S. aureus* of *C. speciosa* stem extracts

Bacterial pathogens	Concentration ($\mu\text{g/mL}$)	Diameter of inhibition zone (mean \pm sd, mm) of extracts					Chloramphenicol disc (30 $\mu\text{g/disc}$)
		<i>n</i> -Hexane	CHCl_3	CHCl_3 : MeOH (1:1)	MeOH	EtOH	
<i>E. coli</i>	100,000	6.22 \pm 0.04 ^A	8.65 \pm 1.63 ^B	6.10 \pm 0.02 ^A	7.09 \pm 0.88 ^C	6.18 \pm 0.11 ^A	21.15 \pm 0.5
	50,000	6.17 \pm 0.02 ^D	7.13 \pm 0.71 ^E	6.07 \pm 0.01 ^D	6.94 \pm 0.80 ^D	6.07 \pm 0.01 ^D	
	25,000	6.13 \pm 0.04 ^F	6.50 \pm 0.45 ^F	6.06 \pm 0.00 ^F	6.17 \pm 0.03 ^F	6.05 \pm 0.00 ^F	
	12,500	6.05 \pm 0.01 ^G	6.44 \pm 0.40 ^G	6.05 \pm 0.00 ^G	6.13 \pm 0.01 ^G	6.04 \pm 0.00 ^G	
<i>P. aeruginosa</i>	100,000	6.13 \pm 0.05 ^H	0.0	6.09 \pm 0.03 ^H	0.0	0.0	9.15 \pm 0.7
	50,000	6.09 \pm 0.03 ^I	0.0	6.08 \pm 0.04 ^I	0.0	0.0	
	25,000	6.07 \pm 0.03 ^J	0.0	6.05 \pm 0.00 ^J	0.0	0.0	
	12,500	0.0	0.0	6.04 \pm 0.00	0.0	0.0	
<i>S. aureus</i>	100,000	0.0	0.0	0.0	0.0	7.55 \pm 0.25	18.92 \pm 0.4
	50,000	0.0	0.0	0.0	0.0	6.79 \pm 0.05	
	25,000	0.0	0.0	0.0	0.0	6.68 \pm 0.06	
	12,500	0.0	0.0	0.0	0.0	6.39 \pm 0.04	

Note: Samples with mean diameter inhibition values of <7 mm were considered as not active, Means with different uppercase letters across rows are significantly different at ($p < 0.05$).

Table 21. Antibacterial inhibitory values (mean \pm sd, mm) against *E. coli*, *P. aeruginosa* and *S. aureus* of compounds **71-75**

Bacterial strains	Concentration ($\mu\text{g/mL}$)	Inhibition diameter zone (mean \pm sd, mm) of isolated compounds 71-75					
		71	72	73	74	75	Chloramphenicol disc (30 $\mu\text{g/disc}$)
<i>E. coli</i>	50	0.0	0.0	0.0	0.0	0.0	20.45 \pm 0.7
	100	0.0	0.0	0.0	0.0	0.0	
	300	0.0	0.0	0.0	0.0	0.0	
	500	0.0	0.0	0.0	0.0	0.0	
	1000	0.0	0.0	0.0	0.0	0.0	
<i>P. aeruginosa</i>	50	0.0	0.0	0.0	0.0	0.0	7.3 \pm 0.4
	100	0.0	0.0	0.0	0.0	0.0	
	300	0.0	0.0	0.0	0.0	0.0	
	500	0.0	0.0	0.0	0.0	0.0	
<i>S. aureus</i>	1000	0.0	0.0	0.0	0.0	0.0	19.26 \pm 0.6
	100	7.03 \pm 0.47	6.33 \pm 0.11	6.94 \pm 0.04	6.48 \pm 0.08	6.87 \pm 0.05	
	300	7.54 \pm 0.7	7.57 \pm 0.25	7.13 \pm 0.04	6.56 \pm 0.03	7.35 \pm 0.35	
	500	7.83 \pm 0.74	8.73 \pm 0.3	7.76 \pm 0.54	6.94 \pm 0.29	10.12 \pm 0.25	
	1000	8.01 \pm 0.22	9.08 \pm 0.06	9.20 \pm 0.76	8.26 \pm 0.6	11.03 \pm 0.6	

As presented in Table 21 none of the five isolated compounds **71-75** were found effective against *E.coli* and *P. aeruginosa*, at doses up to 1000 µg/mL. Whereas against the inflammation causing *S. aureus* bacterium, all the compounds exhibited a slight activity with inhibition diameter zone >7 mm, of which compound **75** showed the higher mean value (11.03 ± 0.6 mm) followed by **73** (9.20 ± 0.76 mm), **72** (9.08 ± 0.06 mm), **74** (8.26 ± 0.6 mm) and **71** (8.01 ± 0.22 mm) at the maximum concentration (1000 µg/mL). The observed susceptibility difference between the Gram-positive and Gram-negative bacteria toward the tested compounds can be related with the variation in biological makeup of the bacteria's outer cell membrane layer. That is, the outer cell membrane of Gram-positive bacteria constitutes simple and thin layers of peptidoglycans which can easily be penetrated by chemical agents; whereas outer cell membrane of Gram-negative bacteria is built from multilayered peptidoglycan and phospholipids which is impermeable to especially less effective compounds¹²¹. Also as stated in literature, glycosylated and hydroxyl group(s) containing pregnane compounds, fractionated from methanol and/or chloroform extracts of the genus *Caralluma*, may exhibit better activity against Gram-positive bacteria like *S. aureus*. This is because, the hydroxyls of the sugar units and/or those present within the pregnane steroids can form a hydrogen bonding with phospholipidic membrane of the bacteria leading to the integration and complex formation of the compounds. This fact may hold true for compounds **73** and **75**, herein, which showed better activity against *S. aureus*. The present result was somewhat comparable with the antibacterial data of *C. umbellata* stem extracts reported by Babu *et al.*¹²². According to these authors, *n*-hexane and methanol extracts of *C. umbellata* stem showed zero inhibition zones against both the Gram-positive (*S. aureus*) and Gram-negative (*E. coli* and *P. aeruginosa*) bacteria at the concentrations of 750 and 1000 µg/mL; whereas chloroform extract of the plant exhibited an inhibitory diameter zone higher than our results against *E.coli* and *S.aureus*, but zero inhibition against *P. aeruginosa* at the same concentration.

***Gloriosa superba* tubers**

The antibacterial activity result of *G. superba* tuber extracts was presented in Tables 22. The result showed that all the extracts indicated an activity (> 7 mm inhibition value) against *E. coli* and *P. aeruginosa* bacteria at all tested concentrations. The better activity against these bacteria was observed in the *n*-hexane extract up to 12,500 µg/mL concentration with the

larger inhibitory values (9.83 ± 0.28 mm and 10.65 ± 0.79 mm, respectively) recorded at the maximum concentration of 100,000 $\mu\text{g/mL}$. The chloroform extract possessed an auspicious activity against *S. aureus* at all concentrations (> 7 mm) by showing a greater inhibition zone value of 10.33 ± 0.34 mm at the higher amount of 100,000 $\mu\text{g/mL}$, comparable to the chloramphenicol (19.16 ± 1.55 mm at 30 μg dose). Generally, the observed inhibitory activity of the extracts, against the *E. coli* and *S.aureus* strains, were found to be weaker than the chloramphenicol (25.29 ± 0.82 mm and 19.16 ± 1.55 mm, respectively). However, against the *P. aeruginosa* bacterium, all the extracts achieved a stronger activity than the chloramphenicol (7.26 ± 0.49 mm at dose of 30 μg) at all tested concentrations.

Table 22. Antibacterial activity inhibitory values (mean \pm sd) of tuber extracts of *G. superba* against *E. coli*, *P. aeruginosa* and *S. aureus*

Bacterial pathogens	Concentration ($\mu\text{g/mL}$)	Zone of inhibition (mean \pm sd, mm) of extracts				
		<i>n</i> -Hexane	CHCl_3	CHCl_3 :MeO H (1:1)	MeOH	Chloramphenicol (30 $\mu\text{g}/\text{disc}$)
<i>E. coli</i>	12,500	9.1 ± 0.0^A	8.4 ± 0.0^B	8.2 ± 0.1^B	8.4 ± 0.0^B	25.3 ± 0.8
	25,000	9.2 ± 0.5^C	8.74 ± 0.0^D	8.5 ± 0.2^D	8.68 ± 0.1^D	
	50,000	9.7 ± 0.1^E	8.8 ± 0.1^F	8.9 ± 0.1^F	8.7 ± 0.2^F	
	100,000	9.8 ± 0.3^G	9.6 ± 0.1^G	9.2 ± 0.1^G	8.9 ± 0.2^H	
<i>P. auregunosa</i>	12,500	7.5 ± 0.1^T	8.8 ± 0.7^U	8.4 ± 0.0^U	8.5 ± 0.5^U	7.3 ± 0.5
	25,000	8.8 ± 0.6^V	8.9 ± 0.7^V	9.7 ± 0.0^W	8.6 ± 0.4^V	
	50,000	10.0 ± 0.4^X	9.1 ± 0.7^Y	9.8 ± 0.1^Y	8.7 ± 0.4^Z	
	100,000	10.7 ± 0.8^{AA}	9.4 ± 0.5^{BB}	10.0 ± 0.0^{AA}	9.1 ± 0.0^{BB}	
<i>S. aureus</i>	12,500	6.7 ± 0.0^I	7.9 ± 0.0^J	6.6 ± 0.0^I	6.5 ± 0.3^I	19.2 ± 1.6
	25,000	7.0 ± 0.2^K	8.5 ± 0.3^L	6.9 ± 0.0^M	6.8 ± 0.4^M	
	50,000	7.3 ± 0.1^N	9.0 ± 0.4^O	7.9 ± 0.0^P	7.1 ± 0.6^N	
	100,000	8.5 ± 0.0^Q	10.3 ± 0.3^R	8.8 ± 0.3^Q	7.2 ± 0.6^S	

Note: Samples with mean diameter inhibition values of <7 mm were considered as not active, Means with different uppercase letters across rows are significantly different at ($p < 0.05$).

***Gomphocarpus purpurascens* leaves extracts**

The antibacterial inhibition zone diameters, expressed as mean \pm standard deviation, recorded by five extracts of *G. purpurascens* leaves against three standard human bacterial pathogens were reported in Table 23.

As Table 23 showed, all the tested concentrations of all extracts indicated positive activities against all strains, except the lowest concentrations (12,500 and 25,000 $\mu\text{g/mL}$) of chloroform (against *S. aureus*), chloroform: methanol (against *P. aeruginosa*), methanol (against *E. coli*) and ethanol (against *S. aureus*) extracts which were found inactive (< 7 mm inhibition zone). The highest inhibitory value (10.1 ± 0.1 mm), against *E. coli* at the highest concentration (100,000 $\mu\text{g/mL}$), was scored by *n*-hexane extract followed by 1:1 of chloroform: methanol (9.4 ± 0.0 mm) and chloroform (9.1 ± 0.3 mm) extracts. The lowest concentration (12,500 $\mu\text{g/mL}$) of the four extracts also inhibited the growth of *E. coli* (7.1 ± 0.1 to 8.1 ± 0.0 mm). The *S. aureus* bacterium was found to be sensitive to all extracts at the maximum concentration (100,000 $\mu\text{g/mL}$) with the larger inhibition diameter value (9.1 ± 0.2 mm) recorded by methanol extract; and with the smallest values provided by the ethanol (7.2 ± 0.0 mm). The *P. aeruginosa* was also found more susceptible to *n*-hexane extract (10.8 ± 0.1 mm), while least sensitive to chloroform: methanol (1:1) extract (8.6 ± 0.0 mm) at the highest dose (100,000 $\mu\text{g/mL}$). Thus far, one similar study was reported by Negash *et al.*⁷⁶ aiming on the evaluation of antibacterial activity of ethanol and methanol leaves extracts of *G. purpurascens* against same standard bacteria mentioned above. However, the tested concentrations (150, 300 and 600 mg/mL) in the reported study, were far higher than the one tested in the present work. According to the report, the ethanol and methanol leaves extracts scored respective inhibition zone values of 6.09 ± 0.18 to 6.90 ± 0.40 mm and 9.19 ± 0.07 to 13.20 ± 0.1 mm against *E. coli*; 9.51 ± 0.1 to 12.7 ± 0.15 mm and 7.1 ± 0.01 to 8.2 ± 0.01 mm against *S. aureus*; and 9.01 ± 0.01 to 9.77 ± 0.15 mm and 9.8 ± 0.01 to 13.8 ± 0.10 mm against *P. aeruginosa*. In this essence, our result was comparable to this report regardless of the huge concentration difference.

Table 23. Antibacterial inhibition zone diameter (mean \pm sd) of leaves extracts of *G. purpurascens* against *E. coli*, *P. aeruginosa* and *S. aureus* standard bacterial strains

Bacterial strains	Concentration ($\mu\text{g/mL}$)	Inhibition zone diameter (mean \pm sd, mm)					
		<i>n</i> -Hexane	CHCl_3	$\text{CHCl}_3\text{:MeOH}$ (1:1)	MeOH	EtOH	Chloramphenicol (30 μg)
<i>E. coli</i>	12,500	8.1 \pm 0.0 ^A	7.8 \pm 0.2 ^B	7.9 \pm 0.3 ^B	6.8 \pm 0.0 ^C	7.1 \pm 0.1 ^B	24.3 \pm 0.8
	25,000	9.2 \pm 0.2 ^D	8.4 \pm 0.4 ^E	9.0 \pm 0.1 ^D	6.9 \pm 0.1 ^F	7.9 \pm 0.4 ^G	
	50,000	9.8 \pm 0.0 ^H	8.7 \pm 0.0 ^I	9.4 \pm 0.0 ^H	7.1 \pm 0.1 ^J	8.4 \pm 0.1 ^I	
	100,000	10.1 \pm 0.1 ^K	9.1 \pm 0.3 ^L	9.4 \pm 0.0 ^L	7.2 \pm 0.0 ^M	8.7 \pm 0.1 ^N	
<i>P. aeruginosa</i>	12,500	9.1 \pm 0.1 ^Y	7.1 \pm 0.0 ^Z	6.5 \pm 0.3 ^{AA}	7.8 \pm 0.0 ^Z	7.5 \pm 0.1 ^Z	7.1 \pm 0.2
	25,000	9.2 \pm 0.0 ^{BB}	7.9 \pm 0.0 ^{CC}	7.7 \pm 0.2 ^{CC}	8.2 \pm 0.2 ^{DD}	8.1 \pm 0.4 ^{DD}	
	50,000	9.7 \pm 0.2 ^{EE}	8.1 \pm 0.2 ^{FF}	8.0 \pm 0.1 ^{FF}	8.6 \pm 0.0 ^{FF}	8.5 \pm 0.0 ^{FF}	
	100,000	10.8 \pm 0.1 ^{GG}	8.8 \pm 0.0 ^{HH}	8.6 \pm 0.0 ^{HH}	9.2 \pm 0.0 ^{II}	9.0 \pm 0.1 ^{JJ}	
<i>S. aureus</i>	12,500	7.0 \pm 0.0 ^O	0.0	7.0 \pm 0.8 ^O	7.1 \pm 0.4 ^O	6.3 \pm 0.0 ^P	19.4 \pm 1.8
	25,000	7.6 \pm 1.2 ^Q	6.9 \pm 0.0 ^R	7.2 \pm 0.7 ^Q	8.3 \pm 0.0 ^S	6.6 \pm 0.0 ^R	
	50,000	8.1 \pm 0.0 ^T	7.5 \pm 0.0 ^U	7.4 \pm 0.7 ^U	8.8 \pm 0.5 ^T	7.0 \pm 0.0 ^U	
	100,000	8.8 \pm 0.5 ^V	8.0 \pm 0.1 ^V	8.1 \pm 0.2 ^V	9.1 \pm 0.1 ^W	7.2 \pm 0.0 ^X	

Note: Samples with mean diameter inhibition values of <7 mm were considered as not active, Means with different uppercase letters across rows are significantly different at ($p < 0.05$).

Antibacterial activity of isolated compounds 76, 78, 79 and 80

Table 24 presented that compounds **76**, **78** and **80** showed an activity (> 7 mm) against all evaluated bacterial strains at all tested concentrations. Compound **78** established the better activity with inhibition zone diameters ranging from 8.22 ± 0.56 to 9.78 ± 0.63 mm against *E. coli*, 7.30 ± 0.10 to 11.07 ± 0.09 mm against *S. aureus* and 9.11 ± 0.67 to 9.99 ± 0.05 mm against *P. aeruginosa*. This compound showed the higher inhibitory value (11.07 ± 0.09 mm) against the *S. aureus* at the maximum concentration of 1000 $\mu\text{g/mL}$. Compound **76** displayed an activity with inhibition zone values of 7.29 ± 0.27 to 9.68 ± 0.88 mm against *E. coli*, 7.20 ± 0.05 to 9.58 ± 0.02 mm against *S. aureus* and 7.49 ± 0.02 to 9.52 ± 0.21 mm against *P. aeruginosa*. Compounds **79** also showed an inhibitory effect against *P. aeruginosa* at all concentrations with the higher zone of inhibition values of 8.8 ± 0.1 at 1000 $\mu\text{g/mL}$ but no activity shown against *S. aureus* bacterium at all concentrations.

Table 24. Antibacterial activity of isolated compounds **76**, **78**, **79** and **80** against *E. coli*, *S. aureus* and *P. aeruginosa* bacterial strains

Bacterial stains	Concentration s ($\mu\text{g/mL}$)	Diameter of inhibition zone (mean \pm sd, mm)				Chloramphenicol (30 $\mu\text{g/disc}$)
		76	78	79	80	
<i>E. coli</i>	50	7.29 ± 0.3	8.22 ± 0.6	6.3 ± 0.0	7.3 ± 0.5	25.3 ± 0.8
	100	8.02 ± 0.2	8.51 ± 0.7	6.8 ± 0.1	8.1 ± 0.1	
	300	8.55 ± 1.0	8.99 ± 0.4	7.7 ± 0.7	8.3 ± 0.0	
	500	8.90 ± 0.1	9.67 ± 0.7	8.1 ± 0.3	8.8 ± 0.1	
	1000	9.68 ± 0.9	9.78 ± 0.6	8.8 ± 0.0	9.1 ± 0.1	
<i>P. aeruginosa</i>	50	7.49 ± 0.0	9.11 ± 0.7	7.4 ± 0.2	7.5 ± 0.0	7.3 ± 0.5
	100	7.70 ± 0.0	9.18 ± 0.4	7.8 ± 0.1	8.3 ± 0.5	
	300	8.34 ± 0.0	9.20 ± 0.0	7.9 ± 0.1	9.1 ± 0.0	
	500	9.34 ± 0.1	9.28 ± 0.0	8.6 ± 0.1	9.4 ± 0.1	
	1000	9.52 ± 0.2	9.99 ± 0.1	8.8 ± 0.1	9.5 ± 0.0	
<i>S. aureus</i>	50	7.20 ± 0.1	7.30 ± 0.1	0.0	6.6 ± 0.1	19.2 ± 1.6
	100	7.39 ± 0.3	7.70 ± 0.1	0.0	6.7 ± 0.1	
	300	7.96 ± 0.3	8.95 ± 0.8	0.0	7.1 ± 0.1	
	500	8.93 ± 0.6	9.53 ± 0.9	0.0	7.5 ± 0.3	
	1000	9.58 ± 0.0	11.07 ± 0.1	0.0	7.6 ± 0.3	

Antibacterial activity of ethyl acetate extracts of endophytic bacterial cultures

The antibacterial activity result of ethyl acetate extracts (1000 $\mu\text{g/mL}$, each) of culture filtrates of GST8 (*B. subtilis*), GST2 (*E. coli*), GST5 (*E. coli*), GST4 (*E. coli*), GSL5 (*B. subtilis*) and GSS7 (*B. amyloliquefaciens*) isolated endophytic bacteria is presented in Table 25.

Table 25. Antibacterial activity of ethyl acetate extracts of isolated endophytic bacteria

Tested organisms	Inhibition zone diameter (mean \pm sd, mm) at 1000 μ g/mL						
	GST8 (<i>B. subtilis</i>)	GST5 (<i>E. coli</i>)	GST2 (<i>E. coli</i>)	GST4 (<i>E. coli</i>)	GSS7 (<i>B. amyloliquefaciens</i>)	GSL5 (<i>B. subtilis</i>)	Chloramph. (30 μ g/disc)
<i>E. coli</i>	7.0 \pm 0.0	7.1 \pm 0.1	6.7 \pm 0.0	8.4 \pm 0.1	8.6 \pm 0.1	9.4 \pm 0.6	25.3 \pm 0.8
<i>P. aeuregunosa</i>	8.0 \pm 1.2	8.2 \pm 0.9	8.4 \pm 0.0	8.8 \pm 0.2	7.6 \pm 0.3	7.6 \pm 0.1	7.3 \pm 0.5
<i>S. aureus</i>	7.9 \pm 0.6	6.9 \pm 0.0	8.4 \pm 0.8	8.3 \pm 0.3	7.1 \pm 0.2	7.1 \pm 0.2	19.2 \pm 1.6

Table 25 showed that all the tested ethyl acetate extracts indicated an activity (≥ 7 mm) against all bacterial strains, except that of GST2 (*E. coli*) and GST5 (*E. coli*), which were found inactive (< 7 mm) against *E. coli* and *S. aureus*, respectively. The higher inhibition zone diameter (9.4 \pm 0.6 mm) against *E. coli* was recorded by the ethyl acetate extract of GSL5 (*B. subtilis*) culture filtrate followed by that of GSS7 (*B. amyloliquefaciens*) (8.6 \pm 0.1 mm) and GST4 (*E. coli*) (8.4 \pm 0.1 mm) (Appendix Figure 6). The ethyl acetate extracts of GST5 (*E. coli*) and GST8 (*B. subtilis*) showed a slight inhibitory effect against the same bacterium with inhibition zone diameters of 7.1 \pm 0.1 mm and 7.0 \pm 0.0 mm, respectively. Whereas the ethyl acetate extract of GST2 (*E. coli*) culture filtrate recorded the higher inhibitory value (8.4 \pm 0.8 mm) against the *S. aureus* strain followed by GST4 (8.3 \pm 0.3 mm) and GST8 (*B. subtilis*) (7.9 \pm 0.6 mm) ethyl acetate extracts. The *P. aeruginosa* bacterium was found vulnerable to all ethyl acetate extracts with greater diameter of inhibition zone scored by GST4 (*E. coli*) (8.8 \pm 0.2 mm) followed by GST2 (*E. coli*) (8.4 \pm 0.0 mm) and GST5 (*E. coli*) (8.2 \pm 0.9 mm) ethyl acetate extracts. The lowest inhibition zone diameters, against *P. aeruginosa*, were measured in the ethyl acetate extracts of GSL5 (7.6 \pm 0.1 mm), GSS7 (*B. amyloliquefaciens*) (7.6 \pm 0.3 mm) and GST8 (*B. subtilis*) (8.0 \pm 1.2 mm).

4.4.2 Antifungal activity assay

The chloroform: methanol (1:1) extracts of *Cadia purpurea* (leaves and roots), *Caralluma speciosa* (stems), *Gloriosa superba* (tubers) and *Gomphocarpus purpurascens* (leaves) were assessed for their potential antifungal activity against *Candida albicans* ATCC 10231 and obtained results were presented in Table 26. The resulted data indicated that the leaves of

Cadia purpurea and tubers of *Gloriosa superba* extracts did not show any activity with zero inhibition values at all tested concentrations. Whereas the roots of *Cadia purpurea* and leaves of *Gomphocarpus purpurascens* extracts displayed a slight activity only at the maximum concentration of 100,000 µg/mL with respective inhibition zone diameter values of 12.67 ± 0.58 mm and 11.00 ± 1.00 mm. The stems extract of *Caralluma speciosa* plant species exhibited prominent inhibitory potential at all evaluated concentrations, except for the minimum concentration (12,500 µg/mL). This stems extract recorded the inhibitory values of 9.00 ± 1.00 mm for 25,000 µg/mL, 14.67 ± 0.58 mm for 50,000 µg/mL and 17.17 ± 1.04 mm for 100,000 µg/mL. The chloroform: methanol (1:1) extract of *Caralluma speciosa* stems in general was found as active as the standard antifungal drug ketoconazole 10 µg/disc (17.67 ± 2.52 mm) mainly at the maximum concentration.

Table 26. Antifungal activity inhibition zone diameters (mean ± sd, mm) against *Candida albicans* of chloroform: methanol (1:1) extracts of four plants

Plant name and standard drug	Tested extract/part	Concentrations (µg/mL) and respective inhibition zone values (mean ± sd, mm)			
		12,5000	25,000	50,000	100,000
<i>C. purpurea</i>	leaves	0.0	0.0	0.0	0.0
	Roots	0.0	0.0	0.0	12.67 ± 0.58
<i>C. speciosa</i>	Stems	0.0	9.00 ± 1.00	14.67 ± 0.58	17.17 ± 1.04
<i>G. superba</i>	Tubers	0.0	0.0	0.0	0.0
<i>G. purpurascens</i>	Leaves	0.0	0.0	0.0	11.00 ± 1.00
Ketoconazole (10 µg/disc)		17.67 ± 2.52			

4.5. *In vitro* antioxidant potential examination

4.5.1 DPPH free radical scavenging assay

Cadia purpurea leaves and roots

The scavenging potential against the DPPH free radical of four roots and leaves extracts (chloroform, 1:1 of chloroform: methanol, methanol and ethanol) and six isolated compounds **65-70** of *C. purpurea* was assessed in reference to the standard antioxidant, ascorbic acid (AA). As presented in Tables 27-29, and depicted in Figures 38-40, each tested analytes showed a dose-dependent activity in which a direct correlation was observed between the DPPH scavenging activity percentage and concentrations of the analytes. As

shown in Table 27 and Figure 43, the ethanol and methanol leaves extracts recorded the higher DPPH radical scavenging percentage (88.23 ± 0.11 and 86.20 ± 0.06 , respectively) with IC_{50} values of 9.22 and 10.94, successively, at the maximum concentration of 500 $\mu\text{g/mL}$. Whereas, at the same concentration, the smaller trapping percentage was observed in the 1:1 of chloroform: methanol (62.31 ± 0.11 , IC_{50} value of 89.73 $\mu\text{g/mL}$) followed by the chloroform (64.89 ± 0.06 and IC_{50} value of 61.55 $\mu\text{g/mL}$) leaves extracts.

Table 27. DPPH scavenging percentage (mean \pm sd) of *C. purpurea* leaves extracts

Concentration ($\mu\text{g/mL}$)	% Scavenging activity (mean \pm sd) of leaves extracts				
	CHCl_3	$\text{CHCl}_3:\text{MeOH}$ (1:1)	MeOH	EtOH	Ascorbic acid
25	42.90 ± 0.00	40.65 ± 0.00	58.75 ± 0.11	60.35 ± 0.22	68.66 ± 0.11
50	50.27 ± 0.00	46.51 ± 0.11	63.83 ± 0.00	65.57 ± 0.11	73.24 ± 0.16
100	53.43 ± 0.06	50.34 ± 0.00	69.04 ± 0.11	70.92 ± 0.06	77.74 ± 0.11
150	55.38 ± 0.06	53.86 ± 0.00	76.50 ± 0.06	76.21 ± 0.11	82.61 ± 0.00
250	58.98 ± 0.06	56.97 ± 0.00	80.42 ± 0.11	80.85 ± 0.22	90.92 ± 0.06
500	64.89 ± 0.06	62.31 ± 0.11	86.20 ± 0.06	88.23 ± 0.11	98.10 ± 0.00
IC_{50} ($\mu\text{g/mL}$)	61.55	89.73	10.94	9.22	4.82

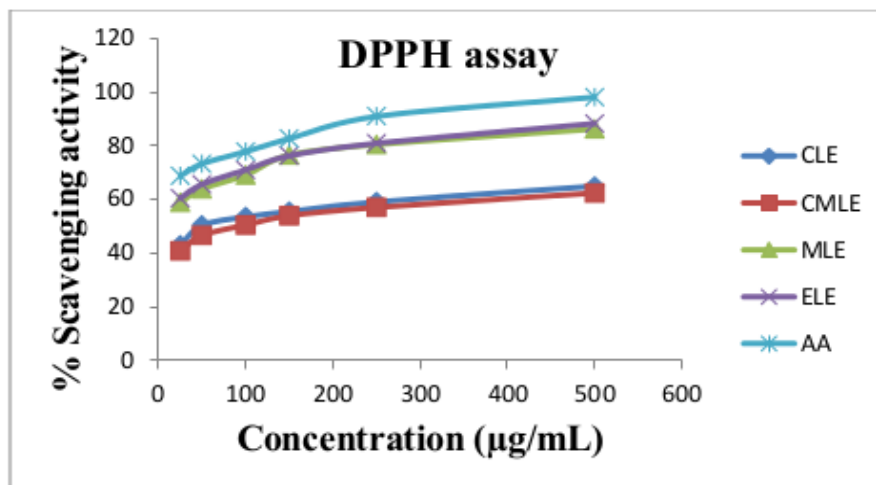


Figure 38. Percentage scavenging activity (means of duplicates) versus different concentrations of *Cadia purpurea* leaves extracts against DPPH radical. CLE, CMLE, MLE and ELE are chloroform, chloroform: methanol (1:1), methanol and ethanol leaves extract, respectively, and AA is ascorbic acid

In the roots part also, the alcoholic extracts (ethanol and methanol) exhibited a better trapping activity percentage (87.51 ± 0.11 and 85.51 ± 0.11 , respectively) on the DPPH radical with respective IC_{50} values of 12.9 and 16.03 $\mu\text{g/mL}$ at the higher concentration (500 $\mu\text{g/mL}$) (Table 28 and Figure 39). Still, the chloroform and chloroform: methanol (1:1) roots extracts provided a comparatively lesser anti-DPPH activity percentage, 77.07 ± 0.00 (IC_{50} value of 27.52 $\mu\text{g/mL}$) and 79.38 ± 0.16 (with 26.14 $\mu\text{g/mL}$ of IC_{50}) for similar concentration. In reference to the observed anti-DPPH potency of ascorbic acid (98.10 ± 0.00 , IC_{50} value of 4.82 $\mu\text{g/mL}$) at the maximum concentration of 500 $\mu\text{g/mL}$, however, the inhibitory activity against the free radical of the tested roots and leaves extracts was found weak.

Table 28. DPPH radical scavenging percentage (mean \pm sd) of *C. purpurea* roots extracts

Concentration ($\mu\text{g/mL}$)	% Scavenging activity (mean \pm sd) against DPPH radical of roots extracts				
	CHCl_3	$\text{CHCl}_3:\text{MeOH}$	Methanol	Ethanol	Ascorbic acid
25	50.28 ± 0.06	50.56 ± 0.11	55.94 ± 0.00	57.77 ± 0.06	68.66 ± 0.11
50	55.46 ± 0.00	56.67 ± 0.11	61.26 ± 0.11	63.98 ± 0.06	73.24 ± 0.16
100	60.16 ± 0.22	61.22 ± 0.00	66.36 ± 0.06	68.01 ± 0.11	77.74 ± 0.11
150	63.83 ± 9.06	65.47 ± 0.16	70.47 ± 0.06	72.33 ± 0.11	82.61 ± 0.00
250	70.94 ± 0.06	72.86 ± 0.11	77.89 ± 0.06	79.68 ± 0.06	90.92 ± 0.06
500	77.07 ± 0.00	79.38 ± 0.16	85.51 ± 0.11	87.51 ± 0.11	98.10 ± 0.00
IC_{50} ($\mu\text{g/mL}$)	27.52	26.14	16.03	12.9	4.82

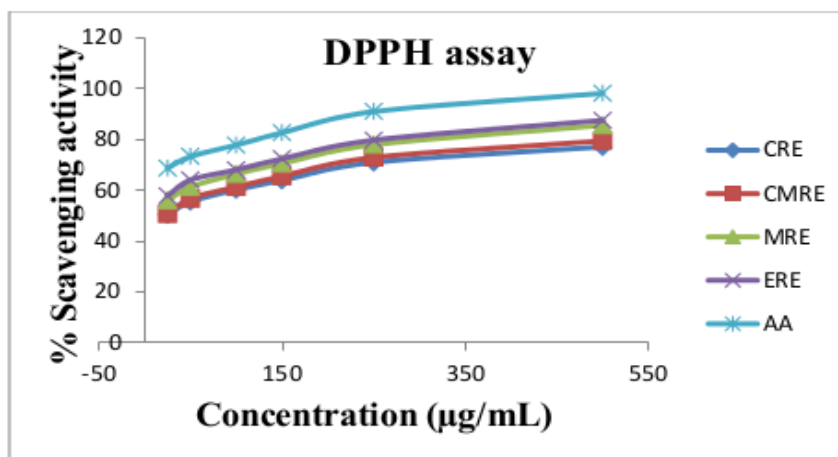


Figure 39. Percentage scavenging activity against DPPH of *C. purpurea* roots extracts at different concentrations. CRE, CMRE, MRE and ERE are chloroform, chloroform: methanol (1:1), methanol and ethanol roots extracts, and AA is ascorbic acid standard

Amongst the examined compounds, the flavonoid compound **66** presented a greater anti-DPPH activity percentage of 83.61 ± 0.06 at concentration of $500 \mu\text{g/mL}$ with smaller IC_{50} value of $6.21 \mu\text{g/mL}$ (Table 29 and Figure 40). The next higher scavenging percentage values were noted by compounds **70** (82.69 ± 0.11 , IC_{50} value of $7.99 \mu\text{g/mL}$) and **67** (80.36 ± 0.00 and IC_{50} value of $8.67 \mu\text{g/mL}$) for the same concentration. Compounds **65**, **69** and **68** exhibited weak DPPH radical scavenging potential by recording higher IC_{50} values of $121.6 \mu\text{g/mL}$, $157.1 \mu\text{g/mL}$ and $208.6 \mu\text{g/mL}$, respectively. Here, the smaller IC_{50} value implies the better DPPH radical scavenging activity and vice versa. Hence, even though compounds **66**, **67** and **70** exhibited relatively good radical inhibitory activity, the overall antioxidative activity against the DPPH radical of all compounds was observed much weaker as compared to the ascorbic acid (IC_{50} value of $4.82 \mu\text{g/mL}$).

Table 29. DPPH radical scavenging activity percentage (mean \pm sd) of compounds **65-70** isolated from leaves and roots of *C. purpurea*

Conc. ($\mu\text{g/mL}$)	Scavenging activity percentage (mean \pm sd) against DPPH of isolated compounds 65-70						
	65	66	67	68	69	70	Ascorbic acid
25	40.25 ± 0.06	63.02 ± 0.00	61.03 ± 0.06	32.48 ± 0.06	32.54 ± 0.00	61.96 ± 0.11	68.66 ± 0.11
50	42.64 ± 0.11	63.55 ± 0.00	61.32 ± 0.11	33.73 ± 0.06	37.52 ± 0.04	62.20 ± 0.06	73.24 ± 0.16
100	45.18 ± 0.11	66.67 ± 0.11	61.42 ± 0.00	34.61 ± 0.07	39.30 ± 0.00	63.59 ± 0.1	77.74 ± 0.11
150	48.44 ± 0.06	68.58 ± 0.06	65.53 ± 0.00	35.48 ± 0.06	47.06 ± 0.00	66.52 ± 0.00	82.61 ± 0.00
250	55.61 ± 0.06	75.86 ± 0.06	73.85 ± 0.00	36.30 ± 0.00	44.27 ± 0.04	74.47 ± 0.06	90.92 ± 0.06
500	65.25 ± 0.06	83.61 ± 0.06	80.36 ± 0.00	40.74 ± 0.06	47.87 ± 0.06	82.69 ± 0.11	98.10 ± 0.00
IC_{50} ($\mu\text{g/mL}$)	121.6	6.21	8.67	208.6	157.1	7.99	4.82

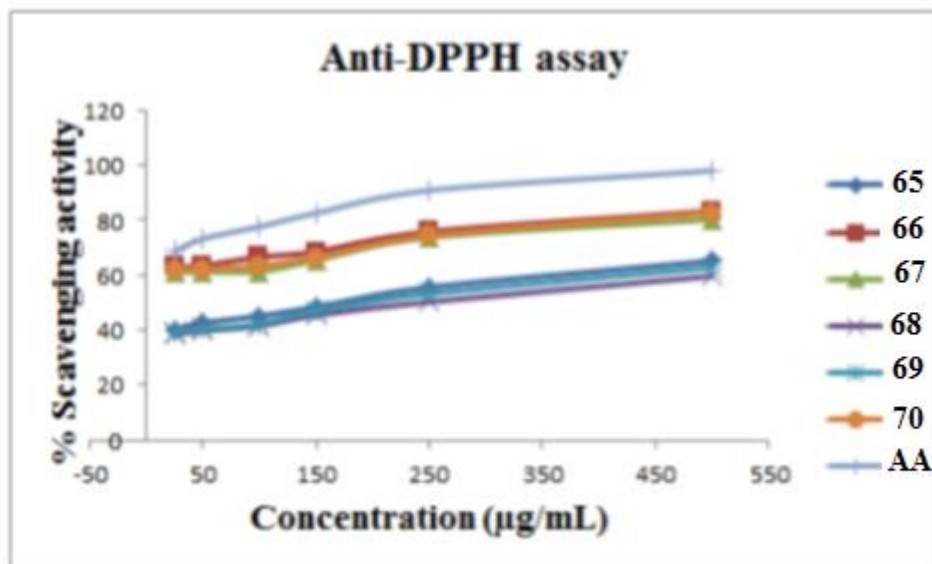


Figure 40. DPPH radical scavenging activity percentage (mean of duplicates) against various concentrations of compounds 65-70 isolated from leaves and roots of *C. purpurea*

Caralluma speciosa stems

The obtained results (Tables 30 and 31, and Figures 41 and 42) revealed that each tested analytes showed a directly correlated (dose-dependent) activity, i.e. the percentage DPPH scavenging activity was getting increased as the concentration increased.

As demonstrated in Table 30 and Figure 41, the ethanol extract (EE) of *C. speciosa* stem showed a better DPPH radical scavenging percentage (58.092 ± 0.00) in comparison to ascorbic acid (95.342 ± 0.02) at the highest concentration of 500 µg/mL followed by chloroform extract (CE, 51.303 ± 0.04). Generally, the obtained IC_{50} values of all the extracts were found to be high compared to the IC_{50} value of ascorbic acid ($5.62 \mu\text{g/mL}$) indicated a negligible inhibitory activity against the DPPH radicals.

Table 30. Percent scavenging activity (mean \pm sd) against DPPH of *C. speciosa* stem extracts

Conc. ($\mu\text{g/mL}$)	% Scavenging activity against DPPH of stem extracts					
	<i>n</i> -Hexane	CHCl_3	CHCl_3 :MeOH (1:1)	MeOH	EtOH	Ascorbic acid
25	6.055 \pm 0.00	8.257 \pm 0.00	6.055 \pm 0.00	6.789 \pm 0.00	11.56 \pm 0.00	65.857 \pm 0.02
50	6.789 \pm 0.00	10.092 \pm 0.00	6.789 \pm 0.00	8.012 \pm 0.21	15.596 \pm 0.00	70.945 \pm 0.02
100	7.156 \pm 0.37	12.196 \pm 0.09	9.541 \pm 0.18	11.56 \pm 0.00	23.67 \pm 0.00	76.254 \pm 0.02
150	7.89 \pm 0.00	12.477 \pm 0.00	11.193 \pm 0.00	14.312 \pm 0.00	27.486 \pm 0.07	80.276 \pm 0.04
250	11.56 \pm 0.00	20.000 \pm 0.00	11.682 \pm 0.21	20.734 \pm 0.00	37.174 \pm 0.07	85.320 \pm 0.04
500	30.765 \pm 0.17	51.303 \pm 0.04	28.037 \pm 0.04	35.229 \pm 0.04	58.092 \pm 0.00	95.342 \pm 0.02
IC ₅₀ ($\mu\text{g/mL}$)	1117.36	512.98	860.01	742.09	400.41	5.62

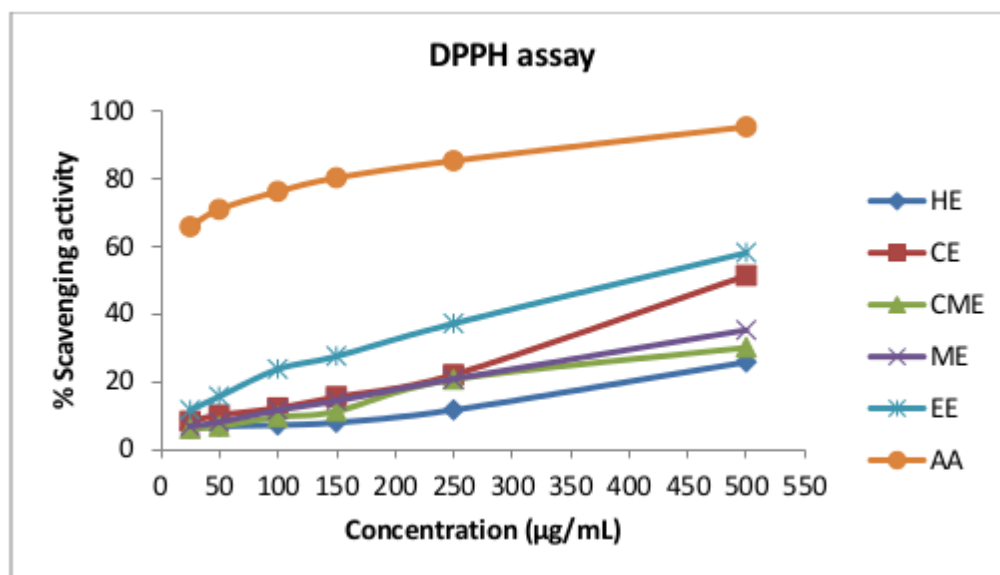


Figure 41. DPPH radical scavenging percentage (%) versus different concentrations of *C. speciosa* crude extracts and ascorbic acid (HE-hexane extract, CE-chloroform extract, CME-chloroform: methanol extract, ME-methanol extract, EE-ethanol extract, AA-ascorbic acid)

As showed in Table 31 and Figure 42, amongst the isolated compounds, compound **74** recorded the highest scavenging percentage (86.225 ± 0.09) followed by compound **73** (72.597 ± 0.11) and compound **75** (56.13 ± 0.11) at the highest concentration ($500 \mu\text{g/mL}$) with IC₅₀ values of 15.67, 73.48 and $270.02 \mu\text{g/mL}$, respectively. Whereas compounds **71** and **72** showed highest IC₅₀ values (3490.64 and $1371.59 \mu\text{g/mL}$, respectively). In compared

to the IC₅₀ value (5.62 µg/mL) of ascorbic acid, the DPPH radical scavenging potential of compounds **71-75** was found to be weak.

Table 31. Scavenging activity percentage (mean ± sd) against DPPH of compounds **71-75** isolated from *C. speciosa* stem extracts

Concentration (µg/mL)	% Inhibitory activity against DPPH of isolated compounds 71-75					
	71	72	73	74	75	Ascorbic acid
25	6.285±0.00	8.609±0.00	41.369±0.09	56.159±0.09	14.79±0.09	65.857±0.02
50	9.609±0.00	11.712±0.11	44.194±0.09	61.280±0.09	27.903±0.04	70.945±0.02
100	13.830±0.00	15.258±0.11	50.521±0.09	67.697±0.07	34.728±0.04	76.254±0.02
150	16.272±0.00	20.038±0.00	56.321±0.16	74.231±0.11	42.252±0.09	80.276±0.04
250	25.038±0.00	30.921±0.04	64.371±0.04	80.721±0.11	52.053±0.09	85.320±0.04
500	35.141±0.11	43.097±0.13	72.597±0.11	86.225±0.09	56.13±0.11	95.342±0.02
IC ₅₀ (µg/mL)	3490.64	1371.59	73.48	15.67	270.02	5.62

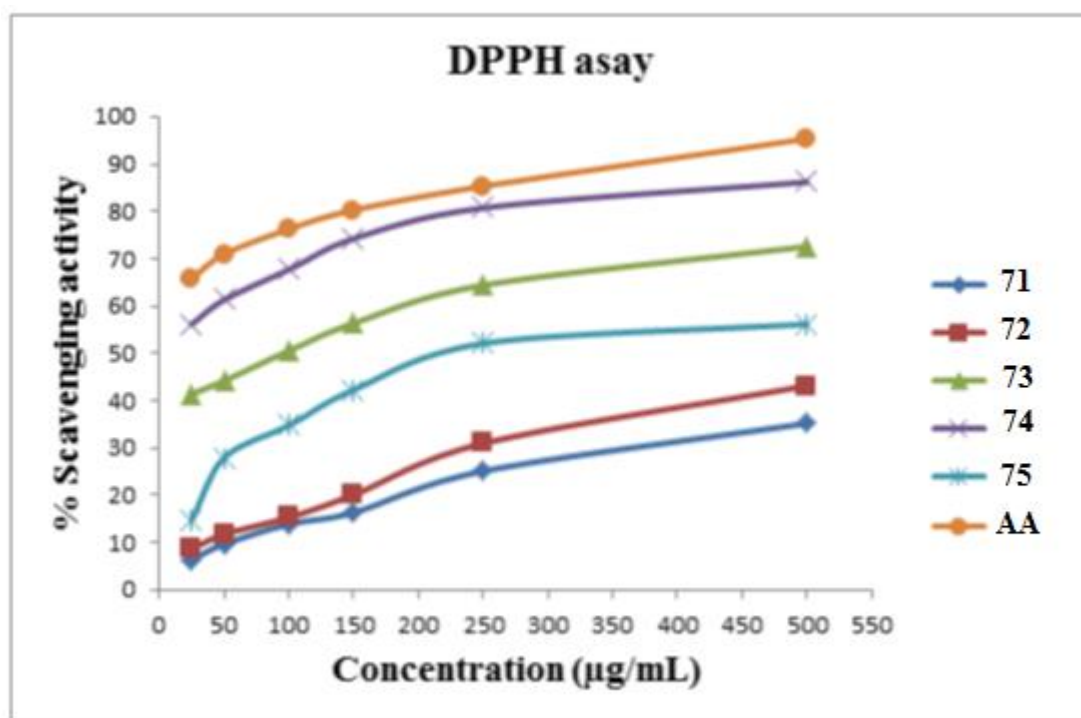


Figure 42. DPPH radical scavenging percentage (%) versus different concentrations (µg/mL) of compounds 71-75 isolated from *C. speciosa* stems and standard ascorbic acid (AA)

Gloriosa superba tubers

All the evaluated tubers extracts and isolated compounds of *G. superba* showed good DPPH free radical inhibitory effect comparable to the ascorbic acid (98.89 ± 0.00 , IC_{50} value of $1.2 \mu\text{g/mL}$) (Table 32 and Figure 43). The methanol extract provided higher scavenging percentage of 90.16 ± 0.00 (IC_{50} value of $1.5 \mu\text{g/mL}$) followed by the 1:1 of chloroform: methanol (89.94 ± 0.03 , IC_{50} of $2.0 \mu\text{g/mL}$) and chloroform (88.91 ± 0.06 , IC_{50} of $3.2 \mu\text{g/mL}$) extracts at the maximum concentration of $500 \mu\text{g/mL}$. Compound **78** indicated a slight DPPH trapping effect with small scavenging percentage of 84.70 ± 0.03 (IC_{50} value of $21.6 \mu\text{g/mL}$) even at the higher concentration ($500 \mu\text{g/mL}$). Whereas compound **76** was found to be weak with scavenging percentage value of 58.73 ± 0.06 and IC_{50} value of $185.9 \mu\text{g/mL}$.

Table 32.: Percentage inhibitory activity (mean \pm sd) of *G. superba* tubers extracts and isolated compounds **76** and **78** against DPPH free radical

Concentration ($\mu\text{g/mL}$)	% Scavenging activity (mean \pm sd) tubers extracts and isolated compounds 76 and 78					
	CHCl_3	$\text{CHCl}_3:\text{MeOH}$ H (1:1)	MeOH	76	78	Ascorbic acid
25	65.27 ± 0.04	68.77 ± 0.03	70.07 ± 0.06	35.73 ± 0.06	52.91 ± 0.03	75.45 ± 0.07
50	72.14 ± 0.07	73.13 ± 0.00	75.15 ± 0.00	40.04 ± 0.00	60.14 ± 0.06	80.99 ± 0.10
100	76.48 ± 0.04	79.55 ± 0.03	80.21 ± 0.00	43.04 ± 0.00	62.76 ± 0.07	84.29 ± 0.07
150	79.89 ± 0.07	82.47 ± 0.00	86.69 ± 0.03	46.79 ± 0.00	67.55 ± 0.10	89.01 ± 0.00
250	83.47 ± 0.00	87.56 ± 0.03	89.82 ± 0.04	53.35 ± 0.07	75.68 ± 0.10	95.79 ± 0.03
500	88.91 ± 0.06	89.94 ± 0.03	90.16 ± 0.00	58.73 ± 0.06	84.70 ± 0.03	98.89 ± 0.00
IC_{50} ($\mu\text{g/mL}$)	3.2	2.0	1.5	185.9	21.6	1.2

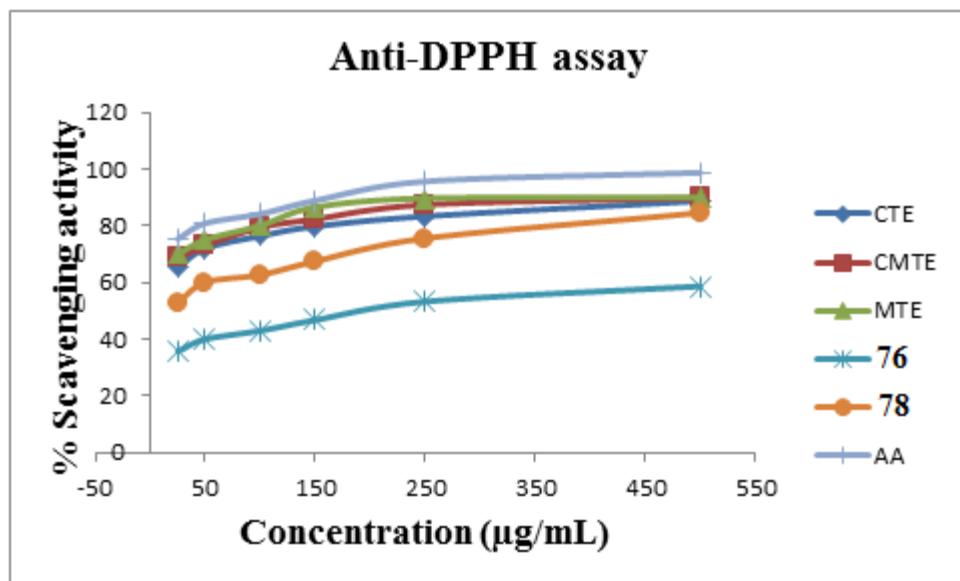


Figure 43. Percentage scavenging activity against DPPH radical versus concentration ($\mu\text{g/mL}$) of *G. superba* tuber extracts and isolated compounds **76** and **78**. CTE, CMTE and MTE are chloroform, chloroform: methanol (1:1) and methanol tubers extract, respectively.

***Gomphocarpus purpurascens* leaves extracts and isolated compound 79**

As presented in Table 33 and depicted in Figure 44, an auspicious anti-DPPH free radical inhibitory effect was observed in all extracts with higher scavenging percentage values (95.7 ± 0.00 and 93.5 ± 0.00 , respectively) recorded by the ethanol and methanol extracts at $500 \mu\text{g/mL}$ with each having the IC_{50} value of $1.1 \mu\text{g/mL}$. The chloroform: methanol (1:1) and chloroform extracts also displayed good DPPH radical scavenging percentage values of 91.2 ± 0.00 (IC_{50} value of $1.7 \mu\text{g/mL}$) and 85.2 ± 0.00 (IC_{50} value of $2.7 \mu\text{g/mL}$). The isolated compound **79** exhibited far less DPPH scavenging percentage (65.09 ± 0.04) at the higher concentration ($500 \mu\text{g/mL}$) with higher IC_{50} value of $134.0 \mu\text{g/mL}$.

Table 33. DPPH scavenging activity percentage of *G. purpurascens* leaves extracts and isolated calotropin (**79**)

Concentration (µg/mL)	% Scavenging activity (mean ± sd) against DPPH free radical					
	CHCl ₃	CHCl ₃ : MeOH	MeOH	EtOH	Calotropin (79)	Ascorbic acid
25	64.30 ± 0.00	70.1 ± 0.00	72.53 ± 0.15	73.7 ± 0.00	36.3 ± 0.00	75.45 ± 0.07
50	70.6 ± 0.00	74.6 ± 0.00	76.83 ± 0.15	78.87 ± 0.06	39.64 ± 0.03	80.99 ± 0.10
100	75.60 ± 0.00	78.07 ± 0.00	79.97 ± 0.06	82.2 ± 0.00	43.7 ± 0.03	85.29 ± 0.07
150	78.30 ± 0.20	82.3 ± 0.00	83.3 ± 0.00	85.43 ± 0.06	48.92 ± 0.07	89.01 ± 0.00
250	80.83 ± 0.06	87.7 ± 0.00	88.4 ± 0.00	90.6 ± 0.00	56.64 ± 0.04	95.79 ± 0.03
500	85.2 ± 0.00	91.2 ± 0.00	93.5 ± 0.00	95.7 ± 0.00	65.09 ± 0.04	98.89 ± 0.00
IC ₅₀ (µg/mL)	2.7	1.7	1.1	1.1	134.0	1.0

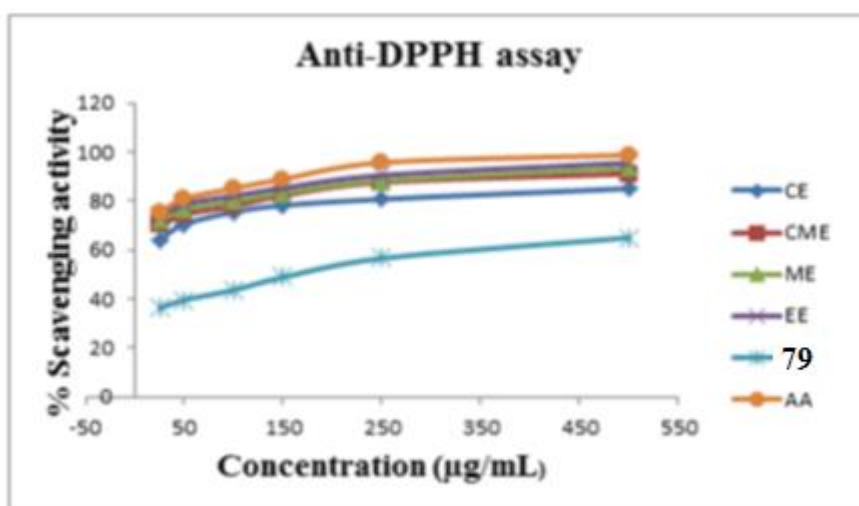


Figure 44. DPPH radical scavenging activity percentage versus concentration (µg/mL) of *G. purpurascens* leaves extracts and isolated calotropin (**79**)

4.5.2 Ferric reducing antioxidant power (FRAP) assay

The ferric reducing antioxidant power of a given analyte could be monitored by the conversion of ferric (Fe^{3+}) into its ferrous (Fe^{2+}) form. That is, ferric ions (Fe^{3+}) originated from ferricyanide complex ($[\text{K}_3\text{Fe}(\text{CN})_6]$) are reduced to the ferrous ions (Fe^{2+}) which can be noticed by the change in color of the reaction solutions from yellow to green in the presence of antioxidants. The produced Fe^{2+} concentration is finally quantified by measuring its absorbance at 700 nm^{104} . In the present work, the same working principle was followed.

***Cadia purpurea* leaves and roots**

The FRAP results of tested leaves and roots extracts, and isolated compounds **65-70** of *C. purpurea* were presented in Tables 34, 35 and 36, respectively. As it can be seen in the Tables, the ferric ion reducing power (expressed in mean absorbance at 700 nm) of each evaluated analytes was found positively related with corresponding concentrations (25-500 µg/mL). That is, the intense of green color and absorbance of mixture was getting increased with the increase of sample concentration indicates a strong ferric reducing potential. Similar to DPPH radical scavenging percentage, the alcoholic leaves extracts showed a better ferric reducing antioxidative power at the maximum concentration of 500 µg/mL with the higher mean absorbance value recorded by methanol extract (0.714 ± 0.001) followed by ethanol extract (0.679 ± 0.001) (Table 34). At the same concentration, the chloroform and chloroform: methanol (1:1) leaves extracts displayed a comparatively weak ferric reducing ability with corresponding absorbance values of 0.397 ± 0.000 and 0.547 ± 0.001 .

Table 34.: FRAP (mean \pm sd) of *C. purpurea* leaves extracts

Concentration (µg/mL)	Absorbance (mean \pm sd, at 700 nm) of leaves extracts				
	CHCl ₃	CHCl ₃ :MeOH	MeOH	EtOH	Ascorbic acid
25	0.372 ± 0.001	0.345 ± 0.001	0.415 ± 0.001	0.411 ± 0.001	0.911 ± 0.001
50	0.373 ± 0.001	0.347 ± 0.001	0.432 ± 0.001	0.430 ± 0.001	0.925 ± 0.001
100	0.380 ± 0.001	0.410 ± 0.001	0.441 ± 0.002	0.435 ± 0.002	1.069 ± 0.002
150	0.381 ± 0.000	0.428 ± 0.001	0.461 ± 0.001	0.458 ± 0.002	1.303 ± 0.002
250	0.384 ± 0.001	0.447 ± 0.001	0.617 ± 0.001	0.558 ± 0.002	1.855 ± 0.001
500	0.397 ± 0.000	0.547 ± 0.001	0.714 ± 0.001	0.679 ± 0.001	2.225 ± 0.000

Likened to the leaves extracts, the extracts of the roots part exhibited stronger ferric reducing antioxidant activity with the higher absorbance values of 0.810 ± 0.001 and 0.788 ± 0.000 observed in the methanol and ethanol extracts, respectively (Table 35). With respect to the standard ascorbic acid (2.225 ± 0.000), however, observed ferric reduction power of studied extracts was not remarkable.

Table 35. FRAP (mean \pm sd) of *C. purpurea* roots extracts

Concentration ($\mu\text{g/mL}$)	Absorbance (mean \pm sd, at 700 nm) of roots extracts				
	CHCl_3	$\text{CHCl}_3:\text{MeOH}$	MeOH	EtOH	Ascorbic acid
25	0.308 ± 0.001	0.429 ± 0.001	0.460 ± 0.001	0.424 ± 0.001	0.911 ± 0.001
50	0.308 ± 0.001	0.524 ± 0.001	0.472 ± 0.001	0.448 ± 0.000	0.925 ± 0.001
100	0.351 ± 0.000	0.542 ± 0.002	0.506 ± 0.000	0.508 ± 0.002	1.069 ± 0.002
150	0.381 ± 0.001	0.573 ± 0.001	0.549 ± 0.000	0.539 ± 0.001	1.303 ± 0.002
250	0.381 ± 0.000	0.610 ± 0.002	0.563 ± 0.002	0.514 ± 0.001	1.855 ± 0.001
500	0.466 ± 0.001	0.653 ± 0.001	0.810 ± 0.001	0.788 ± 0.000	2.225 ± 0.000

Among the compounds evaluated, compounds **70**, **67** and **68** indicated a notable ferric reducing strength with 0.761 ± 0.002 , 0.722 ± 0.000 and 0.621 ± 0.001 , respectively, of absorbance values at the maximum concentration ($500 \mu\text{g/mL}$). The least absorbance values were shown in compounds **65** (0.409 ± 0.001), **69** (0.465 ± 0.001) and **66** (0.510 ± 0.000) for similar concentration (Table 36). Unfortunately, the ferric reducing antioxidant power of all tested compounds **65-70** and that of ascorbic acid was still incomparable for the same concentration.

Table 36. FRAP (mean \pm sd) of compounds **65-70** isolated from *C. purpurea* leaves and roots extracts

Dilutions ($\mu\text{g/mL}$)	FRAP (mean \pm sd) of isolated compounds 65-70						
	65	66	67	68	69	70	Ascorbic acid
25	0.319 \pm 0.001	0.412 \pm 0.001	0.489 \pm 0.003	0.314 \pm 0.001	0.321 \pm 0.001	0.497 \pm 0.001	0.911 \pm 0.001
50	0.335 \pm 0.001	0.430 \pm 0.001	0.493 \pm 0.002	0.344 \pm 0.001	0.332 \pm 0.001	0.510 \pm 0.001	0.925 \pm 0.001
100	0.337 \pm 0.002	0.489 \pm 0.002	0.497 \pm 0.001	0.370 \pm 0.001	0.333 \pm 0.001	0.514 \pm 0.001	1.069 \pm 0.002
150	0.339 \pm 0.001	0.493 \pm 0.001	0.511 \pm 0.001	0.382 \pm 0.001	0.369 \pm 0.02	0.612 \pm 0.001	1.303 \pm 0.002
250	0.393 \pm 0.001	0.500 \pm 0.001	0.608 \pm 0.001	0.486 \pm 0.001	0.459 \pm 0.001	0.623 \pm 0.001	1.855 \pm 0.001
500	0.409 \pm 0.001	0.510 \pm 0.000	0.722 \pm 0.000	0.621 \pm 0.001	0.465 \pm 0.001	0.761 \pm 0.002	2.225 \pm 0.000

Caralluma speciosa stems

The FRAP results of the crude extracts and isolated compounds **71-75** of *C. speciosa* stems are presented in Tables 37 and 38, respectively. As depicted in the Tables, the ferric reducing power (expressed in absorbance at 700 nm) of each tested compounds and extracts showed a positive correlation with corresponding concentrations (from 25-500 µg/mL). That is, at high concentration, intense green color with greater absorbance of mixtures was observed indicating that higher ferric reducing potential.

From Table 37, ethanol extract showed a slightly higher reducing activity (0.794 ± 0.000 , 0.601 ± 0.000 , 0.559 ± 0.003 and 0.497 ± 0.001) at concentrations of 500, 250, 150 and 100 µg/mL. Chloroform extract exhibited the next higher reducing power (0.488 ± 0.001) at the highest concentration.

Table 37. FRAP (mean \pm sd) of *C. speciosa* extracts

Concentration (µg/mL)	Absorbance at 700 nm in FRAP assay of crude extracts					
	<i>n</i> -Hexane	CHCl ₃	CHCl ₃ : MeOH (1:1)	MeOH	EtOH	Ascorbic acid
25	0.297 \pm 0.002	0.339 \pm 0.001	0.351 \pm 0.002	0.374 \pm 0.001	0.425 \pm 0.000	0.593 \pm 0.002
50	0.306 \pm 0.002	0.348 \pm 0.000	0.367 \pm 0.001	0.375 \pm 0.000	0.451 \pm 0.001	1.148 \pm 0.002
100	0.316 \pm 0.002	0.353 \pm 0.005	0.371 \pm 0.001	0.391 \pm 0.000	0.497 \pm 0.001	1.193 \pm 0.003
150	0.316 \pm 0.002	0.354 \pm 0.003	0.381 \pm 0.001	0.398 \pm 0.003	0.559 \pm 0.003	2.145 \pm 0.010
250	0.321 \pm 0.001	0.405 \pm 0.001	0.397 \pm 0.001	0.400 \pm 0.001	0.601 \pm 0.000	2.280 \pm 0.000
500	0.348 \pm 0.001	0.488 \pm 0.001	0.408 \pm 0.004	0.463 \pm 0.002	0.794 \pm 0.000	2.550 \pm 0.000

Table 38 showed that compound **72** recorded highest FRAP with an absorbance of 1.622 ± 0.004 followed by compound **73** (1.608 ± 0.002) at the highest concentration (500 µg/mL); whereas the lowest FRAP (0.291 ± 0.001) was observed in compound **71** at same concentration.

Table 38. FRAP (mean \pm sd) of isolated compounds **71-75** of *C. speciosa* stems extracts

Concentration ($\mu\text{g/mL}$)	Absorbance at 700 nm against ferric ion reduction of compounds 71-75					
	71	72	73	74	75	Ascorbic acid
25	0.224 \pm 0.001	0.262 \pm 0.001	0.338 \pm 0.001	0.247 \pm 0.000	0.242 \pm 0.000	0.593 \pm 0.002
50	0.243 \pm 0.001	0.300 \pm 0.001	0.461 \pm 0.000	0.261 \pm 0.001	0.292 \pm 0.000	1.148 \pm 0.002
100	0.245 \pm 0.001	0.318 \pm 0.001	0.518 \pm 0.003	0.299 \pm 0.001	0.396 \pm 0.001	1.193 \pm 0.003
150	0.250 \pm 0.000	0.397 \pm 0.082	0.565 \pm 0.001	0.434 \pm 0.001	0.473 \pm 0.000	2.145 \pm 0.010
250	0.252 \pm 0.001	0.637 \pm 0.001	0.620 \pm 0.002	0.547 \pm 0.000	0.585 \pm 0.001	2.280 \pm 0.000
500	0.291 \pm 0.001	1.622 \pm 0.004	1.608 \pm 0.002	0.757 \pm 0.002	0.757 \pm 0.001	2.550 \pm 0.000

FRAP of isolated compounds 76, 78 and 79

As presented in Table 39, compound **78** indicated a mild ferric ion reduction capacity with mean absorbance value of 0.665 ± 0.001 despite it was incomparable with the value recorded by the ascorbic acid (2.225 ± 0.000) at the higher concentration of $500 \mu\text{g/mL}$. Whereas compounds **76** and **79** exhibited a very weak ferric reduction antioxidant power with negligible absorbance values (0.366 ± 0.001 and 0.445 ± 0.001 , respectively) at similar concentration.

Table 39. FRAP of isolated compounds **76, 78 and 79**

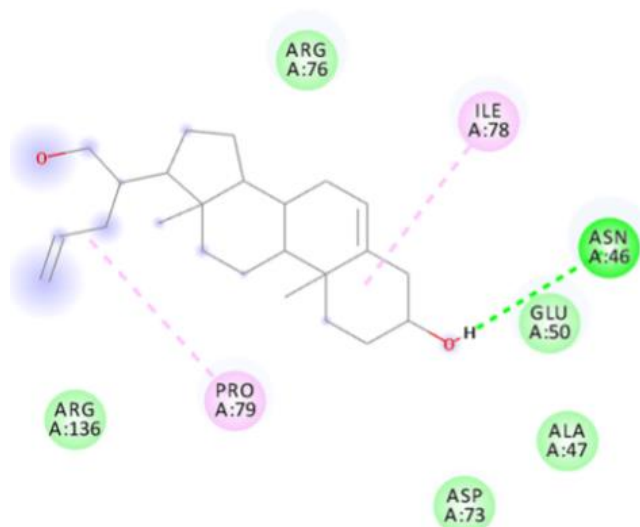
Concentration ($\mu\text{g/mL}$)	FRAP in absorbance at 700 nm (mean \pm sd) of compounds 76, 78 and 79			
	76	78	79	Ascorbic acid
25	0.280 \pm 0.001	0.299 \pm 0.001	0.300 \pm 0.001	0.911 \pm 0.001
50	0.294 \pm 0.001	0.343 \pm 0.001	0.361 \pm 0.001	0.925 \pm 0.001
100	0.350 \pm 0.001	0.370 \pm 0.001	0.391 \pm 0.001	1.069 \pm 0.002
150	0.352 \pm 0.002	0.405 \pm 0.001	0.433 \pm 0.001	1.303 \pm 0.002
250	0.363 \pm 0.002	0.419 \pm 0.001	0.442 \pm 0.001	1.855 \pm 0.001
500	0.366 \pm 0.001	0.665 \pm 0.001	0.445 \pm 0.001	2.225 \pm 0.000

4.6 In silico molecular modeling study

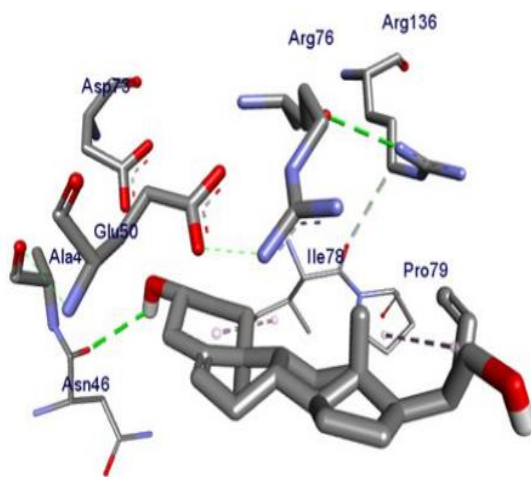
The docking analysis output revealed that the isolated compounds **65-69** showed different interactions including hydrogen-bonding with some active site pockets of *E. coli* gyraseB (6F86), *S. aureus* pyruvate kinase (3T07) and human peroxiredoxin 5 (1HD2) protein models

as presented in Tables 18-20, and depicted in Figures 45-59. Besides, the compounds **65-68**, **70** and **79** formed some interactions with the amino acid residues of *P. aeruginosa* PqsA (5OE3) enzyme (Appendix Table 21 and Figures 60-65). Compounds **65**, **67** and **68** exhibited stronger binding affinity (-6.5, -7.4 and -7.3 kcal/mol, respectively) to the 6F86 protein model than the chloramphenicol (-6.4 kcal/mol) (Figure 66); whereas all the compounds **65-69** showed better binding energy to 3T07 and 1HD2 protein models than chloramphenicol (-4.6 kcal/mol) (Figure 67) and ascorbic acid (-4.5 kcal/mol) (Figure 68). The docking interaction (Figures 45 and 46) indicated that compound **65** formed a hydrogen-bonding interaction with Asn-46 and Glu-352 amino acid residues of 6F86 and 3T07, respectively, while no hydrogen-bonds shown with the 1HD2 enzyme (Figure 47). Apigenin-7-*O*-neohesperidoside (**66**) formed two hydrogen-bonding interactions with Asp-73 and Glu-50 of 6F86 (Figure 48), three with Lys-390, Ser-354 and Leu-269 of 3T07 (Figure 49) and one with Thr-147 of 1HD2 (Figure 50). Calpurnine (**67**) made three hydrogen bonds with Thr-165, Gly-77 and Ile-78 of 6F86 (Figure 51) and two with Glu-352 and Asn-357 of 3T07 enzymes (Figure 52); but did not show any hydrogen-bonding interaction with the amino acid residues of 1HD2 enzyme (Figure 53). Compound **68** showed two hydrogen-bonding interactions both with the 6F86 (with Ile-94 and Val-97, Figure 54) and 3T07 (Thr-387 and Ser-383, Figure 55) enzymes, and one with Ala-42 of 1HD2 (Figure 56). The bis-(2-hydroxybutyl) phthalate (**69**) also established some hydrogen-bondings; three with Asn-46, Glu-50 and Asp-73 of 6F86 (Figure 57), four with Arg-386, Ser-383, Lys-390 and Asn-357 of 3T07 (Figure 58), and three with Gly-46, Thr-44 and Thr-147 of 1HD2 (Figure 59) amino residues. The compounds **65**, **66**, **67**, **68** and **79** recorded respective docking scores of -7.9, -10.9, -8.1, -7.8 and -10.3 kcal/mol against *P. aeruginosa* PqsA (5OE3) which were found higher than that of chloramphenicol (-7.0 kcal/mol) (Figure 69). Compound **65** formed two hydrogen-bonds with Arg-33 and Glu-331 (Figure 60), while compound **66** showed five hydrogen-bonding interactions with Ala-21, Asp-19, Ala-245, Thr-29 and His-24 amino acid residues of 5OE3 (Figure 61). Compounds **67**, **68**, **70** and **79** also established three (with Arg-386, Arg-33 and Glu-388), another three (with Arg-200, Thr-29 and Gln-34), two (with His-24 and Arg-200) and six (with Gly-169, Lys-172, Arg-397, Ala-170, Thr-380 and Thr-164) hydrogen-bonds, respectively, (Figures 62-65) of the protein model 5OE3.

The drug-likeness, ADME and toxicity properties predictions of the isolated compounds **65-69**, **70** and **79** are presented in Appendix Tables 22, 23 and 24. The drug-likeness property prediction report (Appendix Table 22) indicated that apigenin-7-*O*-neohesperidoside (**66**) was found violated three rules of the Lipinski's rule of five (with molecular weight > 500 g/mol, hydrogen-acceptor > 10 and hydrogen-donor > 5). Compound **68**, bis-(2-methylheptyl)phthalate (**70**) and calotropin (**79**) were also found violated, each, one rule of the Lipinski's rule of five (with hydrogen-donor > 5, LogP > 4.15 and molecular weight > 500 g/mol), respectively. The ADME property prediction report (Appendix Table 23) showed that compounds **66**, **79**, **68** and **67** scored higher skin permeation values (logP in cm/s) of -9.94, -8.89, -7.94 and -7.09, respectively. Compounds **66** and **68** exhibited low gastro-intestinal absorption and were found as non blood brain barrier (BBB) permeable. On the other side, compounds **65**, **67**, **68** and **69** did not show any inhibitory interaction with the P-glycoprotein (P-gp) enzyme. Whereas compounds **66**, **68** and **79** were observed as non-inhibitors of all the cytochrome-P (CYP) enzymes. The toxicity property prediction report (Appendix Table 24) revealed that compounds **67** and **79** were found within the toxicity class of two with LD₅₀ values of 32 and 8 mg/Kg, respectively. Apigenin-7-*O*-neohesperidoside (**66**) was found as immunotoxic and mutagenic isolate; and the calotropin (**79**) displayed an immunotoxicity and cytotoxicity properties. Compounds **65** and **68** were also found as immunotoxic and mutagenic isolates, respectively.



(a)



(b)

Figure 45. Ligand-protein interaction (a) and 3D representation (b) between compound 65 and *E. coli* gyraseB enzyme (6F86)

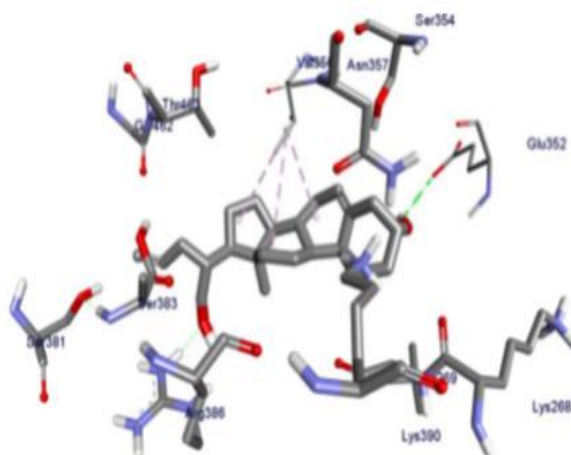
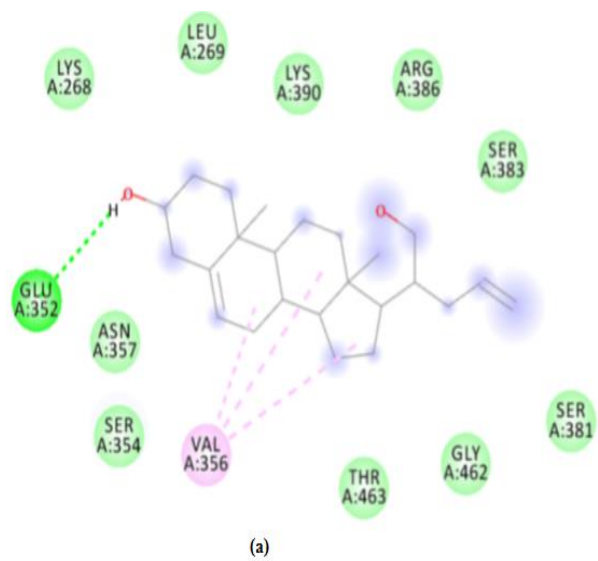


Figure 46. Ligand-protein interaction (a) and 3D representation (b) of compound **65** against *S. aureus* pyruvate kinase (3T07)

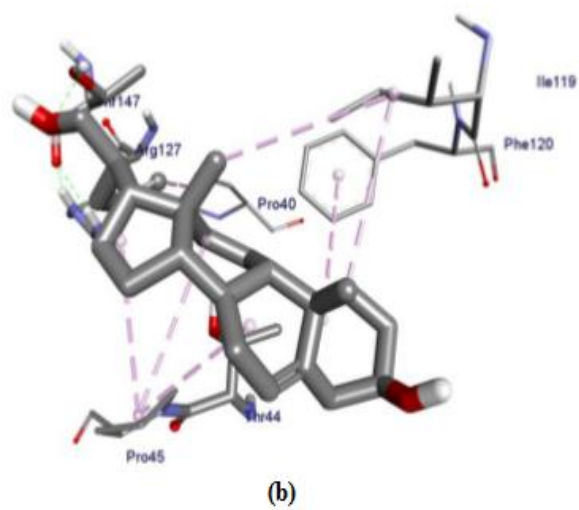
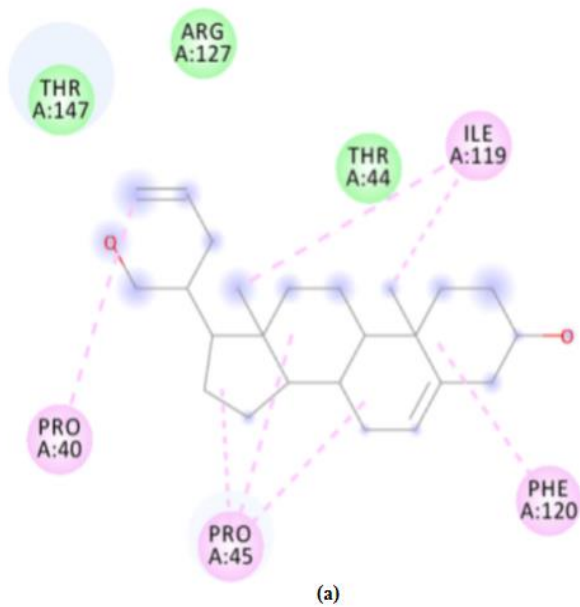


Figure 47. Ligand-protein interaction (a) and 3D representation (b) of compound **65** against human peroxiredoxin (1HD2)

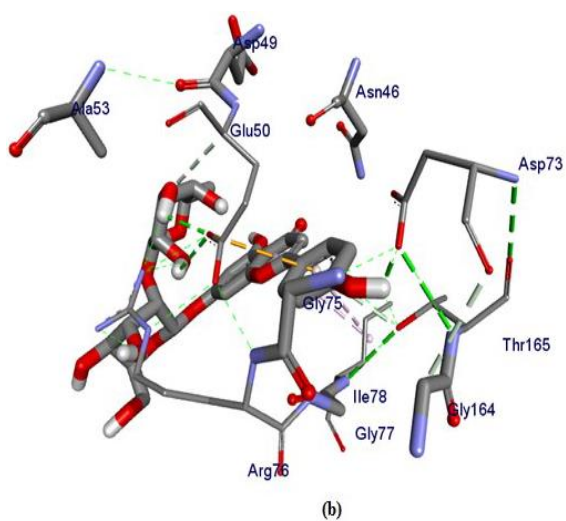
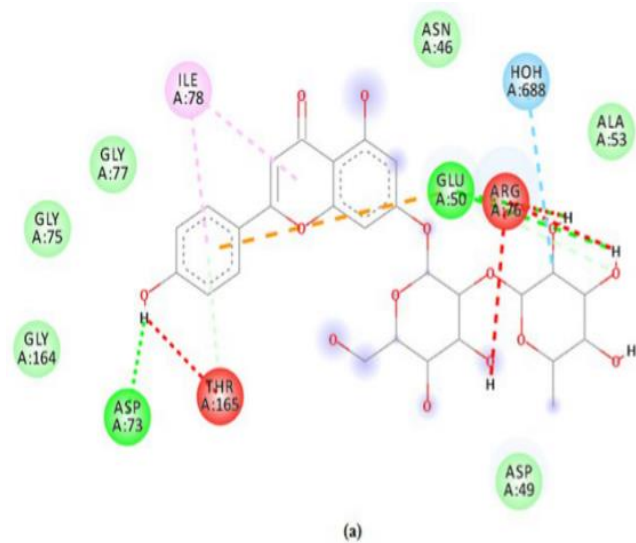


Figure 48. Ligand-protein interaction (a) and 3D representation (b) between apigenin-7-*O*-neohesperidoside (66) and *E. coli* gyraseB enzyme (6F86)

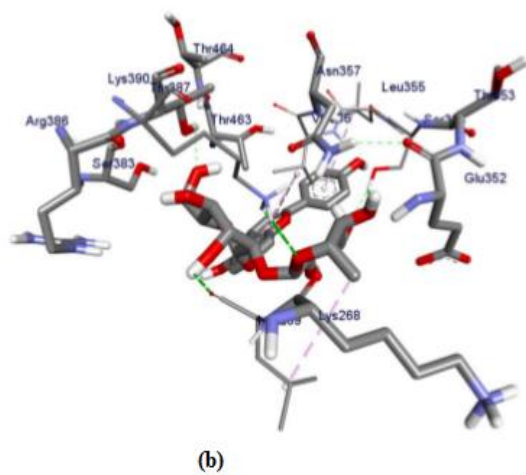
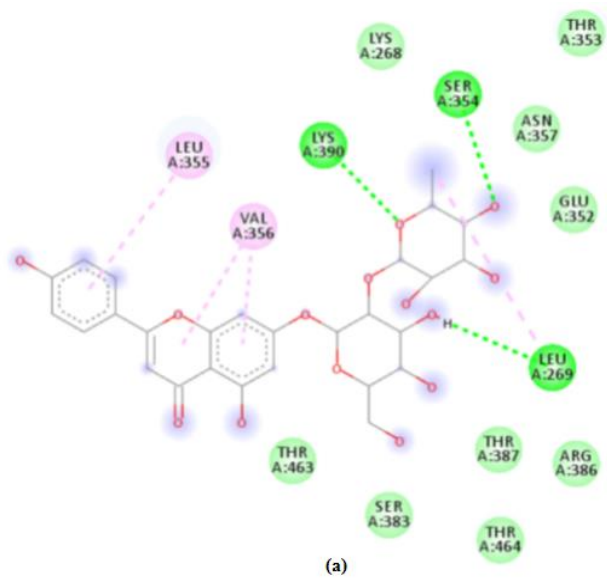
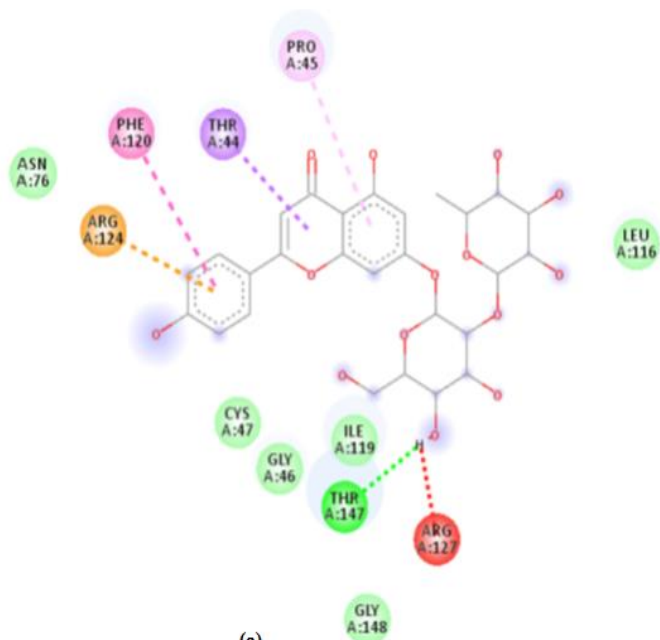
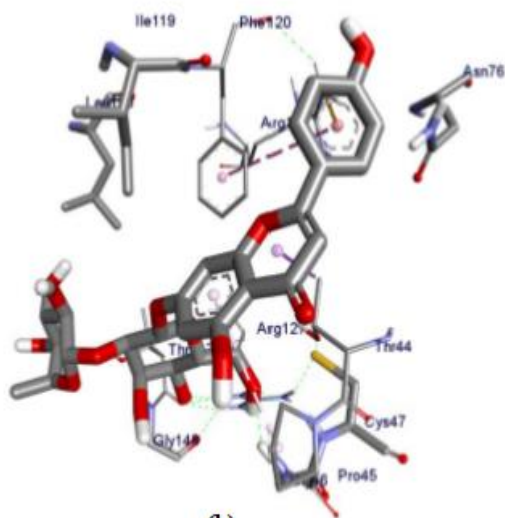


Figure 49. Ligand-protein interaction **(a)** and 3D representation **(b)** between apigenin-7-*O*-neohesperidoside (**66**) and *S. aureus* pyruvate kinase (3T07)



(a)



(b)

Figure 50. Ligand-protein interaction (a) and 3D representation (b) between apigenin-7-*O*-neohesperidoside (66) and human peroxiredoxin 5 (1HD2).

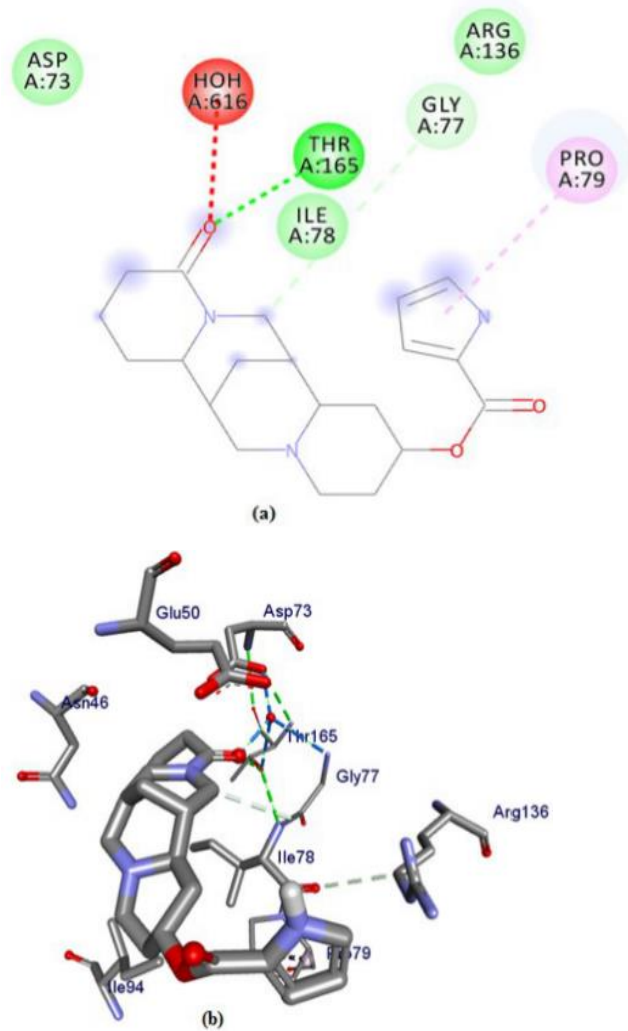
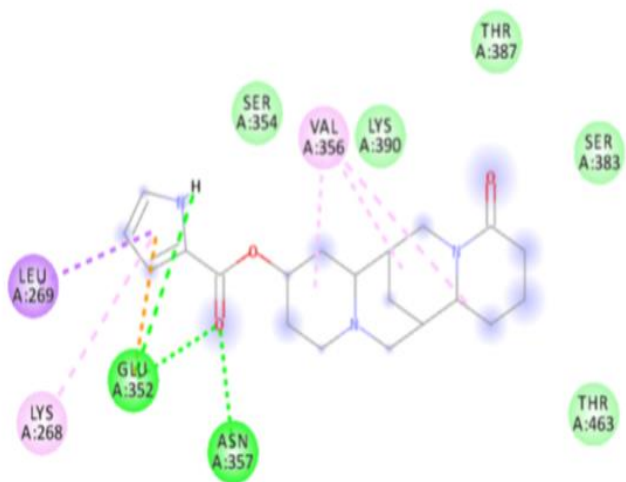
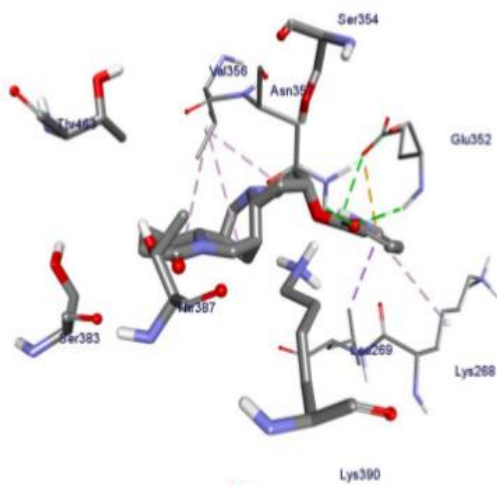


Figure 51. Ligand-protein interaction (a) and 3D representation (b) between calpurnine (67) and *E. coli* gyraseB enzyme (6F86)

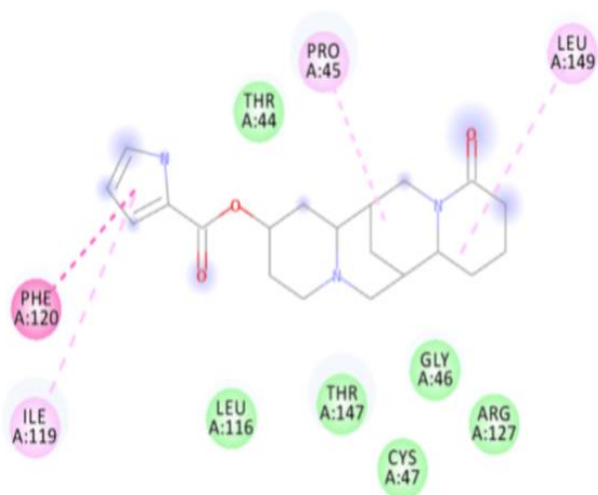


(a)

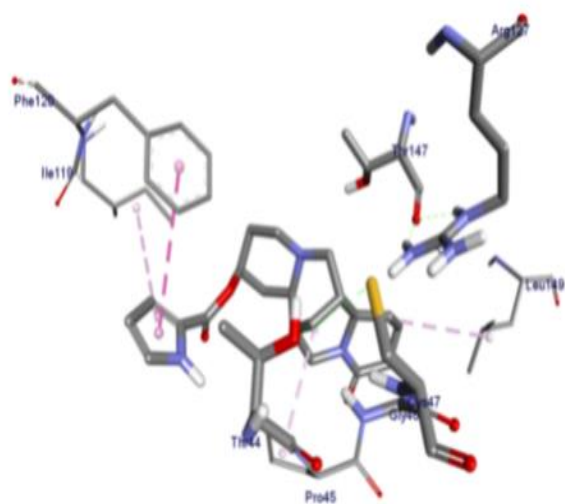


(b)

Figure 52. Ligand-protein interaction (a) and 3D representation (b) between calpurnine (67) and *S. aureus* pyruvate kinase enzyme (3T07)



(a)



(b)

Figure 53. Ligand-protein interaction (a) and 3D representation (b) between calpurnine (67) and human peroxiredoxin 5 (1HD2)

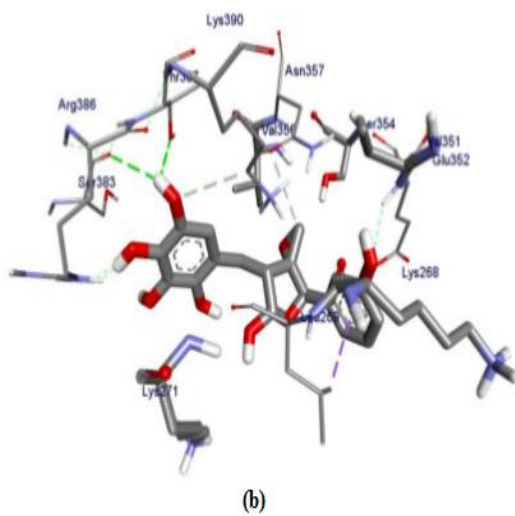
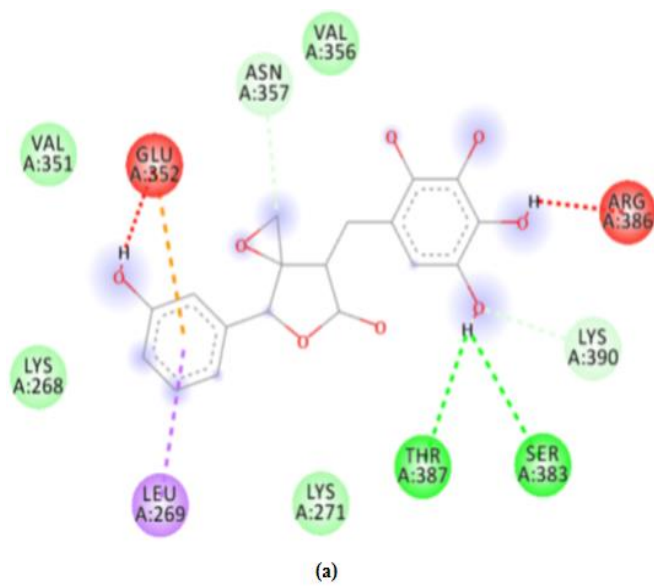


Figure 55. Ligand-protein interaction (a) and 3D representation (b) between compound **68** and *S. aureus* pyruvate kinase (3T07)

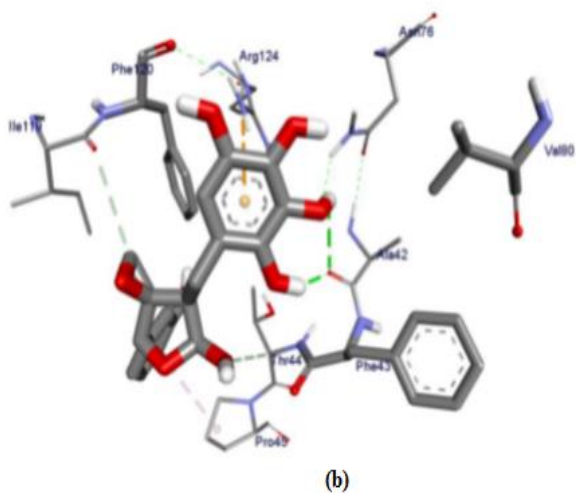
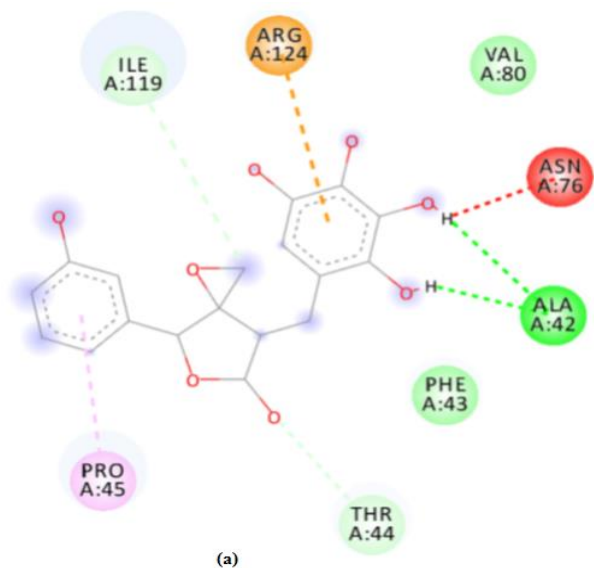


Figure 56. Ligand-protein interaction (a) and 3D representation (b) between compound **68** and human peroxiredoxin 5 (1HD2)

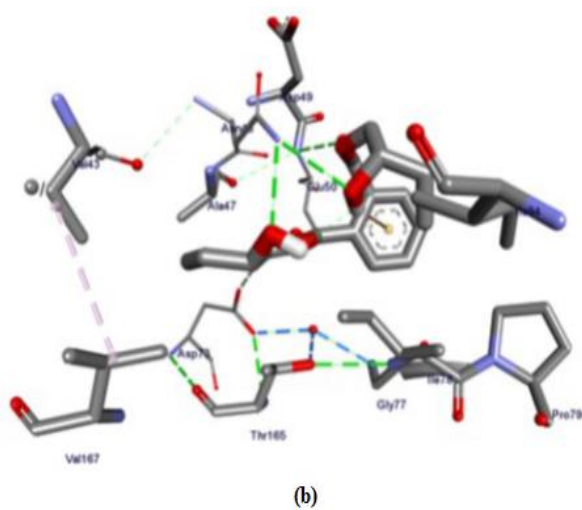
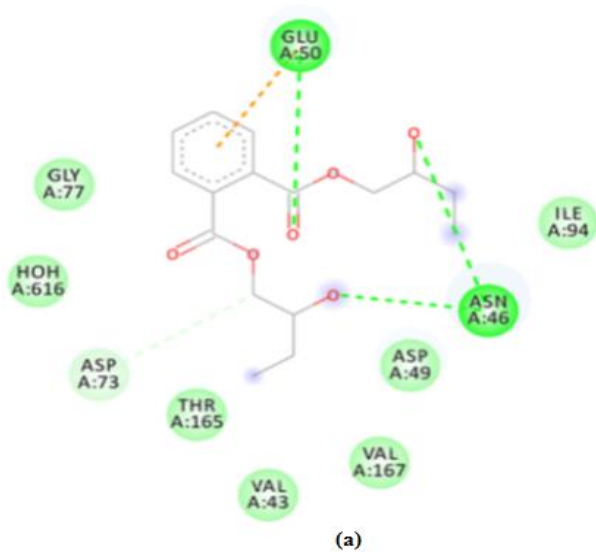


Figure 57. Ligand-protein interaction **(a)** and 3D representation **(b)** between bis-(2-hydroxybutyl) phthalate (**69**) and *E. coli* gyraseB protein (6F86)

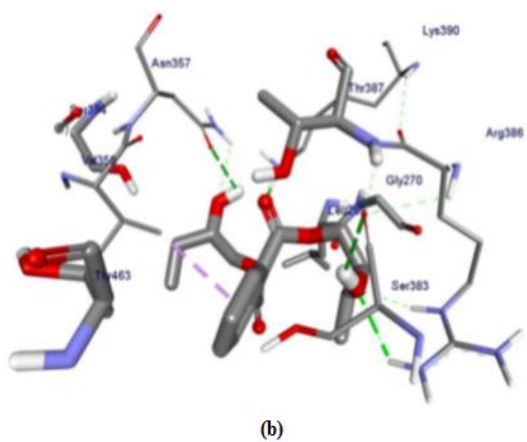
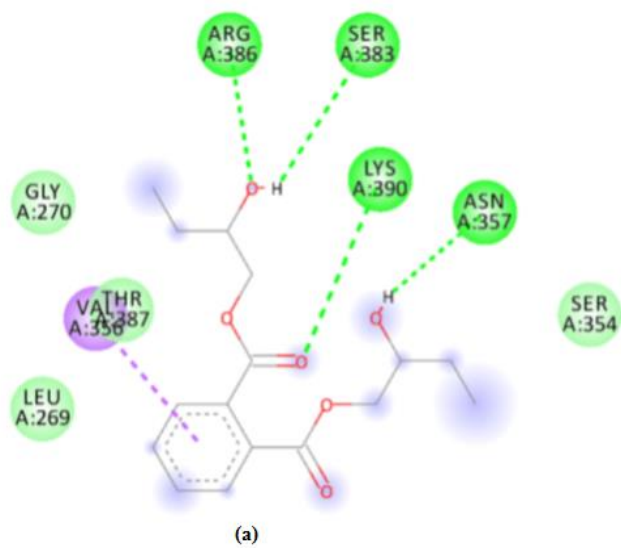


Figure 58. Ligand-protein interaction **(a)** and 3D representation **(b)** between bis-(2-hydroxybutyl) phthalate (**69**) and *S. aureus* pyruvate kinase (3T07)

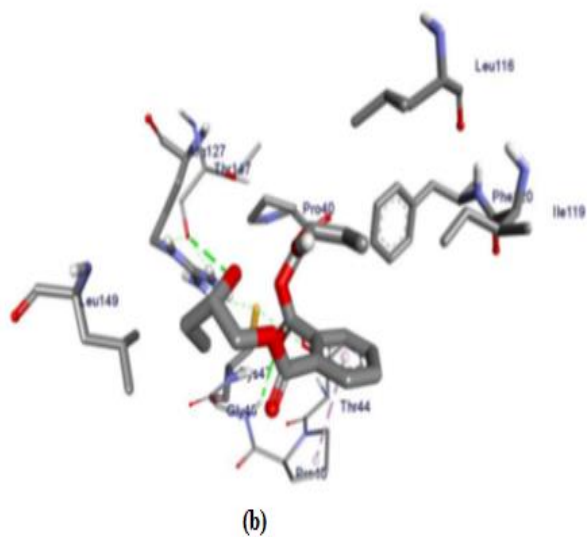
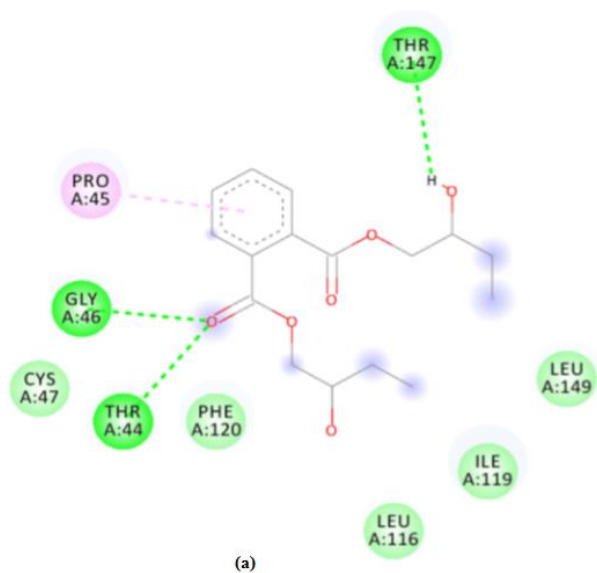
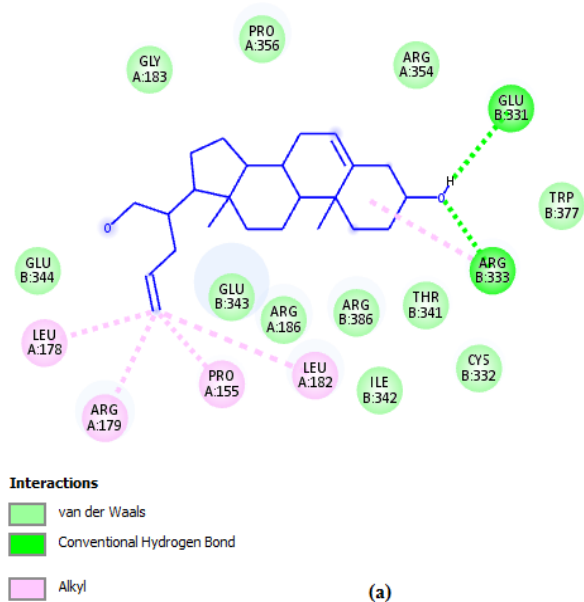
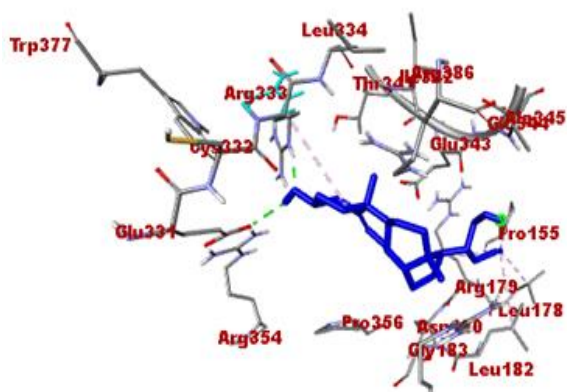


Figure 59. Ligand-protein interaction **(a)** and 3D representation **(b)** between bis-(2-hydroxybutyl)phthalate (**69**) and human peroxiredoxin 5 (1HD2)



(a)



(b)

Figure 60. Ligand-protein interaction (a) and 3D representation (b) between compound 65 and *P. aeruginosa* PqsA (5OE3)

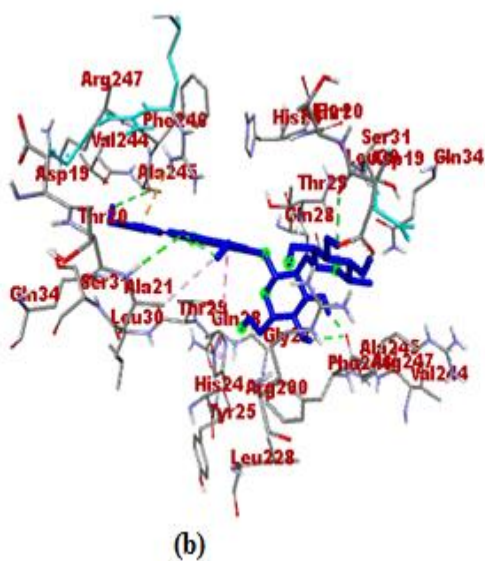
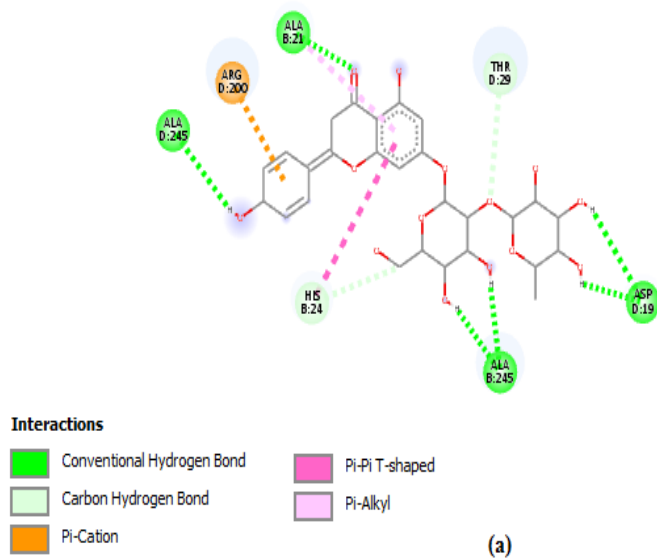


Figure 61. Ligand-protein interaction (a) and 3D representation (b) between apigenin-7-*O*-neohesperidoside (66) and *P. aeruginosa* PqsA (5OE3)

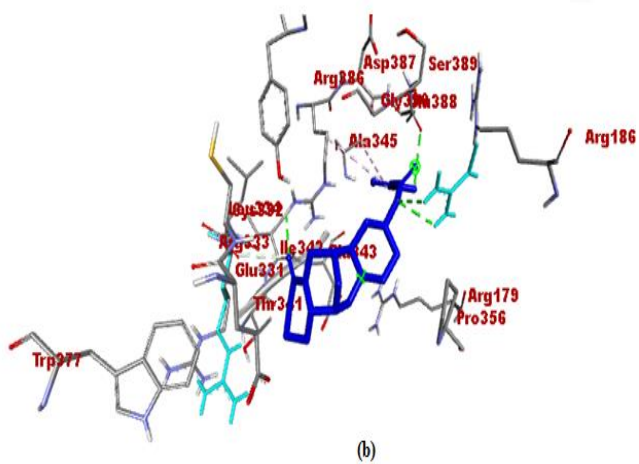
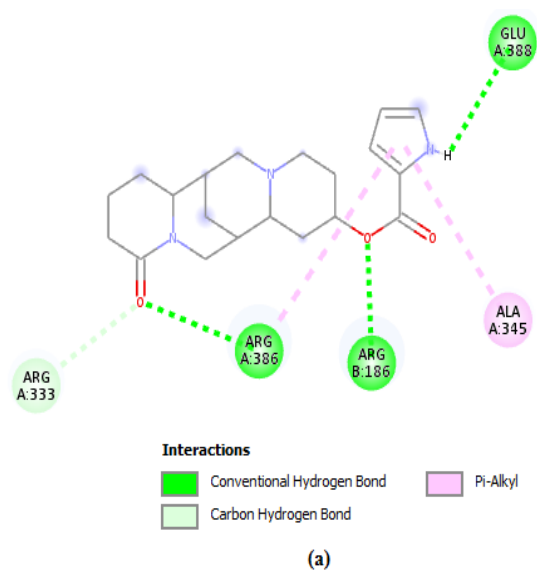
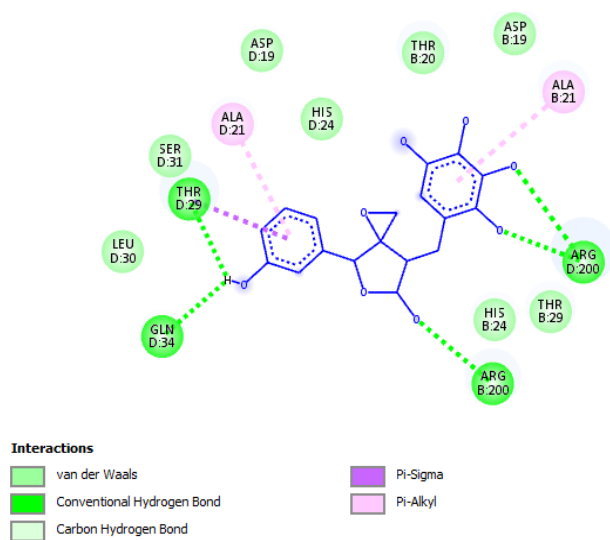
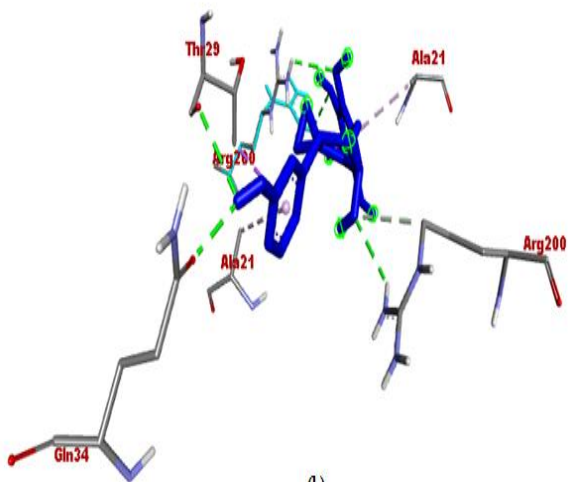


Figure 62. Ligand-protein interaction (a) and 3D representation (b) between calpurnine (67) and *P. aeruginosa* PqsA (5OE3)

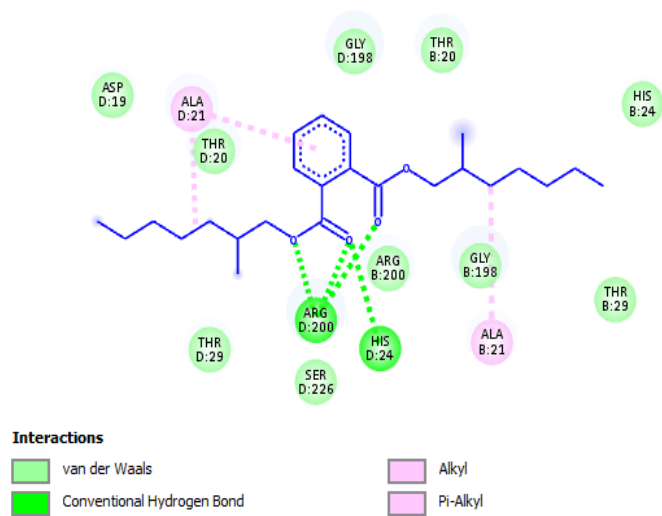


(a)

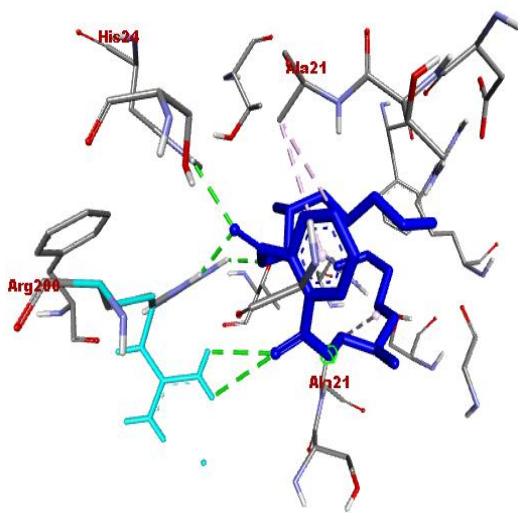


(b)

Figure 63. Ligand-protein interaction (a) and 3D representation (b) between compound 68 and *P. aeruginosa* PqsA (5OE3)

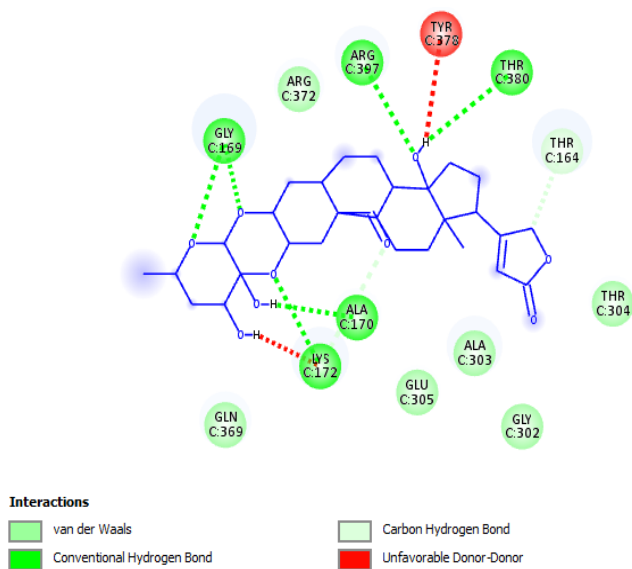


(a)

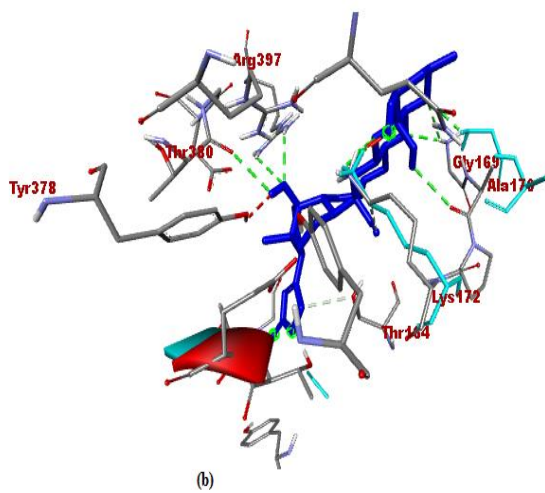


(b)

Figure 64. Ligand-protein interaction (a) and 3D representation (b) between bis-(2-methylheptyl) phthalate (70) and *P. aeruginosa* PqsA (5OE3)



(a)



(b)

Figure 65. Ligand-protein interaction (a) and 3D representation (b) between calotropin (79) and *P. aeruginosa* PqsA (5OE3)

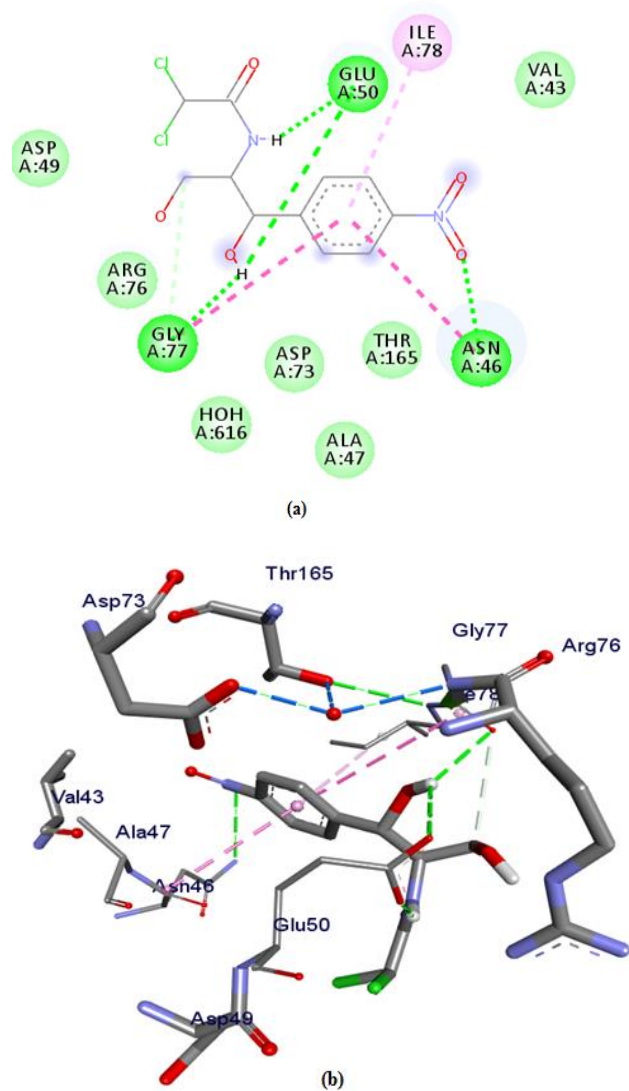


Figure 66. Ligand-protein interaction (a) and 3D representation (b) between chloramphenicol and *E. coli* gyraseB enzyme (6F86)

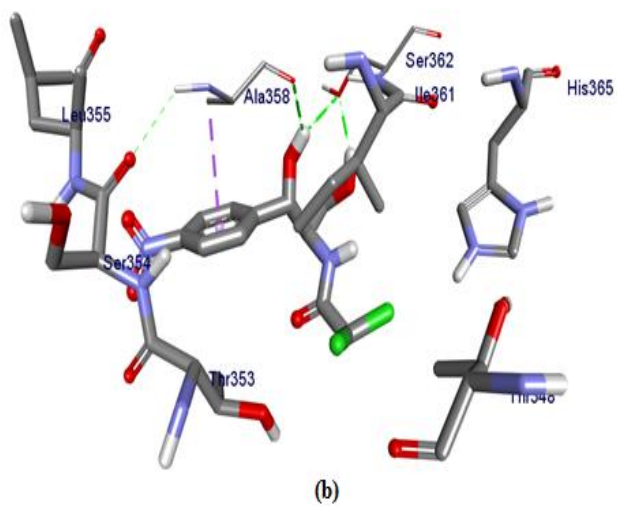
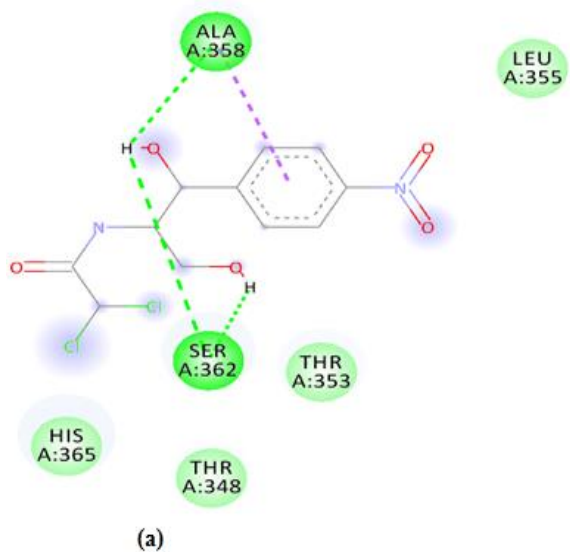


Figure 67. Ligand-protein interaction (a) and 3D representation (b) between chloramphenicol and *S. aureus* pyruvate kinase (3T07)

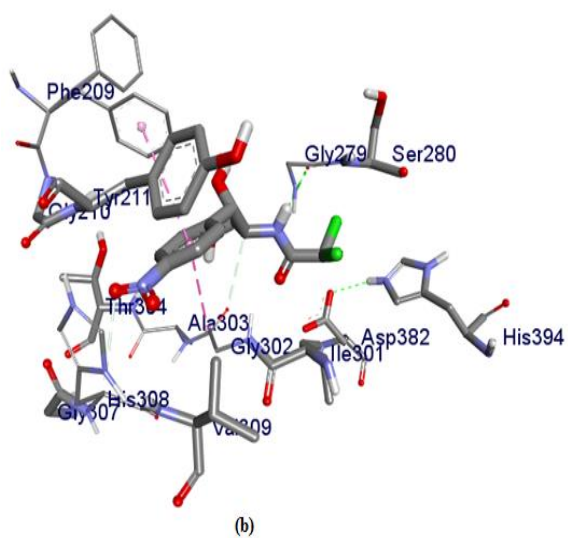
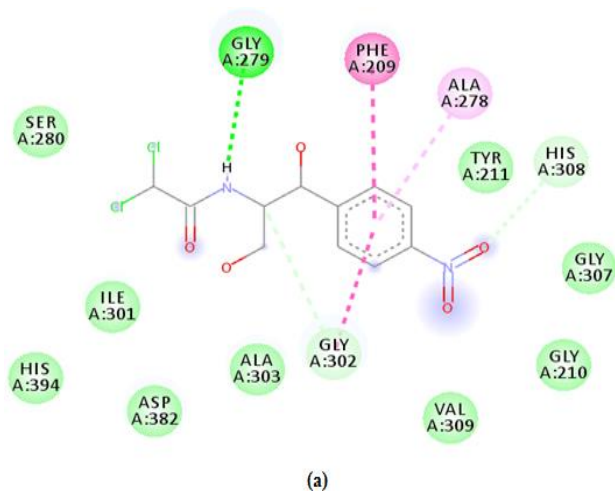


Figure 68. Ligand-protein interaction (a) and 3D representation (b) between chloramphenicol and *P. aeruginosa* PqsA (5OE3)

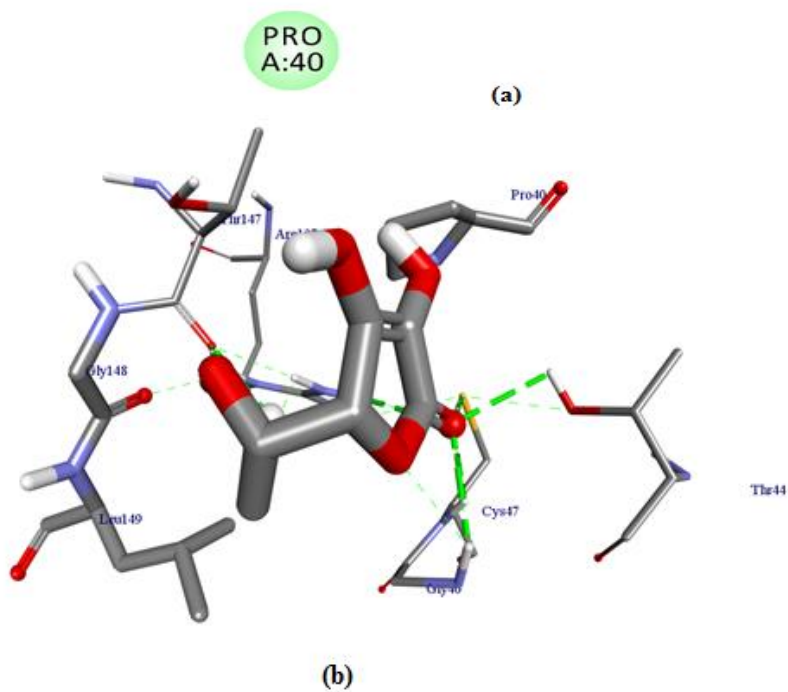
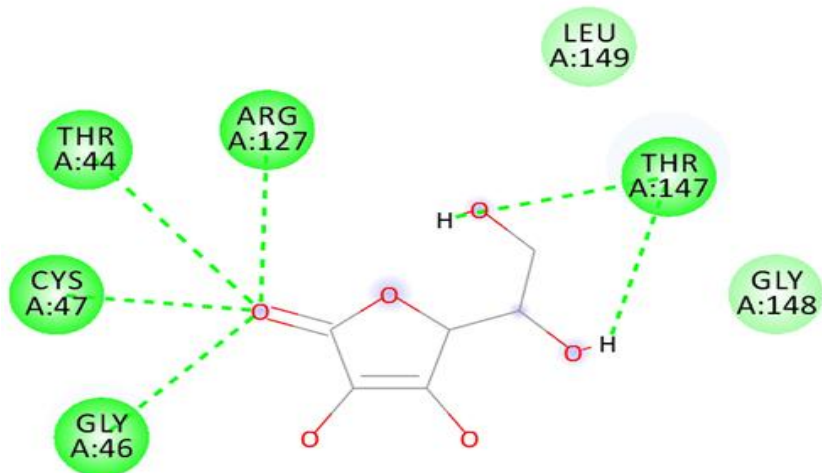


Figure 69. Binding interaction (a) and 3D structure (b) between ascorbic acid and human peroxiredoxin 5 (1HD2)

5 Conclusion and Recommendation

The phytochemical investigation on *C. purpurea* (leaves and roots), *C. speciosa* (stems), *G. superba* (tubers) and *G. purpurascens* (leaves) led to the isolation of 17 compounds **65-80**, of which 1-undecene (**80**) was isolated from ethyl acetate extract of *Escherichia coli* culture (GST5) endophytic bacterial isolate. The endophytic study resulted in isolation of thirty endophytic bacteria from leaves, stems and tubers of *G. superba* for the first time. Majority (21, 70%) of the isolates were found to be Gram-positive, of which 19 (90.5 %) exhibited *bacilli* shape while the rest showed *cocci* and rod cell shape. Besides, of the 21 Gram-positive isolates, 19 were found as spore formers. The MALDI-TOF MS analysis resulted in identification of 26 isolates, whereas 4 of the 30 isolates were not identified. Based on the biochemical and MALDI-TOF MS analyses, the thirty isolated endophytic bacteria were fall into four categories, viz., *Bacillus* spp. (66.7%), *Escherichia* spp. (26.7%), *Providencia* spp. (3.3%) and *Corynebacterium* spp. (3.3%). All extracts and isolated compounds of *G. superba*, *C. purpurea* and *G. purpurascens* displayed better antibacterial activity against *P. aeruginosa* strain than chloramphenicol (7.2 ± 0.6 - 8.2 ± 0.6 mm) almost at all tested concentrations. The ethyl acetate extracts of the culture filtrates of the representative endophytic bacterial isolates, GST8 (*B. subtilis*), GST2 (*E. coli*), GST5 (*E. coli*), GST4 (*E. coli*), GSL5 (*B. subtilis*) and GSS7 (*B. amyloliquefaciens*), also showed slight activity against the tested bacterial strains at concentration of 1000 $\mu\text{g/mL}$. The chloroform:methanol (1:1) extracts of all plant species were found with almost no antifungal activity, except that of *C. speciosa* stem which exhibited a promising result (9.00 ± 1.00 to 17.17 ± 1.04 mm) up to 100,000 $\mu\text{g/mL}$. Besides, a dose depended antioxidant activity was noticed both by the extracts and isolated compounds against DPPH radical and ferric ion reduction up to 500 $\mu\text{g/mL}$ concentration. The obtained antioxidant activity data indicated that apigenin-7-*O*-neohesperidoside (**66**) and calpurnine (**67**) provided a good scavenging potential against DPPH radical (IC_{50} values of 6.21 and 8.67 $\mu\text{g/mL}$, respectively) comparable to ascorbic acid (4.82 $\mu\text{g/mL}$) at similar concentrations (25-500 $\mu\text{g/mL}$). The extracts of *G. superba* tuber and *G. purpurascens* leaves also exhibited promising DPPH radical scavenging activity with IC_{50} values ranging from 1.1-3.2 $\mu\text{g/mL}$ equivalence to ascorbic acid (1.0-1.3 $\mu\text{g/mL}$) at the same tested concentrations. The molecular docking

result showed that the studied compounds **65-69** formed some hydrogen-bonding, hydrophobic and Van der Waals interactions with some amino acid residues of *E. coli* gyraseB (6F86) and *S. aureus* pyruvate kinase (3T07) protein models with stronger binding affinity shown by compound **65**, calpurnine (**67**) and compound **68** (-6.5, -7.4 and -7.3 kcal/mol, respectively) to the 6F86 protein model, compared to chloramphenicol (-6.4 kcal/mol). Whereas all the compounds **65-69** showed a better binding energy to *S. aureus* pyruvate kinase (3T07) and human peroxiredoxin 5 (1HD2) better than chloramphenicol (-4.6 kcal/mol) and ascorbic acid (-4.5 kcal/mol), respectively. Besides, the studied compounds **65, 66, 67, 68** and **79** recorded respective docking scores of -7.9, -10.9, -8.1, -7.8 and -10.3 kcal/mol against *P. aeruginosa* PqsA (5OE3) which were higher than that of the chloramphenicol (-7.0 kcal/mol). The drug-likeness candidacy and the pharmacokinetic property result showed that apigenin-7-*O*-neohesperidoside (**66**) violated three rules of the Lipinski's rule of five (with molecular weight > 500 g/mol, hydrogen-acceptor > 10 and hydrogen-donor > 5) and was found to be as immunotoxic and mutagenic compound. Compound **68**, bis-(2-methylheptyl)phthalate (**70**) and calotropin (**79**) were also found violated, each, one rule of the Lipinski's rule of five (with hydrogen-donor > 5, LogP > 4.15 and molecular weight > 500 g/mol), respectively. Calotropin (**79**) was found as immunotoxic and cytotoxic isolate; whereas compounds **65** and **68** showed an immunotoxicity and mutagenicity properties, respectively. The present finding concluded that calpurnine (**67**) was isolated both from the leaves and roots of the *C. purpurea* plant using two different extraction techniques. This can be considered as an advantage to conserve the ecosystem of the plant in case an isolation of the compound is needed in large scale for various applications. The present research finding also provided an assertion to the possibility of exploration of endophytic bacterial species and associated chemical constituents from their host plants in the context of Ethiopia. This study recommends further instrumental analysis, including the 2D-NMR and HRMS, to fully confirm the structures of the newly isolated compounds **65, 68** and **69**. The present study also recommends further molecular characterization of the isolated endophytic bacteria using 16S rRNA gene sequencing to identify them in strain level. Further extensive biochemical investigations would be needed on the mentioned plant species, by giving a special emphases to the *G.*

superba and *G. purpurascens* plant species, to increase the chance of obtaining additional phytochemicals and endophytic microbes including fungi with better efficacy.

Additionally, we are advising a PhD student who is conducting further related study on endophytic which is supported by this project. The summary of his work is as follows.

A total of 20 potential endophytic bacterial isolates were obtained from a root of *Echinops Kebaricho* (16 isolate, 80%) and seed of *Lepidium sativum* (4 isolates, 20%), Ethiopian traditional medicinal plants. These endophytic bacteria were shown different morphological characteristics. In this study, (15 isolates, 75%) of isolates were shown gram positive and (5 isolates, 25%) gram negative results. The motility test was also performed and (14 isolates, 70%) of isolates were motile whereas (6 isolates, 30%) of isolates were non-motile. With regard to Citrate test, (10 isolates, 50%) were positive and (10 isolates, 50%) were shown negative results. Moreover, Triple sugar iron test, H₂S production, Methyl red test and others were also conducted. These bacterial isolates were identified using high throughput MILD-TOF mass spectrometers based on their protein profile. Among these isolates, *Bacillus cereus* (9%) was dominantly identified endophytic bacterial isolates followed by *Pseudomonas fluorescens* (3%). Moreover, *Proteus mirabilis* (2%) and *Salmonella species* (1%) were also identified in this study. Pikoviskya medium supplemented with Ca₃(PO₄)₂ was employed for phosphate solubilization of endophytic bacteria isolate. Among tested isolates, Ls5I1 isolate was exhibited a highest phosphate solubilization with 5.32 solubilization index. The lowest Phosphate solubilization was also recorded for EKF3I2 isolates with 1.05 solubilization index. Moreover, Zinc solubilization assay was also carried out using MSM medium supplemented with ZnO. Among these identified endophytic bacteria, Ls5I1 isolate was exhibited a highest mean, (19.97mm) of clearing zone around colony with highest Zinc solubilization index of 5.82 followed by EKWG1I3 isolate with 4.36 solubilization index. The 16S rRNA gene sequencing was performed for the present isolates such as Ls5I1, EKWG1I3, EKWG2I3 and EKWG2I1 and also phylogenetic tree was constructed for isolate Ls5I1 using MEGA 11 software. A suitable growth conditions were performed for isolate Ls5I1 to evaluate growth efficiency against various Carbon source using Luria–Bertani broth medium. This endophytic bacterial isolate (Ls5I1) was exhibited a best growth condition when Glucose was used as a carbon source. The highest cell biomass (CDW, g/L) with (0.046 ± 0.001) and Optical density (OD_{600nm}) with (1.292

± 0.001) were recorded for Glucose against this isolate. With regarding to N_2 source, Peptone was used as best cell growth with the highest OD ($_{600nm}$) value of (1.360 ± 0.006) and cell biomass (CDW, g/L) (0.058 ± 0.001). Moreover, the effect of various pH value and salt concentration (NaCl conc.) was also evaluated. This study showed identified endophytic bacterial isolates were candidate for growth promotion of host plants and solubilizing insoluble phosphate and zinc minerals.

Ongoing activities: LC-MS analysis, Crude extraction of secondary metabolite,

Future activities will be:

- TLC analysis
- Antimicrobial activities of the bacterial extracts
- Anti-oxidant activities
- Structural elucidation of these bioactive compounds and
- Molecular characterization of the isolates (PCR and WGS)

6 References

- (1) Gulluce, M.; Aslan, A.; Sokmen, M.; Sahin, F.; Adiguzel, A.; Agar, G.; Sokmen, A. Screening the Antioxidant and Antimicrobial Properties of the Lichens *Parmelia Saxatilis*, *Platismatia Glauca*, *Ramalina Pollinaria*, *Ramalina Polymorpha* and *Umbilicaria Nylanderiana*. *Phytomedicine* **2006**, *13* (7), 515–521.
<https://doi.org/10.1016/j.phymed.2005.09.008>.
- (2) Mbeng, W. O.; Prof, S.; Grierson, D. S. Antifungal Evaluation and Phytochemical Analysis of Selected Medicinal Plants Used in the Treatment of Fungal Diseases Associated with HIV Infection in the Eastern Cape, South Africa. Thesis, **2013**.
- (3) Debebe, D.; Debella, A.; K. Urga. Medicinal Plants and Other Useful Plants of Ethiopia; 1993.
- (4) Strobel, G. The Emergence of Endophytic Microbes and Their Biological Promise. *Journal of Fungi* **2018**, *4* (2). <https://doi.org/10.3390/jof4020057>.
- (5) Patil, R. H.; Patil, M. P.; Maheshwari, V. L. Bioactive Secondary Metabolites From Endophytic Fungi: A Review of Biotechnological Production and Their Potential Applications. *Studies in Natural Products Chemistry* **2016**, *49*, 189–205.
<https://doi.org/10.1016/B978-0-444-63601-0.00005-3>.
- (6) Prasad, M. P.; Dagar, S. Identification and Characterization of Endophytic Bacteria from Fruits like Avacado and Black Grapes. *International Journal of Current Microbiology and Applied Sciences* **2014**, *3* (8), 937–947.
- (7) Martinez-Klimova, E.; Rodríguez-Peña, K.; Sánchez, S. Endophytes as Sources of Antibiotics. *Biochemical Pharmacology* **2017**, *134*, 1–17.
<https://doi.org/10.1016/j.bcp.2016.10.010>.
- (8) Strobel, G.; Daisy, B.; Castillo, U.; Harper, J. Natural Products from Endophytic Microorganisms. *Journal of Natural Products* **2004**, *67*, 257–268.
<https://doi.org/10.1021/np030397v>.
- (9) van Wyk, A. S.; Prinsloo, G. Medicinal Plant Harvesting, Sustainability and Cultivation in South Africa. *Biological Conservation* **2018**, *227*, 335–342.
<https://doi.org/10.1016/j.biocon.2018.09.018>.
- (10) Demie, G.; Negash, M.; Awas, T. Ethnobotanical Study of Medicinal Plants Used by Indigenous People in and around Dirre Sheikh Hussein Heritage Site of South-

- Eastern Ethiopia. *Journal of Ethnopharmacology* **2018**, *220*, 87–93.
<https://doi.org/10.1016/j.jep.2018.03.033>.
- (11) Mohammed, T.; Teshale, C. Ethnopharmacology Preliminary Phytochemical Screening and Evaluation of Antibacterial Activity of *Dichrocephala*. *Journal of Intercultural Ethnopharmacology* 2012, *1* (1), 30–34.
- (12) Abebe, D. and Ahadu, A. Medicinal Plants and Enigmatic Health Practices of Northern Ethiopia; 1993.
- (13) Mavuti, K. M.; Kimani, E. N.; Mukiyama, T. Growth Patterns of the Pearl Oyster *Pinctada Margaritifera* L. in Gazi Bay, Kenya. *African Journal of Marine Science* **2005**, *27* (3), 567–575. <https://doi.org/10.2989/18142320509504117>.
- (14) Satyajit D. Sarker, Zahid Latif, A. I. G. *Natural Products Isolation*, 2nd ed.; Satyajit D. Sarker, Zahid Latif, A. I. G., Ed.; Totowa, New Jersey 07512, 2006.
- (15) Bekele, E. Study on Actual Situation of Medicinal Plants in Ethiopia. *Japan Association for International Collaboration of Agriculture and Forestry* **2007**, 1–5.
- (16) Belayneh, A.; Asfaw, Z.; Demissew, S.; Bussa, N. F. Medicinal Plants Potential and Use by Pastoral and Agro-Pastoral Communities in Erer Valley of Babile Wereda, Eastern Ethiopia. *Journal of Ethnobiology and Ethnomedicine* **2012**, *8*.
<https://doi.org/10.1186/1746-4269-8-42>.
- (17) Belayneh, A.; Bussa, N. F. Ethnomedicinal Plants Used to Treat Human Ailments in the Prehistoric Place of Harla and Dengego Valleys, Eastern Ethiopia. *Journal of Ethnobiology and Ethnomedicine* **2014**, *10* (1), 1-17.. <https://doi.org/10.1186/1746-4269-10-18>.
- (18) Yuan, H.; Ma, Q.; Ye, L.; Piao, G. The Traditional Medicine and Modern Medicine from Natural Products. *Molecules* **2016**, *21* (5), 559.
<https://doi.org/10.3390/molecules21050559>.
- (19) Gupta, R.; Gabrielsen, B.; Ferguson, S. Natures Medicines: Traditional Knowledge and Intellectual Property Management. Case Studies from the National Institutes of Health (NIH), USA. *Current Drug Discovery Technologies* **2005**, *2* (4), 203–219.
<https://doi.org/10.2174/157016305775202937>.
- (20) Dias, D. A.; Urban, S.; Roessner, U. A Historical Overview of Natural Products in Drug Discovery. *Metabolites* **2012**, *2* (2), 303–336.

<https://doi.org/10.3390/metabo2020303>.

- (21) Gurib-Fakim, A. Medicinal Plants: Traditions of Yesterday and Drugs of Tomorrow. *Molecular Aspects of Medicine* **2006**, 27 (1), 1–93.
<https://doi.org/10.1016/j.mam.2005.07.008>.
- (22) Newman, D. J.; Cragg, G. M.; Snader, K. M. Natural Products as Sources of New Drugs over the Period 1981-2002. *Journal of Natural Products* **2003**, 66 (7), 1022–1037. <https://doi.org/10.1021/np030096l>.
- (23) Chikezie, P. C. Herbal Medicine: Yesterday, Today and Tomorrow. *Alternative & Integrative Medicine* **2015**, 04 (03). <https://doi.org/10.4172/2327-5162.1000195>.
- (24) Kashani, H. H.; Hoseini, E. S.; Nikzad, H.; Aarabi, M. H. Pharmacological Properties of Medicinal Herbs by Focus on Secondary Metabolites. In *Life Science Journal* **2012**, 9, 509–520.
- (25) Namita, P.; Mukesh, R. Issn 2230 – 8407 Medicinal Plants Used As Antimicrobial Agents : A Review. *International research journal of pharmacy* **2012**, 3 (1), 31–40.
- (26) Duraipandiyar, V.; Ignacimuthu, S. Antifungal Activity of Traditional Medicinal Plants from Tamil Nadu, India. *Asian Pacific Journal of Tropical Biomedicine* **2011**, 1, S204–S215. [https://doi.org/10.1016/S2221-1691\(11\)60157-3](https://doi.org/10.1016/S2221-1691(11)60157-3).
- (27) Vashist, H.; Jindal, A. Antimicrobial Activities of Medicinal Plants–Review. *Journal of Research in Pharmaceutical and Biomedical Sciences* **2012**, 3 (1), 222–230.
- (28) Nascimento, G. G. F.; Locatelli, J.; Freitas, P. C.; Silva, G. L. Antibacterial Activity of Plant Extracts and Phytochemicals on Antibiotic-Resistant Bacteria. *Brazilian Journal of Microbiology* **2000**, 31 (4), 247–256. <https://doi.org/10.1590/S1517-83822000000400003>.
- (29) Chanda, S.; Rakholiya, K. Combination Therapy : Synergism between Natural Plant Extracts and Antibiotics against Infectious Diseases. *Microbiology Book Series* **2011**, 520–529.
- (30) Laxmipriya Padhi, Y.; Kishore Mohanta, S. K. P. Endophytic Fungi with Great Promises : A Review. *Journal of Advanced Pharmacy Education & Research* **2013**, 3 (3), 152–170.
- (31) Stierle, A. A. and Stierle, D. B. Bioactive Compounds from Four Endophytic

- Penicillium* spp. of a Northwest Pacific Yew Tree. In *Studies in Natural Products Chemistry* 2000, 24, 933–977. [https://doi.org/10.1016/S1572-5995\(00\)80058-7](https://doi.org/10.1016/S1572-5995(00)80058-7).
- (32) Lai, D., Heike, B.-O., Werner, E.G.M., Victor, W., Peter, P. Bioactive Polyketides and Alkaloids from *Penicillium Citrinum*, a Fungal Endophyte Isolated from *Ocimum Tenuiflorum*. *Fitoterapia* **2013**, 9, 100–106.
- (33) Chen, M.; Fu, Y.; Zhou, Q. Penifupyrone , a New Cytotoxic Funicone Derivative from the Endophytic Fungus *Penicillium* spp . HSZ-43. *Natural Product Research* **2014**, 28 (19), 15544-1548. <https://doi.org/10.1080/14786419.2014.924932>.
- (34) Du, X.-P., Su, W.-J. Two New Polyketides from Mangrove Endophytic Fungus spp. *Chemistry of Natural Compounds* **2014**, 2 (50), 214–216.
- (35) Giridharan, P., Verekar, S.A., Khanna, A., Mishra, P.D., Deshmukh, S. Anticancer Activity of Sclerotiorin , Isolated from an Endophytic Fungus. *Indian Journal of Experimental Biology* **2012**, 50 (7), 464–468.
- (36) Xu, Y.-M., Patricia, E.-A., Mangping, X.L., Elizabeth, A.A., Gunatilaka, L. A. Secoemestrin D, a Cytotoxic Epitetrahydrodioxopiperazine, and Emericellenes A–E, Five Sesterterpenoids from *Emericella* spp. AST0036, a Fungal Endophyte of *Astragalus Lentiginosus*. *Journal of Natural Products* **2013**, 76 (12), 2330–2336.
- (37) Gu, W., Ge, H.M., Song, Y.C., Ding, H., Zhu, H.L., Zhao, X.A., Tan, R. Cytotoxic Benzo[j] Fluoranthene Metabolites from *Hypoxylontruncatum* IFB-18, an Endophyte of *Artemisia Annuua*. *Journal of Natural Products* **2007**, 70 (1), 114–117.
- (38) Yu, H.; Zhang, L.; Li, L.; Zheng, C.; Guo, L.; Li, W.; Sun, P.; Qin, L. Recent Developments and Future Prospects of Antimicrobial Metabolites Produced by Endophytes. *Microbiological Research* **2010**, 165 (6), 437–449. <https://doi.org/10.1016/j.micres.2009.11.009>.
- (39) Patil, R. H.; Patil, M. P.; Maheshwari, V. L. Bioactive Secondary Metabolites from Endophytic Fungi: A Review of Biotechnological Production and Their Potential Applications. *Studies in Natural Products Chemistry* **2016**, 49, 189–205. <https://doi.org/10.1016/B978-0-444-63601-0.00005-3>.
- (40) Izumi, H.; Anderson, I. C.; Killham, K.; Moore, E. R. B. Diversity of Predominant Endophytic Bacteria in European Deciduous and Coniferous Trees. *Canadian Journal of Microbiology* **2008**, 54 (3), 173–179. <https://doi.org/10.1139/w07-134>.

- (41) Jana, S.; Shekhawat, G. S. Critical Review on Medicinally Potent Plant Species: *Gloriosa Superba*. *Fitoterapia* **2011**, 82 (3), 293–301. <https://doi.org/10.1016/j.fitote.2010.11.008>.
- (42) Sebsebe, D. and Gilbert, M. Hydrocharitaceae to Arecaceae. In: Sue Edwards, Sebsebe Demissew and Inga Hedberg (Eds.), *Flora of Ethiopia and Eritrea Volume 6*. 1997, pp 184–185.
- (43) Rajak, R. C; Rai, M. K. Herbal Medicines, Biodiversity and Conservation Strategies; 1996; pp 75–79.
- (44) Mats, T. Pittosporaceae to Araliaceae. In: Inga Hedberg & Sue Edwards (Eds.), *Flora of Ethiopia, Volume 3*; The National Herbarium, Addis Ababa and the Department of Biology, 1989.
- (45) Gilbert, M. *Flora of Ethiopia and Eritrea Volume 4, Part 1*; Inga Hedberg (Ed.), *Apiaceae to Dipsacaceae*. The National Herbarium, Addis Ababa and the Department of Biology, 2003.
- (46) Olof, R. *Flora of Ethiopia and Eritrea, Volume 5*; Gentianaceae to Cyclocheilaceae. The National Herbarium, Addis Ababa University, Addis Ababa, 2006.
- (47) Ajao, A. A.; Sibiya, N. P.; Moteetee, A. N. Sexual Prowess from Nature: A Systematic Review of Medicinal Plants Used as Aphrodisiacs and Sexual Dysfunction in Sub-Saharan Africa. *South African Journal of Botany* **2018**, 122, 342–359. <https://doi.org/10.1016/j.sajb.2018.08.011>.
- (48) Zahir, A. A.; Rahuman, A. A.; Pakrashi, S.; Ghosh, D.; Bagavan, A.; Kamaraj, C.; Elango, G.; Chatterjee, M. Evaluation of Antileishmanial Activity of South Indian Medicinal Plants against *Leishmania Donovanii*. *Experimental Parasitology* **2012**, 132 (2), 180–184. <https://doi.org/10.1016/j.exppara.2012.06.012>.
- (49) Agrawal, P.; Laddha, K. Rapid Separation of Phenethylisoquinoline Alkaloid from *Gloriosa Superba* Tubers. *Journal of Applied Research on Medicinal and Aromatic Plants* **2015**, 2 (4), 200–202. <https://doi.org/10.1016/j.jarmap.2015.08.001>.
- (50) Singh, V. K. Selected Indian Folk Medicinal Claims and Their Relevance in Primary Health Care Programme. *Glimpses Plant Res* **1993**, No. 10, 147–152.
- (51) Le Roux, L. G.; Robbertse, P. J. Aspects Relating to Seed Production in *Gloriosa Superba* L. *South African Journal of Botany* **1997**, 63 (4), 191–197.

[https://doi.org/10.1016/S0254-6299\(15\)30743-2](https://doi.org/10.1016/S0254-6299(15)30743-2).

- (52) Mali, R. G.; Hundiwale, J. C.; Gavit, R. S.; Patil, D. A.; Patil, K. S. Herbal Abortifacients Used in North Maharashtra. *Natural Product Radiance* **2006**, 5 (4), 315–318.
- (53) Samy, R. P.; Thwin, M. M.; Gopalakrishnakone, P.; Ignacimuthu, S. Ethnobotanical Survey of Folk Plants for the Treatment of Snakebites in Southern Part of Tamilnadu, India. *Journal of Ethnopharmacology* **2008**, 115 (2), 302–312. <https://doi.org/10.1016/j.jep.2007.10.006>.
- (54) Mats, T. Pittosporaceae to Araliaceae. In: Inga Hedberg & Sue Edwards (Eds.), *Flora of Ethiopia, Volume 3; The National Herbarium, Addis Ababa and the Department of Biology, 1989*.
- (55) Moravec, I.; Fernandez, E.; Vlkova, M.; Milella, L. Ethnobotany of Medicinal Plants of Northern Ethiopia. *Bol. latinoam. Caribe plantas med. aromat* **2014**, 13 (2), 126–134. <https://doi.org/10.1016/j.numecd.2009.04.003>.
- (56) Yemane, B.; Medhanie, G.; K, S. R. Survey of Some Common Medicinal Plants Used in Eritrean Folk Medicine Abstract. *American Journal of Ethnomedicine* **2017**, 4 (2), 14. <https://doi.org/10.21767/2348-9502.100014>.
- (57) Dutt, H. C.; Singh, S.; Avula, B.; Khan, I. A.; Bedi, Y. S. Pharmacological Review of *Caralluma* R.Br. with Special Reference to Appetite Suppression and Anti-Obesity. *Journal of Medicinal Food* **2011**, 15 (2), 108–119. <https://doi.org/10.1089/jmf.2010.1555>.
- (58) Kuriyan, R.; Raj, T.; Srinivas, S. K.; Vaz, M.; Rajendran, R.; Kurpad, A. V. Effect of *Caralluma Fimbriata* Extract on Appetite, Food Intake and Anthropometry in Adult Indian Men and Women. *Appetite* **2007**, 48 (3), 338–344. <https://doi.org/10.1016/j.appet.2006.09.013>.
- (59) van Heerden, F. R.; Marthinus Horak, R.; Maharaj, V. J.; Vleggaar, R.; Senabe, J. V.; Gunning, P. J. An Appetite Suppressant from *Hoodia* Species. *Phytochemistry* **2007**, 68 (20), 2545–2553. <https://doi.org/10.1016/j.phytochem.2007.05.022>.
- (60) Ramesh, M.; Nageshwar Rao, Y.; Appa Rao, A. V. N.; Prabhakar, M. C.; Seshagiri Rao, C.; Muralidhar, N.; Madahava Reddy, B. Antinociceptive and Anti-Inflammatory Activity of a Flavonoid Isolated from *Caralluma Attenuata*. *Journal*

- of Ethnopharmacology* **1998**, 62 (1), 63–66. [https://doi.org/10.1016/S0378-8741\(98\)00048-8](https://doi.org/10.1016/S0378-8741(98)00048-8).
- (61) Hemaiswarya, S.; Raja, R.; Anbazhagan, C.; Thiagarajan, V. Antimicrobial and Mutagenic Properties of the Root Tubers of *Gloriosa Superba* Linn. (Kalihari). *Pakistan Journal of Botany* **2009**, 41 (1), 293–299.
- (62) Khan, H.; Ali Khan, M.; Mahmood, T.; Choudhary, M. I. Antimicrobial Activities of *Gloriosa Superba* Linn (Colchicaceae) Extracts. *Journal of Enzyme Inhibition and Medicinal Chemistry* **2008**, 23 (6), 855–859. <https://doi.org/10.1080/14756360701747409>.
- (63) Ashokkumar, N.; Shanthi, A.; Sivakumar, M.; Rajamani, K. Studies on Antifungal Activity of Different Plant Parts of Glory Lily (*Gloriosa Superba* L .) against Fungal Wilt Pathogen , *Fusarium Oxysporum*. *International Journal of Current Microbiology and Applied* **2017**, 6 (9), 428–433.
- (64) Mahidol, C.; Ruchirawat, S.; Prawat, H.; Pisutjaroenpong, S.; Engprasert, S.; Chumsri, P.; Tengchaisri, T.; Sirisinha, S.; Picha, P. Biodiversity and Natural Product Drug Discovery. *Pure and Applied Chemistry* **1998**, 70 (11), 2065–2072. <https://doi.org/10.1351/pac199870112065>.
- (65) Khan, H.; Khan, M. A.; Hussan, I. Enzyme Inhibition Activities of the Extracts from Rhizomes of *Gloriosa Superba* Linn (Colchicaceae). *Journal of Enzyme Inhibition and Medicinal Chemistry* **2007**, 22 (6), 722–725. <https://doi.org/10.1080/14756360601164853>.
- (66) Jayakumar, F. A.; Group, S. E.; Simon, S. E.; Group, S. E. Characteristic and Optimized Use of Bioactive Compounds from *Gloriosa Superba* and *Albizia Amara* with Apoptotic Effect on Hepatic and Squamous Skin Carcinoma. *IJPSR* **2018**, 9 (5), 1769-1778. <https://doi.org/10.13040/IJPSR.0975-8232>.
- (67) Latha, K. P.; Girish, H. N.; Kirana, H. Anti-Arthritic Activity of Chloroform Extract of Tubers of *Gloriosa Superba* Linn. *International Journal of Research in Pharmacy and Chemistry* **2015**, 5 (4), 662–667.
- (68) Pare, S. R.; Zade, V. S.; Thakare, V. G. Evaluation of the Potential Aphrodisiac Activity of Aqueous , Chloroform and Alcohol Extract of *Gloriosa Superba* in Male Albino Rat. *International Journal of Theoretical and Applied Sciences* **2014**, 6 (2),

39–46.

- (69) Suryavanshi, S.; Rai, G.; Malviya, S. N.; Suryavanshi, S. Evaluation of Anti-Microbial and Anthelmintic Activity of *Gloriosa Superba Tubers*. *ARPB* **2012**, *2* (1), 45–52.
- (70) Wink, M.; Wyk, B.-E. Mind-Altering and Poisonous Plants of the World. In *Choice Reviews* **2013**, *46*, 46–6198. <https://doi.org/10.5860/choice.46-6198>.
- (71) Abdel-Sattar, E.; Shehab, N. G.; Ichino, C.; Kiyohara, H.; Ishiyama, A.; Otaguro, K.; Omura, S.; Yamada, H. Antitrypanosomal Activity of Some Pregnane Glycosides Isolated from *Caralluma* Species. *Phytomedicine* **2009**, *16* (6–7), 659–664. <https://doi.org/10.1016/j.phymed.2009.02.009>.
- (72) Abdel-Sattar, E.; Harraz, F. M.; Al-ansari, S. M. A.; El-Mekawy, S.; Ichino, C.; Kiyohara, H.; Ishiyama, A.; Otaguro, K.; Omura, S.; Yamada, H. Acylated Pregnane Glycosides from *Caralluma Tuberculata* and Their Antiparasitic Activity. *Phytochemistry* **2008**, *69* (11), 2180–2186. <https://doi.org/10.1016/j.phytochem.2008.05.017>.
- (73) Al-Harbi, M. D.; Qureshi, S.; Raza, M.; Ahmed, M. M.; Afzal, M.; Shah, A. Evaluation of *Caralluma Tuberculata* Pretreatment for the Protection of Rat Gastric Mucosa against Toxic Damage. *Toxicology and Applied Pharmacology* **1994**, 1–8.
- (74) Kumar, K. P.; Khan, K. A.; Anupama, K.; Prakash, K. V. Antifungal and Anthelmintic Activity of *Caralluma Fimbriata* Stem: A Herb. *International Journal of Chemical Sciences* **2008**, *6* (3), 1486–1490.
- (75) Jitwasinkul, T.; Charoensuksai, P. Antiproliferative Effects of *Pereskopsis Diguetii*, *Caralluma Speciosa* and *Euphorbia Ritchiei* Hydroalcoholic Extract; 2018; Vol. 42.
- (76) Negash, W.; Sahile, S.; Misganaw, D. *In vitro* Antimicrobial Effects of *Gomphocarpus Purpurascens* A . Rich Against Standard and Clinically Isolated Microorganisms. *Global Scientific Journals* **2019**, *7* (6), 1–17.
- (77) Dvoráčková, S.; Sedmera, P.; Potěšilová, H.; Šantavý, F.; Simánek, V. Alkaloids of *Gloriosa Superba* L. *Collection of Czechoslovak Chemical Communications* **1984**, *49*, 1536–1542. <https://doi.org/10.1135/cccc19841536>.
- (78) Pieters, L., Apers, S., Capistrano, R. *Gloriosa Superba* l. Extracts, Compositions

and Use There of in Treatment of Pancreatic Cancer. *European patent application* **2016**.

- (79) Chaudhuri, P. K. Nonalkaloidal Constituents of the Seeds of *Gloriosa Superba*. *Indian Journal of Chemistry Section B* **1998**, *37*, 98-99.
- (80) Kaul, S.K. and Thakur, R. Chemical Constituents of the Flowers of *Gloriosa Superba* Linn. *Physical Sciences* **1997**, *1* (47), 21–22.
- (81) Shobha, M.; Sampath Kumara, K. K.; Prakash, H. S. Fungal Endophytes Associated with *Gloriosa Superba* (L.). *Proceedings of the National Academy of Sciences, India Section B: Biological Sciences* **2018**. <https://doi.org/10.1007/s40011-018-1053-2>.
- (82) Murali, T.S., Satyamoorthy, K., Bhat, D. V. A Method of Producing Colchicine from an Endophytic *Phomopsis* Using Epigenetic Modifiers. *Indian Pat. Appl* **2018**.
- (83) Devi, L. S.; Bareh, D. A.; Joshi, S. R. Studies on Biosynthesis of Antimicrobial Silver Nanoparticles Using Endophytic Fungi Isolated from the Ethno-Medicinal Plant *Gloriosa Superba* L. *Proceedings of the National Academy of Sciences India Section B - Biological Sciences* **2014**, *84* (4), 1091–1099. <https://doi.org/10.1007/s40011-013-0185-7>.
- (84) Budhiraja, A.; Nepali, K.; Sapra, S.; Gupta, S.; Kumar, S.; Dhar, K. L. Bioactive Metabolites from an Endophytic Fungus of *Aspergillus* Species Isolated from Seeds of *Gloriosa Superba* Linn. *Medicinal Chemistry Research* **2013**, *22* (1), 323–329. <https://doi.org/10.1007/s00044-012-0032-z>.
- (85) Zweekhorst-Van Laer, A. M. H., Nelen, T. H. Flavanoids from *Cadia Purpurea* (Picc.) Ait. *Pharmaceutisch Weekblad* **1976**, *51* (111), 1289–1293.
- (86) van Rijk, J. L. and M.H. Radema. New Quinolizidine Alkaloids from *Cadia Purpurea*. *Tetrahedron Letters* **1976**, No. 24, 2053–2054.
- (87) Van Eijk, J. L. and Radema, M. H. Lupanine Alkaloids and Other Compounds from *Cadia Purpurea*. *Planta Medica* **1975**, *2* (28), 139–142.
- (88) Radema, B. M. H. Ethoxylupanine, a New Alkaloid from *Cadia Purpurea*. *Planta Medica* **1975**, *2* (28), 143.
- (89) M van Laer, A.; F Uffellie, O. Luteoline in *Cadia Purpurea* (Picc.) Ait; 1971; *106*, 890-892..

- (90) Bader, A.; Braca, A.; De Tommasi, N.; Morelli, I. Further Constituents from *Caralluma Negevensis*. *Phytochemistry* **2003**, *62* (8), 1277–1281.
[https://doi.org/10.1016/S0031-9422\(02\)00678-7](https://doi.org/10.1016/S0031-9422(02)00678-7).
- (91) Al-massarani, S. M.; Bertrand, S.; Nievergelt, A.; El-shafae, A. M.; Al-howiriny, T. A.; Al-musayeib, N. M.; Cuendet, M.; Wolfender, J. Acylated Pregnane Glycosides from *Caralluma Sinaica*. *Phytochemistry* **2012**, *79*, 129–140.
<https://doi.org/10.1016/j.phytochem.2012.04.003>.
- (92) Xia, Z. -H.; Mao, S. -L.; Lao, A. -N.; Uzawa, J.; Yoshida, S.; Fujimot, Y. Five New Pregnane Glycosides from the Stems of *Marsdenia Tenacissima*. *Journal of Asian Natural Products Research* **2011**, *13* (6), 477–485.
<https://doi.org/10.1080/10286020.2011.570263>.
- (93) Deepak, D.; Srivastava, S.; Khare, A. Pregnane Glycosides from *Hemidesmus Indicus*. *Phytochemistry* **1997**, *44* (1), 145–151. [https://doi.org/10.1016/S0031-9422\(96\)00393-7](https://doi.org/10.1016/S0031-9422(96)00393-7).
- (94) Oyama, M.; Iliya, I.; Tanaka, T.; Inuma, M. Five New Steroidal Glycosides from *Caralluma Dalzielii*. *Helvetica Chimica Acta* **2007**, *90* (1), 63–71.
<https://doi.org/10.1002/hlca.200790022>.
- (95) Rizwani, G.; Aslam, M.; Ahmad, M.; Usmanghani, K.; Ahmad, V. Lipid Components of *Caralluma Edulis* (Edgew.) Hook; 1993; Vol. 6, 19-27.
- (96) Zito, P.; Sajeve, M.; Bruno, M.; Maggio, A.; Rosselli, S.; Formisano, C.; Senatore, F. Essential Oil Composition of Stems and Fruits of *Caralluma Europaea* N.E.Br. (Apocynaceae). *Molecules* **2010**, *15* (2), 627–638.
<https://doi.org/10.3390/molecules15020627>.
- (97) Yannai, S. Dictionary of Food Compounds with CD-ROM: Additives, Flavors, and Ingredients; Boca Raton: Chapman and Hall. CRC Press, 2004.
- (98) Gerrans, G. C.; Harley-mason, J. The Alkaloids of *Virgilia Oroboides*. *Journal of the Chemical Society* **1964**, 2202–2206.
- (99) Ododo, M. M.; Choudhury, M. K.; Dekebo, A. H. Structure Elucidation of β -Sitosterol with Antibacterial Activity from the Root Bark of *Malva Parviflora*. *SpringerPlus* **2016**, *5*, 1–11. <https://doi.org/10.1186/s40064-016-2894-x>.
- (100) Breed, R. S.; Murray, E. G. D.; Smith, N. R. *Bergey's Manual of Determinative*

- Bacteriology*, 7th ed.; The Willaims and Wilkins Company: Baltimore, 1957.
- (101) Kunert, O.; Rao, B. V. A.; Babu, G. S.; Padmavathi, M.; Kumar, B. R.; Alex, R. M.; Schühly, W.; Simic, N.; Kühnelt, D.; Rao, A. V. N. A. Novel Steroidal Glycosides from Two Indian *Caralluma* Species, *C. Stalagmifera* and *C. Indica*. *Helvetica Chimica Acta* **2006**, *89* (2), 201–209. <https://doi.org/10.1002/hlca.200690022>.
- (102) Collee, J. G.; Mackie, T. J.; McCartney, J. E. *Practical Medical Mycology*, 14th ed.; Church Livingston: New York, 1996, p. 978. [https://doi.org/10.1016/0021-8707\(56\)90012-0](https://doi.org/10.1016/0021-8707(56)90012-0).
- (103) Khorasani, E. A.; Mat, T. R.; Mohajer, S.; Banisalam, B. Antioxidant Activity and Total Phenolic and Flavonoid Content of Various Solvent Extracts from *in Vivo* and *in Vitro* Grown *Trifolium Pratense* L. (Red Clover). *BioMed Research International* **2015**, 643285.
- (104) Do, Q. D.; Angkawijaya, A. E.; Tran-Nguyen, P. L.; Huynh, L. H. Effect of Extraction Solvent on Total Phenol Content, Total Flavonoid Content, and Antioxidant Activity of *Limnophila* Aromatic. *Journal of Food and Drug Analysis* **2014**, *22* (3), 296–302.
- (105) Mabry, T. J.; Kagan, J.; Rosler, H. *Nuclear Magnetic Resonance Analysis of Flavonoids*; The University of Texas Publication, University Station, Austin, Texas, 1964.
- (106) Padorinat, W. G. Secoiridoid and Flavonoid Glycosides from *Gonocaryum Calleryanum*. *Phytochemistry* **1996**, *39* (1), 115–120.
- (107) Asres, K.; Greeonst, W.A.; Phillipson, J. D.; Mascagni, P. Alkaloids of Ethiopian *Calpurnia Aurea* Subsp. *Aurea*. *Phytochemistry* **1986**, *25* (6), 1443–1447.
- (108) Rameshthangam, P.; Ramasamy, P. Antiviral Activity of Bis-(2-Methylheptyl)Phthalate Isolated from *Pongamia Pinnata* Leaves against White Spot Syndrome Virus of *Penaeus Monodon Fabricius*. *Virus Research* **2007**, *126*, 38–44.
- (109) Ortiz, A.; Sansinenea, E. Di-2-Ethylhexylphthalate May Be a Natural Product. *Journal of Chemistry* **2018**, 1–7.
- (110) Namikoshi, M.; Fujiwara, T.; Nishikawa, T.; Ukai, K. Natural Abundance ¹⁴C Content of Dibutyl Phthalate (DBP) from Three Marine Algae. *Marine Drugs* **2006**,

4, 290–297.

- (111) Lotfy, M. M.; Hassan, H. M.; Hetta, M. H.; El-Gendy, A. O.; Mohammed, R. Di-(2-Ethylhexyl) Phthalate , a Major Bioactive Metabolite with Antimicrobial and Cytotoxic Activity Isolated from the Culture Filtrate of Newly Isolated Soil *Streptomyces* (*Streptomyces Mirabilis* Strain NSQu-25). *BJBAS* **2018**, 7, 263–269. <https://doi.org/10.5829/idosi.wasj.2012.20.09.2868>.
- (112) Shafikova, T. N.; Maksimova, L. A.; Omelichkina, Yu.-V.; G. Enikeev, A.; Semenov, A. A. Endogenous Phthalates in Plants and Their Alleged Participation in Defense Response against Phytopathogens Endogenous Phthalates in Plants and Their Alleged Participation in Defense Response against Phytopathogens. In *IOP Conf. Series: Earth and Environmental Science* **2020**, 408, 1–6. <https://doi.org/10.1088/1755-1315/408/1/012076>.
- (113) Zhang, H.; Hua, Y.; Chen, J.; Li, X.; Bai, X.; Wang, H. Organism-Derived Phthalate Derivatives as Bioactive Natural Products. *Journal of Environmental Science and Health, Part C* **2018**, 36 (3), 125–144. <https://doi.org/10.1080/10590501.2018.1490512>.
- (114) Nair, J. J.; Ndhhlala, A. R.; Chukwujekwu, J. C.; Staden, J. Van. Isolation of Di-(2-Ethylhexyl) Phthalate from a Commercial South African Cognate Herbal Mixture. *South African Journal of Botany* **2012**, 80, 21–24. <https://doi.org/10.1016/j.sajb.2012.01.008>.
- (115) Lotfy, M. M.; Hassan, H. M.; Hetta, M. H.; El-gendy, A. O.; Mohammed, R. Di-(2-Ethylhexyl) Phthalate , a Major Bioactive Metabolite with Antimicrobial and Cytotoxic Activity Isolated from River Nile Derived Fungus *Aspergillus Awamori*. *Beni-Suef University Journal of Basic and Applied Sciences* **2018**, 7 (3), 263–269. <https://doi.org/10.1016/j.bjbas.2018.02.002>.
- (116) Marzouk, A. M.; Osman, S. M.; Gohar, A. A. A New Pregnane Glycoside from *Gomphocarpus Fruticosus* Growing in Egypt. *Natural Product Research* **2016**, 30 (9), 1060–1067.
- (117) Tagele, S. B.; Lee, H. G.; Kim, S. W.; Lee, Y. S. Phenazine and 1-Undecene Producing *Pseudomonas Chlororaphis* Subsp . *Aurantiaca* Strain KNU17Pc1 for Growth Promotion and Disease Suppression in Korean Maize Cultivars. *Journal of*

Microbiology and Biotechnology **2019**, 29 (1), 66–78.

- (118) Zhou, J. Y.; Zhao, X. Y.; Dai, C. C. Antagonistic Mechanisms of Endophytic *Pseudomonas Fluorescens* against *Athelia Rolfsii*. *Journal of Applied Microbiology* **2014**, 117, 1144–1158. <https://doi.org/10.1111/jam.12586>.
- (119) Luo, J.; Lehtinen, T.; Efimova, E.; Santala, V.; Santala, S. Synthetic Metabolic Pathway for the Production of 1 - Alkenes from Lignin - Derived Molecules. *Microbial Cell Factories* **2019**, 18 (48), 1–13. <https://doi.org/10.1186/s12934-019-1097-x>.
- (120) Prakash, D.; Ms, A.; Radhika, B.; Venkatesan, R.; Chalasani, S. H. 1 -Undecene from *Pseudomonas Aeruginosa* Is an Olfactory Signal for Flight-or-Fight Response in *Caenorhabditis Elegans*. *The EMBO Journal* **2021**, 40, 1–12. <https://doi.org/10.15252/emj.2020106938>.
- (121) Malladi, S.; Ratnakaram, V. N.; Babu, K. S.; Pullaiah, T. Evaluation of *in Vitro* Antibacterial Activity of *Caralluma Lasiantha* for Scientific Validation of Indian Traditional Medicine. *Cogent Chemistry* **2017**, 105 (1), 1–16. <https://doi.org/10.1080/23312009.2017.1374821>.
- (122) Babu, K. S.; Malladi, S.; Nadh, R. V. Evaluation of *in Vitro* Antibacterial Activity of *Caralluma Umbellata* Haw Used in Traditional Medicine by Indian Tribes. *Annual Research & Review in Biology* **2014**, 4 (6), 840–855.

7 Appendices

Appendix Table 1. ^1H , ^{13}C and DEPT-135 NMR (CDCl_3) spectroscopic data of compound 65

Position	δ_{H} (multiplicity and coupling)	δ_{C}	DEPT-135
1	1.17 (m)	29.3	-CH ₂ -
2	1.17 (m)	29.3	-CH ₂ -
3	3.63 (m)	73.9	-CH-OH
4	2.22(m)	39.7	-CH ₂ -
5	-	138.9	-C- (Q)
6	5.27 (m)	122.6	=CH-
7	1.78 (m)	29.1	-CH ₂ -
8	1.17 (m)	38.6	-CH-
9	1.17 (m)	49.9	-CH-
10	-	42.1	-C- (Q)
11	1.17 (m)	22.6	-CH ₂ -
12	1.17 (m)	33.8	-CH ₂ -
13	-	48.8	-C- (Q)
14	1.17 (m)	56.6	-CH-
15	1.17 (m)	27.1	-CH ₂ -
16	1.17 (m)	27.1	-CH ₂ -
17	1.17 (m)	55.9	-CH-
18	0.60 (s)	13.9	-CH ₃
19	0.94 (s)	14.0	-CH ₃
20	2.69 (m)	45.8	-CH-
21	3.91 (dd, $J = 1.79, 1.79$)	66.7	-CH ₂ -OH
22	1.78 (m)	31.9	-CH ₂ -
23	5.73 (m)	139.4	=CH-
24	4.85 (br d, H- <i>cis</i> , $J = 10.55$), 4.92 (br d, H- <i>trans</i> , $J = 17.02$)	113.9	=CH ₂
3/21-OH	1.96 (s)	-	-

Appendix Table 2. ^1H , ^{13}C and DEPT-135 NMR (CD_3OD) spectral data of apigenin-7-*O*-neohesperidoside (**66**)

Compound 66				Apigenin-7- <i>O</i> -neohesperidoside (DMSO, d_6) ¹⁰⁶
Position	δ_{H} (m and <i>J</i>)	δ_{C}	DEPT-135	δ_{C}
1	-	-	-	-
2	-	161.5	Q	164.2
3	6.71 (s)	104.2	=CH-	103.1
4	-	181.2	Q (C=O)	181.8
5	-	160.1	Q (hydroxylated)	161.1
6	6.48 (d, <i>J</i> = 2.02)	96.9	=CH-	99.6
7	-	163.9	Q (oxygenated)	162.6
8	6.82 (d, <i>J</i> = 2.02)	92.7	=CH-	94.7
9	-	156.1	Q	157.9
10	-	105.6	Q	105.6
1'	-	120.2	Q	121.1
2'/6'	7.94 (d, <i>J</i> = 8.69)	126.9	=CH-	128.5
3'/5'	6.98 (d, <i>J</i> = 9.09)	114.3	=CH-	115.9
4'	-	160.0	Q (hydroxylated)	161.4
4'/5-OH	4.59 (intense s)	-	-	-
Glucose-1''	5.25 (d, <i>J</i> = 7.46)	99.6	O-CH-O-	98.6
2''	3.58 (m)	77.4	-CH-O	77.1
3''	3.64 (m)	76.1	-CH-OH	77.0
4''	3.45 (t, <i>J</i> = 18.32)	69.3	-CH-OH	70.6
5''	3.75 (m)	76.1	-CH-O	77.4
6''	3.93 (m)	59.4	-CH ₂ -OH	61.0
Rhaminose-1'''	5.31 (d, <i>J</i> = 1.70)	101.4	-O-CH-O-	100.5
2'''	3.64 (m)	68.5	-CH-OH	70.2
3'''	3.58 (m)	70.7	-CH-OH	70.6
4'''	3.45 (t, <i>J</i> = 18.32)	75.4	-CH-OH	72.3
5'''	3.98 (m)	67.2	-CH-O-	68.6
6'''	1.36 (d, <i>J</i> = 6.17)	15.5	-CH ₃	18.1
OHs of sugars	2.65	-	-	-

Appendix Table 3. ^1H , ^{13}C and DEPT-135 NMR (CDCl_3) data of 13-*O*-pyrrolecarboxyl lupanine (**67**) and literature data

Compound 67				Calpurnine ¹⁰ ₇
C/H	δ_H	δ_C	DEPT-135	δ_C
1	-	-	-	-
2	-	171.9	Q (C=O)	171.6
3	2.73 (m)	33.0	-CH ₂ -	33.1
4	1.89 (m)	19.4	-CH ₂ -C-O-	19.5
5	1.89 (m)	26.5	-CH ₂ -	26.6
6	4.36 (m)	60.7	-CH-N-	60.7
7	2.09 (m)	33.9	-CH-	34.2
8	1.37 (m)	27.3	-CH ₂ -	27.3
9	2.09 (m)	32.4	-CH-	32.6
10	4.57 (br d, $J = 4.54$)	46.9	-CH ₂ -N-	46.9
11	3.02 (m)	57.5	-CH-N-	57.6
12	2.22 (m)	36.4	-CH ₂ -	36.1
13	5.24 (m)	67.6	-CH-O-	68.0
14	2.57 (m)	28.4	-CH ₂ -	28.7
15	3.39 (m)	49.9	-CH ₂ -N-	49.9
16	-	-	-	-
17	3.62 (m)	51.9	-CH ₂ -N-	52.1
13-pyrrolicarboxyl moiety				
1'	-	160.0	Q (-C=O)	160.1
2'	-	122.8	Q	122.9
3'	4.98 (br s, 2 ⁰ amine)	-	-	-
4'	6.97 (br s)	123.3	=CH-NH	123.4
5'	6.24 (dd, $J = 6.23, 6.22$)	110.3	=CH-	110.3
6'	6.95 (br s)	116.2	=CH-	116.1

Appendix Table 4. ^1H , ^{13}C and DEPT-135 NMR (CDCl_3) spectral data of compound **68**

Position	δ_{H}	δ_{C}	DEPT-135
1	-	154.2	Q
2	5.92 (d, $J = 1.6$)	103.7	=CH-
3	-	157.0	Q
4	6.43 (br s)	104.7	=CH-
5	7.37 (br d, $J = 8.3$)	132.1	=CH-
6	6.72 (br s)	109.8	=CH-
7	5.46 (s, overlapping)	78.5	-CH-O-
8	-	77.2	Q
9	1.25 (s)	66.5	C-CH ₂ -O-
1'	-	112.7	Q
2'	-	148.1	Q
3'	-	141.7	Q
4'	-	117.9	Q
5'	-	156.7	Q
6'	5.90 (d, $J = 1.7$)	101.1	=CH-
7'	2.37 (m)	29.7	C=C-CH ₂ -
8'	3.67 (m)	40.2	-CH-
9'	5.48 (d, $J = 6.7$)	93.9	O-CH-OH
OH groups	5.34	-	-

Appendix Table 5. ^1H , ^{13}C and DEPT-135 NMR (CDCl_3) spectral data for bis-(2-hydroxybutyl) phthalate (**69**)

C/H	δ_{H}	δ_{C}	DEPT-135
1/2	-	132.2	Q (-C=C-)
3/6	7.72 (dd, $J = 3.2, 3.7$)	128.9	=CH-
4/5	7.53 (dd, $J = 3.2, 3.7$)	130.9	=CH-
7/8	-	167.7	Q (C=O)
1'/1''	4.37 (quart., $J = 21.4$)	61.7	CH ₂ -O-
2'/2''	3.81 (m)	77.2	-CH-OH
3'/3''	1.25 (m)	29.7	-CH ₂ -CH ₃
4'/4''	0.89 (t, $J = 11.0$)	14.1	-CH ₃

Appendix Table 6. ^1H , ^{13}C and DEPT-135 NMR (CD_3OD) data of compound **70** and di-(2-methylheptyl)phthalate

Compound 70				di-(2-methylheptyl)phthalate (CDCl_3) ¹⁰⁸	
Attribution	δ_{H} (multiplicity and coupling)	δ_{C}	DEPT-135	δ_{H}	δ_{C}
1'/1''	4.24 (dd, $J = 1.82, 2.11$)	67.7	-CH ₂ -O-	4.15 (m)	68.1
2'/2''	1.71 (m)	38.8	-CH-	1.25(m)	38.7
3'/3''	1.36 (m)	23.6	-CH ₂ -	1.25(m)	23.7
4'/4''	1.36 (m)	28.7	-CH ₂ -	1.25(m)	28.9
5'/5''	1.36 (m)	30.2	-CH ₂ -	1.25(m)	30.3
6'/6''	1.36 (m)	22.7	-CH ₂ -	1.25 (m)	22.9
7'/7''	0.94 (t, $J = 10.98$)	13.1	-CH ₃	0.82	14.1
8'/8''	0.98 (d, $J = 7.28$)	10.1	-CH ₃	0.82	10.9
7/8	-	167.9	Q (C=O)	-	167.8
1/6	-	132.2	Q		130.9
2/5	7.74 (dd, $J = 3.68, 3.68$)	128.5	=CH-	7.65 (dd)	128.8
3/4	7.64 (dd, $J = 3.68, 3.68$)	131.0	=CH-	7.45 (dd)	132.4

Appendix Table 7.: ^1H , ^{13}C and DEPT-135 NMR (CDCl_3) spectral data of heptacos-1-ene (**71**)

C/H	δ_{H}	δ_{C}	DEPT-135
1	(4.96, dd, $J = 16.4, 11.1$)	114.5	=CH ₂
2	5.80 (m)	139.8	=CH-
3	2.04 (m)	34.3	-CH ₂ -
4	1.38 (m)	30.2	-CH ₂ -
5	1.25 (m)	29.9	-CH ₂ -
6	1.25 (m)	29.9	-CH ₂ -
7	1.25 (m)	30.2	-CH ₂ -
8	1.25 (m)	30.2	-CH ₂ -
9	1.25 (m)	30.2	-CH ₂ -
10	1.25 (m)	30.2	-CH ₂ -
11	1.25 (m)	30.2	-CH ₂ -
12	1.25 (m)	30.2	-CH ₂ -
13	1.25 (m)	30.2	-CH ₂ -
14	1.25 (m)	30.2	-CH ₂ -
15	1.25 (m)	30.2	-CH ₂ -
16	1.25 (m)	30.2	-CH ₂ -
17	1.25 (m)	30.2	-CH ₂ -
18	1.25 (m)	30.2	-CH ₂ -
19	1.25 (m)	30.2	-CH ₂ -
20	1.25 (m)	30.2	-CH ₂ -
21	1.25 (m)	30.2	-CH ₂ -
22	1.25 (m)	30.2	-CH ₂ -
23	1.25 (m)	30.2	-CH ₂ -
24	1.25 (m)	30.2	-CH ₂ -
25	1.25 (m)	30.2	-CH ₂ -
26	1.38 (m)	23.2	-CH ₂ -
27	0.88 (t, $J = 12.87$)	14.6	-CH ₃

Appendix Table 8. ^1H , ^{13}C and DEPT-135 NMR (CDCl_3) spectral data of di-(2-ethylhexyl)phthalate (**72**)

Compound 72				$(\text{CDCl}_3)^{115}$		$(\text{CDCl}_3)^{114}$	
C/H	δ_{H}	δ_{C}	DEPT-135	δ_{H}	δ_{C}	δ_{H}	δ_{C}
1,1'	4.21 (4H, br t, $J=12.38$)	68.0	-CH ₂ - O-	4.12 (4H, d)	66.9	4.20-4.24 (4H, dd, $J = 10.90, 6.00$)	68.5
2,2'	2.33 (2H, m)	38.5	-CH-	1.58 (2H, m)	37.8	1.67 (2H, m)	39.1
3,3'	1.25-1.36 (4H, m)	29.5	-CH ₂ -	1.24-1.34 (2H, m)	29.4	1.35 (4H, m)	30.7
4,4'	1.25-1.36 (4H, m)	28.7	-CH ₂ -	1.24-1.34 (2H,m)	21.9	1.32 (4H, m)	29.3
5,5'	1.25-1.36 (4H, m)	22.8	-CH ₂ -	1.24-1.34 (2H, m)	22.8	1.39 (4H, m)	23.3
6,6'	0.78 (6H, t, $J = 8.56$)	13.9	-CH ₃	0.80 (6H, t)	9.9	0.89 (6H, t, $J = 6.84$)	14.4
7,7'	1.25-1.36 (4H, m)	23.5	-CH ₂ -	1.34 (2H, m)	27.9	1.46 (4H, m)	24.1
8,8'	0.89 (6H, dd, $J = 9.83, 12.04$)	10.8	-CH ₃	0.84 (6H, t)	12.9	0.92 (6H, t, $J = 7.48$)	11.3
9,9'	-	167.6	Q (C=O)	-	166.5	-	168.1
1'',2''	-	132.2	-C- (Q)	-	131.5	-	132.8
3'',6''	7.70 (2H, dd, $J = 4.45, 4.87$)	128.6	=CH-	7.59 (2H, dd)	127.7	7.70 (2H, dd, $J = 5.68, 3.32$)	129.1
4'',5''	7.53 (2H, dd, $J = 4.45, 4.87$)	130.7	=CH-	7.39 (2H, dd)	129.8	7.52 (2H, dd, $J = 5.68, 3.32$)	131.2

Appendix Table 9. ¹H, ¹³C and DEPT-135 NMR (CDCl₃) spectroscopic data of the aglycone moiety of compound **73**

Compound 73				Compound 52 (CD ₃ OD) ⁹¹		Compound 58 (Pyridine- <i>d</i> ₅) ⁹²	Compounds 59- 61 (CDCl ₃) ⁹³
C/ H	δ _H	δ _C	DEPT- 135	δ _H	δ _C	δ _C	δ _C
1	1.38 (m)	33.7	-CH ₂ -	1.10/1.75 (m, α,β)	38.4	38.1	40.4
2	1.38 (m)	29.5	-CH ₂ -	1.90/1.51 (m, α,β)	30.6	29.6	30.3
3	3.33 (m)	72.2	-CH-O-	3.50 (m)	78.9	76.7	77.4
4	1.38 (m)	33.5	-CH ₂ -	2.38/2.17 (m, α,β)	39.4	34.6	39.5
5	1.79 (m)	47.3	-CH-	-	140.8(Q)	45.3	141.8 (Q)
6	1.38 (m)	29.5	-CH ₂ -	5.49 (br s)	122.9 (- CH-)	25.2	122.5 (-CH-)
7	1.38 (m)	29.5	-CH ₂ -	1.92/2.25 (m, α,β)	28.1	34.4	32.5
8	1.79 (m)	44.9	-CH-	1.87 (m)	37.7	76 (C-OH)	34.0
9	1.79 (m)	49.8	-CH-	1.37 (m)	44.5	46.9	45.8
10	-	35.2	Q	-	38.2	36.7	36.8
11	1.79 (m)	22.5	-CH ₂ -	1.84/1.65 (m, α,β)	27.4	24.6	24.4
12	4.79 (br d, <i>J</i> = 9.91)	73.8	-CH-O-	4.98 (m)	80.1	75.9	71.5 (C-OH)
13	-	53.2	Q	-	53.5	57.5	56.0
14	-	86.5	-C-OH (Q)	-	87.3	88.4	84.9
15	1.38 (m)	31.7	-CH ₂ -	1.65/1.87 (m, α,β)	32.3	32.8	32.5
16	1.38 (m)	29.5	-CH ₂ -	1.70/2.04 (m, α,β)	25.5	33.8	27.5
17	2.02 (m)	55.7	-CH-	2.28 (m)	51.1	88.8	52.7
18	1.04 (s)	10.5	-CH ₃	1.14 (s)	10.2	12.2	12.2
19	0.88 (s)	12.6	-CH ₃	1.01 (s)	19.8	13.0	17.8
20	5.39 (m)	70.4	-CH-O-	5.25 (m)	75.3	70.7	71.7
21	1.24 (br s)	19.2	-CH ₃	1.21 (d, <i>J</i> = 5.0)	19.7	19.5	20.6

14-OH	2.17 (br s)	-	-	-	-	-	-
Bz (12)							
1'	-	165.8	C=O (Q)	-	167.3	166.6	
2'	-	130.4	Q	-	131.7	131.7	
3', 7'	7.92 (dd, $J=7.74, 7.74$)	129.2	=CH-	7.75 (br d, $J = 8.5$)	130.3	130.4	
4', 6'	7.28 (t, $J = 12.95$)	127.9	=CH-	7.25 (t, $J=8.0$)	129.5	128.8	
5'	7.59 (tt or sep., $J = 12.95, 14.10$)	132.3	=CH-	7.52, t ($J = 7.5$)	133.9	133.2	
Bz (20)							
1'	-	166.4	C=O (Q)	-	167.9	-	
2'	-	130.5	Q	-	132.5	-	
3', 7'	8.18 (br t, $J=18.32$)	129.6	=CH-	8.05 (br d, $J = 8.5$)	130.7	-	
4', 6'	7.34 (t, $J = 12.95$)	128.3	=CH-	7.50 (t, $J = 8.5$)	129.8	-	
5'	7.73 (br quar., $J = 26.07$)	132.8	=CH-	7.68 (t, $J = 7.5$)	134.3	-	

Note: Bz: Benzoyl

Appendix Table 10. ^1H , ^{13}C and DEPT-135 NMR (CDCl_3) spectral data for the sugar moieties of compound **73**

Compound 73				Compound 52 ⁹¹		Compound 58 ⁹²		Compounds 59-61 ⁹³
C/H	δ_{H}	δ_{C}	DEPT-135	δ_{H}	δ_{C}	δ_{H}	δ_{C}	δ_{C}
Cym-I								
1''	4.98 (br d, $J = 10.52$)	95.3	CH-O-	4.89 (d, $J = 10.5$)	97.2	5.33 (dd, $J = 9.8, 2.0$)	95.9	97.8
2''	1.79 (m)	36.1	-CH ₂ -	1.65/2.15 (m)	36.4	1.82/2.35 (m)	37.3	35.8
3''	3.98 (m)	78.8	-CH-O-	3.84 (m)	78.5	4.11 (m)	78.1	77.3
4''	3.73 (m)	82.3	-CH-O-	3.22 (m)	83.7	3.53 (dd, $J = 9.0, 3.1$)	83.5	83.0
5''	3.98 (m)	68.3	-CH-O-	3.80 (m)	69.9	4.28 (m)	69.0	68.8
6''	1.32 (br s)	17.9	-CH ₃	1.21 (d, $J = 6.5$)	18.5	1.42 (d, $J = 6.0$)	18.7	18.5
7''	3.53 (s)	57.0	-OCH ₃	3.44 (s)	58.4	3.65 (s)	58.9	55.2
Cym-II								
1'''	4.90 (br d, $J = 6.89$)	99.1	-CH-O-	4.80 (d, $J = 8.0$)	101.1	5.13 (dd, $J = 9.8, 2.1$)	100.5	99.4
2'''	1.79 (m)	36.1	-CH ₂ -	1.62/2.1 (m)	36.7	1.88/2.33 (m)	37.0	36.0
3'''	3.98 (m)	78.8	-CH-O-	3.92 (m)	78.7	4.02 (m)	77.8	77.0
4'''	3.73 (m)	82.3	-CH-O-	3.32 (m)	83.9	3.44 (dd, $J = 9.1, 3.0$)	83.2	73.8
5'''	3.98 (m)	68.3	-CH-O-	3.90 (m)	70.1	4.18 (m)	68.9	69.3
6'''	1.32 (br s)	18.1	-CH ₃	1.31 (d, $J = 6.5$)	18.6	1.38 (d, $J = 6.0$)	18.5	18.8
7'''	3.54 (s)	57.7	-OCH ₃	3.45 (s)	58.6	3.58 (s)	59.0	57.5

Cym-I and **Cym-II**: Cymarose

Appendix Table 11. ^1H , ^{13}C and DEPT-135 NMR (CDCl_3) spectral data of compound **74**

C/H	δ_{H}	δ_{C}	DEPT-135
1	1.22 (m)	33.9	-CH ₂ -
2	1.22 (m)	23.1	-CH ₂ -
3	1.22 (m)	29.8	-CH ₂ -
4	1.22 (m)	29.8	-CH ₂ -
5	2.30 (m)	38.8	-CH-
6	1.22 (m)	29.8	-CH ₂ -
7	1.22 (m)	29.8	-CH ₂ -
8	3.59 (m)	31.7	-CH-
9	2.01 (m)	52.7	-CH-
10	-	34.8	Q
11	1.63 (m)	22.8	-CH ₂ -
12	3.84 (m)	38.8	-CH-O-
13	-	52.2	Q
14	2.01 (m)	57.3	-CH-
15	1.22 (m)	23.8	-CH ₂ -
16	1.22 (m)	32.0	-CH ₂ -
17	4.19 (m)	55.9	-CH-
18	0.87 (s)	11.1	-CH ₃
19	0.87 (s)	14.2	-CH ₃
20	6.83 (m)	139.4	=CH-
21	5.78 (d, $J = 17.40$, H- <i>trans</i>), 5.33 (d, $J = 15.20$, H- <i>cis</i>)	114.2	=CH ₂
22	4.98 (m)	68.3	-CH ₂ -O-
Bz (12)			
1'	-	167.9	C=O (Q)
2'	-	132.5	Q
3',7'	8.04 (br s)	129.9	=CH-
4',6'	7.57 (br t, $J = 17.70$)	128.9	=CH-
5'	7.80 (br t, $J = 16.82$)	131.0	=CH-

Appendix Table 12. ^1H , ^{13}C and DEPT-135 NMR (CDCl_3) spectral data for the aglycone moiety of compound **75**

C/H	δ_{H}	δ_{C}	DEPT-135
1	1.30 (m)	33.2	-CH ₂ -
2	1.30 (m)	25.9	-CH ₂ -
3	3.19 (m)	76.9	-CH-O-
4	1.30 (m)	39.1	-CH ₂ -
5	1.83 (m)	45.5	-CH-
6	1.30 (m)	30.0	-CH ₂ -
7	1.30 (m)	32.3	-CH ₂ -
8	1.83 (m)	30.1	-CH-
9	1.83 (m)	44.8	-CH-
10	-	36.7	Q
11	1.70 (m)	23.1	-CH ₂ -
12	4.84 (br d, $J = 9.40$)	74.4	-CH-O-
13	-	53.8	Q
14	-	87.1	-C-O-(Q)
15	1.30 (m)	31.1	-CH ₂ -
16	1.30 (m)	18.0	-CH ₂ -
17	2.37 (m)	50.4	-CH-
18	0.90 (s)	13.2	-CH ₃
19	0.75 (s)	14.8	-CH ₃
20	5.24 (m)	74.9	-CH-O-
21	1.10 (br s)	19.5	-CH ₃
Bz (12)			
1'	-	166.4	C=O (Q)
2'	-	131.0	Q
3',7'	7.80 (dd, $J = 7.42, 7.42$)	129.8	=CH
4',6'	7.14 (t, $J = 14.84$)	128.6	=CH
5'	7.45 (tt, $J = 13.38, 14.11$)	132.9	=CH
Bz (20)			
1'	-	166.7	C=O (Q)
2'	-	131.3	Q
3',7'	8.04 (br t, $J = 18.62$)	130.1	=CH
4',6'	7.20 (t, $J = 14.11$)	128.8	=CH
5'	7.59 (br quar., $J = 20.01$)	133.3	=CH
Acetoxy (14)			
1''	-	175.7	C=O (Q)
2''	2.81 (s)	22.3	-CH ₃

Appendix Table 13. ^1H , ^{13}C and DEPT-135 NMR (CDCl_3) spectroscopic data for the sugar moieties of compound **75**

Compound 75				Literature value⁹¹	
C/H	δ_{H}	δ_{C}	DEPT-135	δ_{H}	δ_{C}
Cym-I					
1'''	4.73 (br d, $J = 9.33$)	95.9	-CH-O-	4.87 (dd, $J = 10.0, 2.5$)	97.3
2'''	2.01 (m)	37.2	-CH ₂ -	1.57 (br dd, $J = 16.00, 12.00, H_{\alpha}$), 2.08 (br dd, $J = 15.0, 3.0, H_{\beta}$)	36.9
3'''	3.88 (m)	80.9	-CH-O-	3.86 (q, $J = 4.0$)	78.6
4'''	3.40 (m)	85.3	-CH-O-	3.25 (dd, $J = 10.0, 4.0$)	84.1
5'''	3.88 (m)	71.2	-CH-	3.86 (m)	70.1
6'''	1.34 (br s)	21.2	-CH ₃	1.21 (d, $J = 6.0$)	18.5
7'''	3.62 (br s)	60.6	-OCH ₃	3.45 (s)	58.5
Cym-II					
1''''	4.57 (br d, $J = 9.03$)	99.9	-CH-O-	4.81 (dd, $J = 8.5, 2.0$)	101.1
2''''	2.01 (m)	38.3	-CH ₂ -	1.70 (m, H_{α}), 2.11 (m, H_{β})	36.4
3''''	3.88 (m)	81.9	-CH-O-	3.86 (m)	78.6
4''''	3.40 (m)	85.4	-CH-O-	3.28 (m)	84.3
5''''	3.88 (m)	71.3	-CH-	3.85 (dq, $J = 6.0, 9.5$)	70.3
6''''	1.34 (br s)	22.3	-CH ₃	1.32 (d, $J = 6.0$)	18.8
7''''	3.62 (br s)	60.7	-OCH ₃	3.44 (s)	58.7
Thev					
1'''''	4.27 (br d, $J = 4.26$)	104.7	-CH-O-	4.31 (d, $J = 8.0$)	104.3
2'''''	3.40 (m)	74.8	-CH-OH	3.20 (m)	75.7
3'''''	3.40 (m)	86.7	-CH-O-	3.25 (m)	86.2
4'''''	3.40 (m)	85.7	-CH-OH	3.30 (m)	82.9
5'''''	3.88 (m)	72.8	-CH-O-	3.70 (m)	72.7
6'''''	1.34 (br s)	18.2	-CH ₃	1.39 (d, $J = 6.0$)	18.6
7'''''	3.77 (s)	61.0	-OCH ₃	3.64 (s)	61.3

Note: **Cym-I** and **Cym-II**: Cymarose, **Thev**: Thevetose

Appendix Table 14. ^1H , ^{13}C and DEPT-135 NMR (CDCl_3) spectral data of β -sitosterol (**76**) and β -sitosterol oleate (**77**)

Compound 76				Compound 77		β- sitosterol⁹⁹	
C/H	δ_{H} (multiplicity)	δ_{C}	DEPT-135	δ_{H}	δ_{C}	δ_{H}	δ_{C}
1	1.51 (m)	37.1	-CH ₂ -	1.58 (m)	37.0	1.46 (m)	37.3
2	1.60 (m)	31.7	-CH ₂ -	1.62 (m)	33.9	1.56 (m)	31.7
3	3.56 (m)	71.8	-CH-OH	4.65 (m)	73.7 (-CH-O-)	3.54 (m)	71.8
4	2.31 (m)	42.3	-CH ₂ -	2.34 (m)	39.7	2.32 (m)	42.3
5	-	140.8	Q	-	139.8	-	140.8
6	5.36 (m)	121.8	=CH-	5.37 (m)	122.6	5.37 (overlapping, t)	121.7
7	2.02 (m)	31.9	-CH ₂ -	2.34 (m)	31.9	2.04 (m)	31.9
8	1.67 (m)	31.9	-CH-	1.90 (m)	31.9	1.69 (m)	31.9
9	1.60 (m)	50.1	-CH-	1.62 (m)	50.1	1.55 (m)	50.2
10	-	36.5	Q	-	36.6	-	36.5
11	1.51 (m)	21.1	-CH ₂ -	1.58 (m)	21.0	1.52 (m)	21.1
12	1.51 (m)	39.8	-CH ₂ -	1.58 (m)	38.2	1.51 (m)	39.8
13	-	42.3	Q	-	42.3	-	42.3
14	1.51 (m)	56.8	-CH-	1.58 (m)	56.7	1.50 (m)	56.8
15	1.60 (m)	24.3	-CH ₂ -	1.62 (m)	24.3	1.58 (m)	24.3
16	1.86 (m)	28.3	-CH ₂ -	1.90 (m)	28.3	1.85 (m)	28.3
17	1.37 (m)	56.0	-CH-	1.33 (m)	56.1	1.45 (m)	56.1
18	0.67 (s)	11.9	-CH ₃	0.71 (s)	12.0	0.70 (s)	11.9
19	1.00 (s)	19.4	-CH ₃	1.05 (s)	19.4	1.03 (s)	19.4
20	1.60 (m)	36.2	-CH-	1.58-1.62 (m)	36.2	1.60 (m)	36.2
21	0.92 (d, $J = 6.46$ Hz)	18.8	-CH ₃	0.95 (d, $J = 6.48$ Hz)	18.8	0.94 (overlapping, d)	18.8
22	1.25 (m)	33.9	-CH ₂ -	1.33 (m)	33.9	0.93 (m)	33.9
23	1.25 (m)	29.7	-CH ₂ -	1.33 (m)	29.7	1.15 (m)	26.1
24	1.35 (m)	45.8	-CH-	1.33 (m)	45.9	1.38 (m)	45.9
25	1.60 (m)	29.1	-CH-	1.62 (m)	29.1	1.57 (m)	29.2
26	0.82 (d, $J = 1.92$ Hz)	19.8	-CH ₃	0.87 (d, $J = 2.13$ Hz)	19.8	0.84 (overlapping, d)	19.4

27	0.86 (d, $J = 7.68$ Hz)	19.0	-CH ₃	0.91 (d, $J = 6.77$ Hz)	19.1	0.86 (d)	19.1
28	1.25 (m)	23.1	-CH ₂ -	1.27-1.33 (m)	22.7	1.10 (m)	23.1
29	0.80 (br t, $J = 16.18$ Hz)	12.0	-CH ₃	0.84 (dd, $J = 2.58, 6.72$ Hz)	11.9	0.82 (overlapping, t)	12.0
3-OH	1.95 (s)	-	-	-	-	1.98 (s)	-
1'				-	173.3 (C=O)		
2'				2.33 (m)	34.7 (-CH ₂)		
3'				1.62 (m)	25.1 (-CH ₂)		
4'				1.33 (m)	26.1 (-CH ₂)		
5'				1.33 (m)	29.1 (-CH ₂)		
6'				1.33 (m)	27.2 (-CH ₂)		
7'				1.33 (m)	29.7 (-CH ₂)		
8'				2.05 (m)	33.9 (-CH ₂)		
9'				5.40 (m)	130.0 (=CH-)		
10'				5.38 (m)	129.8 (=CH-)		
11'				2.05 (m)	33.9 (-CH ₂)		
12'				1.33 (m)	29.3 (-CH ₂)		
13'				1.33 (m)	29.3 (-CH ₂)		
14'				1.33 (m)	27.8 (-CH ₂)		
15'				1.33 (m)	27.1 (-CH ₂)		
16'				1.33 (m)	31.9 (-CH ₂)		
17'				1.33 (m)	23.1 (-CH ₂)		
18'				0.90 (t, $J = 5.79$ Hz)	14.1 (-CH ₃)		

Appendix Table 15. ^1H , ^{13}C and DEPT-135 NMR (CDCl_3) spectral data of 1,2-dipropyl phthalate (**78**)

C/H position	δ_{H}	δ_{C}	DEPT-135
1'/1''	4.39 (br q)	61.7	-CH ₂ -O-
2'/2''	1.36 (m)	29.7	-CH ₂ -
3'/3''	0.89 (t, $J = 11.18$)	14.1	-CH ₃
1/2	-	132.2	Q
3/6	7.73 (br t, $J = 7.98$)	128.9	=CH-
4/5	7.53 (br t, $J = 7.98$)	131.0	=CH-
7/8	-	167.7	Q (C=O)

Appendix Table 16. ^1H , ^{13}C and DEPT-135 NMR (CD_3OD) data of calotropin (**79**)

Compound 79				Calotropin ¹¹⁶ in $\text{CDCl}_3:\text{CD}_3\text{OD}$ (4:1)	
Attribution	δ_{H}	δ_{C}	DEPT-135	δ_{H}	δ_{C}
1	2.47 (m)	30.2	-CH ₂ -	*	34.2
2	4.0 (br d, $J = 6.06$)	70.5	-CH-O-	4.00 (dd, $J = 12.5, 4.0$)	68.1
3	3.89 (m)	77.9	-CH-O-	3.85 (m)	71.2
4	1.68 (m)	33.0	-CH ₂ -	*	32.6
5	1.68 (m)	43.0	-CH-	*	44.1
6	1.41 (m)	28.7	-CH ₂ -	*	28.9
7	1.41 (m)	27.4	-CH ₂ -	*	27.2
8	1.26 (m)	38.8	-CH-	*	42.9
9	1.68 (m)	49.3	-CH-	*	49.9
10	-	52.6	Q	-	52.4
11	1.41 (m)	24.2	-CH ₂ -	*	21.4
12	1.26 (m)	33.4	-CH ₂ -	*	38.5
13	-	49.0	Q	-	49.2
14	-	84.4	Q	-	83.9
15	2.12 (m)	36.8	-CH ₂ -	*	38.7
16	1.68 (m)	26.5	-CH ₂ -	*	26.3
17	2.85 (dd, $J = 10.2, 6.4$)	50.4	-CH-	2.69 (dd, $J = 9.0, 4.5$)	50.1
18	0.83 (s)	14.8	-CH ₃	0.89 (s)	15.1
19	10.05 (s)	208.0	Q (C=O)	*	207.7
20	-	175.9	Q	-	175.7
21	4.53 (br d, $J = 24.52$)	73.9	-CH ₂ -O-	4.63 (dd, $J = 18.0, 1.0$)	73.5
22	5.93 (d, $J = 7.35$)	116.6	=CH-	5.69 (br s)	116.8
23	-	175.9	Q (C=O)	-	175.5
1'	4.72 (br s)	94.1	-O-CH-O-	4.78 (s)	95.5
2'	-	90.4	Q	-	90.9

3'	3.64 (m)	71.9	-CH-OH	3.72 (m)	72.3
4'	2.37 (m)	35.4	-CH ₂ -	*	37.8
5'	3.45 (m)	66.3	-CH-O-	3.38 (m)	67.8
6'	0.94 (d, <i>J</i> = 7.1)	19.9	-CH ₃	1.02 (d, <i>J</i> = 6.0)	20.4
OHs	2.05 (s)	-	-	*	-

* Values not reported

Appendix Table 17. ¹H, ¹³C and DEPT-135 NMR (CDCl₃) data of 1-undecene (**80**)

C/H	δ_H (multiplicity)	δ_C	DEPT-135
1	4.99 (<i>trans</i> , d, <i>J</i> = 17.33), 4.93 (<i>cis</i> , d, <i>J</i> = 9.76)	114.1	=CH ₂
2	5.82 (m)	139.3	=CH
3	2.04 (br q or m)	33.8	-CH ₂ -
4	1.26 (m)	29.2	-CH ₂ -
5	1.26 (m)	29.6	-CH ₂ -
6	1.26 (m)	29.5	-CH ₂ -
7	1.26 (m)	29.4	-CH ₂ -
8	1.26 (m)	28.9	-CH ₂ -
9	1.26 (m)	31.9	-CH ₂ -
10	1.26 (m)	22.7	-CH ₂ -
11	0.88 (t, <i>J</i> = 13.52)	14.1	-CH ₃

Appendix Table 18. Molecular binding capacity of isolated compounds **65-69** and chloramphenicol against *E. coli DNA gyraseB* (PDB ID: 6F86) for antibacterial activity

Compounds	Binding Affinity (kcal/mol)	H-bond	Residual amino acid interactions	
			Hydrophobic/Pi-Cation/Anion/Alkyl	Van-der Waals
65	-6.5	Asn-46	Pro-79, Ile-78	Asp-73, Ala-47, Glu-50, Arg-76, Arg-136
66	-6.4	Asp-73, Glu-50	Ile-78, Arg-76	Asp-49, Ala-53, Asn-46, Gly-77, Thr-165
67	-7.4	Thr-165, Gly-77, Ile-78	Pro-79	Asp-73
68	-7.3	Ile-94, Val-97	Ile-78	Asn-46, Ser-121, Gly-119, Val-120
69	-5.7	Asn-46, Glu-50, Asp-73	Ile-78	Asp-49, Gly-77, Val-43, Ile-94, Val-167, Thr-165
Chloramphenicol	-6.4	Glu-50, Gly-77, Asn-46	Ile-78	Val-43, Asp-49, Arg-76, Asp-73, Ala-47, Thr-165

Appendix Table 19. Molecular binding capacity of isolated compounds **65-69** and chloramphenicol against *S. aureus pyruvate kinase* (PDB ID: 3T07) for antibacterial activity

Appendix Table 20. Molecular binding capacity of isolated compounds **65-69** and ascorbic acid against *human peroxiredoxin 5* (PDB ID: 1HD2) for antioxidant activity

Compounds	Binding affinity (kcal/mol)	H-bond	Residual amino acid interactions	
			Hydrophobic/Pi-Cation/Anion/Alkyl	Van-der Walls
65	-6.1	Glu-352	Val-356	Lys-268, Leu-269, Lys-390, Arg-386, Ser-383, Ser-381, Gly-462, Thr-463, Ser-356, Asn-357
66	-5.5	Lys-390, Ser-354, Leu-269	Leu-355, Val-356, Leu-269	Lys-268, Thr-353, Asn:357, Glu-352, Thr-387, Arg-386, Thr-464, Ser-383, Thr-463
67	-6.3	Glu-352, Asn-357	Leu-269, Lys-268, Glu-352, Val-356	Ser-356, Lys-390, Thr-387, Ser-383, Thr-463
68	-6.7	Thr-387, Ser-383	Gly-352, Leu-269, Arg-386, Asn-357, Lys-390	Val-351, Val-356, Lys-271, Lys-268
69	-6.3	Arg-386, Ser-383, Lys-390, Asn-357	Val-356	Gly-270, Leu-269, Thr-387, Ser-354
Chloramphenicol	-4.6	Ala-358, Ser-362	-	Lu-355, Thr-353, Thr-348, His-365
Compounds	Binding affinity (kcal/mol)	H-bond	Interactions with amino acid residues	
			Hydrophobic/Pi-Cation/Anion/Alkyl	Van-der Walls
65	-5.4	-	Pro-40, Por-45, Ile-119, Phe-120	Thr-147, Arg-127, Thr-44
66	-4.8	Thr-147	Arg-127, Phe-120, Thr-44, Pro-45, Arg-127	Asn-76, Leu-116, Gly-148, Ile-119, Gly-46, Cys-47,
67	-6.2	-	Phe-120, Ile-119, Pro-45, Leu-149	Thr-44, Leu-116, Thr-147, Cys-47, Arg-127, Gly-46

68	-6.0	Ala-42	Pro-45, Thr-44, Ile-119, Arg-124, Asn-76	Val-80, Phe-43
69	-5.9	Gly-46, Thr-44, Thr-147	Pro-45	Cys-47, Phe-120, Leu-116, Ile-119, Leu-149
Ascorbic acid	-4.5	Thr-44, Thr-147, Arg-127, Cys-47, Gly-46	-	Leu-149, Gly-148, Pro-40

Appendix Table 21. Molecular binding capacity of isolated compounds **65-68, 70** and **79**, and chloramphenicol against *P. aeruginosa* PqsA (PDB ID: 5OE3) for antibacterial activity

Compounds	Binding affinity (kcal/mol)	H-bond	Residual amino acid interactions	
			Hydrophobic/Pi-Cation/Anion/Alkyl	Van-der Walls
65	-7.9	Arg-333, Glu-331	Arg-333, Pro-155, Leu-178, Arg-179, Leu-182	Trp-377, Cyc-332, Thr-341, Arg-386, Ile-342, Arg-186, Glu-343, Glu-344, Gly-183, Pro-356, Arg-354
66	-10.9	Ala-21, Asp-19, Ala-245, Thr-29, His-24	Arg-200, His-24, Ala-21	Thr-29
67	-8.1	Arg-386, Glu-388, Arg-333	Ala-345, Arg-386	-

68	-7.8	Arg-200, Thr-29, Gln-34	Thr-29, ALA-21	Asp-19, Thr-20, His-24, Ser-31, Leu-30, Thr-29
70	-6.1	His-24, Arg-200	Ala-21	His-24, Thr-20, Gly-198, Asp-19, Thr-29, Ser-226, Arg-200
79	-10.3	Gly-169, Lys-172, Arg-397, Ala-170, Thr-380, Thr-164	Arg-333	Thr-164, Thr-304, Gly-302, Ala-303, Glu-305, Gln-369
Chloramphenicol	-7.0	Gly-279	Phe-209, Ala-278, His-308, Gly-302	Ser-280, Ile-307, His-394, Asp-382, Ala-303, Val-309, Gly-210, Gly-307, Tyr-211

Appendix Table 22. Drug-likeness property prediction of isolated compounds **65-69, 70** and **79**

Compounds	Formula	Mol. Wt.(g/mol)	NRB	NHA	NHD	TPSA (Å²)	LogP (cLogP)	Lipinski's rule of five violation
65	C ₂₄ H ₃₈ O ₂	358.58	4	2	2	40.46	3.89	0
66	C ₂₇ H ₃₀ O ₁₄	578.52	6	14	8	228.97	2.07	3
67	C ₂₀ H ₂₇ N ₃ O ₃	357.45	3	4	1	65.64	3.04	0
68	C ₁₈ H ₁₈ O ₈	362.33	3	8	6	143.14	1.33	1
69	C ₁₆ H ₂₂ O ₆	310.32	8	4	2	58.92	3.14	0
70	C ₂₄ H ₃₈ O ₄	390.56	16	4	0	52.6	6.36	1
79	C ₂₉ H ₄₀ O ₉	532.02	2	9	3	131.75	1.84	1

Note: NHD = Number of Hydrogen donor, NHA = Number of Hydrogen acceptor, NRB = Number of rotatable bonds, and TPSA = total polar surface area

Appendix Table 23. ADME property prediction of isolated compounds **65-69, 70** and **79**

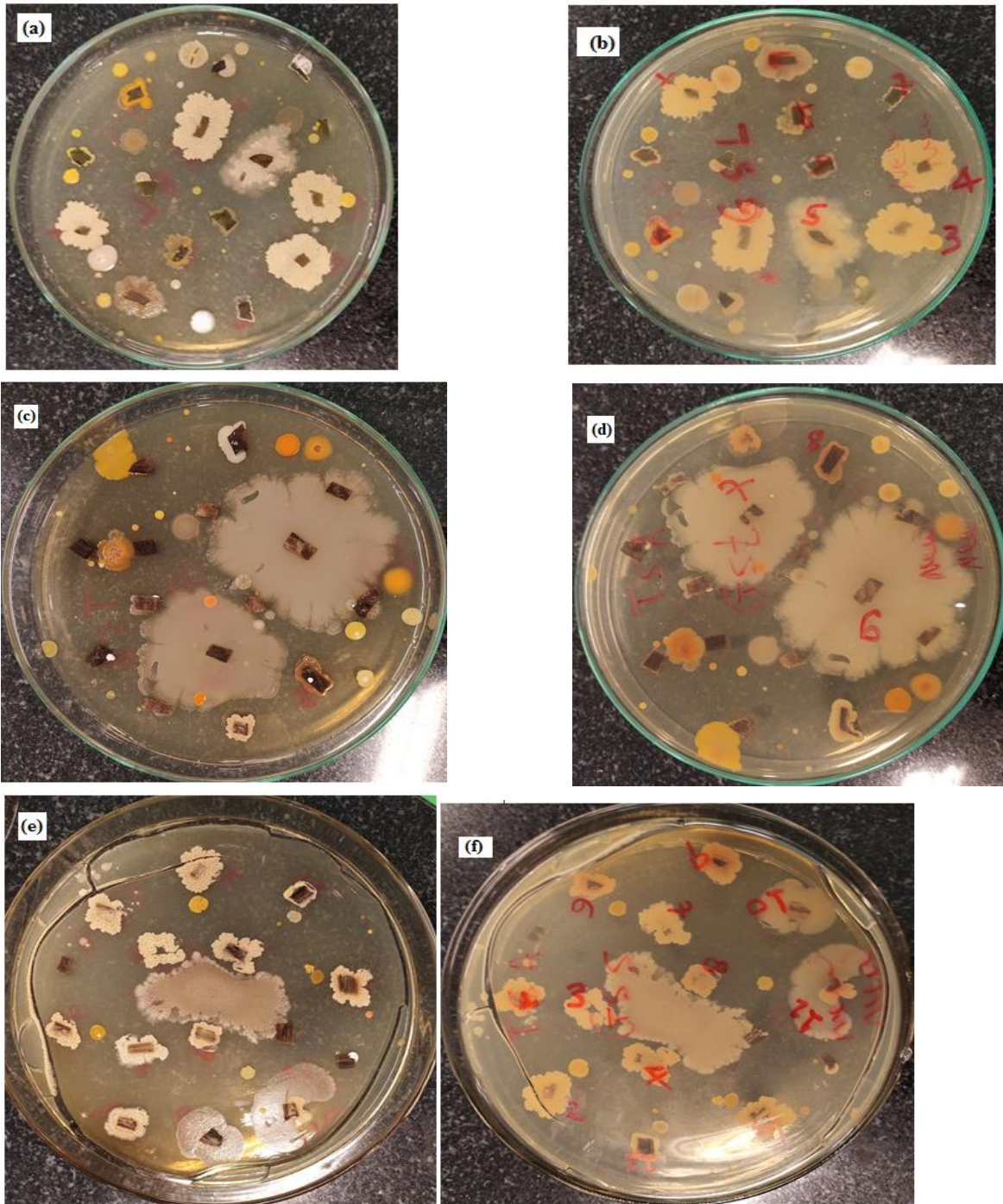
Cpd	Chemical formula	logKp cm/s	GI Absorption	BBB Permeability	Inhibitor interaction (SwissADME/PreADMET)					
					P-gp substrate	CYP1A2 inhibitor	CYP2C19 inhibitor	CYP2C9 inhibitor	CYP2D6 inhibitor	CYP3A4 inhibitor
65	C ₂₄ H ₃₈ O ₂	-4.41	High	Yes	No	No	No	Yes	No	No
66	C ₂₇ H ₃₀ O ₁₄	-9.94	Low	No	Yes	No	No	No	No	No
67	C ₂₀ H ₂₇ N ₃ O ₃	-7.09	High	Yes	No	No	No	No	Yes	No
68	C ₁₈ H ₁₈ O ₈	-7.94	Low	No	No	No	No	No	No	No
69	C ₁₆ H ₂₂ O ₆	-6.26	High	Yes	No	Yes	No	No	Yes	No
70	C ₂₄ H ₃₈ O ₄	-2.95	High	No	Yes	No	No	Yes	No	Yes
79	C ₂₉ H ₄₀ O ₉	-8.89	High	No	Yes	No	No	No	No	No

Note: LogKp = Skin permeation value, GI = Gastro-Intestinal, BBB = Blood Brain Barrier, P-gp = P-glycoprotein, CYP = Cytochrome-P

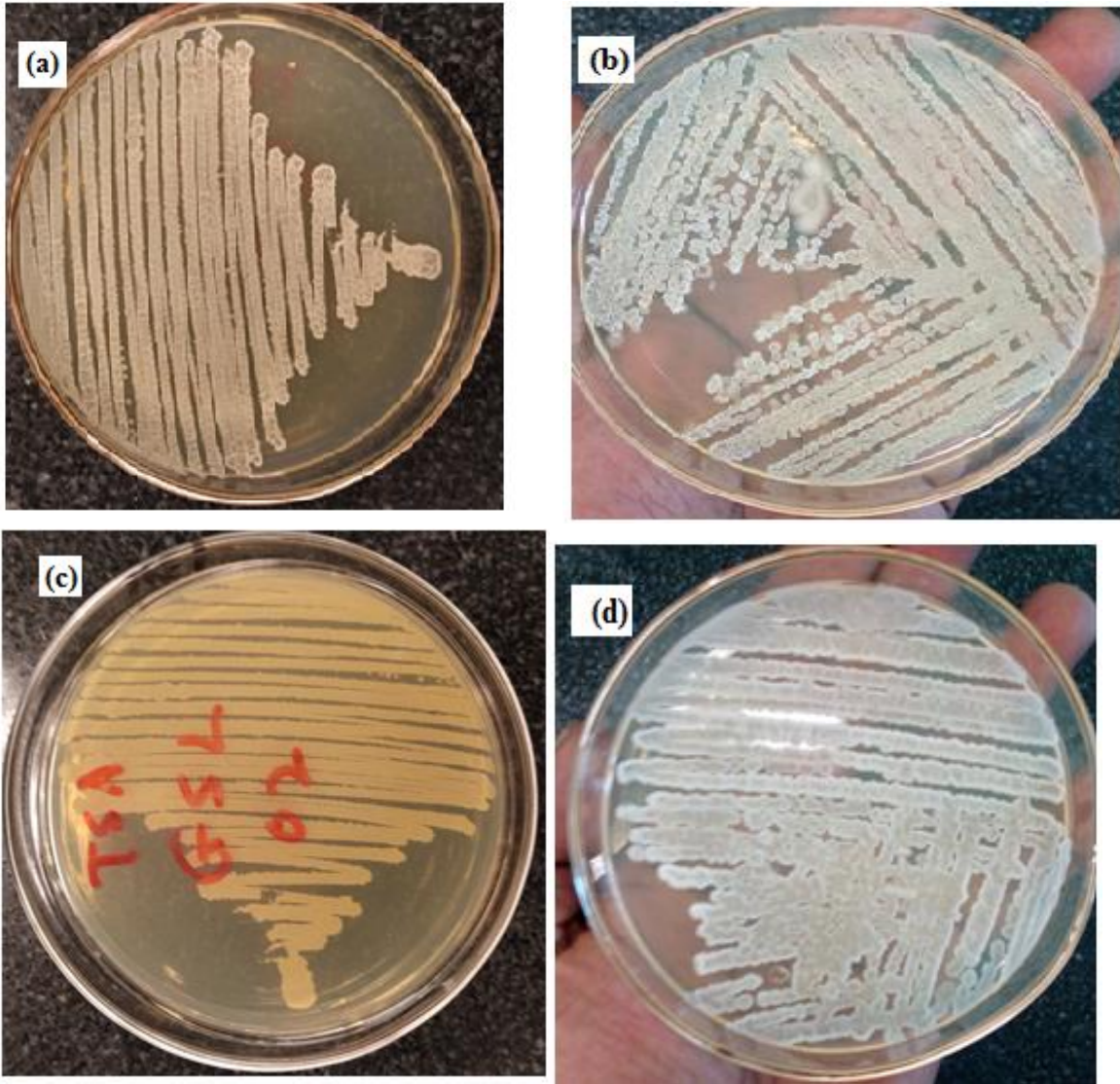
Appendix Table 24. Predication of toxicity property of isolated compounds **65-69, 70** and **79**

Cpd	Chemical formula	LD ₅₀ (mg/Kg)	Toxicity class	Organ toxicity				
				Hepatotoxicity	Carcinogenicity	Immunotoxicity	Mutagenicity	Cytotoxicity
65	C ₂₄ H ₃₈ O ₂	890	4	No	No	Yes	No	No
66	C ₂₇ H ₃₀ O ₁₄	5000	5	No	No	Yes	Yes	No
67	C ₂₀ H ₂₇ N ₃ O ₃	32	2	No	No	No	No	No
68	C ₁₈ H ₁₈ O ₈	2000	4	No	No	No	Yes	No
69	C ₁₆ H ₂₂ O ₆	2830	5	No	No	No	No	No
70	C ₂₄ H ₃₈ O ₄	1340	4	No	Yes	No	No	No
79	C ₂₉ H ₄₀ O ₉	8	2	No	No	Yes	No	Yes

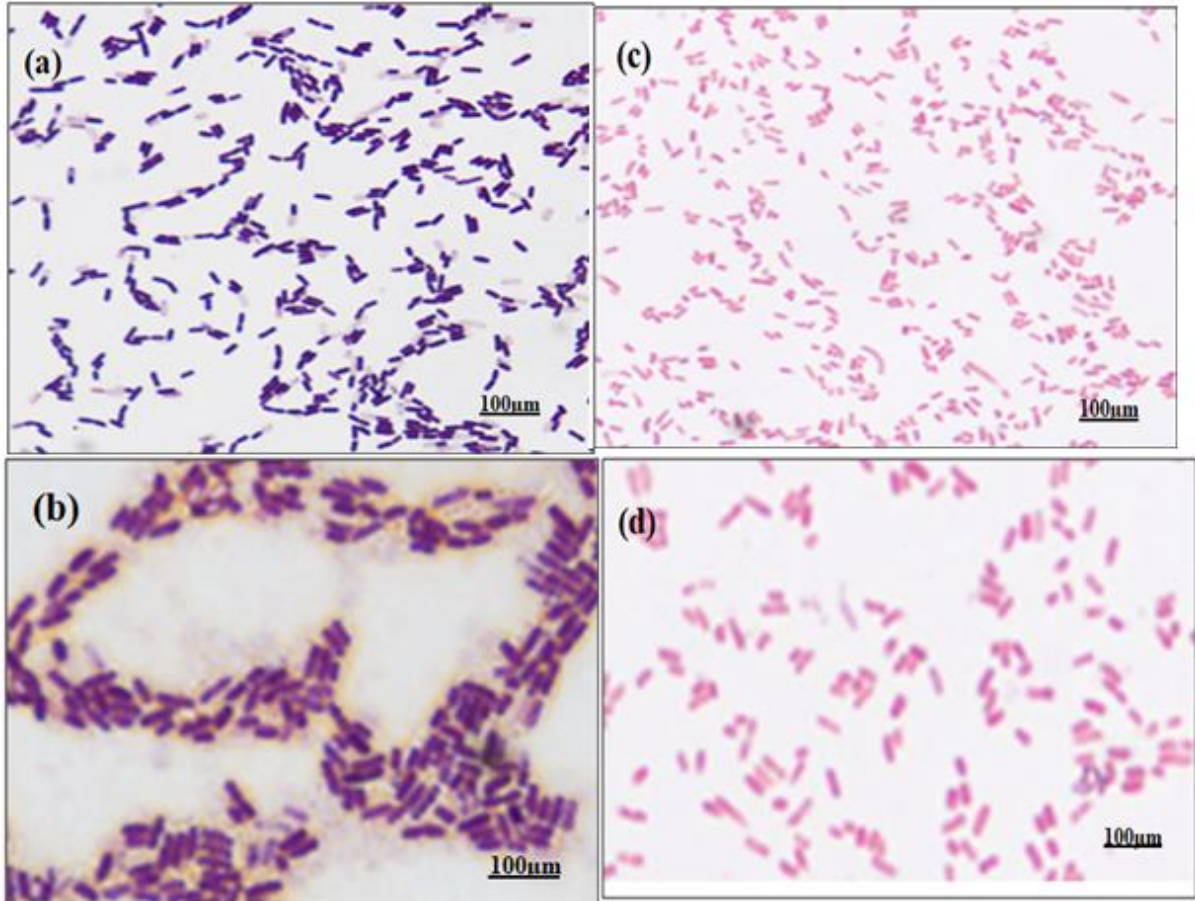
Appendix Figure 1. Representatives of emerging endophytic bacteria of plant segments on TSA medium containing Petri plate. (a) *B. subtilis* (GSL2), (b) *B. megaterium* (GSL3), (c) *E. coli* (GSS11), (d) *E. coli* (GST5), (e) *B. amyloliquefaciens* (GSS7) and (f) *Providencia rettgeri* (GSS1)



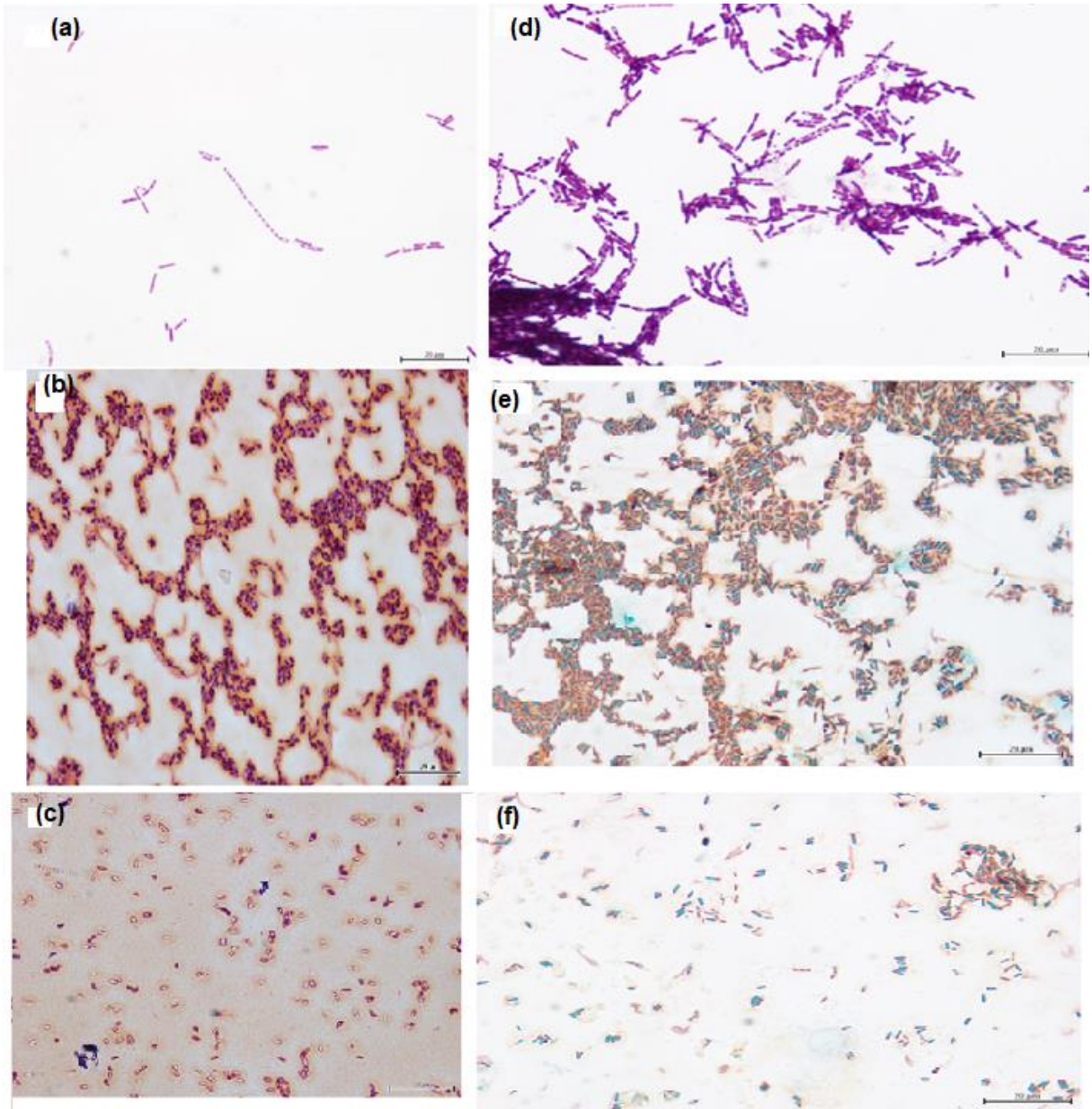
Appendix Figure 2. Representatives of sub-cultured (pure) endophytic bacterial isolates. (a) indicates for *Bacillus subtilis* (GSL1), (b) indicates *Bacillus megaterium* (GSL3) with gel colony, (c) indicates for *Bacillus subtilis* (GSL2) and (d) indicates *B. amyloliquefaciens* (GSS7)



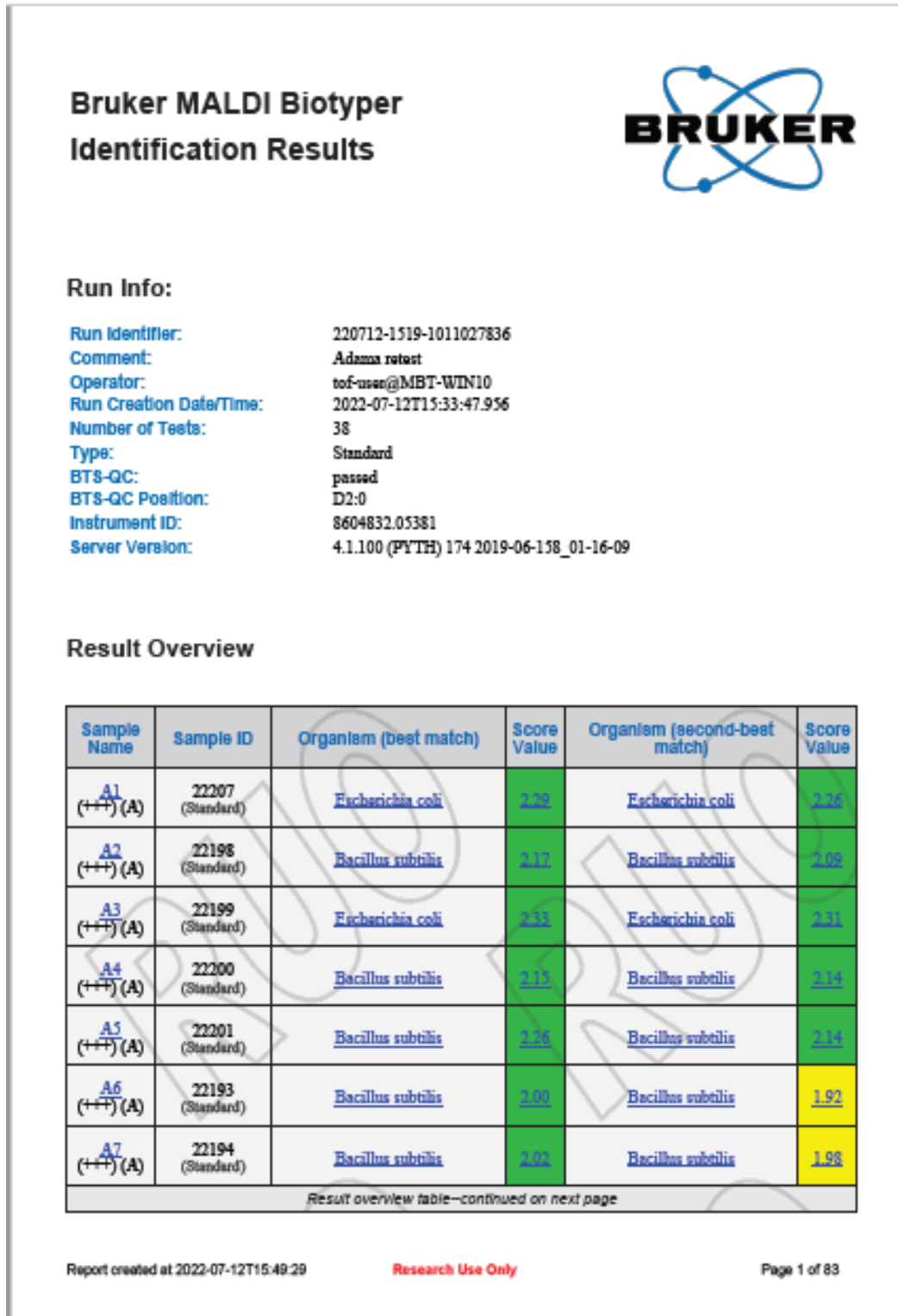
Appendix Figure 3. Representatives of Gram-positive (purple color) and Gram-negative (red color) endophytic bacterial isolates. (a) *Bacillus subtilis* (GSL1), (b) *Bacillus megatirium* (GSL3), (c) *Escherichia coli* (GST5) and (d) *Providencia rettgeri* (GSS1).



Appendix Figure 4. Representatives of spore forming endophytic bacteria against Gram-staining (a-d) and spore-staining (e & f) tests. (a) *B. subtilis* (GSL2), (b) *B. subtilis* (GSS2), (c) *B. amyloliquefaciens* (GSS7), (d) *B. subtilis* (GSS8), (e) *B. subtilis* (GST8) and (f) *B. subtilis* (GST1)



Appendix Figure 5. MALDI-TOF MS analysis data of endophytic bacteria isolated from leaves, stems and tubers of *Gloriosa superba*



Result overview table—continued from previous page

Sample Name	Sample ID	Organism (best match)	Score Value	Organism (second-best match)	Score Value
A8 (+++)(A)	22195 (Standard)	Bacillus subtilis	2.01	Bacillus subtilis	1.92
A9 (-)(C)	22196 (Standard)	No Organism Identification Possible	1.74	No Organism Identification Possible	1.71
A10 (+++)(A)	22197 (Standard)	Escherichia coli	2.22	Escherichia coli	2.22
A11 (+)(B)	22190 (Standard)	Bacillus subtilis	1.85	Bacillus subtilis	1.83
A12 (-)(C)	22191 (Standard)	no peaks found	0.00	no peaks found	0.00
B1 (+)(B)	22192 (Standard)	Bacillus subtilis	1.94	Bacillus subtilis	1.81
B2 (+++)(A)	22206 (Standard)	Escherichia coli	2.22	Escherichia coli	2.22
B3 (+++)(A)	22205 (Standard)	Bacillus subtilis	2.03	Bacillus subtilis	1.94
B4 (+++)(A)	22204 (Standard)	Escherichia coli	2.01	Escherichia coli	2.00
B5 (+)(B)	22203 (Standard)	Bacillus subtilis	1.83	Bacillus subtilis	1.78
B6 (+++)(A)	22202 (Standard)	Bacillus subtilis	2.08	Bacillus subtilis	1.92

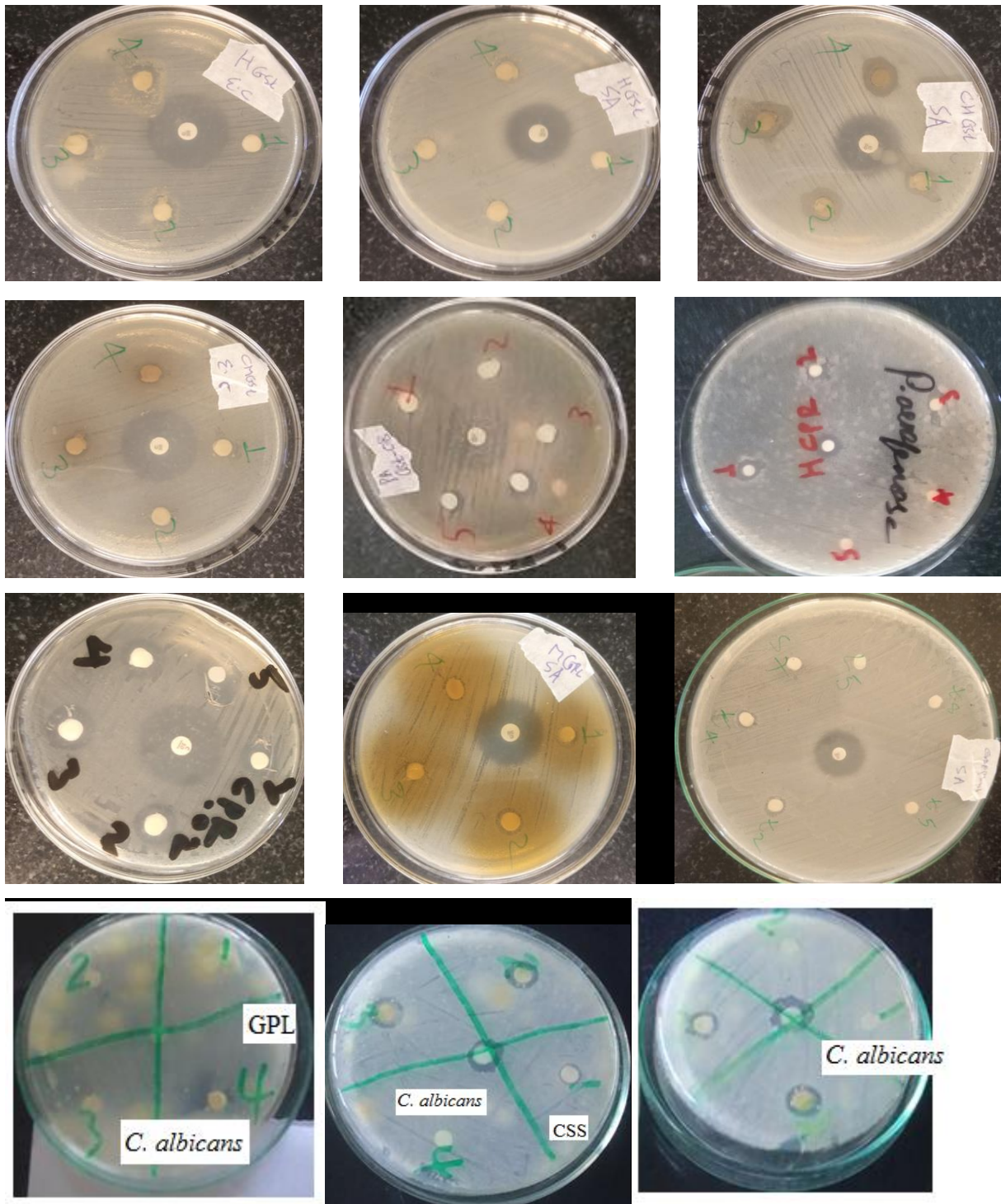
Meaning of Score Values

Range	Interpretation	Symbols	Color
2.00 - 3.00	High-confidence identification	(+++)	green
1.70 - 1.99	Low-confidence identification	(+)	yellow
0.00 - 1.69	No Organism Identification Possible	(-)	red

Meaning of Consistency Categories (A - C)

Category	Interpretation
(A)	High consistency: The best match is a high-confidence identification. The second-best match is (1) a high-confidence identification in which the species is identical to the best match, (2) a low-confidence identification in which the species or genus is identical to the best match, or (3) a non-identification.
(B)	Low consistency: The requirements for high consistency are not met. The best match is a high- or low-confidence identification. The second-best match is (1) a high- or low-confidence identification in which the genus is identical to the best match or (2) a non-identification.
(C)	No consistency: The requirements for high or low consistency are not met.

Appendix Figure 6. Representatives of antimicrobial inhibition zones of extracts, isolated compounds and ethyl acetate extracts of endophytic bacterial cultures



Approval of Investigators

We hereby declare that the research report entitled

“Phytochemical Investigation and *In-Vitro* Biological Activities evaluation of Selected Ethiopian Medicinal Plants and their Endophytes in Eastern Ethiopia”

incorporating the necessary comments and suggestions given by the reviewers.

	Name	Signature	Date
Principal Investigator	_____	_____	_____
Co- Investigator	_____	_____	_____
Co- Investigator	_____	_____	_____
Co- Investigator	_____	_____	_____

Approval of Reviewers

I hereby confirm that (PI)Dr./Mr. _____ has accomplished his/her work as per the approved proposal and incorporated all the comments given by the reviewers in his/her terminal report of the project entitled “Phytochemical Investigation and *In-Vitro* Biological Activities evaluation of Selected Ethiopian Medicinal Plants and their Endophytes in Eastern Ethiopia”

and hence the report qualifies for submission as standard research output.

	Name	Signature	Date
Reviewer 1.	_____	_____	_____
Reviewer 2.	_____	_____	_____

Approval: School Ethical Review Board (School Scientific Committee)

	Name	Signature	Date
1.	_____	_____	_____
2.	_____	_____	_____
3.	_____	_____	_____
4.	_____	_____	_____